



**HAL**  
open science

## Biodegradation of chloroacetanilide herbicides in wetlands

Omniea Elsayed

► **To cite this version:**

Omniea Elsayed. Biodegradation of chloroacetanilide herbicides in wetlands. Ecosystems. Université de Strasbourg, 2015. English. NNT : 2015STRAJ003 . tel-01280603

**HAL Id: tel-01280603**

**<https://theses.hal.science/tel-01280603>**

Submitted on 29 Feb 2016

**HAL** is a multi-disciplinary open access archive for the deposit and dissemination of scientific research documents, whether they are published or not. The documents may come from teaching and research institutions in France or abroad, or from public or private research centers.

L'archive ouverte pluridisciplinaire **HAL**, est destinée au dépôt et à la diffusion de documents scientifiques de niveau recherche, publiés ou non, émanant des établissements d'enseignement et de recherche français ou étrangers, des laboratoires publics ou privés.

# UNIVERSITÉ DE STRASBOURG

*ÉCOLE DOCTORALE des sciences de la Vie et de la Santé*

UMR 7156 UNISTRA - CNRS

Génétique Moléculaire, Génomique, Microbiologie (GMGM)

**THÈSE** présentée par :

**Omniea ELSAYED**

## Biodegradation of chloroacetanilide herbicides in wetlands

soutenue le : **23 Janvier 2015**

pour obtenir le grade de: **Docteur de l'université de Strasbourg**

Discipline: Sciences du Vivant

Spécialité : Aspects moléculaires et cellulaires de la biologie

**THÈSE dirigée par :**

**M. IMFELD Gwenaël** Chargé de recherche, CNRS, Université de Strasbourg, France  
**M. VUILLEUMIER Stéphane** Professeur, Université de Strasbourg, France

**RAPPORTEURS :**

**M. BAYONA Josep M** Professeur, IDAEA, Espagne  
**M. TRUU Jaak** Professeur, Université de Tartu, Estonie

---

**AUTRES MEMBRES DU JURY :**

**M. MILLET Maurice** Professeur, Université de Strasbourg, France  
**Mme. NIJENHUIS Ivonne** Senior scientist, UFZ, Allemagne



*“A PhD is a journey, not a destination”*

Adapted from Ralph Waldo Emerson

## Acknowledgments

The work of this PhD thesis was performed at the “Laboratory of Hydrology and Geochemistry of Strasbourg (LHyGeS)” UMR 7517-CNRS-Université de Strasbourg, and the laboratory “Génétique Moléculaire, Génomique, Microbiologie (GMGM)” UMR 7156-CNRS-Université de Strasbourg. Thanks to all the members of both laboratories. This PhD work was funded by the European Union under the 7<sup>th</sup> Framework Programme (Marie Curie Initial Training Network CSI:Environment, Contract Number PITN-GA-2010-264329).

Thank you Dr. Gwenaël Imfeld and Prof. Stéphane Vuilleumier, directors of this PhD thesis for their continuous support and guidance, especially during the last year. Gwenaël, I’m very grateful for the moral support and encouragement during the ups and downs (and there has been many) of this four year long journey. I’m very grateful to Stéphane for pointing me towards this PhD position when I first contacted him more than four years ago, it was a great opportunity for me. I would also like to thank you both for the time and effort spent on corrections and feedback of different parts of this manuscript.

I would also like to thank members of my PhD jury: Prof. Josep M Bayona, Prof. Jaak Truu, Dr. Ivonne Nijenhuis and Prof. Maurice Millet for kindly accepting to evaluate my work.

I would like to thank Dr. Ivonne Nijenhuis and all the members of the Isotope biogeochemistry in the Helmholtz Centre for Environmental Research – UFZ in Leipzig for welcoming me in your lab and helping me with the CSIA measurements. A special thanks to Mathias Gehre, Ursula Günther and Falk Bratfisch for their help with the IRMS machines (Benny). My heartfelt thanks to Sara Herrero Martin for advice and support during my stay in Leipzig and through all different organisational aspects of CSI:Environment project.

My PhD experience was a bit particular in that I had two offices, two teams and two supervisors. This experience was overall enriching, though challenging at times. This work wouldn’t have been possible without the help and support of members of both teams at the LHyGes and the GMGM. Thanks to Elodie, Marie, Ivan, Benoit, Clio and Izabella in the LHyGeS not only for the good cooperation and scientific discussions but also for their

friendship that made a huge difference in my PhD experience. Thank you for the warm welcome to the team and for the effort you made to speak in English when I first started in the lab, although it didn't last long. Thank you Nicolas Trottier and Yi for being great office-mates. I'm also very grateful to Benoit and Eric for their technical help in the lab and good company. I also thank all 3<sup>rd</sup> floor PhD students for always keeping a good atmosphere in the lab. I am lucky to have you all as friends and as colleagues. Thanks to all members of the LHyGeS for "les tournois de pétanque" and "les fêtes de la moustache" which were always a lot of fun. On the other side (GMGM) I thank Christelle and Yousra for guiding me through the tips and tricks of the lab and for preparing the agarose gels for me during the last two months of lab-work. Thank you Thierry for always accepting to help with different bits of lab-work with a welcoming attitude. Thank you Françoise for the continuous good energy and cheerfulness, it always helped to lift my mood. Thank you Farhan for showing me how things are done when I first started doing lab work at the GMGM. Thanks to all PhD students at the GMGM: Pauline, Farah who were always a good company. I also wish to express my gratitude to all the trainees who helped in different parts of this work, especially Renata, Ana and Julie. Your contributions were very valuable to my work.

To all CSI:Environment fellows: thanks for your friendship, for your cooperation and the good times we had together touring Europe while learning about isotopes!

A final and big thank you goes to my family who have encouraged me to start this project and supported me all the way. Thank you Adham for always being there and for believing in me. Thank you baby Donya for bearing up with me through the final phases of write-up and helping me keep things in perspective. My deep thanks goes to all who enjoyed the company of Donya to allow me to finish this manuscript (mama, Noura & Hend).

## Remerciements

Ce travail de thèse a été réalisé au Laboratoire d'Hydrologie et de Géochimie de Strasbourg (LHyGeS) UMR 7517 CNRS-Université de Strasbourg, et dans l'unité de recherche Génétique Moléculaire, Génomique, Microbiologie (GMGM) UMR 7156 Université de Strasbourg - CNRS. Merci à tous les membres de ces deux laboratoires. Ce travail de thèse a été financé par l'Union européenne au titre du 7<sup>ème</sup> programme-cadre (Réseau de formation initiale Marie Curie, CSI: Environnement, contrat Nombre PITN-GA-2010-264329).

Merci Dr. Gwenaël Imfeld et Prof. Stéphane Vuilleumier, directeurs de ce travail de doctorat pour leur soutien et leur supervision, en particulier au cours de la dernière année. Dr. Imfeld, je suis très reconnaissante pour ton soutien moral et tes encouragements pendant les hauts et les bas (et il y en a eu beaucoup) de ce voyage de quatre ans. Je suis très reconnaissante au Prof. Vuilleumier pour m'avoir orienté vers cette position de doctorat quand je l'ai contacté il y a plus de quatre ans, et qui s'est révélée être une grande opportunité pour moi. Je tiens également à vous remercier tous les deux pour le temps et les efforts consacrés aux corrections et à l'évaluation des différentes parties de ce manuscrit.

Je tiens également à remercier les membres de mon jury de thèse: Prof. Josep M Bayona, Prof. Jaak Truu, Dr. Ivonne Nijenhuis et Prof. Maurice Millet d'avoir bien voulu accepter d'évaluer mon travail de thèse.

Je tiens à remercier Dr. Ivonne Nihenhuis et tous les membres de l'équipe biogéochimie des isotopes dans le Centre Helmholtz pour la recherche environnementale - UFZ de Leipzig de m'avoir accueillie dans votre laboratoire et de m'avoir aidé avec les analyses CSIA. Un grand merci à Mathias Gehre, Ursula Günther et Falk Bratfisch pour leur aide avec la machine IRMS (Benny). Mes sincères remerciements à Sara Herrero Martin pour tous les conseils et le soutien pendant mon séjour à Leipzig ainsi que son aide pour tous les différents aspects organisationnels du projet CSI: Environnement.

Mon expérience de doctorat était particulière étant donné que j'avais deux bureaux, deux équipes et deux directeurs de thèse. Cette expérience a été stimulante et enrichissante. Ce travail n'aurait pas été possible sans l'aide et le soutien des membres des deux équipes au LHyGes et au GMGM. Merci à Elodie, Marie, Ivan, Benoît, Clio et Izabella au LHyGes non seulement pour le bon travail en collaboration et pour les discussions scientifiques

enrichissantes mais aussi pour leur amitié qui a eu un impact très positif sur mon expérience globale de ce doctorat. Merci pour l'accueil chaleureux de toute l'équipe et pour l'effort que vous avez fait de parler en anglais quand j'ai commencé dans le laboratoire, même si cela n'a pas duré très longtemps 😊. Merci Nicolas Trottier et Yi Pan pour avoir été de merveilleux « co-bureau ». Je suis également très reconnaissante à Benoît Guyot et à Eric Pernin pour leur aide technique dans le laboratoire et leur bonne compagnie. Je remercie également tous les doctorants du 3ème étage d'avoir gardé toujours une bonne ambiance dans le laboratoire. Je suis très heureuse de vous avoir comme amis et collègues. Merci à tous les membres du LHyGeS pour la convivialité "des tournois de pétanque" et "des fêtes de la moustache". Du côté (GMGM), je remercie Christelle Gruffaz et Yousra Louhichi pour leurs aides précieuses et leurs conseils pratiques pour le travail au laboratoire et spécialement pour leur assistance à la préparation des gels d'agarose pendant les deux derniers mois de manips. Merci à Thierry Nadalig d'avoir toujours accepté de m'aider faire les manips avec gentillesse. Merci à Françoise Bringel pour son énergie et sa bonne humeur, qui m'ont toujours aidé à garder le moral. Merci à Muhammad Farhan Ul Haque pour m'avoir guidé au démarrage quand j'ai commencé à faire des manips au GMGM. Merci à tous les doctorants au GMGM: Pauline et Farah. Je tiens également à exprimer ma gratitude à tous les stagiaires qui m'ont aidé dans les différentes parties de ce travail, en particulier Renata, Ana et Julie. Vos contributions ont été très précieuses pour mon travail.

A tous les doctorants dans le réseau CSI: Environnement: merci pour votre amitié, votre coopération et les bons moments que nous avons passés ensemble partout en Europe, tout en découvrant les isotopes!

Finalement, un très grand merci à ma famille qui m'a encouragé à commencer ce projet et m'a soutenu tout au long du chemin. Merci Adham d'être toujours là et de croire en moi. Merci bébé Donya d'avoir supporté les phases finales de la rédaction de la thèse et de m'avoir aidé à garder les choses en perspective et merci à tous ceux qui ont gardé Donya pour me permettre de terminer ce manuscrit (maman, Noura et Hend).



# Résumé étendu

## La biodégradation de chloroacétanilides dans les zones humides

### Introduction

Les chloroacétanilides (métolachlore, alachlore et acétochlore ; Figure I) sont une famille d'herbicides largement utilisés pour le contrôle des graminées annuelles et des mauvaises herbes sur une grande variété de cultures, notamment maïs, tournesol et betterave sucrière (Pereira *et al.*, 2009). Les chloroacétanilides sont des herbicides de pré-levée (c'est-à-dire appliqués avant le développement du couvert végétal), dont la solubilité élevée dans l'eau les rends particulièrement sujets à une mobilisation lors d'événements ruisselants (Reid *et al.*, 2000). Les chloroacétanilides et leurs produits de dégradation sont ainsi fréquemment détectés comme contaminants dans les nappes phréatiques et les eaux de surface, soulevant des interrogations quant à leurs impacts sur les écosystèmes et la santé humaine (Baran et Gourcy, 2013).

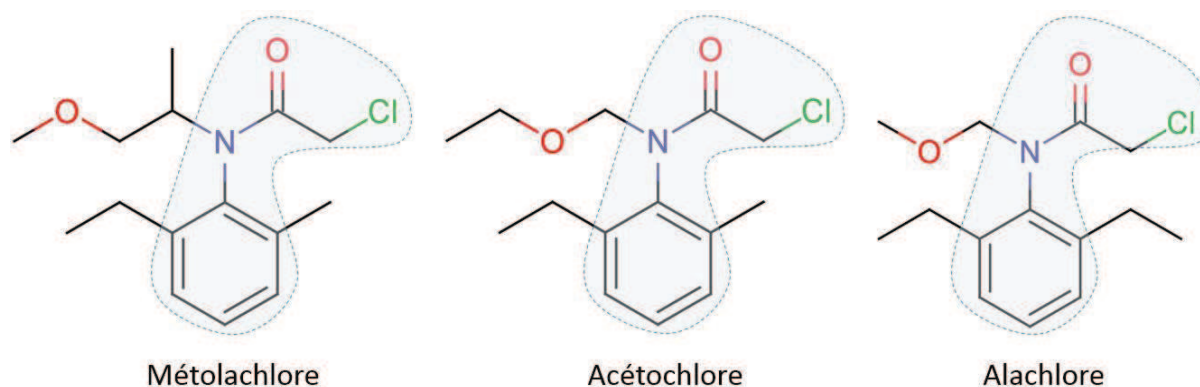


**Figure I. Structure moléculaire des herbicides métolachlore, acétochlore et alachlore.** La structure moléculaire commune des chloroacétanilides est mise en évidence en bleu clair.

La compréhension des processus de transport et de dégradation régissant le devenir des pesticides est donc essentielle pour l'optimisation de stratégies de remédiation et une meilleure évaluation des risques environnementaux de contamination par les pesticides. Cependant, les processus régissant le transport et la biodégradation des chloroacétanilides en terres agricoles, en passant par les zones réactives, telles que les zones humides, et ce avant d'atteindre les écosystèmes aquatiques, restent mal connus. Les zones humides sont des écosystèmes dans lesquelles une grande variété de processus permettent la dégradation des pesticides (Stehle *et*

*al.*, 2011). La dégradation des pesticides est notamment déterminée par les communautés bactériennes et les processus biogéochimiques actifs dans les zones humides (Borch *et al.*, 2010). La biodégradation est considérée actuellement comme le principal processus de transformation des chloroacétanilides dans l'environnement (Fenner *et al.*, 2013), tandis que les transformations abiotiques, tels que la photolyse ou l'hydrolyse, semblent jouer un rôle mineur (Zhang *et al.*, 2011). Parallèlement, la composition et le fonctionnement microbiens sont impactés par l'exposition aux pesticides (Imfeld et Vuilleumier, 2012). Potentiellement, les communautés microbiennes représentent ainsi des bio-indicateurs de l'exposition aux pesticides dans les zones humides (Sims *et al.*, 2013). Cependant, la connaissance des communautés microbiennes associées à la dégradation des chloroacétanilides dans les zones humides, et les paramètres environnementaux associés est encore rudimentaire.

Traditionnellement, les études sur l'atténuation des pesticides dans les zones humides consistent en des bilans massiques entrée-sortie des pesticides, et portent rarement sur les processus de dégradation *in situ*. Dans le cas des chloroacétanilides, une grande variété de processus de dégradation peut être envisagée, bien que les connaissances sur les conditions dans lesquelles chaque processus est pertinent sont encore limitées, et les approches pour l'évaluation de la dégradation *in situ* de chloroacétanilides manquent largement. De nouvelles approches expérimentales peuvent fournir un aperçu sur les processus de dégradation *in situ* des pesticides. Celles-ci comprennent notamment l'analyse isotopique composé-spécifique (CSIA) et l'analyse chirale (Milosevic *et al.*, 2013), ainsi que les techniques moléculaires de l'écologie microbienne. Avant le début de la présente thèse, ces différentes approches n'avaient pas été développés ou appliqués de conjointement et de façon ciblée à l'étude de la dégradation des chloroacétanilides dans les zones humides.

### **Objectifs du projet de doctorat**

L'objectif général de la thèse a été d'évaluer la dégradation *in situ* des chloroacétanilides, et de caractériser la diversité bactérienne associée dans les zones humides. Les objectifs spécifiques de cette thèse étaient les suivants:

- développer et valider une méthode CSIA pour évaluer la dégradation *in situ* d'herbicides chloroacétanilides dans l'environnement;
- suivre les communautés bactériennes associées à la dégradation des chloroacétanilides à l'aide d'outils moléculaires;

- évaluer la dégradation *in situ* de chloroacétanilides dans les zones humides et sa relation avec les conditions biogéochimiques;
- évaluer l'impact des conditions hydrauliques et du mode d'exposition aux herbicides sur la biogéochimie, la dissipation des chloroacétanilides et sur les communautés bactériennes dans les zones humides.

Des zones humides expérimentales ont été choisies comme systèmes-modèles pour étudier le devenir de chloroacétanilides dans des conditions dynamiques d'oxydo-réduction. Ces zones humides expérimentales intègrent les principales caractéristiques des zones humides (par exemple les interactions de sédiments, eau et plantes), tout en permettant un meilleur contrôle des paramètres environnementaux (par exemple les flux de contaminants), et donc une meilleure interprétation des processus de dégradation *in situ*. Plusieurs outils ont été développés et combinés pour étudier la dégradation de chloroacétanilides dans les zones humides étudiées. Des méthodes d'analyse hydrogéochimique et analytique ont été appliquées à l'étude du lien entre les conditions biogéochimiques et la dégradation des chloroacétanilides. L'analyse CSIA, l'analyse des produits de dégradation et (dans le cas de métolachlore) l'analyse de chiralité ont été utilisées pour démontrer la dégradation des chloroacétanilides *in situ*, et pour fournir des indications sur les processus impliqués. Le génotypage T-RFLP et le pyroséquençage 454 ont été utilisés pour caractériser la diversité des communautés bactériennes dans les zones humides contaminées par les chloroacétanilides, et déterminer leur réponse à l'exposition aux chloroacétanilides et aux conditions hydrochimiques.

### ***Résumé des résultats obtenus au cours du projet de doctorat***

La transport et la dégradation des chloroacétanilides ont d'abord été étudiés dans des zones humides à écoulement vertical au laboratoire, pour mieux comprendre les processus de dégradation du métolachlore, de l'acétochlore et de l'alachlore à l'interface oxiqve/anoxiqve dans les zones humides, et leur lien avec les communautés bactériennes aquatiques (Elsayed *et al.*, 2014b). La diminution de charge d'acétochlore et d'alachlore entre l'entrée et la sortie des zones humides ont été respectivement de 56 et 51%, alors que le métolachlore s'est montré plus persistant, avec seulement 23% de dissipation. Ceci suggère que les différences structurales entre les trois chloroacétanilides semblent déterminer en partie leur dégradation. La dégradation des trois chloroacétanilides s'est produite en particulier dans la rhizosphère, en

condition anaérobie (Figure II).

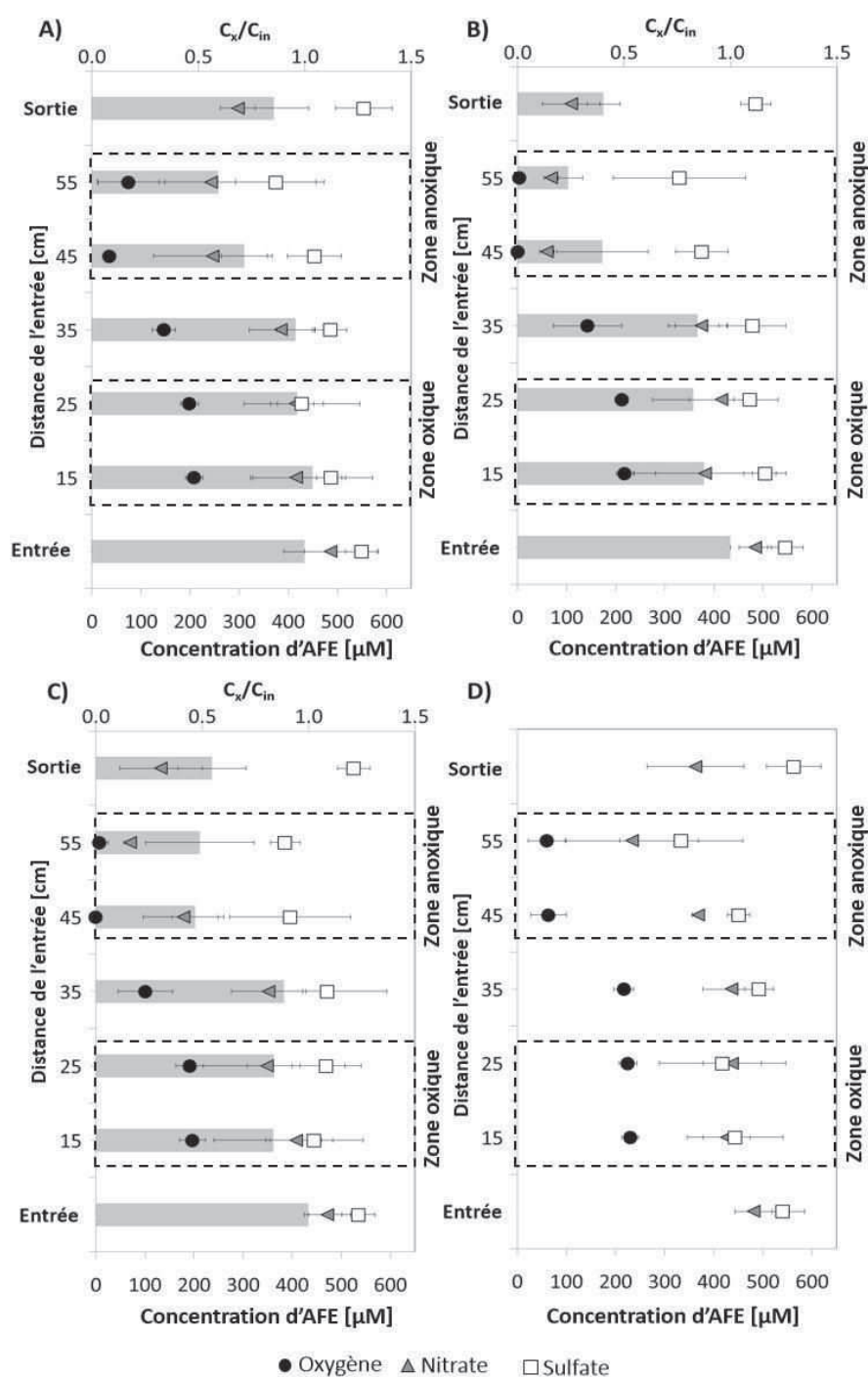


**Figure II. Concentrations d'accepteurs terminaux d'électrons (AFE) : oxygène (cercles noirs), nitrate (triangles gris) et sulfate (carrés blancs) dans les zones humides expérimentales contaminés par le métolachlore (A), l'acétochlore (B), et l'alachlore (C), et (D) par le contrôle sans herbicide. Les concentrations relatives des chloroacétanilides ( $C_x / C_{in}$  = concentration au point (x) divisée par la concentration d'entrée) aux différentes profondeurs des zones humides de laboratoire sont indiquées par des barres grises, comme la moyenne  $\pm$  écart-type ( $\mu \pm \sigma$ ) de l'ensemble des valeurs obtenues tout au long de l'expérience.**

Une méthode d'analyse isotopique composé-spécifique (carbone) du métolachlore, de l'alachlore et de l'acétochlor dans les échantillons d'eau a été développée. Un fractionnement isotopique prononcé a été observé (Figure III), suggérant une biodégradation *in situ* de l'alachlore ( $\epsilon_{\text{bulk}} = -2,0 \pm 0,3$ ) et de l'acétochlor ( $\epsilon_{\text{bulk}} = -3,4 \pm 0,5$ ).

Malgré une faible dissipation, les rapports énantiomériques du métolachlore diffèrent entre la zone oxique ( $0,494 \pm 0,006$ ) et la zone rhizosphérique ( $0,480 \pm 0,005$ ), indiquant la biodégradation préférentielle de l'énantiomère *S*. Les paramètres hydrochimiques, et en particulier la concentration en oxygène, corrént avec les profils bactériens, contrairement aux concentrations en chloroacétanilides.

La rhizosphère était dominée par des bactéries Gram-positives anaérobies affiliées aux *Clostridia* et aux *Actinobacteria*, et par des *Proteobacteria*. Des taxons connus pour leur capacité à réduire le sulfate comme *Deltaproteobacteria* (*Desulfobacteraceae*, *Desulfovibrionaceae*, et *Desulfobulbaceae*) et *Clostridium* (*Peptococcaceae*) ont également été détectés. Les communautés bactériennes de la rhizosphère anoxique ont probablement contribué à la dégradation des chloroacétanilides, soit directement en catalysant leur biodégradation, soit en fournissant des molécules soufrées agissant comme des nucléophiles avec les chloroacétanilides. Les résultats obtenus soulignent l'importance de la dégradation anaérobie des chloroacétanilides, et illustrent le potentiel d'outils innovants tels que le CSIA et l'analyse énantiomérique, en combinaison avec des approches plus traditionnelles comme les analyses hydrochimiques, la quantification de pesticides et les analyses de produits de dégradation, pour évaluer le devenir des chloroacétanilides dans les zones humides.

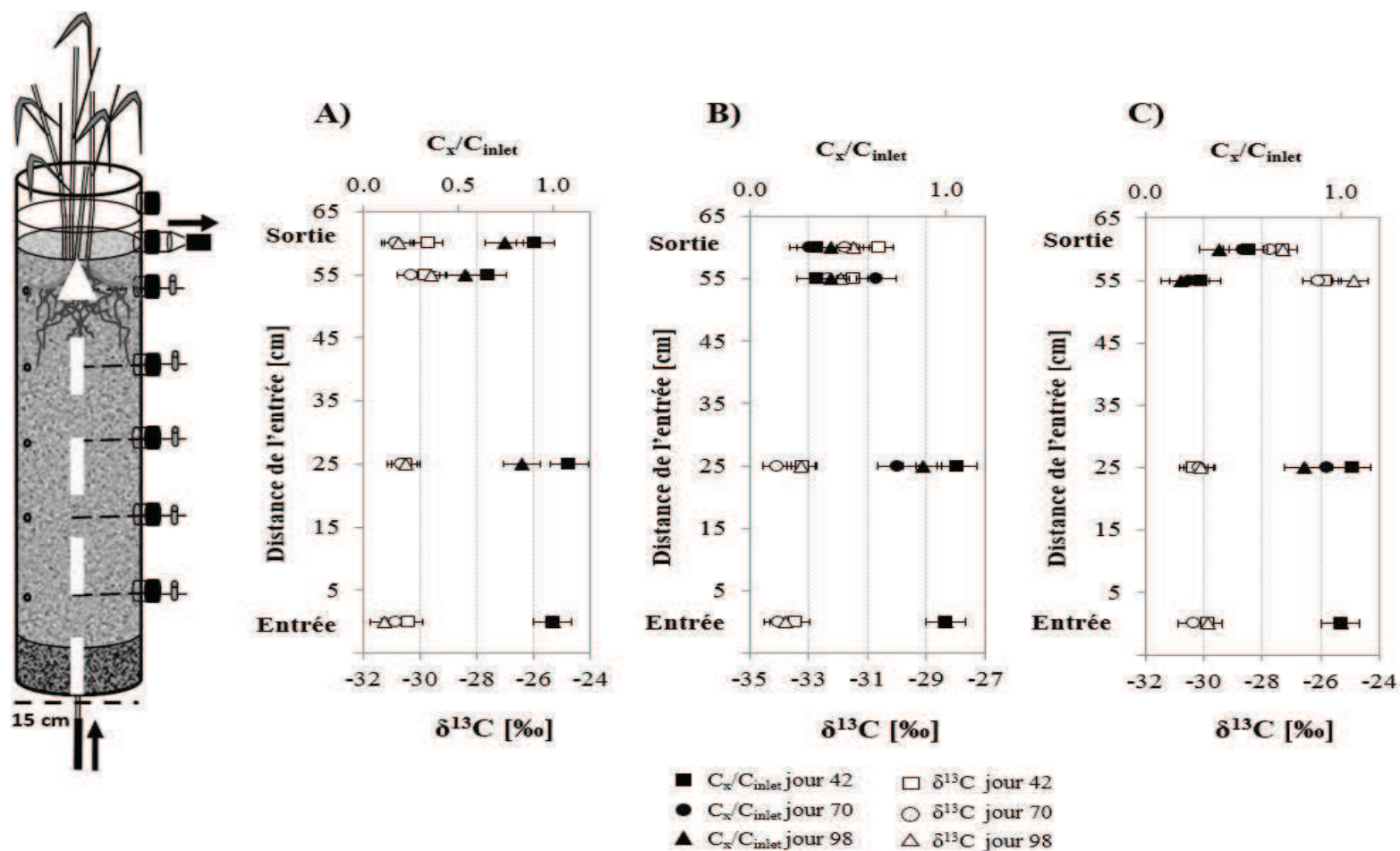


**Figure III. Signatures isotopiques du carbone du métolachlore, de l'acétochlor et de l'alachlore dans les zones humides expérimentales.** La composition isotopique de carbone est représentée en notation  $\delta^{13}C$  (symboles blancs) et  $C_x / C_{in}$ : concentration au point (x) divisée par la concentration d'entrée (symboles noirs) de métolachlore en A) alachlore en B) et acétochlor en C) à l'intérieur des zones humides en colonnes le jour 42 (carrés), le jour 70 (cercles) et le jour 98 (triangles). Les flèches indiquent la direction d'écoulement de l'eau. Les barres d'erreur indiquent l'incertitude de  $\delta^{13}C$  ( $\pm 0,5$  ‰) et l'erreur propagée de  $C_x/C_{inlet}$  sur la base des écarts-types des concentrations.

Le régime hydraulique joue également un rôle majeur dans l'évolution biogéochimique des zones humides et influence la dégradation des contaminants organiques, y compris les pesticides (Faulwetter *et al.*, 2009). Dans un deuxième volet de ce travail, l'impact des conditions hydrauliques et le mode d'exposition aux herbicides sur les conditions biogéochimiques, la dissipation des chloroacétanilides, et la diversité des communautés bactériennes associées a été évalué, et le transport du *S*-métolachlore a été suivi dans une zone humide expérimentale à ciel ouvert (Elsayed *et al.*, 2014a). L'influence des conditions hydrauliques et hydrochimiques sur la dégradation du *S*-métolachlore et sur les communautés bactériennes a été caractérisée dans deux zones humides artificielles identiques, imitant pour l'une des conditions d'exposition chronique et continue (flux continu), et pour l'autre une exposition aiguë et transitoire au *S*-métolachlore (bâchées).

Les deux zones humides ont montré des conditions d'oxydo-réduction distinctes, correspondant aux différents régimes hydrauliques appliqués. La zone humide à écoulement continu se distinguait par des conditions anaérobies (potentiels redox variant de -190 mV à -400 mV), tandis que le système de traitement en discontinu alternait entre conditions aérobies et anaérobies (320 mV à -400 mV). Une réduction des nitrates, du manganèse et des sulfates a été observée dans les deux zones humides, mais de manière généralement plus prononcée dans la zone humide opérée en bâchées. De même, l'atténuation de *S*-métolachlore était plus élevée dans le système en bâchées (93-97%) que dans celui en flux continu (40-79%), en accord avec des études précédentes décrivant une activité biogéochimique et une élimination des contaminants organiques plus élevées dans les systèmes alternant les phases de saturation et d'insaturation que dans les zones humides saturées en continu et fonctionnant à faible potentiel redox (Avila *et al.*, 2013; Dytczak *et al.*, 2008).

Les différences de composition bactérienne observées dans les deux systèmes étaient modestes bien que significatives ( $p = 0,008$ ), et une corrélation entre le *S*-métolachlore, les nitrates, et les concentrations totales de carbone inorganique a été notée (Figure IV). La composition bactérienne des eaux interstitielles des zones humides a évolué graduellement au fil du temps dans les zones humides à flux continu, et plus brusquement dans la zone humide en discontinu, reflétant les conditions distinctes de fonctionnement hydraulique et de potentiel redox dans les deux systèmes (Figure V). Les résultats obtenus suggèrent que les profils de composition bactérienne et leur dynamique pourraient servir comme bioindicateurs de l'exposition aux herbicides et aux perturbations hydrauliques dans les zones humides

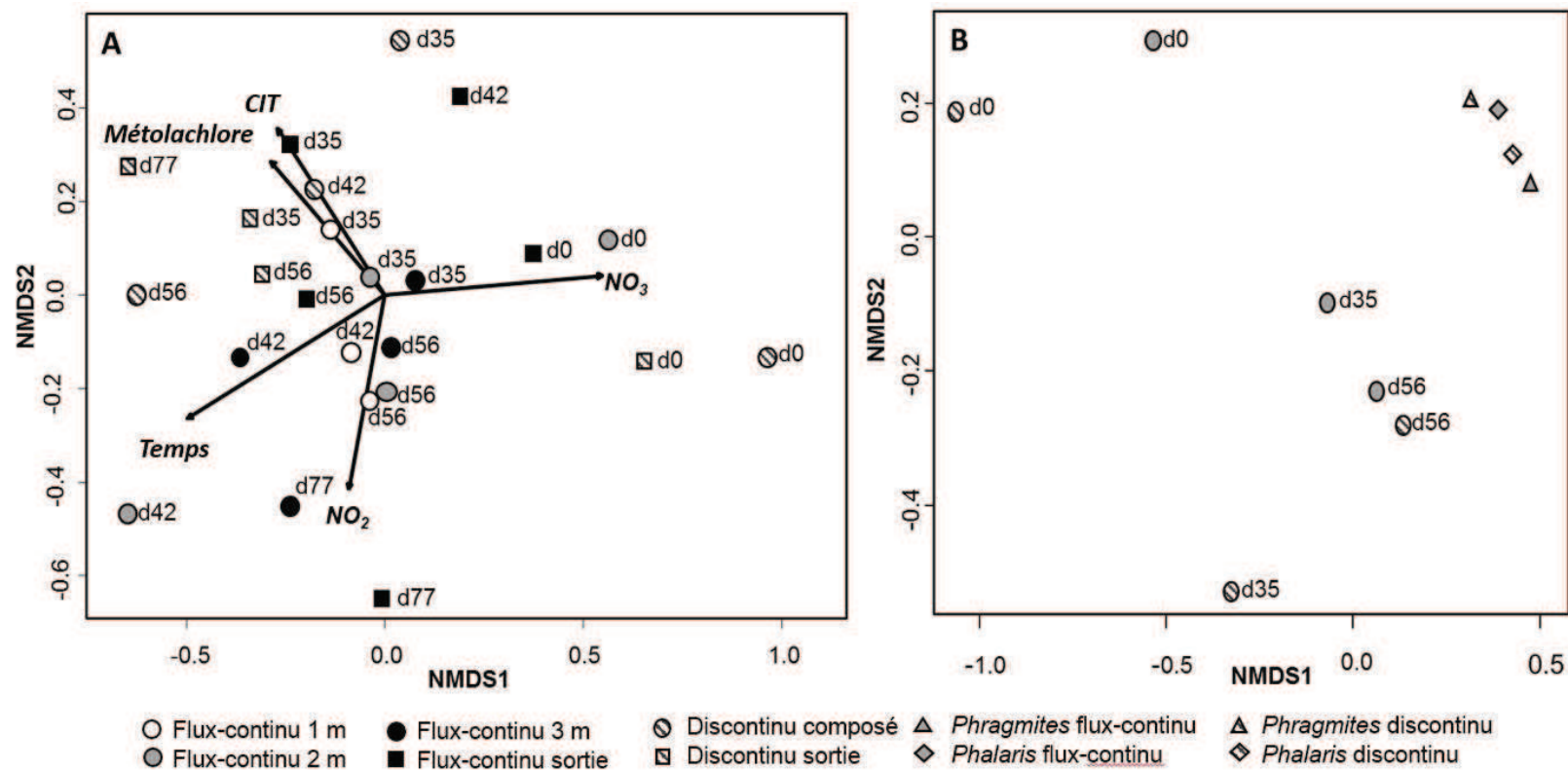


**Figure IV. Représentation 2D-NMDS des profils des communautés bactériennes basée sur (A) la T-RFLP et (B) le pyroséquençage de la région hypervariable V1-V3 du gène ARNr 16S des échantillons d'eau de zones humides et de la rhizosphère. Les symboles sont libellés par jour d'échantillonnage (jours 0, 35, 42, 56 et 77). 1m, 2m, 3m: 1, 2 et 3 mètres de l'entrée, respectivement. En (A), les vecteurs correspondent aux variables qui corrént significativement avec la structure de la communauté bactérienne (temps, *S*-métochlorure, nitrate, nitrite et carbone inorganique total). Stress : (A) 0,18%, (B) 0,04%**



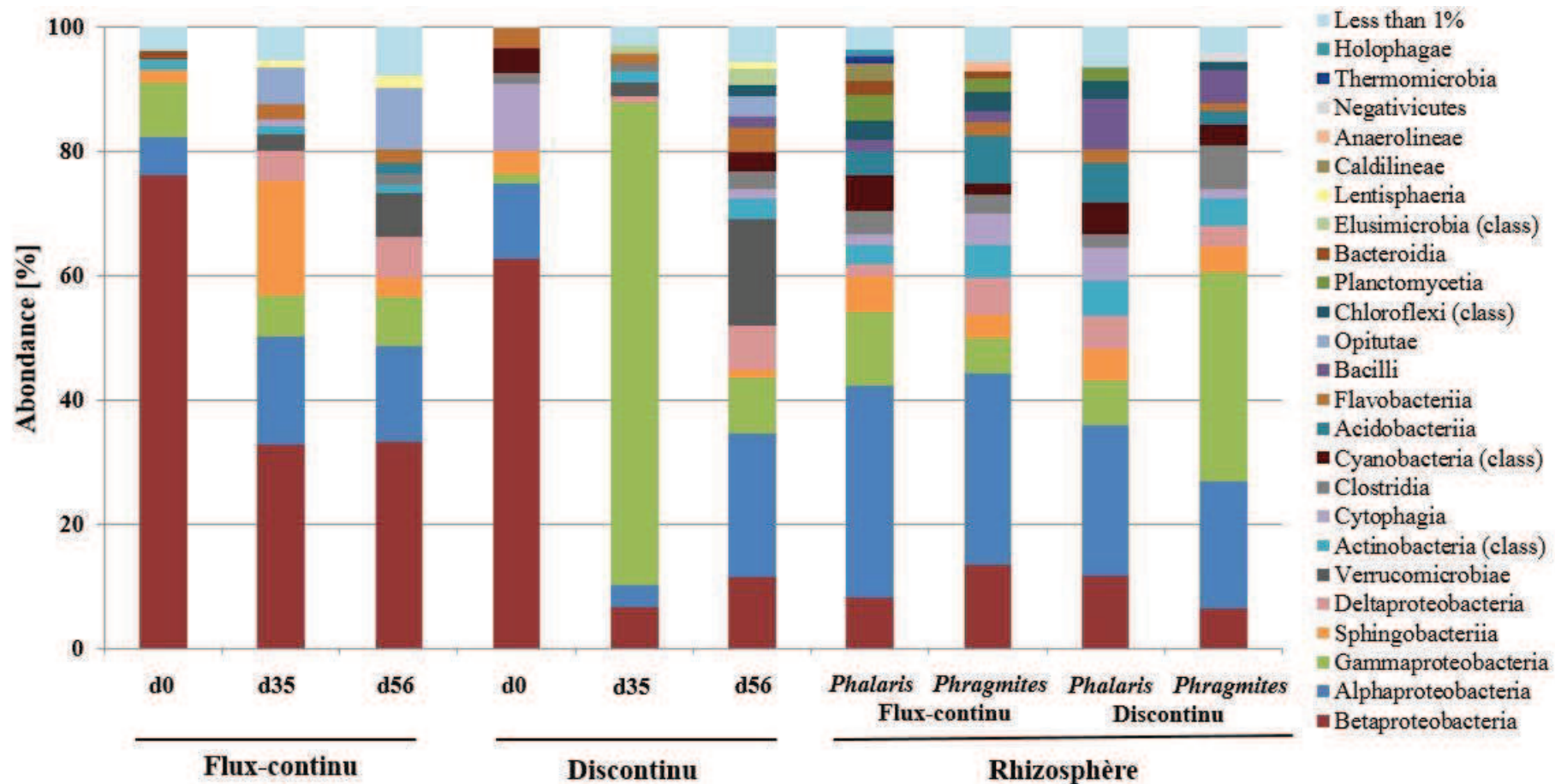


Figure V. Abondance relative [%] des classes bactériennes dominantes (seuil d'identité de séquence = 80%) dans les échantillons d'eau des zones humides pour les différents jours d'échantillonnage (jours 0, 35 et 56) ainsi que dans les échantillons de la rhizosphère. Les échantillons d'eau interstitielle de zone humide en flux continu représentés étaient ceux prélevés à 2 m de l'entrée.

Pris conjointement, les résultats obtenus au cours de cette thèse de doctorat démontrent le rôle prévalent des conditions biogéochimiques dans le devenir des chloroacétanilides. L'importance des conditions anaérobies pour la dégradation de chloroacétanilides dans des environnements rédox-dynamiques a été démontrée. De plus, ce travail a mis en évidence la valeur d'outils innovants tels que le CSIA, l'analyse d'énantiomères, et l'analyse moléculaire de l'ADN environnemental pour caractériser le devenir d'herbicides chloroacétanilides dans l'environnement.

En perspective de ce travail, la détermination de facteurs d'enrichissement isotopique des chloroacétanilides dans différentes conditions d'oxydo-réduction ainsi que l'identification de souches bactériennes dégradant les chloroacétanilides permettront d'améliorer la compréhension mécanistique des voies de dégradation de chloroacétanilides et des gènes cataboliques correspondants. L'application de ces approches expérimentales complémentaires contribuera à améliorer l'évaluation de la biodégradation des chloroacétanilides dans des environnements contaminés, et de mieux prédire à long-terme le devenir de pesticides en évaluant les risques environnementaux associés. Du point de vue de la remédiation, l'amélioration des connaissances sur la dégradation des chloroacétanilides servira également à l'optimisation de la conception de zones humides artificielles pour le traitement et l'élimination des chloroacétanilides et de micropolluants similaires.

## List of Abbreviations

(Q)-ToF	Quadrupole time-of-flight mass spectrometry
2,4-D	2,4-Dichlorophenoxyacetic acid
AKIE	Apparent kinetic isotope effect
ANOSIM	Analysis of similarities
ANOVA	Analysis of variance
BLAST	Basic local alignment search tool
BTEX	Benzene, toluene, ethylbenzene, and xylenes
CA	Correspondence analysis
CCA	Canonical correspondence analysis
CSIA	Compound-specific isotope analysis
DCM	Dichloromethane
DDT	Dichlorodiphenyltrichloroethane
DEET	N,N-Diethyl-meta-toluamid
DGGE	Denaturing gradient gel electrophoresis
DMSO	Dimethyl sulfoxide
DNA	Deoxyribonucleic acid
dNTP	Deoxyribonucleotide triphosphate
EA-IRMS	Elemental analyzer-isotope ratio mass spectrometry
EE	Enantiomeric excess
EF	Enantiomer-fraction
ESA	Ethane sulfonic acid
ESIA	Enantiomer-specific isotope analysis
GC	Gas chromatography
GC-C-IRMS	Gas chromatography-combustion-isotope ratio mass spectrometry
GSH	Glutathione
GST	Glutathione S-transferase
HESI	Heated electrospray ionization
HRMS	High resolution mass spectrometry
KIE	Kinetic isotope effect
LC	Liquid chromatography
LC-IRMS	Liquid chromatography-isotope ratio mass spectrometry
MAFFT	Multiple alignment using fast fourier transform
MRM	Multiple reaction monitoring
MTBE	Methyl tertiary-butyl ether
NMDS	Nonmetric multidimensional scaling
OTU	Operational taxonomic unit
OXA	Oxanilic acid
PCA	Principle component analysis
PCoA	Principle coordinate analysis
PCR	Polymerase chain reaction
PFLA	Phospholipid ester-linked fatty acid
PICT	Pollution-induced community tolerance

qPCR	Quantitative polymerase chain reaction
RAPD	Random Amplified Polymorphic DNA
RDA	Redundancy analysis
RNA	Ribonucleic acid
SIP	Stable isotope probing
SPE	Solid phase extraction
SRM	Selective reaction monitoring
TEA	Terminal electron acceptor
TEAP	Terminal electron-accepting process
T-RF	Terminal-restriction fragment
T-RFLP	Terminal-restriction fragment length polymorphism
U-HPLC	Ultra-high performance liquid chromatography
V-PDP	Vienna-Pee Dee Belemnite

# Table of contents

Chapter I: Introduction.....	1
1. Pesticides.....	2
1.1. Use, ecological and human health impact.....	2
1.2. Transport and attenuation in the environment .....	4
2. Chloroacetanilide herbicides.....	8
2.1. Properties and use .....	8
2.2. Environmental fate of chloroacetanilide herbicides .....	9
3. Evaluating pesticide (bio)degradation in the environment .....	15
3.1. Hydrogeochemistry.....	16
3.2. Degradation product analysis.....	17
3.3. Enantiomer analysis .....	18
3.4. Compound-specific isotope analysis.....	19
3.5. Molecular microbiology.....	23
3.6. Data analysis .....	26
4. Wetland systems .....	28
4.1. Wetland biogeochemistry and hydrology .....	29
4.2. Processes governing pesticides in wetlands.....	30
4.3. Impact of pesticides on wetland bacterial communities .....	33
5. Research focus and objectives .....	35
5.1. Research focus: Degradation of chloroacetanilides.....	35
5.2. Research objectives.....	37
5.3. Thesis layout .....	38
Chapter II: Methodology.....	41
1. CSIA to assess <i>in situ</i> degradation of chloroacetanilides .....	42
1.1. Materials and Methods.....	44
1.2. Results and discussion .....	46
2. Investigation of putative genes for chloroacetanilide biodegradation .....	51
2.1. Materials and methods .....	53
2.2. Results and discussion .....	57
3. T-RFLP on lab-scale wetland samples .....	61
3.1. Materials and methods .....	63
3.2. Results and discussion .....	66

Chapter III: Degradation of chloroacetanilide herbicides in lab-scale wetlands .....	69
Section 1. Using compound specific isotope analysis to assess the degradation of chloroacetanilide herbicides in lab-scale wetlands .....	70
Abstract .....	71
1. Introduction.....	72
2. Materials and Methods.....	73
2.1. Chemicals.....	73
2.2. Chloroacetanilide extraction from water samples and quantification.....	74
2.3. Carbon isotope analysis .....	74
2.4. Lab-scale wetlands characteristics and set-up .....	74
2.5. Pore water sampling.....	77
2.6. Hydrochemical analysis .....	77
2.7. Data analysis .....	77
2.8. Carbon isotope notation and calculation.....	78
3. Results and discussion .....	78
3.1. Transport and attenuation of chloroacetanilide herbicides .....	78
3.2. Chloroacetanilide carbon isotope fractionation .....	80
4. Conclusion .....	85
5. Acknowledgments.....	86
Appendix Chapter III - section 1 .....	86
Section 2. Degradation of chloroacetanilide herbicides and bacterial community composition in lab-scale wetlands .....	93
Abstract .....	94
1. Introduction.....	95
2. Material and methods.....	97
2.1. Chemicals.....	97
2.2. Lab-scale wetlands.....	97
2.3. Hydrogeochemical analysis .....	98
2.4. Quantification of chloroacetanilides and degradation products.....	98
2.5. Molecular analysis .....	99
2.6. Data analysis .....	100
3. Results.....	101
3.1. Biogeochemical evolution and chloroacetanilide dissipation.....	101
3.2. Detection of ESA and OXA degradation products in the wetlands.....	103
3.3. Enantiomer analysis of <i>rac</i> -metolachlor .....	103

3.4.	Composition of water bacterial communities .....	104
4.	Discussion .....	111
4.1.	Biogeochemical conditions and chloroacetanilide degradation.....	111
4.2.	Enantioselective degradation of metolachlor.....	112
4.3.	Putative degradation pathways of chloroacetanilides in the rhizosphere .....	112
4.4.	Influence of hydrogeochemical conditions and contamination on wetland bacterial populations .....	113
4.5.	Bacterial taxonomic structure in wetland water.....	114
5.	Conclusions.....	116
6.	Acknowledgements.....	116
7.	Appendix Chapter III- section 2 .....	117
Chapter IV: Bacterial communities in batch and continuous-flow wetlands treating <i>S</i> -metolachlor .....		128
Abstract.....		129
1.	Introduction.....	130
2.	Materials and methods .....	132
2.1.	Experimental design.....	132
2.2.	Sampling .....	134
2.3.	Hydrochemical and pesticide analysis .....	135
2.4.	DNA extraction.....	135
2.5.	T-RFLP analysis .....	136
2.6.	454 pyrosequencing .....	136
2.7.	Data analysis .....	136
3.	Results and discussion .....	137
3.1.	Biogeochemical evolution .....	137
3.2.	<i>S</i> -metolachlor dissipation.....	139
3.3.	T-RFLP analysis of hydraulic regime effects on bacterial communities.....	140
3.4.	Comparison of T-RFLP and 454 pyrosequencing approaches .....	143
3.5.	Bacterial composition of wetland water .....	144
3.6.	Bacterial composition of the wetland rhizosphere.....	147
3.7.	Towards identification of <i>S</i> -metolachlor degraders .....	148
4.	Acknowledgments.....	149
5.	Appendix Chapter IV .....	150

Chapter V: General discussion and perspectives .....	160
1. Monitoring pesticide degradation in wetlands .....	168
<b>Perspectives</b> .....	165
2. Following pesticide degradation in wetlands using CSIA .....	168
<b>Perspectives</b> .....	169
3. Bacterial composition and activity in chloroacetanilide-contaminated wetlands .....	172
<b>Perspectives</b> .....	174
References .....	177



# Table des matières

Chapitre I: Introduction.....	1
1. Les pesticides .....	2
1.1. Utilisation, impact sur la santé et l'environnement .....	2
1.2. Transport et dissipation dans l'environnement.....	4
2. Les herbicides chloroacétanilides .....	8
2.1. Caractéristiques et utilisation.....	8
2.2. Le devenir environnemental des chloroacétanilides .....	9
3. Evaluation de la (bio)dégradation des pesticides dans l'environnement.....	15
3.1. Hydrogéochimie.....	16
3.2. Analyse des produits de dégradation .....	17
3.3. Analyse énantiomérique.....	18
3.4. Analyse isotopique composé-spécifique.....	19
3.5. Microbiologie moléculaire.....	23
3.6. Analyse de données.....	26
4. Les zones humides .....	28
4.1. Biogéochimie et hydrologie des zones humides .....	29
4.2. Processus régissant les pesticides dans les zones humides.....	30
4.3. Impact des pesticides sur les communautés bactériennes des zones humides.....	33
5. Axes de recherche et objectifs du projet.....	35
5.1. La dégradation des chloroacétanilides dans les zones humides.....	35
5.2. Objectifs de la thèse .....	37
5.3. Plan du manuscrit de thèse.....	38
Chapitre II: Méthodologie.....	41
1. CSIA pour évaluer la dégradation des chloroacétanilides <i>in situ</i> .....	42
1.1. Matériels et méthodes .....	44
1.2. Résultats et discussion .....	46
2. Investigation des gènes potentiellement impliqués dans la dégradation des chloroacétanilides .....	51
2.1. Matériels et méthodes .....	53
2.2. Résultats et discussion .....	57
3. T-RFLP des échantillons des zones humides en colonnes.....	61
3.1. Matériels et méthodes .....	63
3.2. Résultats et discussion .....	66

Chapitre III: La dégradation de chloroacétanilides dans des zone humides en colonnes.....	69
Section 1. Utilisation de l'analyse isotopique composé-spécifique pour évaluer la dégradation des chloroacétanilides dans des zones humides en colonnes.....	70
Résumé.....	71
1. Introduction.....	72
2. Matériels et méthodes .....	73
2.1. Produits chimiques.....	73
2.2. Extraction et quantification de chloroacétanilides dans l'eau.....	74
2.3. Analyses isotopiques du carbone .....	74
2.4. Présentation et caractéristiques de ces zones humides .....	74
2.5. Echantillonnage.....	77
2.6. Analyses hydrochimiques .....	77
2.7. Analyses des données .....	77
2.8. Notations et calculs des isotopes de carbone .....	78
3. Résultats et discussion .....	78
3.1. Transport et dissipation des chloroacétanilides .....	78
3.2. Fractionnement isotopique du carbone .....	80
4. Conclusion .....	85
5. Remerciements.....	86
Annexe Chapitre III - section 1.....	86
Section 2. La dégradation des herbicides chloroacétanilides et la composition des communautés bactériennes dans des zones humides en colonnes .....	93
Résumé.....	94
1. Introduction.....	95
2. Matériels et méthodes .....	97
2.1. Produits chimiques.....	97
2.2. Les zones humides en colonnes .....	97
2.3. Analyses hydrogéochimiques .....	98
2.4. Quantification des chloroacétanilides et leurs produits de dégradation.....	98
2.5. Analyses moléculaires .....	99
2.6. Analyse de données.....	100
3. Résultats.....	101
3.1. Evolution biogéochimique et dissipation de chloroacétanilides.....	101
3.2. Détection d'ESA et OXA dans les zones humides .....	103

3.3.	Analyse énantiomérique du métolachlore racémique .....	103
3.4.	Composition des communautés bactériennes dans l'eau .....	104
4.	Discussion .....	111
4.1.	Conditions biogéochimiques et la dégradation des chloroacétanilides.....	111
4.2.	Dégradation énantio-sélective du métolachlore.....	112
4.3.	Voies de dégradation supposées des chloroacétanilides dans la rhizosphère .....	112
4.4.	Influence des conditions hydrogéochimiques et de la contamination sur les populations bactériennes des zones humides .....	113
4.5.	Composition taxonomique bactérienne dans l'eau des zones humides.....	114
5.	Conclusions.....	116
6.	Remerciements.....	116
7.	Annexe Chapitre III- section 2.....	117
Chapitre IV: Les communautés bactériennes dans des zones humides en flux discontinu et flux continu exposées au <i>S</i> -métolachlore.....		128
Résumé.....		129
1.	Introduction.....	130
2.	Matériels et méthodes .....	132
2.1.	Conception expérimentale .....	132
2.2.	Echantillonnage.....	134
2.3.	Hydrochimie et analyse de pesticides .....	135
2.4.	Extraction de l'ADN .....	135
2.5.	Génotypage par T-RFLP .....	136
2.6.	Pyroséquençage 454.....	136
2.7.	Analyse des données .....	136
3.	Résultats et discussion .....	137
3.1.	Evolution biogéochimique .....	137
3.2.	Dissipation du <i>S</i> -métolachlore .....	139
3.3.	Analyse T-RFLP de l'effet du régime hydraulique sur les communautés bactériennes des zones humides .....	140
3.4.	Comparaison de la T-RFLP et du pyroséquençage .....	143
3.5.	Composition bactérienne de l'eau des zones humides .....	144
3.6.	Composition bactérienne de la rhizosphère des zones humides .....	147
3.7.	Vers l'identification des populations bactériennes dégradant le <i>S</i> -métolachlore... 148	
4.	Remerciements.....	149
5.	Annexe Chapitre IV .....	150

Chapitre V: Discussion générale et perspectives .....	160
1. Suivi de la dégradation de pesticides dans les zones humides.....	168
Perspectives.....	165
2. CSIA pour évaluer la dégradation des pesticides dans les zones humides .....	168
Perspectives.....	169
3. Composition et activité des communautés bactériennes dans les zones humides contaminés par les chloroacétanilides.....	172
Perspectives.....	174
Références.....	177

## List of figures

Figure I-1. Processes driving the fate of pesticides in the environment. ....	5
Figure I-4: Chloroacetanilide herbicides and their degradation products.....	14
Figure I-5: Example Rayleigh plots of carbon and nitrogen isotope fractionation during the oxidation of nitrobenzene by <i>Comamonas sp.</i> strain JS765 .....	21
Figure I-6: Biogeochemical cycles of nitrogen, carbon and sulphur in wetlands.....	30
Figure I-7: Processes of pesticide removal in wetlands.....	31
Figure I-8: Graphical outline representing Chapters III and IV of this PhD thesis. ....	40
Figure II-1. The principle (A) and instrumentation (B) of compound-specific isotope analysis by gas chromatography combustion isotope ratio mass spectrometry.....	43
Figure II-3. Linearity tests for (A) metolachlor, (B) acetochlor and (C) alachlor.. ....	48
Figure II-4: Pathway of acetochlor degradation by <i>Sphingobium DC2</i> .....	52
Figure II-5: Main steps of the T-RFLP procedure .....	62
Figure II-6. Example T-RFLP electropherogram as visualised using PeakScanner software showing sample peaks (blue) and size marker peaks (red).....	66
Figure III-1. Picture (A) and schematic representation (B) of the vertical flow lab-scale wetlands .....	76
Figure III-2. Carbon isotope signatures of metolachlor, acetochlor and alachlor in lab-scale wetlands .....	82
Figure III-3. Relative concentrations ( $C_x/C_{in}$ = concentration at point (x) divided by inlet concentration) for metolachlor (triangles), alachlor (squares) and acetochlor (circles) and corresponding average oxygen concentrations at different depths in lab-scale wetlands .....	90
Figure III-4. Linearized Rayleigh plots for alachlor A) and acetochlor B). ....	92
Figure III-5. Concentrations of terminal electron acceptors (TEAs) oxygen (black circles), nitrate (grey triangles) and sulphate (white squares) in column wetlands.....	102
Figure III-6. Mean enantiomer fraction ( $\pm$ SD) of metolachlor along the flow path for the period between day 0 and day 112.....	104
Figure III-7. 2D-NMDS ordination of T-RFLP bacterial profiles (A) and a posteriori fitting of environmental parameters (B).....	106
Figure III-8. 2D-NMDS ordination of A) pyrosequencing (97% sequence identity) and B) corresponding T-RFLP bacterial community profiles of sequenced lab-scale wetland samples.. ..	108

Figure III-9. Relative abundance [%] of bacterial classes (defined at 80% sequence identity) in lab-scale wetland outlets on day 0 and day 70, and in the anoxic zone (at 45 cm from inlets) of wetlands contaminated with metolachlor (Met), acetochlor (Acet) and alachlor (Ala) on day 70.....	110
Figure III-10. Chromatogram of metolachlor diastereoisomers obtained with chiral GC-MS analysis.....	123
Figure III-11. Reddish-brown ferric iron oxide precipitates along <i>Phragmites australis</i> root periphery in a lab-scale wetland. ....	123
Figure III-12. Load removal of metolachlor, alachlor and acetochlor between two sampling campaigns from day 0 to day 112. ....	124
Figure III-13. 2D-NMDS ordination of T-RFLP bacterial community profiles.....	125
Figure III-14. Rarefaction curves for bacterial OTUs. ....	126
Figure IV-1. Schematic representation of (A) subsurface-flow constructed wetlands investigated in this study (B) hydraulic operation and contamination for the two wetlands.	133
Figure IV-2. Biogeochemical processes and metolachlor degradation in the two wetlands.	139
Figure IV-3. 2D-NMDS ordination of bacterial community profiles based on (A) T-RFLP and (B) pyrosequencing of the V1-V3 hypervariable region of the 16S rRNA gene in total DNA from wetland water and rhizosphere samples. ....	142
Figure IV-4. Relative abundance [%] of dominant bacterial classes (80% sequence identity threshold) in the wetland water samples on different sampling days (days 0, 35 and 56) and in the rhizosphere samples. ....	146
Figure IV-5. 2D-NMDS ordination of bacterial profiles based on T-RFLP of the 16S rRNA gene from wetland inlet, outlet and piezometer samples. ....	157
Figure IV-6. Rarefaction curves for bacterial sequences of the V1-V3 hypervariable region of the 16S rRNA gene with OTUs defined at 97% sequence identity.. ....	158
Figure V-1. Proposed approaches for improving assessments of chloroacetanilide-contaminated wetlands.....	162

## Liste de figures

Figure I-1. Processus régissant le devenir des pesticides dans l'environnement .....	5
Figure I-4: Les herbicides chloroacétanilides et leurs produits de dégradation.....	14
Figure I-5: Exemple de fractionnement isotopique du carbone et de l'azote au cours de l'oxydation du nitrobenzène par la souche <i>Comamonas</i> sp. JS765.....	21
Figure I-6: Cycles biogéochimiques de l'azote, du carbone et du soufre dans les zones humides .....	30
Figure I-7: Processus de l'élimination des pesticides dans les zones humides .....	31
Figure I-8: Aperçu graphique pour les chapitres III et IV du manuscrit de thèse. ....	40
Figure II-1. Principe (A) et instrumentation (B) de l'analyse isotopique composé-spécifique par chromatographie gazeuse – combustion-spectrométrie de masse de rapport isotopique ..	43
Figure II-3. Test de linearité pour (A) le métolachlore, (B) l'acétochlore et (C) l'alachlore..	48
Figure II-4: Voie de dégradation de l'acétochlore par <i>Sphingobium</i> sp. DC2.....	52
Figure II-5: Principales étapes de la T-RFLP .....	62
Figure II-6. Exemple d'électrophérogramme de T-RFLP visualisé à l'aide du logiciel PeakScanner.....	66
Figure III-1. Photographie (A) et représentation schématique (B) des zones humides en colonnes .....	76
Figure III-2. Signatures isotopiques du carbone du métolachlore, de l'acétochlore et de l'alachlore dans les zones humides en colonnes.....	82
Figure III-3. Concentrations relatives ( $C_x/C_{in}$ = concentration au point (x) divisée par la concentration d'entrée) pour le métolachlore (triangles), l'alachlore (carrés) et l'acétochlore (cercles) et les concentrations moyennes d'oxygène à différentes profondeurs dans les zones humides en colonnes .....	90
Figure III-4. Graphique de Rayleigh pour l'alachlore A) et l'acétochlore B).....	92
Figure III-5. Concentrations d'accepteurs terminaux d'électrons: oxygène (cercles noirs), nitrate (triangles gris) et sulfate (carrés blancs) dans les zones humides en colonnes..	102
Figure III-6. Fraction énantiomérique moyenne ( $\pm$ écart-type) du métolachlore entre les jours 0 et 112.....	104
Figure III-7. Représentation 2D-NMDS des profils bactériens T-RFLP (A) et des paramètres environnementaux (B). ....	106

Figure III-8. Représentation 2D-NMDS des profils bactériens basés sur A) le pyroséquençage (97% d'identité de séquence) et B) la T-RFLP des échantillons des zones humides en colonnes. ....	108
Figure III-9. L'abondance relative [%] des classes bactériennes (seuil d'identité de séquence = 80%) dans les sorties des zones humides en colonnes au jour 0 et au jour 70, ainsi que dans la zone anoxique (à 45 cm de l'entrée) des zones humides contaminées avec le métolachlore (Met), l'acétochlore (Acet) et l'alachlore (Ala) au jour 70 et au jour 110 .....	110
Figure III-10. Chromatogramme des diastéréoisomères du métolachlore obtenu en utilisant l'analyse GC-MS chirale.....	123
Figure III-11. Précipité brun rougeâtre de l'oxyde de fer(II) le long des racines de <i>Phragmites australis</i> dans une zone humide en colonne. ....	123
Figure III-12. Réduction de masse du métolachlore, de l'alachlore et de l'acétochlore entre deux campagnes d'échantillonnage entre le jour 0 et le jour 112. ....	124
Figure III-13. Représentation 2D-NMDS de profils T-RFLP de communautés bactériennes. ....	125
Figure III-14. Courbes de raréfaction des OTUs bactériennes .....	126
Figure IV-1. Représentation schématique des zones humides artificielles aux flux aquatique souterrain examinés dans cette étude. (A) fonctionnement hydraulique et (B) contamination pour les deux zones humides .....	133
Figure IV-2. Processus biogéochimiques et dégradation du métolachlore dans les deux zones humides.....	139
Figure IV-3. Représentation 2D-NMDS des profils de communautés bactériennes basés sur (A) la T-RFLP et (B) le pyroséquençage de la région hypervariable V1-V3 du gène ARNr 16S de l'eau des zones humides et des échantillons de la rhizosphère .....	142
Figure IV-4. . L'abondance relative [%] des classes bactériennes dominantes (seuil d'identité de séquence = 80%) dans les échantillons d'eau des zones humides pour les différents jours d'échantillonnage (jours 0, 35 et 56) et dans les échantillons de la rhizosphère.....	146
Figure IV-5. Représentation 2D-NMDS des profils bactériens basés sur T-RFLP du gène ARNr 16S à l'entrée des zones humides, à la sortie et aux échantillons des piézomètres.....	157
Figure IV-6. Courbes de raréfaction pour les séquences bactériennes des régions hypervariables V1-V3 du gène ARNr 16S avec les OTUs définis à un seuil d'identité de séquence de 97%. ....	158
Figure V-1. Approches proposées pour l'amélioration de l'évaluation des zones humides contaminées par les chloroacétanilides .....	162



# List of tables

Table I-3. Approaches of evaluation of pesticide degradation .....	16
Table II-2. Target functional genes and their corresponding primer pairs. ....	56
Table II-3. Detection of target functional genes in constructed wetland samples .....	60
Table II-4. Comparison of the two T-RFLP data treatment methods. ....	67
Table III-1. Bulk enrichment factors and AKIE values calculated for alachlor and acetochlor for sampling campaigns at days 42, 70 and 98 and for data from the three campaigns combined .....	84
Table III-2. Average values (mean $\pm$ standard deviation) for hydrochemical parameters of inlets and outlets of lab-scale wetlands from day 0 to day 98. ....	88
Table III-3. Average mass removal [%] of metolachlor, alachlor and acetochlor between inlets and outlets of lab-scale wetlands between day 28 and 98, and during the three periods of isotope investigation. ....	89
Table III-4. Mean and standard deviations of stable carbon isotope ( $\delta^{13}\text{C}$ ) triplicate measurements for two weeks old inlets (two weeks inlet), freshly spiked inlets (fresh inlet) and outlets at days 42, 70 and 98. ....	91
Table III-5. Physicochemical properties of the filling materials used for the lab-scale wetlands. ....	121
Table III-7. Diversity and richness indices calculated for lab-scale wetland water samples by T-RFLP and by 454 pyrosequencing (OTUs at 97% sequence identity) for days 0, 14, 70 and 98. ....	127
Table IV-1. Inlet water volumes and injected <i>S</i> -metolachlor concentrations and masses in both studied wetlands. ....	154
Table IV-2. Hydrochemical parameters of water samples from the inlet (tap water), outlet and piezometers of the continuous and the batch wetlands. ....	155
Table IV-3. Daughter ions and transition SRM used for GC-MS/MS quantification of <i>S</i> -metolachlor and LC-MS/MS quantification of its ionic degradation products ESA and OXA. ....	156
Table IV-4. Shannon diversity index $H'$ and number of OTUs calculated for wetland samples by T-RFLP (T-RFs) and by 454 pyrosequencing (97% sequence identity), and for rhizosphere samples. ....	159

# Liste des tableaux

Table I-3. Approches de l'évaluation de la dégradation des pesticides.....	16
Table II-2. Les gènes fonctionnels ciblés et leurs correspondants amorces. ....	56
Table II-3. Détection de gènes fonctionnels dans 60 échantillons de zones humides artificielles .....	60
Table II-4. Comparaison de deux méthodes de traitement des données T-RFLP .....	67
Table III-1. Facteurs d'enrichissement et valeurs AKIE calculés pour l'alachlore et l'acétochlore pour les campagnes d'échantillonnage à jour 42, 70 et 98 et pour les données combinées des trois campagnes .....	84
Table III-2. Les valeurs moyennes (moyenne $\pm$ écart-type) des paramètres hydrochimiques des entrées et sorties des zones humides à l'échelle du laboratoire du jour 0 au jour 98 .....	88
Table III-3. Réduction de masse moyenne [%] du métolachlore, de l'alachlore et de l'acétochlore entre les entrées et les sorties des zones humides en colonnes entre le jour 28 et 98, ainsi que pendant les trois périodes d'analyse des isotopes. ....	89
Table III-4. Moyennes et écarts-types des mesures isotopiques en triplicat du carbone stable ( $\delta^{13}\text{C}$ ) pour les entrées datant de deux semaines, les entrées fraîchement préparées et les sorties aux jours 42, 70 et 98.....	91
Table III-5. Des propriétés physico-chimiques des matériaux de remplissage utilisés pour les zones humides en colonnes.....	121
Table III-7. Indices de diversité et de richesse calculés pour les échantillons d'eau des zones humides en colonnes par T-RFLP et par pyroséquençage 454 (OTU à 97% d'identité de séquence) pour les jours 0, 14, 70 et 98.....	127
Table IV-1. Les volumes d'eau d'entrée, les concentrations et masses de <i>S</i> -métolachlore injectés dans les deux zones humides étudiées.....	154
Table IV-2. Paramètres hydrochimiques d'eau d'entrée (eau du robinet), de sortie et des piézomètres des zones humides en flux continu et en discontinu.....	155
Table IV-3. Ions fils et transition SRM utilisées pour la quantification GC-MS/MS du <i>S</i> - métolachlore et la quantification LC-MS/MS de produits de dégradation ionique ESA et OXA. .....	156
Table IV-4. Indices de diversité Shannon <i>H</i> et nombre d'OTUs pour les échantillons d'eau des zones humides et pour les échantillons de rhizosphère par T-RFLP (T-RFs) et par pyroséquençage 454 (identité de séquence de 97%).....	159



# Chapter I

## Introduction

This Chapter provides background information about the main subjects of interest of this PhD work, namely reactive transport of pesticides in wetland systems. First, the relevance of studying pesticide contamination and degradation in the environment, focusing on our target family: the chloroacetanilide herbicides, is reviewed. Then, methods for monitoring pesticide degradation in the environment are presented and the advantages and limitations of each tool are highlighted. The main biogeochemical characteristics and functioning of wetlands, our chosen ‘model’ ecosystems for studying pesticide (bio)degradation, are discussed. We then discuss wetland biogeochemical and pesticide degrading processes as well as the impact of pesticides on wetland bacterial communities. Finally, the focus and objectives of this PhD thesis are presented.

## 1. Pesticides

### 1.1. Use, ecological and human health impact

Since the introduction of the first synthetic organic pesticide DDT (dichlorodiphenyltrichloroethane) in the 1940s, pesticides have been increasingly used to increase agricultural crop yields. The number of pesticide molecules developed has been steadily rising along with the global pesticide production. Currently, there are more than 536 and 1,055 different registered pesticides molecules in the EU and the USA (Sierka, 2013; EU, 2014). An estimated 2.4 million tons of pesticide active ingredient is applied worldwide every year, 90% of which is applied on agricultural fields. Herbicides comprise the largest portion of the pesticides used (39%), followed by insecticides (18%), and fungicides (10%) (EPA, 2011). Due to this extensive worldwide use, pesticides became a major source of diffuse environmental pollution (Mostafalou and Abdollahi, 2013). Nine out of the twelve dangerous persistent organic pollutants of the initial list identified by the Stockholm Convention in 2004 were pesticides (Patterson et al., 2009). Numerous persistent pesticides were still detected in environment several years after the ban of their use. Organochlorine pesticides including p,p'-dichlorodiphenyltrichloroethane (DDT), hexachlorobenzene, endoslfan, and  $\beta$ -hexachlorocyclohexane could still be detected in soil, water, fish and even in human milk decades after the ban of their use (Kurt-Karakus et al., 2006; Darko et al., 2008; Mueller et al., 2008). Another example is atrazine that remained the most abundant pesticide in groundwater in Germany almost two decades after its ban (Jablonowski et al., 2011). A recent study revealed the extent of pesticide contamination of freshwater ecosystems in the EU by monitoring pesticide concentrations in 4,001 sites distributed in 91 European rivers. Pesticides exceeded the acute risk threshold for fish, invertebrates and algae in 81%, 87%, and 96% of the tested samples, respectively (Malaj et al., 2014). Pesticides were also found to be among the most relevant and important contaminants of ground water in Europe. The insecticide N,N-Diethyl-meta-toluamide (DEET) was detected in 84% of groundwater samples while other pesticides such as atrazine, diuron, simazine and isoproturon were detected in 20 to 56% of the samples (Loos et al., 2010). The above mentioned examples give a glimpse of the extent of the pesticide contamination in different environmental compartments.

The widespread pesticide contamination comes with consequences on the environment and human health. The landmark book "Silent Spring" by Rachel Carson (1962) was the first to

expose potential damage to the environment and human health caused by pesticides, and thereby drew public attention to the issue. Numerous scientific studies showed the detrimental impact of pesticide exposure on humans, and a wide diversity of flora and fauna (Dawson et al., 2010; Kohler and Triebkorn, 2013). For example, long-term pesticide exposure has been linked to increased incidence of prostate cancers by hindering DNA repair mechanisms in pesticide applicators and pesticide manufacturing workers (Barry et al., 2012). Another study reported the link between residential pesticide use and increased risk of melanoma cancers (Fortes et al., 2007). Similarly, higher serum levels of DDE (dichlorodiphenyldichloroethylene), a metabolite of the pesticide DDT, correlated with an increased risk for Alzheimer disease (Richardson et al., 2014) while an increased risk for Parkinson's disease among other neurodegenerative diseases was linked with chronic, non-occupational exposure to pesticides (Parron et al., 2011). Numerous pesticides have raised concerns due to their endocrine disruptive properties including: insecticides such as chlorpyrifos, chlordane, parathion, lindane, and malathion; herbicides such as diuron, proflaminate, thiazopyr, trifluralin; and fungicides such as vinclozolin, phenylphenol, and carbendazim (Murray et al., 2010). Pesticides were also associated with toxicity to aquatic organisms (Groner and Relyea, 2011), animals (Amaral et al., 2012), and plants (Andresen et al., 2012). Recently, the role of neonicotinoid insecticides in the decline of populations of pollinator bees has been demonstrated (Whitehorn et al., 2012), where imidacloprid-contaminated bumble bee colonies were found to be significantly smaller in size and produced less queens than non-contaminated colonies. Given their crucial role as pollinators, the decline of bee populations threatens crop production potentially on a global scale. In addition to their toxic effects on humans, animals, insects and aquatic organisms, pesticides also impact microorganisms in soil and water ecosystems (Imfeld and Vuilleumier, 2012), subsequently influencing nutrient and biogeochemical cycles (Kinney et al., 2005; Schafer et al., 2012). As a result of the numerous deleterious effects of pesticides on the environment and human health, the understanding of the behaviour and fate of pesticides in the environment has become a subject of main interest for the scientific community, reflecting the societal concerns.

## 1.2. Transport and attenuation in the environment

Pesticide contamination is mainly diffuse and caused by losses of intentionally applied pesticides in agricultural fields, but can also be caused by high-level point source pesticide release (e.g. accidental spills) (Vega et al., 2007). Most of the load of pesticides applied in agriculture reaches non-target compartments causing contamination of soil, water and air. During application, 1 to 75% of pesticides can be transported via drift to non-target areas (Lefrancq et al., 2013; Barbash, 2014). After application, 50 - 60% of the pesticides are typically transported to the atmosphere via volatilisation (Grégoire et al., 2009). The volatilised loads of pesticides can then contaminate soil and water bodies through water deposition (rainfall), or dry deposition (gaseous and solid particles precipitation). Once on the soil, a part of the pesticides can be attenuated by destructive processes which are mainly mediated by soil micro-organisms (Fenner et al., 2013). The non-degraded fraction of pesticides can, however, be mobilised by rain and transported through runoff to downstream water bodies, or leach through the soil until reaching groundwater ecosystems (Botta et al., 2012; Farlin et al., 2013). An estimated range of 1-10% of pesticide load applied is found in downstream surface water bodies that include streams, rivers and lakes in areas surrounding agricultural catchments (Schulz, 2004).

The contribution of the different routes of transport and degradation on the fate of pesticides in the environment depends on a number of extrinsic factor (e.g. climate conditions, agricultural landscape and practices, additives in pesticide formulations), and intrinsic factors specific to each pesticide molecule (e.g. volatility, hydrophobicity, solubility). For instance, highly volatile pesticides are mostly influenced by spray drift and volatilisation. Pesticides with relatively high organic carbon water coefficients ( $K_{oc} \geq 410$ ) have a strong tendency to sorb to organic material in soil and sediment and more likely to persist for long periods of time with low perspective of degradation (De Wilde et al., 2009), and are mainly transported by soil erosion or by transport on soil particles (Maillard et al., 2011). On the contrary, polar pesticides with higher water solubility are more likely to be transported via rainfall-runoff and leach to receptor water bodies. Their high bioavailability increases their risk to aquatic and soil organisms as well as their potential for biodegradation (Yu et al., 2006). Likewise, pesticide degradation products which are typically more polar than their precursors are thus more prone to mobilisation (Escher and Fenner, 2011). Their high mobility makes degradation products

relevant contaminants of surface and ground water (Huntscha et al., 2008). Pesticide degradation products are of particular relevance if they are formed in large amounts and/or are persistent, if they are more mobile than the parent compounds, and/or if they are highly toxic (Escher and Fenner, 2011). Unlike physical attenuation processes (e.g. sorption, volatilisation), degradation processes are the only true means of removal of pesticide contamination in the environment. Generally, microbial degradation is considered to be the dominant process of pesticide degradation (Fenner et al., 2013). Yet, abiotic degradation processes can also be of relevance under certain circumstances. For example, photodegradation contributed considerably to the degradation of several pesticides in surface prairie lakes water (Zeng and Arnold, 2013). Other ‘dark’ abiotic degradation processes occur at very low rates and therefore usually of little importance. However, this trend can be reversed under specific conditions, e.g. in environments with high pH (e.g. hydrolysis at  $\text{pH} \geq 8$  (Zhang et al., 2013b)), or in the presence of suitable catalysts (e.g. chloroacetanilide herbicides degradation in sulphidic environments (Zeng et al., 2011)). The interplay between the different transport and degradation processes determine the fate of pesticides in the environment and consequently the levels of exposure to pesticide contamination in downstream ecosystems (Rice et al., 2007).

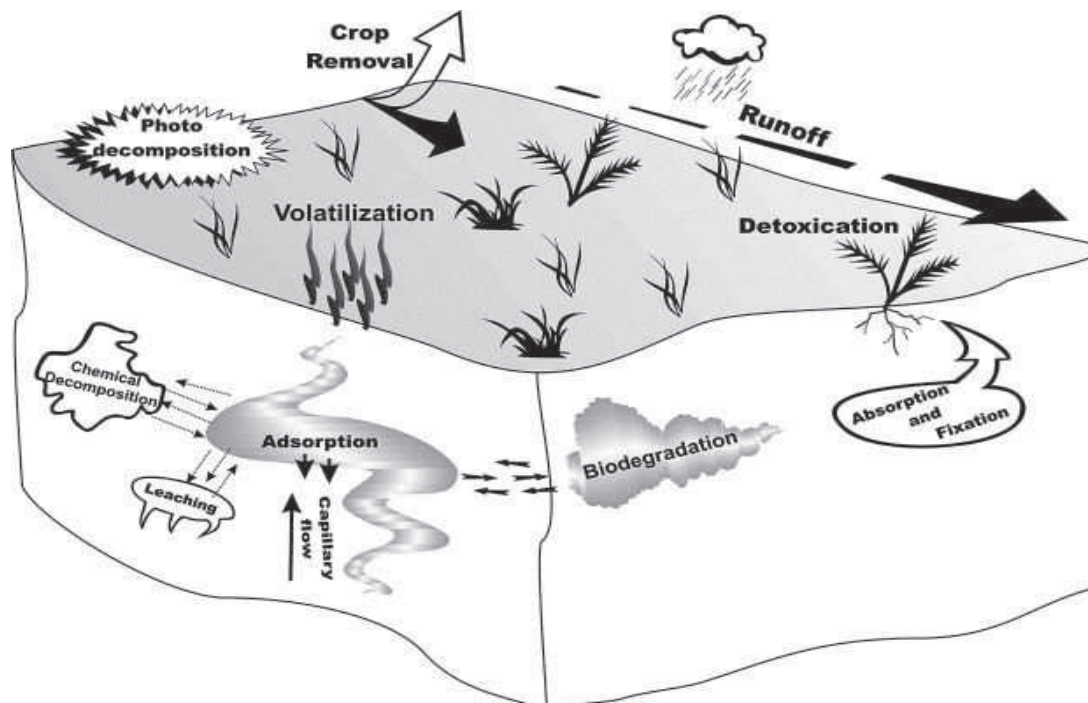


**Figure I-1. Processes driving the fate of pesticides in the environment** (Andreu and Picó, 2004).



Several factors add to the severity of the issue of pesticide contamination. One of these factors is the increasing proportion of chiral pesticides with the introduction of pesticides with more complex molecular structures. More than 30% of currently used pesticides are chiral compounds, including pyrethroids, organophosphate insecticides, imidazolinone and metolachlor (Liu et al., 2005). Chiral molecules contain at least one stereo-centre that is often an asymmetrically substituted carbon atom giving rise to two or more enantiomers which are non-superimposable mirror images of each other. Figure I-2 shows stereoisomers of the chiral pesticide metolachlor. Enantiomers of chiral pesticides have identical physicochemical properties (solubility, vapour pressures, and partition coefficients among air, water and octanol) and transport processes (advection, deposition, volatilisation, diffusion) and abiotic reactions (photolysis, hydrolysis) will not change enantiomer proportions (Bidleman et al., 2013). On the contrary, enantiomers may differ in their binding to stereo-sensitive biological receptors and naturally occurring chiral biomolecules because of their different molecular configurations (Hegeman and Laane, 2002).

Accordingly, enantiomers may exhibit different biological activities, toxicities, and degradation processes in organisms and the environment (Ye et al., 2010). In many of the chiral pesticides that are commercialised as racemates, only one of the enantiomers possesses the target activity (e.g. herbicidal) while the other enantiomer is present in the commercial formulation as a by-product of the pesticide synthesis process (Diao et al., 2010; Ye et al., 2013). Enantiomers of pesticides need therefore to be assessed separately for toxicity, and environmental fate. Likewise, additives (e.g. surfactants) are concomitantly released in the environment with pesticides and represent new potential contaminants with different environmental behaviour and toxicity, and therefore need to be taken into account for the approval of pesticide commercial formulations (Schenker et al., 2007; Oliver-Rodríguez et al., 2013). Pesticide degradation products are also increasingly being considered in pesticide risk assessments, in particular if they prove to be more toxic, more persistent or more mobile than their parent compounds (Escher and Fenner, 2011). Finally, the emerging nanopesticide technology present a new challenge for pesticide risk assessments (Kah and Hofmann, 2014). Nanopesticides refer to an emerging class of pesticides in which nanotechnology (e.g., use of materials that have a physical form with at least one size dimension in the range of 1–100 nm) is employed to enhance the efficacy or reduce the environmental footprint of a pesticide active

ingredient. For example, the encapsulation of pesticide active ingredient in nanocapsules for controlled release or targeted delivery of pesticide active ingredient. New risk assessment procedures will be needed to take into consideration the impact of the use of such nanoformulations on the activity and toxicity of known pesticide active ingredients (Kookana et al., 2014).

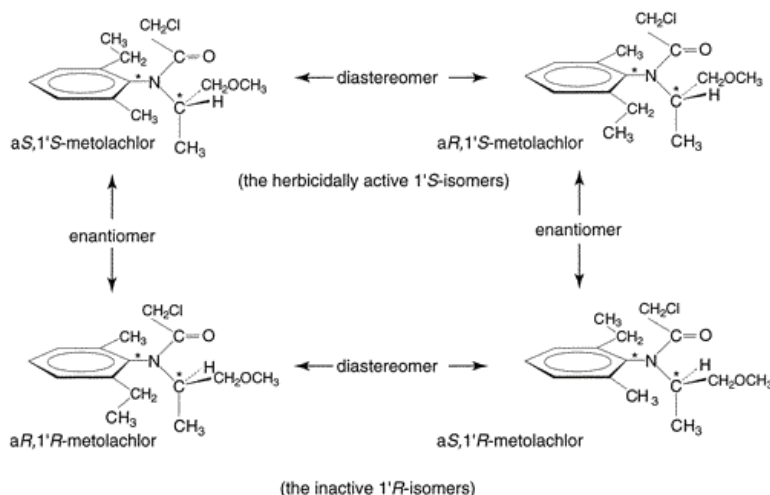


**Figure I-2. Stereoisomers of metolachlor. Chiral centres are denoted by asterisks. Also indicated are the diastereomeric and enantiomeric relationships between isomers.** (Muller et al., 2001).

In spite of decades-long use of pesticides, predictions of pesticide fate in the environment remain elusive. It is therefore important to understand the interplay of processes that control fate of pesticides in the environment; transport routes (e.g. *via* aerial deposition, erosion, runoff) phase transfer processes (e.g. sorption and volatilisation) and degradation processes. Pesticide degradation is of particular importance since it is the only process that effectively eliminates pesticide molecules from the environment. The type and rate of degradation processes of pesticides in a given environment is determined by intrinsic factors to the pesticide molecule (e.g. molecular structure, hydrophobicity) and environmental factors (e.g. redox, pH, temperature) (Knabel et al., 2012; Fenner et al., 2013b). Traditionally studies of pesticide degradation in the environment mainly depend on concentration analysis and mass balance approaches to demonstrate pesticide attenuation, but these approaches provide little information on *in situ* removal processes. Consequently, new approaches are needed to i) demonstrate the occurrence of *in situ* pesticide degradation, ii) identify conditions under which

degradation takes place, and iii) when possible, quantify the extent of degradation. Methods for assessing pesticide degradation in the environment are discussed in section 3. In the following section we focus on the properties and environmental fate the target family of herbicides of this PhD thesis work: chloroacetanilide herbicides.

## 2. Chloroacetanilide herbicides

### 2.1. Properties and use

Chloroacetanilide herbicides form a sub-group of amide herbicides. They share a chloroacetanilide core moiety and mainly differ in their alkoxyalkyl group attached to the nitrogen atom of the amide group, and the methyl or ethyl benzene ring substituents (Figure I-3). They are widely used to control annual grasses and broad-leaved weeds on a variety of crops including maize, sugar beet and sunflower (Zhang et al., 2011). Chloroacetanilides act by inhibiting the elongation of C16 and C18 to C20 fatty acids to very long chain fatty acids in susceptible weeds, leading to imbalance in fatty acid composition and thus to the weakening of cell membranes (Gotz and Boger, 2004). Chloroacetanilides include metolachlor, acetochlor, alachlor, propachlor and butachlor among others. Alachlor was widely used in the 1990s until the EU banned its use in 2006 due to concerns regarding elevated human exposure due to extensive ground water contamination and potential carcinogenicity (Heydens et al., 1999). Alachlor was largely replaced by acetochlor that was also banned in the EU in 2012. The ban came after evidence of the high human exposure of acetochlor and its metabolite *t*-norchloroacetochlor, and the high risk of acetochlor to aquatic organisms and birds (European food safety authority, 2011). Metolachlor is a chiral molecule containing two stereogenic centres; an asymmetrically substituted carbon and a chiral axis giving rise to four stereoisomers; two pairs of enantiomers and two pairs of diastereoisomers (Figure I-2). Metolachlor was first introduced in 1979 as a racemic mixture, containing equal ratios of the two enantiomers, which was later replaced in 1990s by a formulation enriched with the herbicidally active *S*-enantiomer (*S*-metolachlor) (Ma et al., 2006). *S*-metolachlor and acetochlor were the fourth and fifth most commonly used pesticides in the USA between 2001 and 2007 (EPA, 2011).

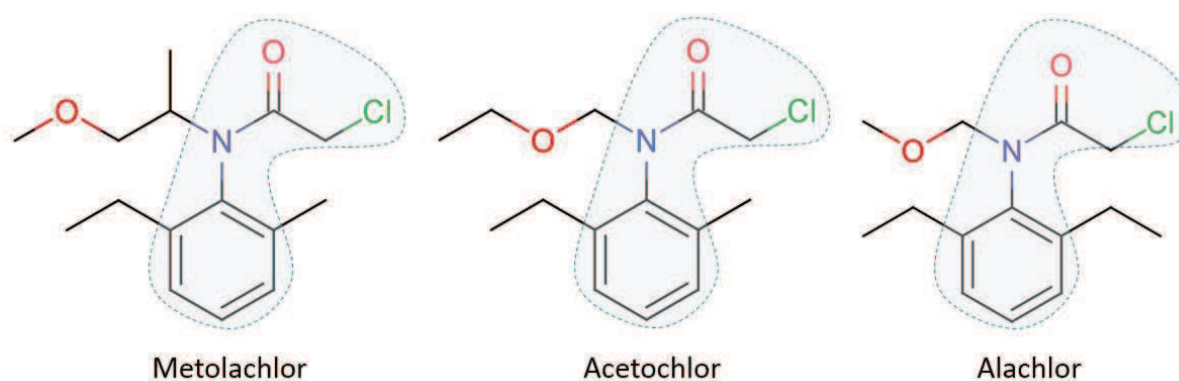


**Figure I-3. Molecular structure of the chloroacetanilide herbicides metolachlor, acetochlor and alachlor.** The chloroacetanilide common moiety is highlighted in pale blue.

*S*-metolachlor is currently the most widely used chloroacetanilide herbicide despite its higher persistence and recalcitrance to degradation in soil and water compared to other chloroacetanilides, as was demonstrated in several studies (Graham et al., 1999; Zhang et al., 2011a). In addition to differences in herbicidal activity, metolachlor enantiomers exhibit different toxicities towards earthworms (Xu et al., 2010), aquatic organisms (Liu and Xiong, 2009), and rice and maize roots (Liu et al., 2012a). Preferential degradation of the *S*-enantiomer was observed in soil and sludge (Muller et al., 2001; Ma et al., 2006), whereas another study reported the absence of enantioselective degradation of metolachlor in soil (Klein et al., 2006). The environmental conditions under which enantiomer-specific degradation of metolachlor occurs, the microbial populations, pathways and enzymes involved in this enantioselective degradation process remain unknown.

## 2.2. Environmental fate of chloroacetanilide herbicides

Chloroacetanilide herbicides are pre-emergence herbicides (i.e. applied before the development of a vegetal cover) to inhibit seed germination which, along with their relatively high water solubility, makes them prone to mobilisation by runoff and to contaminate aquatic ecosystems (Reid et al., 2000). Indeed, chloroacetanilides and their degradation products are frequently detected in ground and surface water which raises concerns about their environmental and human health impacts (Baran and Gourcy, 2013b; Postigo and Barcelo, 2014). Chloroacetanilides are characterised by low volatility (Henry constants  $> 10^{-3}$  Pa m<sup>3</sup>

mol<sup>-1</sup>), and stability to hydrolysis (half-life  $\geq$  100 days; Table I-1) (Carlson et al., 2006). Metolachlor and acetochlor are also relatively stable to photolysis, whereas alachlor is more photo-labile with a half-life of < 1 day. Therefore, photolysis may be a relevant dissipation pathway for alachlor in surface waters. The major dissipation route of chloroacetanilides in the environment is believed to be biodegradation. A number of bacterial strains that are able to aerobically degrade alachlor, acetochlor, or metolachlor have been characterised. Known aerobic chloroacetanilide degraders include members of *Streptomyces* (Sette et al., 2005a), *Bacillus* (Wang et al., 2008), *Pseudomonas* (Xu et al., 2006), *Paracoccus* (Zhang et al., 2011), *Rhodococcus* (Liu et al., 2012b) and *Sphingomonads* (Chen et al., 2014b) genera. Yet, anaerobic degraders of chloroacetanilides have not been identified, and the biodegradation pathways governing the fate of chloroacetanilide under different redox conditions remain poorly understood.

**Table I-1. Physicochemical properties of metolachlor, alachlor and acetochlor.** Source: Pesticide Properties DataBase online (<http://sitem.herts.ac.uk/aeru/projects/ppdb/index.htm>).

	<b>Metolachlor</b>	<b>Alachlor</b>	<b>Acetochlor</b>
<b>Molecular formula</b>	C <sub>15</sub> H <sub>22</sub> ClNO <sub>2</sub>	C <sub>14</sub> H <sub>20</sub> ClNO <sub>2</sub>	C <sub>14</sub> H <sub>20</sub> ClNO <sub>2</sub>
<b>Molar mass [g mol<sup>-1</sup>]</b>	283.8	269.8	269.8
<b><i>DT50</i><sub>photolysis</sub> [days]</b>	Stable	0.5	stable
<b><i>DT50</i><sub>hydrolysis</sub> [days]</b>	Stable	0.5	stable
<b><i>DT50</i><sub>soil</sub> [days]</b>	90	14	14
<b><i>K</i><sub>oc</sub> [mL g<sup>-1</sup>]</b>	200	124	156
<b>Log<i>K</i><sub>ow</sub></b>	3.4	3.1	4.1
<b><i>H</i><sub>cc</sub> 20 °C [dimensionless]</b>	4.13 × 10 <sup>-07</sup>	1.31 × 10 <sup>-06</sup>	8.64 × 10 <sup>-09</sup>

Table I-2 summarises the main degradation processes for the chloroacetanilide herbicides metolachlor, acetochlor and alachlor. Chloroacetanilide degradation products are the most frequently detected pesticide degradation products in ground water in France and Germany (Amalric et al., 2013; Reemtsma et al., 2013). The most frequently detected of these degradation products are the ionic ethane sulfonic acid (ESA) and oxanilic acid (OXA) degradates, which are found in surface and ground water samples at similar or higher concentrations than the parent molecules (Steele et al., 2008). For example, ESA and OXA

degradation products of metolachlor, acetochlor and alachlor were found at concentrations of 0.05 to 0.9  $\mu\text{g L}^{-1}$  which were up to 100 times higher than those of their parent compounds in drinking water samples (Hladik et al., 2008a). In a survey of herbicide concentrations in the Mississippi river basin, ESA and OXA degradates of metolachlor, acetochlor and alachlor were detected in 66 to 100% of the samples, compared to 31 and 60% for acetochlor and metolachlor (Rebich et al., 2004). The trend can also be seen in ground water samples; metolachlor ESA was found at average concentrations of  $(0.21 \pm 0.12 \mu\text{g L}^{-1})$  comparable to concentrations of *S*-metolachlor  $(0.25 \pm 0.32 \mu\text{g L}^{-1})$ , while metolachlor OXA was found at 10 times lower concentrations  $(0.05 \pm 0.04 \mu\text{g L}^{-1})$  in an alluvial aquifer (Baran and Gourcy, 2013b). ESA and OXA degradation products are thought to be mainly formed through biologically-mediated glutathione conjugation (Graham et al., 1999). However, the involved glutathione *S*-transferase (GST) enzyme and the genes coding it have not been identified in microorganisms. ESA degradation products were also found to be formed abiotically through chloroacetanilide dechlorination by reduced sulphur species in highly sulphidic environments (Cai et al., 2007; Bian et al., 2009). Both reactions involve a  $\text{S}_{\text{N}}2$  nucleophilic substitution mechanism, where the nucleophile is the reduced sulphur specie in the case of abiotic, and glutathione in the case of biologically-catalysed reactions. Nucleophilic substitution reactions of the chloride atom in the chloroacetanilide molecule also occur in the presence of polysulphides, resulting in the formation of mercaptoacetanilides (Zeng et al., 2011).

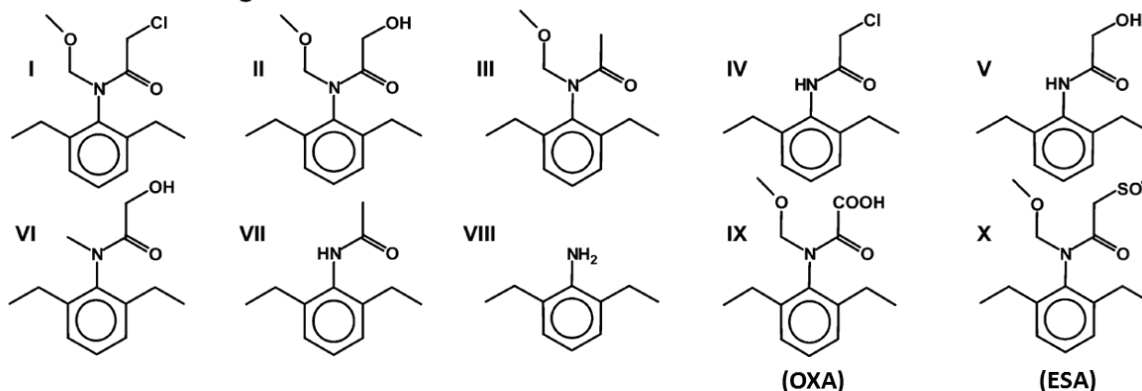
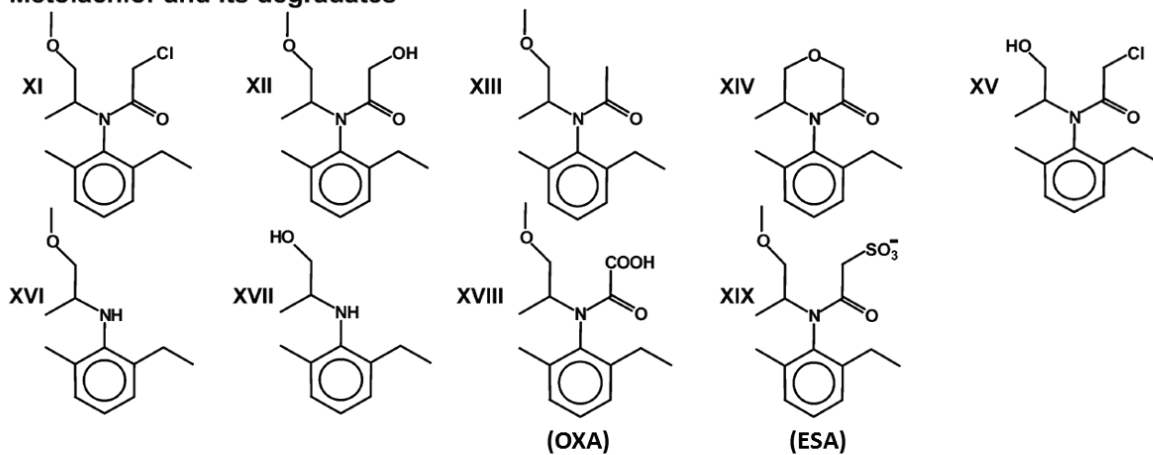
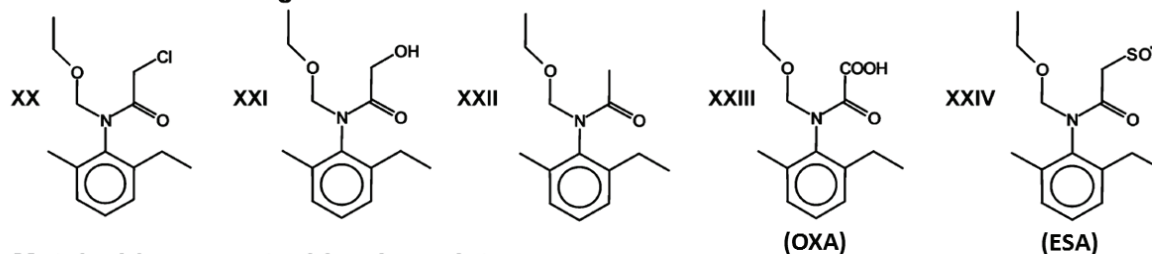
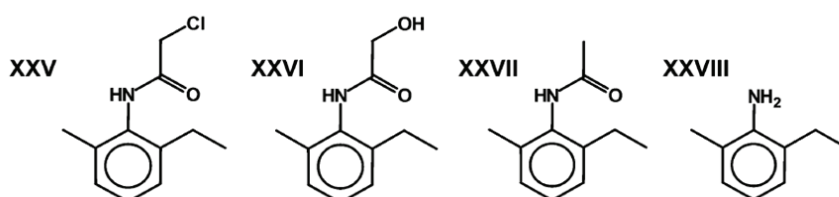
**Table I-2. Main biotic and abiotic degradation processes of chloroacetanilide herbicides.** Latin numbers in brackets indicate corresponding structures in Figure I-4.

	<b>Degradation process</b>	<b>Mechanism</b>	<b>Degradation products</b>	<b>Reference</b>
<b>Biotic</b>	Biologically catalysed (glutathione is nucleophile)	Nucleophilic substitution (S <sub>N</sub> 2)	Glutathione conjugates → ESA (X, XIX and XXIV) and OXA (IX, XVIII and XXIII)	(Aga et al., 1996; Rebich et al., 2004)
	Biologically catalysed	Oxidative N-dealkylation	N-dealkylated chloroacetanilide (IV and XXV) → 2,6-diethylaniline (VIII) or 2-methyl-6-ethylaniline (XXVIII)	(Chen et al., 2014b)
<b>Abiotic</b>	Bisulphite Bisulfide Thiosulphate	Nucleophilic substitution (S <sub>N</sub> 2)	Thiosulfate acetanilides → ESA (X, XIX and XXIV)	(Cai et al., 2007; Bian et al., 2009)
	Polysulphates	Nucleophilic substitution (S <sub>N</sub> 2)	Mercaptoacetanilides	(Zeng et al., 2011)
	Zero valent iron Dithonite	Reductive dechlorination (hydrogenolysis)	Non-chlorinated acetanilide (III, XIII and XXII)	(Eykholt and Davenport, 1998; Boparai et al., 2006)
	Acid/ Alkaline hydrolysis	Nucleophilic substitution (S <sub>N</sub> 2)	Hydroxy-substituted acetanilides (II, XII and XXI) N-dealkylated chloroacetanilide (IV and XXV)	(Carlson et al., 2006)

In addition to the ionic ESA and OXA, a large number of neutral degradation products of chloroacetanilides have been identified (Figure I-4) (Hladik et al., 2008b). Neutral chloroacetanilide degradates have been detected in surface and ground water, although in concentrations 10 - 20 × lower than those of the ionic ESA and OXA degradates (0.005 - 0.95  $\mu\text{g L}^{-1}$ ) (Hladik et al., 2008a; Amalric et al., 2013). However, the biogeochemical conditions and the pathways governing their formation in the environment are mostly unknown. An exception is the pathway involving N-dealkylation followed by hydrolysis of the amide bond of acetochlor in *Sphingobium quisquiliarum* cultures. The amide hydrolysis step was found to be catalysed by an amidase enzyme encoded by the *cmeH* gene (Li et al., 2013). Very recently, the hydrolase responsible for the first dealkylation step was also identified as CndA, a three component Rieske non-heme oxygenase encoded by the *cndA* gene (Chen et al., 2014b). The N-dealkylase catalysed the degradation of acetochlor and alachlor but not metolachlor. The rate of N-dealkylation reactions for tertiary amides including chloroacetanilides were found to be lower than biologically catalysed GST-dependant dechlorination in sludge-seeded bioreactors. The contribution of this pathway to chloroacetanilides dissipation is therefore expected to be low under conditions where faster reactions are possible (e.g. GST-dependant dechlorination) (Helbling et al., 2010). Indeed, the N-dealkylated products of metolachlor and/or acetochlor, and alachlor were among neutral degradates found in ground and surface water (Hladik et al., 2008b), in lower concentrations than ESA and OXA degradation products as discussed above.

Several challenges face our understanding of the degradation of chloroacetanilide herbicides in the environment. Given the numerous potential degradation pathways and degradation products mentioned above, the identification of the main relevant chloroacetanilide transformation processes, and the biogeochemical conditions under which they occur is not a straightforward task. Furthermore, although anaerobic degradation of chloroacetanilides was demonstrated in several studies (Graham et al., 2000; Seybold et al., 2001; Lauga et al., 2013a), the involved degradation pathways have not yet been explored. Also, concepts and approaches to evaluate qualitatively and quantitatively *in situ* assessments of chloroacetanilide degradation are essentially lacking.



**Alachlor and its degradates****Metolachlor and its degradates****Acetochlor and its degradates****Metolachlor or acetochlor degradates**

**Figure I-4: Chloroacetanilide herbicides and their degradation products** (Hladik et al., 2005). Structures I-X represent alachlor (I) and its degradation products, structures XI-XIX represent metolachlor (XI) and its degradation products, structures XX-XXIV represent acetochlor (XX) and its degradation products, structures XXV-XXVIII are degradation products that can result from either metolachlor or acetochlor degradation.

### 3. Evaluating pesticide (bio)degradation in the environment

Because of the ubiquity of pesticide pollution and its deleterious effects on biota, assessments of their environmental risks are essential. Risk assessments require a thorough understanding of the fate and degradation of pesticides in the environment (Rice et al., 2007). Comprehensive assessments of pesticide fate should provide evidence of the occurrence of attenuation processes, identify the main processes involved and the conditions under which they occur, and ideally quantify the extent of the degradation, and the share of different attenuation processes in overall pesticide dissipation (Penning et al., 2010). In this perspective, simple monitoring of pesticide concentrations or calculations of pesticide mass dissipation are insufficient. These approaches provide no distinction between destructive and non-destructive processes and give no indication of relevant/prevaling degradation processes. Instead, a combination of different chemical and biomolecular tools can be used to obtain complementary lines of evidence on pesticide *in situ* degradation. Approaches for assessment of pesticide degradation are listed in Table I-3.

Pesticide and degradation product analysis can demonstrate the occurrence of degradation and the prevailing degradation pathways (Baran and Gourcy, 2013b). More innovative methods such as compound specific isotope analysis (CSIA) and enantiomer analysis can indicate *in situ* degradation, but also help understanding of degradation mechanisms, and in some cases enable the quantification of degradation in field conditions (Maier et al., 2013). Meanwhile, hydrogeochemical analysis is useful to indicate the biogeochemical conditions under which a given degradation process takes place (Imfeld et al., 2008). Molecular tools (e.g. microcosm studies, functional gene assays) allow the identification of degrading microbial populations and enzymes, demonstrating the potential of *in situ* biodegradation (Li et al., 2013; Monard et al., 2013). Moreover, 16S rRNA gene based techniques in combination with data analysis tools (e.g. multivariate statistical analysis) can be used to evaluate the dynamics of bacterial composition in contaminated sites and its use in the identification of potential indicators to pesticide contamination (Imfeld and Vuilleumier, 2012).

**Table I-3. Approaches of evaluation of pesticide degradation**

Evidence based on	
Parent pesticide degradation	Quantitative chemical analysis of pesticide Compound-specific isotope analysis (label-free) Enantiomer analysis
Products	Chemical analysis of degradation products (target/non-target)
Degradation potential	Hydrogeochemical analysis to characterise pH, redox, TEAPs Demonstrating biodegradation in microcosms Functional gene analysis Detection of $^{13}\text{C}$ -labelled carbon in bacterial DNA from $^{13}\text{C}$ -labelled pesticide (DNA-stable isotope probing) Identification of known degrading bacterial populations

### 3.1. Hydrogeochemistry

The prevailing redox conditions and the availability of TEAs indicate the possibility of the occurrence certain degradation processes in a given system (Avila et al., 2013). For example, the determination of methanogenic conditions in granular sludge may favor the occurrence of reductive dechlorination of cyclodiene insecticides (Baczynski et al., 2004), since this reaction is not energetically possible under different redox conditions (e.g. under aerobic conditions). While hydrogeochemical analysis is mainly applied to decipher biodegradation processes, it can also be beneficial to demonstrate the capacity of the system to support certain abiotic degradative processes. An example is the abiotic dechlorination of chloroacetanilides by reduced sulphur species in prairie pothole porewater (Zeng et al., 2011). In the latter study, hydrochemical analysis was essential to demonstrate the occurrence of sulphate reduction and the presence of the required reduced sulphur species.

A limitation of hydrogeochemical monitoring is that it usually fails to take into account the heterogeneity of redox conditions possibly present in the study site (Bombach et al., 2010). This is especially true in redox dynamic systems such as wetlands, and is complicated by the existence of micro redox gradients in the wetland rhizosphere zone, and more generally heterogeneity of biogeochemical conditions. Thus, hydrochemical data should be carefully interpreted in parallel with data obtained using other approaches.

### 3.2. Degradation product analysis

Detection and quantification of degradation products is one of the most common methods for the assessment of pesticide degradation in the environment. This approach has the advantage of providing evidence of *in situ* degradation, and knowledge on the dominant degradation pathways (Padilla-Sanchez et al., 2012). Pesticide degradation products are also frequent ground water contaminants (see (Postigo and Barcelo, 2014) for a review on pesticide degradation products in ground water). Consequently, degradation products are increasingly being accounted for in pesticide risk assessments (European food safety authority, 2011).

On the other hand, the application of degradation product analysis in pesticide fate assessment faces several obstacles. Knowledge about degradation pathways is needed, which is not always the case in particular for complex pesticide molecules that may undergo various degradation pathways and form many different degradation products (Bombach et al., 2010). An additional challenge to this approach is the need for sensitive analytical tools for a large number of degradation products whose structures are mostly unknown. This analytical limitation can be addressed by coupling liquid chromatography LC or (ultra-) high performance liquid chromatography (U-) HPLC, with high accuracy and high resolution mass detectors such as (quadrupole) time of flight (Q)ToF and the recently developed Orbitrap®. These high-resolution mass spectrometry (HRMS) methods enable the analysis of a large numbers of degradation products for which analytical standards are not available (Reemtsma et al., 2013). The identification of pesticides transformation products has been carried out in most cases with time-of-flight (TOF) analysers in soil (Padilla-Sanchez et al., 2012), and in water (Pareja et al., 2012; Lopez et al., 2014), while studies using the Orbitrap® mass analyser are less common (Helbling et al., 2012). Additional bottlenecks in the analysis of degradation products in environmental samples include tedious extraction and sample pre-concentration methods.

Labour and time intensive sample pre-treatments are usually needed to reduce matrix contents that typically co-elute with the target analyte, and to enrich target compounds (Petrovic et al., 2010). Further improvements in extraction, pre-concentration methods and instrumentation are expected, encouraging wide-scope screening of pesticide degradation products in different environmental matrices (Petrovic et al., 2010; Hernandez et al., 2012).

### 3.3. Enantiomer analysis

Enantioselectivity plays an important role in the environmental fate and ecological risks of a chiral pesticide, as many biological processes are enantioselective. As a result, the enantiomeric composition may be changed by the preferential degradation of one of the enantiomers, and an enrichment of the other enantiomer in the non-degraded fraction of the parent pesticide molecules would indicate the occurrence of biodegradation (Celis et al., 2013). The chromatographic separation of a compound's enantiomers can be done using chiral stationary phase (chiral column) that can resolve the specific target enantiomers of interest (Eljarrat et al., 2008). The shifts in enantiomeric composition are usually represented using the enantiomeric excess (EE; Eq.(1)), or the enantiomeric fraction (EF; Eq.(2)) notations.

$$EE = \frac{S-R}{S+R} \quad (1)$$

$$EF = \frac{S}{S+R} \quad (2)$$

where  $S$  and  $R$  are the peak areas corresponding to the  $S$ - and  $R$ - enantiomers of the compound.

Enantiomer analysis of chiral pesticides has the advantage of providing an indication of the occurrence of *in situ* biodegradation that is independent of prior knowledge on degradation pathways, and of the detection of degradation products. The enantioselective degradation of pesticides can be redox dependant, implying the prevalence of different degrading microbial populations with different enantiomer preferences under different redox conditions (Kato et al., 2010). This has been demonstrated for phenoxy herbicides in a field study where enantiomeric shifts indicating preferential degradation of the  $S$ -enantiomer were observed at one site and preferential degradation of the  $R$ -enantiomer in another, which suggested the presence of different bacterial populations with different enantiomer preferences between the two sites

(Milosevic et al., 2013). This approach has been successfully applied to assess the biodegradation of metalaxyl (Celis et al., 2013) and organochlorine pesticides (Xue et al., 2014) in agricultural soil and marine sediment respectively. The preferential degradation of one enantiomer could also imply the possible persistence and accumulation of the non-degraded enantiomer under certain environmental conditions. This underscores the need for environmental fate assessments for each of the pesticide enantiomers under different biogeochemical conditions (Ye et al., 2010). The benefits of this method are however limited to chiral pesticides, and its use fails for chiral pesticides if microbial enzymes happen to degrade both enantiomers equally well, or if enzymes with preferences towards both *S*- and *R*-enantiomers are present concomitantly (Hegeman and Laane, 2002).

### 3.4. Compound-specific isotope analysis

#### 3.4.1. *CSIA basics*

Elements usually have a major common isotope and can have one or more additional stable isotopes. For example, 98.93% of carbon in nature is  $^{12}\text{C}$  while only 1.07% is  $^{13}\text{C}$ . Stable isotope ratios (*R*) are measured by mass spectrometry either in bulk samples by elemental analysis- isotope ratio mass spectrometry (EA-IRMS), or in specific compounds by gas chromatography- combustion- isotope ratio mass spectrometry (GC-C-IRMS) (Elsner et al., 2012). Stable isotope variations are usually reported in the delta ( $\delta$ ) notation, in parts per thousand (‰; per mil) relative to an international standard of known isotopic composition as shown for carbon stable isotopes  $^{12}\text{C}$  and  $^{13}\text{C}$  in the equation below (Eq. (3)):

$$\delta^{13}\text{C}_{\text{sample}} = \frac{(R_{\text{sample}} - R_{\text{standard}})}{R_{\text{standard}}} \quad (3)$$

where  $R_{\text{sample}}$  and  $R_{\text{standard}}$  are the ratios  $^{13}\text{C}/^{12}\text{C}$  of sample and standard. Hence, positive  $\delta$  values represent an enrichment in  $^{13}\text{C}$  in the sample relative to the standard, whereas negative values represent a depletion in  $^{13}\text{C}$ .

Heavier isotopes exhibit lesser vibrational frequencies than lighter isotopes of the same element, which translates to shorter bond lengths, stronger bonds and greater activation energies (Elsner et al., 2005). Transformation reactions differ in their reaction rate depending

on whether a heavy or light isotope of an element is present at the bond that is broken during the first irreversible transformation step (Elsner et al., 2005). This phenomenon is called the kinetic isotope effect (KIE). In general, lighter isotopes react faster than heavier isotopes of the same element leading to an enrichment of the heavy isotope in the remaining unreacted fraction of the compound (Hofstetter and Berg, 2011). This gives rise to a measurable fractionation factor ( $\alpha$ ) that is often expressed as the enrichment factor ( $\epsilon$ ) according to Eq.(4).

$$\epsilon = (\alpha - 1) \times 1000 [\text{‰}] \quad (4)$$

The Rayleigh equation (Eq.(5)) relates the isotope ratio of an element in a molecule (e.g.,  $\delta^{13}\text{C}$ ) at time point zero ( $\delta^{13}\text{C}_0$ ) and at time point t ( $\delta^{13}\text{C}_t$ ) to the corresponding concentration at time point zero ( $C_0$ ) and at time point t ( $C_t$ ) during degradation, via the kinetic isotope enrichment factor ( $\epsilon$ ) of the isotope pair and the degradation process.

$$\ln \left( \frac{\delta^{13}\text{C} + 1000}{\delta^{13}\text{C}_0 + 1000} \right) = \frac{\epsilon}{1000} \times \ln \frac{C}{C_0} \quad (5)$$

Using the Rayleigh equation (Eq.(5)), enrichment factors can be derived from laboratory studies for different compounds and transformation reactions. These enrichment factors relate changes in concentrations that occur during degradation to concomitant changes in isotope ratios of the target compound. The extent of *in situ* degradation may therefore be inferred from measured isotope ratios in field samples, provided that an appropriate enrichment factor is known.

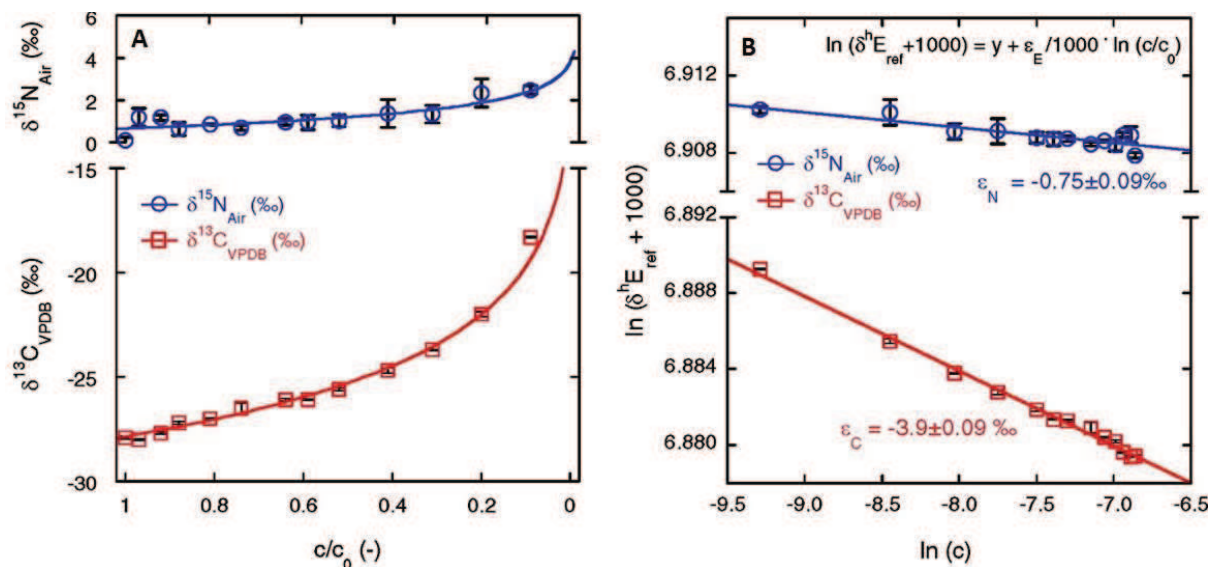


**Figure I-5: Example Rayleigh plots of carbon and nitrogen isotope fractionation during the oxidation of nitrobenzene by *Comamonas sp.* strain JS765.** (A) Measured  $\delta^{15}\text{N}$  and  $\delta^{13}\text{C}$  values of nitrobenzene at different stages of transformation ( $c/c_0$  is the fraction of remaining substrate) and calculated  $\delta^{15}\text{N}$  and  $\delta^{13}\text{C}$  enrichment of nitrobenzene. (B) Linearized  $\delta^{15}\text{N}$  and  $\delta^{13}\text{C}$  enrichment and bulk  $\delta^{15}\text{N}$  and  $\delta^{13}\text{C}$  enrichment factors ( $\epsilon_N$  and  $\epsilon_C$ ) of nitrobenzene (Hofstetter et al., 2008).

### 3.4.2. CSIA for assessments of pesticide degradation

CSIA can provide valuable insights on contaminant degradation directly in the field. For example, CSIA is typically used to i) indicate the occurrence of (bio)degradation, ii) identify the prevailing degradation pathways, and to iii) quantify the extent of (bio)degradation. CSIA has been widely applied to evaluate the environmental fate of various organic contaminants, mainly in groundwater, and most notably: chlorinated ethenes (Imfeld et al., 2008), petroleum hydrocarbons (Richnow et al., 2003), and alkanes (Bouchard et al., 2008). For reviews on CSIA of organic contaminants see (Elsner, 2010; Hofstetter and Berg, 2011; Elsner et al., 2012; Schmidt and Jochmann, 2012; Hatzinger et al., 2013). In contrast, the use of CSIA to trace the fate of emerging micropollutants (e.g. pesticides and pharmaceuticals) is still in its infancy (Spahr et al., 2013). CSIA methods have been developed for a handful of pesticides: lindane (Badea et al., 2009), isoproturon (Penning et al., 2010), atrazine (Meyer et al., 2008), 2,6-dichlorobenzamide (BAM), a metabolite of dichlobenil, (Reinnicke et al., 2012), phenoxy-acid herbicides (Maier et al., 2013), and organophosphorus herbicides (Wu et al., 2014). (Zhang et al., 2014) demonstrated the potential of CSIA to differentiate between photolysis, hydrolysis,



abiotic reductive dechlorination and bacterial reductive dechlorination of lindane. Likewise, CSIA could distinguish between abiotic hydrolysis and microbially-catalysed hydrolysis of isoproturon in laboratory experiments owing to differences in reaction mechanisms between biotic and abiotic hydrolysis (Penning et al., 2010). Still, the application of CSIA has rarely been reported in field assessments of pesticides (Milosevic et al., 2013), due to several limitations.

On the down side, several challenges face field applications of CSIA. Analytical challenges include the analysis of low-concentration contaminants in complex environmental matrices, analysis of polar pesticides which are non GC-amenable (Elsner et al., 2012). The analytical challenges are gradually being overcome by progress in the instrumentation and analysis methods, for example through the development of liquid chromatography-based CSIA methods (Gilevska et al., 2014). Another crucial factor in CSIA-based field assessments is the choice of enrichment factors (Thullner et al., 2012). Different enrichment factors are derived from laboratory studies and that are reaction- and in some cases microorganism-specific. Therefore, complementary methods such as degradation product analysis, and biogeochemical analysis are essential to give hints on prevailing degradation pathways and guide the choice of enrichment factors (Stelzer et al., 2009). Moreover, measured isotope fractionation in the field may be smaller than expected if other rate limiting steps (e.g. substrate uptake, transport or binding to enzyme) precede the first fractionating step (i.e. bond breaking by enzymatic catalysis). If the reverse step of the preceding process is slow, every substrate molecule that reaches the reactive site will be transformed, irrespective of its isotopic composition. The observed isotopic fractionation will therefore be smaller than expected, or “masked” (Penning et al., 2010). For example, toluene oxidation rates in suspension were found to be limited by the transport of toluene to the bacteria colonizing mineral particles and the isotope fractionation associated with the bond-cleavage was masked (Tobler et al., 2008). This “masking” effect can complicate the interpretation of the observed isotope fractionation in field samples since measured isotope fractionation may be much smaller than expected for a given mechanistic scenario (Thullner et al., 2012).

### 3.5. Molecular microbiology

Investigations of different aspects of microbial communities in pesticide-contaminated environments can demonstrate the intrinsic potential of *in situ* biodegradation and/or elucidate degradation pathways in laboratory experiments. Several culture-dependant and culture-independent tools are available for this purpose.

#### 3.5.1. *Microcosm studies*

Microcosms and bacterial cultures based on inocula from pesticide-contaminated environments can be set-up and used in laboratory experiments to demonstrate the potential of occurrence of biodegradation in the field. This can be done by simply monitoring the dissipation of the target pesticide (Konopka, 1994), or by integrating other methods for a more thorough understanding of pesticide degradation.

For instance, degrading communities can be isolated and identified, and TEAs involved in the anaerobic degradation of some pesticides can be identified. A pesticide can degrade optimally in the presence of a certain TEAs in anaerobic environments, and may be recalcitrant in their absence (Hägglom et al., 2000). Therefore, knowledge on TAEs coupled to pesticide degradation is important to predict the degradability of a pesticide under given redox conditions. For example, the herbicide dicamba was mineralised in methanogenic cultures, degraded (but not mineralised) in sulphate reducing cultures, and was recalcitrant in nitrate, and iron reducing cultures (Milligan and Hägglom, 1999). Degradation products can also be analysed to elucidate degradation pathways (Liu et al., 2012b). Understanding of abiotic degradation processes can also be improved using microcosm studies. For example, the abiotic dechlorination of the pesticide DDT by reduced sulphur species was demonstrated in sulphate reducing cultures of a *Clostridium sp.* strain isolated from paddy soils (Bao et al., 2012). This example illustrates microbially-mediated abiotic pesticide degradation, where categorical distinction between biotic and abiotic degradation becomes difficult (Fenner et al., 2013). Microcosm degradation studies can thus provide valuable detailed information of degradation processes, and the involved degrading microbial populations. However, these oversimplified systems fail to represent the complexity and heterogeneity of conditions present in the environment. In addition, they are limited to the cultivable fraction of environmental bacterial

diversity which represents < 1% of the total bacterial diversity (Bombach et al., 2010). Therefore, the application of microcosm-derived data to field assessments should be done with caution.

### 3.5.2. *Molecular techniques*

The on-going developments of biomolecular tools allow the exploration of links between contaminant degradation and the structure and functions of bacterial communities (Imfeld et al., 2009). Information about the genetic potential of biodegradation of the target pesticide in the field can be obtained using PCR-based detection and/or quantification of genes coding for key catabolic enzymes (i.e. functional gene analysis). A crucial prerequisite of functional gene analysis is the understanding of degradation pathways and the corresponding genetic basis. For example, the *atzD* gene encoding cyanuric acid hydrolase has been found to correlate with atrazine biodegradation in the surface layers of an agricultural soil, consistent with the knowledge that cyanuric acid hydrolase cleaves the s-triazine ring during bacterial atrazine metabolism (Monard et al., 2013). The application of functional gene analysis to other pesticides, in particular chloroacetanilides, is discussed in further detail in Chapter II.

Molecular techniques based on 16S rRNA gene analysis allow the investigation of previously known degrading bacterial populations either by DNA-based community fingerprinting or by sequencing methods. Bacterial 16S rRNA genes are used for phylogenetic identification of bacteria as they generally contain nine “hypervariable regions” that demonstrate considerable sequence diversity among different bacterial species and can be used for species identification (Mills et al., 2006). Hypervariable regions are flanked by conserved DNA sequence stretches, enabling PCR amplification of target 16S rRNA sequences from total bacterial populations using universal primers (Winsley et al., 2012).

DNA fingerprinting techniques (e.g. DGGE and T-RFLP) provide a specific pattern or profile of a given microbial community and can be used to reveal the dynamics of dominant bacterial phylotypes in response to different stressors (e.g. pesticide contamination). The advent of high throughput sequencing technologies reduced considerably the cost and time needed for analysis of large numbers of samples, in comparison to previous cloning and sequencing methods (Loman et al., 2012). High throughput sequencing techniques enabling parallel pyrosequencing

of a large number of samples in picoliter volumes (Ahmadian et al., 2006). Among high-throughput sequencing techniques, barcoded pyrosequencing (Roche 454) of 16S rRNA gene amplicons is widely applied for high-level resolution analysis of the diversity and composition of microbial communities in high-diversity environments (e.g. agricultural and wetland soils) (Kuramae et al., 2012; Serkebaeva et al., 2013). The 454 pyrosequencing technology is based on the "sequencing by synthesis" principle which involves using a single strand DNA as a template for sequencing and synthesising its complementary strand with enzymatic action, meanwhile detecting the release of pyrophosphate during the incorporation of each newly added nucleotide. Another popular high throughput sequencing technology is Illumina sequencing technology. Both methods have advantages and limitations. The Illumina platform produces more reads than 454 (up to 1.5 billion reads per run, compared with 1 million reads per run on a 454 plate of comparable cost), but produces fewer base pairs (bp) per read (75–150bp per read compared with 250–400bp per read on 454) (Werner et al., 2012). The shorter Illumina reads may reduce phylogenetic resolution, while the higher number of reads allow the identification of rare and novel taxa. (Ong et al., 2013). The availability of these high throughput techniques encourages the development of bacterial proxies for organic contaminant pollution, for instance by monitoring the changes of abundances of pollutant-sensitive taxonomic groups (dos Santos et al., 2011). In addition, the identification of degrading populations using sequencing techniques and comparison of their abundances can help identify preferential zones of pesticide biodegradation in heterogeneous ecosystems or 'degradation hotspots'. For instance, hotspots of toluene degradation were identified by correlating abundance of known toluene degraders and toluene concentrations over a redox gradient in a contaminated aquifer (Larentis et al., 2013).

However, ecologic functions can be dispersed between phylogenetically diverse groups (Wang and He, 2013), and linking the presence of specific phylogenetic group and a given function may therefore give false estimates of the metabolic potential of the system. Other tools can provide more accurate knowledge on a given metabolic capacity (e.g. target pesticide degradation) in the environment. The identification of pesticide-degraders *in situ* without prior knowledge on their identity can be achieved using stable isotope probing (SIP) (Cupples and Sims, 2007). The method involves the supply of stable isotope-labelled pesticide (e.g. C<sup>13</sup>-labelled pesticide) to a field sample (e.g. water or soil), and tracing the isotope label to

biomarker molecules such as DNA, RNA or proteins. This allows the cultivation-independent identification of bacterial populations that are actively assimilating the target pesticide. This technique allowed the identification of novel toluene degraders in various environments (e.g. agricultural soil, granular sludge and groundwater) (Martinez-Lavanchy et al., 2011), and was rarely used for identification of pesticide degraders (Uhlik et al., 2014).

### 3.6. Data analysis

Integrated approaches of environmental pesticide assessments combine the use of several of the tools discussed above over a space and/or time gradients. This can result in large data-sets that require further treatment to be accurately summarised and interpreted.

In this regard, multivariate analysis can be used to enable the exploration of links between pesticide degradation, hydrogeochemical parameters, and aspects of bacterial communities (e.g. abundance of different phylotypes) in a contaminated ecosystem. After appropriate treatment of data-sets (e.g. standardisation, transformation), they can be subjected either to exploratory (e.g. principal component analysis, PCA; correspondence analysis, CA; principal coordinate analysis, PCoA; and nonmetric multidimensional scaling, NMDS) or to interpretation analyses (e.g. indirect gradient analyses; redundancy analysis, RDA; canonical correspondence analysis, CCA; variation partitioning) (Ramette, 2007; Buttigieg and Ramette, 2014). Exploratory multivariate analyses can be done using species  $\times$  samples datasets and are used to reveal patterns (e.g. existence of clusters or groups of objects) in large data sets, but do not directly explain their occurrence. Output plots represent relationships between samples (e.g.(dis)similarities) and allow the recognition of patterns in datasets. For instance, NMDS analysis demonstrated the grouping or “clustering” of bacterial composition profiles according to their degree of exposure to organochlorine pesticides thus suggesting an impact of organochlorine pesticides on bacterial composition of the common reed *Phragmites australis* (San Miguel et al., 2014). PCA was used to demonstrate seasonal variations in hydrogeochemistry of a constructed wetland, which were in turn linked to seasonal differences in pesticide removal rates from the wetland (Maillard et al., 2011). Similarly, PCA indicated the importance of hydraulic residence time as a key parameter influencing herbicide dissipation in microcosms simulating storm water basins (Bois et al., 2013).

On the other hand, interpretative analyses combine information from different data-sets (e.g. bacterial phylotype abundance and hydrogeochemical parameters) to identify correlations between species patterns and environmental variables (Legendre and Fortin, 2010). For example, CCA was used to identify the correlation between long-term copper exposure (used as inorganic fungicide), and pH on bacterial community composition in agricultural soil (de Boer et al., 2012). In another study, PCA and RDA analyses indicated the correlation between bacterial community fatty acid profiles and the degradation of polychlorinated biphenyls under different redox conditions in rice paddy field soils (Chen et al., 2014a). It should be noted that while statistical analysis can be useful to indirectly infer relationships, for example links between prevailing redox conditions and degradation, it cannot be used to demonstrate cause and effect relationships.

Another useful approach to data interpretation is the use of reactive transport models to evaluate and predict pesticide transport and degradation in agroecosystems (Knabel et al., 2012). Reactive transport models can be helpful to interpret trends of pesticide concentration changes, pesticide mass balance and degradation products at complex field sites. Data from laboratory studies (e.g. degradation rates under different conditions, physicochemical properties like  $K_{ow}$ ) are used as input parameters in these models (Kidmose et al., 2010). Data from field studies on pesticide fate are used to validate the output of the model by showing that the model can reproduce reality (i.e. field data) with sufficient accuracy. Once validated, the model may be used to predict pesticide transport and degradation under different meteorological or hydrological conditions or agricultural contexts at significantly lower cost and time than field experiments require (Ghafoor et al., 2011). New pesticide reactive transport models are being developed to include data from new techniques, most notably CSIA to decipher processes of pesticide degradation at a large-scale (e.g. catchment scale) (Lutz et al., 2013).

The approaches discussed in the previous section can be used to assess qualitatively and quantitatively pesticide degradation processes and predict pesticide degradation potential in soil and/or water ecosystems such as wetlands. The interest of studying pesticide fate in wetlands is twofold. First, natural and artificial wetlands present in the vicinity of agricultural catchments receive pesticide contamination and act as buffer zones where pesticides are attenuated before reaching aquatic ecosystems. Consequently, an improved understanding of

pesticide transport and degradation in wetlands would allow the estimation of the exposure of downstream ecosystems such as rivers and streams to pesticide contamination. Second, constructed wetlands are increasingly being used for treatment of pesticide contamination. Knowledge on operational and environmental parameters, in particular biogeochemical parameters, governing pesticide attenuation would provide guidance for design and operation of constructed wetlands. The next section gives an overview of wetlands, focusing on biogeochemical cycling and pesticide attenuation processes occurring in wetlands. The impact of pesticides on wetland bacterial communities is also discussed.

#### **4. Wetland systems**

Wetlands are transitional ecosystems between terrestrial and aquatic ecosystems. They are characterised by the presence of soil that is permanently or periodically saturated with water, and plants that are adapted for life in saturated soil conditions. Wetlands currently represent 6% of the world's surface area (> 270 million hectares) (Junk et al., 2013). They are one of the most biologically active and productive ecosystems with a net primary productivity of 2,000 g C m<sup>-2</sup> yr<sup>-1</sup>. Different types of wetlands exist with different hydrological characteristics, water chemistry, vegetation, morphology and fauna, and include bogs, fens, swamps and marshes (Keddy, 2010). Wetlands provide many essential ecosystem services for human kind including floods control, groundwater replenishment, nutrient cycling, supporting wildlife, and improvement of water quality. In spite of their ecological importance, an estimated 30 - 90% of wetlands worldwide have been destroyed as a result of industrial land use (e.g. agriculture, forestry), urban expansion and climate change (Morissette et al., 2013). As awareness regarding their benefits increased, efforts of wetland restoration increased, and international treaties for wetland protection were adopted (Ramsar convention, 1971). Moreover, constructed wetlands were designed in order to mimic processes of nutrient and organic contaminant removal of natural wetlands to be used for water quality improvement (Vymazal, 2011a).

#### 4.1. Wetland biogeochemistry and hydrology

The main factors contributing to wetland nutrient cycling and contaminant removal functions are the interactions between soil, plants and water over space and time, resulting the heterogeneity of biogeochemical conditions present in wetlands. Biogeochemical conditions in wetlands are mainly driven by hydrology and metabolic activities of microorganisms (Sims et al., 2013). All wetlands are permanently or periodically saturated with water. Given that the rate of oxygen diffusion in water is significantly lower than in air, the inundation of wetland soil with water leads to decreased oxygen diffusion to sub-surface wetland soils (Zhou et al., 2002). Microorganisms consume available oxygen as a terminal electron acceptor (TEA) in respiration processes coupled to the break-down of organic carbon substrates (electron donor) and use the energy differential for growth and reproduction (Faulwetter et al., 2009). In the absence of oxygen, (e.g. in submerged wetland sediments) microorganisms reduce the TEA which yields the highest energy in the following order (from higher to lower redox) nitrate ( $\text{NO}_3^-$ ), ferric iron (Fe III), manganese (Mn IV), sulphate ( $\text{SO}_4^{2-}$ ) and organic carbon (Kirk, 2004). As a consequence, wetlands are characterised by steep redox gradients that sustain a variety of biogeochemical cycles (e.g. carbon, nitrogen and sulphur) and contaminant degradation processes (Pester et al., 2012; Avila et al., 2013). Several studies documented the impact of wetland hydrology on biogeochemical cycling in natural and constructed wetlands (Hefting et al., 2004; Burgin et al., 2011). Fewer studies focused on organic contaminant degradation, in particular pharmaceuticals, in constructed wetlands (Zhang et al., 2012; Avila et al., 2013). Knowledge on the influence of hydrological conditions on pesticide degradation in wetlands remains very scarce.



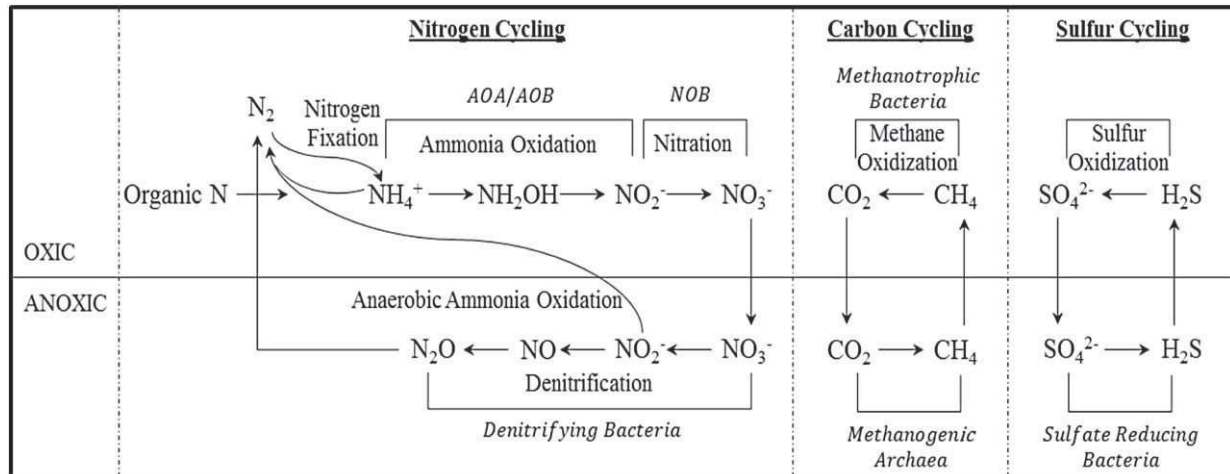


**Figure I-6: Biogeochemical cycles of nitrogen, carbon and sulphur in wetlands.** AOA: Ammonia-oxidising archaea, AOB: Ammonia oxidising bacteria, NOB: nitrite-oxidising bacteria (Sims et al., 2013).

Plants may also play an important role in wetland biogeochemical development through the release of oxygen by plant roots as a result of diffusive and/or convective gas transport processes from the atmosphere through the plant tissues into the root system (Laanbroek, 2010). This leads to the formation of a small oxidised layer around the root, creating a spatial redox gradient ranging from  $\approx +500$  mV close to the root surface to  $\approx -250$  mV at 1-20 mm from the root surface, which adds to the heterogeneity of redox conditions occurring in the wetlands (Faulwetter et al., 2009). The resulting redox gradient along with the abundance of carbon sources from plant exudates, sloughed-off root tissues, and mucilages make the rhizosphere zone a hotspot for microbial activity. Rhizosphere bacterial processes are essential in the cycling of nitrogen, sulphur iron and carbon (Neubauer et al., 2005). Enhanced degradation of organic contaminants in the rhizosphere zone has been repeatedly demonstrated for a variety of organic contaminants, including pesticides (Yu et al., 2003; Singh et al., 2004).

#### 4.2. Processes governing pesticides in wetlands

Pesticides can reach wetlands (natural or constructed) located downstream of agricultural catchments through contaminated runoff or through discharge of pesticide-contaminated ground water during flood periods (Kidmose et al., 2010; Tournebize et al., 2013). Constructed wetlands have proven to be efficient systems for treatment of pesticide-contaminated water

(Krone-Davis et al., 2013). The ability of wetlands to attenuate pesticide contamination is owing to the interplay of several physical, chemical, and biological processes governing the transport and degradation of pesticides in wetlands (Tournebize et al., 2013). Pesticide attenuation in wetlands can occur through destructive or non-destructive processes. Among non-destructive processes, sorption to wetland soil or plant material represents an important process of pesticide attenuation, in particular for hydrophobic pesticides (Budd et al., 2011; Passeport et al., 2011). Plant uptake can be a route of dissipation for pesticides in with octanol-water partition coefficient ( $\log K_{ow}$ ) between 1 and 3. Pesticides with lower  $\log K_{ow}$  values will hardly penetrate the lipid-containing root epidermis, whereas pesticides with  $\log K_{ow}$  values  $> 3$  will be increasingly retained by the lipids in the root epidermis and the organic matter surrounding the root (Verkleij et al., 2009). Volatilisation is of particular relevance in the case of (semi)volatile pesticides including some organochlorine and organophosphate pesticides, especially in dry, hot climates (Schneider et al., 2013). While non-destructive attenuation processes can decrease pesticide concentrations in contaminated water, they do not lead to mass depletion of pesticides from the environment, but rather to their transfer to different phases or compartments.

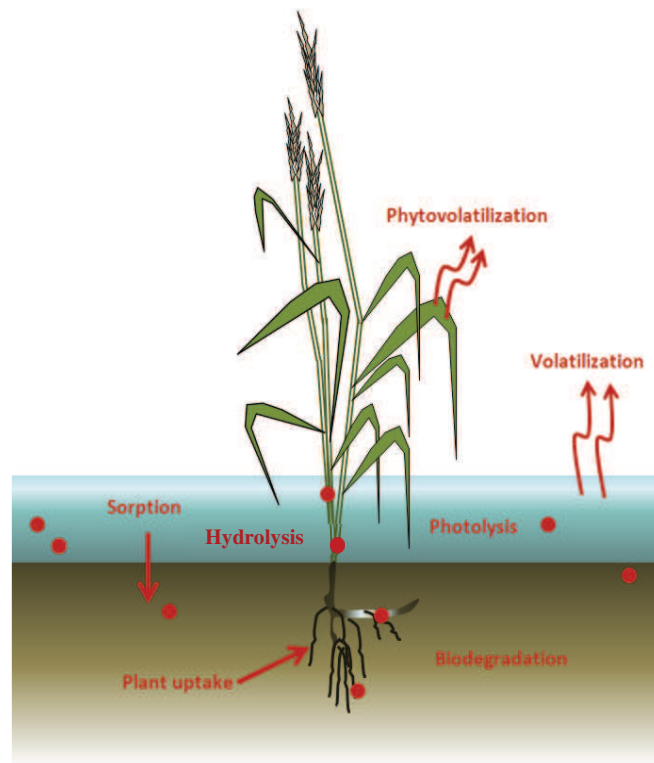


**Figure I-7: Processes of pesticide removal in wetlands** (Maillard, 2014)

Biotic and abiotic destructive degradation processes on the other hand leads to real removal of pesticides. Abiotic degradative processes in wetlands include photolysis and hydrolysis. Indirect photolysis of liable pesticides can occur in surface water of wetlands in the presence of suitable photosensitizers such as humic acids, as previously demonstrated for alachlor (Miller and Chin, 2005; Zeng and Arnold, 2013). Other chemical degradation processes may occur in wetlands. However to occur at relevant rates they require specific conditions (e.g. high or low pH), and the presence of suitable abiotic catalysts (e.g., sulphides) which are usually produced during microbial metabolic activities (e.g. sulphate reduction) (Fenner et al., 2013). Unlike inorganic contaminants (e.g. nitrate and metals) that are influenced by redox conditions, organic pollutants including pesticides are indirectly influenced by redox conditions during microbial degradation reactions that can be coupled to these redox reactions (Borch et al., 2010).

Bacterial degradation is recognised as a major removal process for pesticides in wetlands (Maillard and Imfeld, 2014). Pesticide degradation can be coupled with growth and proliferation leading to the conversion of pesticide molecules to non-toxic inorganic end products e.g. CO<sub>2</sub>, H<sub>2</sub>O and NH<sub>4</sub> (i.e. mineralisation) (Cederlund et al., 2007). Alternatively, co-metabolic degradation of pesticides can occur, during which the pesticide is transformed during the metabolism of another growth substrate (Luo et al., 2008). Cometabolism, occurs when a growth substrate induces microbes to produce enzymes that “fortuitously” degrade a non-growth substrate, even though the non-growth substrate does not provide energy to the microbe (Haws et al., 2006). Cometabolism is particularly important in the degradation of some otherwise recalcitrant contaminants, but is more likely to result in the formation of recalcitrant degradation products. However, in some cases two or more bacterial populations can work in concert to perform different steps of the pesticide degradation leading to its mineralisation. An example is the mineralisation of acetochlor in a mixed culture of two *Sphingobium* strains in which *S. quisquiliarum* performed the first step of degradation of acetochlor (N-dealkylation) while *S. baderi* metabolised the degradation product (Li et al., 2013). Due to the important role of microbial degradation in pesticide removal in wetlands and in the environment in general, the link between pesticide biodegradation and biogeochemical conditions is a subject of interest in pesticide research.

Biodegradation of pesticides in wetlands largely depends on the prevailing redox and TEAPs. Studies on the biodegradation of pesticides mainly focused on aerobic degradation, which is usually faster than anaerobic degradation (Zhang and Bennett, 2005; Faulwetter et al., 2009). Nonetheless, anaerobic conditions are prevalent in several ecosystems that frequently receive pesticide contamination including wetlands, soil, and aquifers. Anaerobic processes are involved in the degradation of a number of chlorinated pesticides including chloroacetanilides, atrazine, 2,4-D, and lindane (Zhang and Bennett, 2005). Anaerobic pesticide degradation has been observed under iron, sulphate and methane reducing conditions reduction (Kuhlmann and Kaczmarczyk, 1995). In addition, some pesticides can be used by the bacteria as TEAs during reductive dehalogenation processes (Adrian et al., 2007). The heterogeneity of redox conditions and TEAPs present in wetland systems give them unique ability to promote the biodegradation of a wide variety of pesticide molecules, which in turn makes wetlands interesting ecosystems for the study of pesticide biodegradation in the environment.

#### 4.3. Impact of pesticides on wetland bacterial communities

As discussed above, bacterial communities play a key role in wetland functions and in particular nutrient cycling and contaminant degradation. The structure and functions of bacterial communities in wetlands are impacted by environmental (e.g. soil pH) and operational parameters (e.g. water table fluctuations) (Ishida et al., 2006; Hartman et al., 2008; Ligi et al., 2013). Pesticides have been shown in a large number of studies to affect the composition and functions of bacterial communities (Lo, 2010). Mechanisms of pesticide toxicity in bacteria vary, depending on the type of pesticide and the microbial species exposed. For example, herbicides targeting inhibition of photosynthesis in plants are most toxic to phototrophic microorganisms, usually exhibiting toxicity by disrupting photosynthesis. Other mechanisms of pesticide toxicity in microbes include inhibition of respiration, biosynthetic reactions, cell growth and division (DeLorenzo et al., 2001).

The effects of transient pesticide exposure on bacterial communities can be temporary. Alternatively, long-term pesticide exposure more likely leads to the adaptation of bacterial communities by increase in abundance of tolerant communities, or through genetic modifications (e.g. horizontal gene transfer) (Springael and Top, 2004; Imfeld and Vuilleumier,

2012). Pesticide exposure can impact total bacterial community composition as evidenced by decreased soil bacterial diversity, which can be due to its toxicity and to the dominance of pesticide-tolerant and/or pesticide-degrading populations (Johnsen et al., 2001). However, the impacts of pesticide exposure on bacterial communities of wetlands that receive agricultural runoff are unexplored. This understanding is essential to assess if, and how does pesticide exposure impacts bacterial community composition, and ecological functions and services in natural and artificial wetlands. Consequently, this information help predicting the ability of natural wetlands to sustain its microbially-mediated functions after acute or chronic exposure to pesticide loads (Weber et al., 2011), and also to guide the optimisation of design and operation of constructed wetlands for pesticide treatment (Faulwetter et al., 2009).

In addition, because of their sensitivity and rapid response to environmental disturbance, bacteria can provide suitable proxies for the assessment of wetland biological integrity. Recently, interest in the development of bacterial bioindicators for wetland assessment has increased (Sims et al., 2013). For example, the normalised ratio of *Acidobacteria* to *Proteobacteria* has been proposed as a broad indicator of wetland trophic status (Hartman et al., 2008), while the ratio of ammonia-oxidising bacteria to ammonia-oxidising archaea has been proposed as an indicator of oligotrophic conditions (Sims et al., 2012). Yet, only a few studies suggested bacterial indicators of pesticide contamination in soil ecosystems (Yu et al., 2006), and none were proposed in wetlands.

Biomolecular tools such as DNA fingerprinting techniques and functional gene analysis have been widely used to study the link between pesticide exposure and microbial community structure in different environments. For example, T-RFLP revealed significant shifts in freshwater sediment bacterial structure after exposure to captan and glyphosate (Widenfalk et al., 2008). Similarly, the chloroacetanilide herbicide alachlor caused shifts in bacterial community structure as revealed by DGGE in anoxic slurries (Lauga et al., 2013). Functional gene analysis showed the increase of abundance of bacterial genes coding 2,4-D-degrading enzymes in soil bacteria as a response to exposure to 2,4-D (Gonod et al., 2006). Effects of pesticide exposure on soil biogeochemical cycles including the inhibition of nitrification/denitirfication processes were also reported (Kinney et al., 2005). Progress in high throughput sequencing techniques paved the way to the study of yet largely unknown bacterial diversity of redox dynamic environments such as wetlands. Several recent studies have used

high throughput sequencing to explore the bacterial diversity of a variety of constructed wetlands (Ligi et al., 2013; Menon et al., 2013; Zhong et al., 2014) and natural wetlands including acidic *Sphagnum*-dominated wetlands (Serkebaeva et al., 2013), peatlands (Lin et al., 2012), salt marshes (Bowen et al., 2011) and freshwater wetlands (Peralta et al., 2013). Yet, high throughput sequencing techniques have rarely been used to investigate the link between organic contaminant, in particular pesticides, and wetland microbial communities (Yergeau et al., 2012; San Miguel et al., 2014).

## 5. Research focus and objectives

### 5.1. Research focus: Degradation of chloroacetanilides in wetlands

One of the major challenges in pesticide studies is to predict their environmental fate aided by a thorough understanding of their transport and degradation under different environmental conditions. Wetlands located in the vicinity of agricultural catchments can act as buffer zones for the attenuation of pesticide pollution before it reaches downstream aquatic ecosystems. Detailed understanding of pesticide behaviour in wetlands can help predict the extent of contamination in downstream aquatic ecosystems (e.g. rivers and streams). Moreover, wetlands have the advantage of combining heterogeneous redox conditions and high microbial activity, they can thus accommodate a wide variety of contaminant degradation processes which makes them suitable systems for the study of the environmental fate of pesticides. Therefore, there is a need to decipher the processes of *in situ* degradation controlling the fate of widely used herbicides, such as chloroacetanilides in wetland systems. From a remediation perspective, knowledge on pesticide removal processes and the biogeochemical conditions under which they occur in wetlands can guide the optimisation of design and operation of treatment wetlands. Since hydrology is the main driver of wetland biogeochemistry, understanding the impact of hydrology on pesticide removal is also essential. Studies on pesticide attenuation in wetlands traditionally depended on inlet-outlet balances of pesticide loads, and rarely explored *in situ* degradation processes. Tools for *in situ* assessments of pesticide degradation are therefore needed.

Chloroacetanilide herbicides are of the most widely pesticides in the EU and the USA. The major dissipation route of chloroacetanilides in the environment is believed to be

biodegradation. However, the degradation pathways involved and the conditions under which each pathway is relevant are poorly understood. Their wide use, frequent detection as water contaminants, and the scarcity of knowledge regarding their degradation in redox-dynamic ecosystems make them interesting target compounds for this PhD work on pesticide degradation in wetlands.

Accordingly, in this PhD work we aim to address the following gaps of knowledge in order to improve our understanding of chloroacetanilide degradation in wetlands: i) the lack of tools for the assessment of *in situ* degradation of chloroacetanilides and ii) the scarcity of knowledge on impacts of wetland hydrology and biogeochemistry on chloroacetanilide degradation.

Given the essential role of wetland microbiome in wetland ecological functions, knowledge on their composition and its changes in response to hydrochemical parameters, operational parameters (in case of constructed wetlands), and pesticide disturbances is relevant to predict wetlands' ability to adapt to these disturbances. This highlights a third iii) gap of knowledge on the bacterial composition of pesticide-contaminated wetlands and environmental factors influencing it over space and time.

Field-scale studies provide information about the overall fate of pesticides, but due to their complexity, they are not well suited for detailed investigations of degradation processes and the associated bacterial populations. On the other hand, microcosm-scale studies, can provide detailed understanding of single degradation processes under given conditions, but fail to represent the heterogeneity and interactions present in the field (Caquet et al., 2000). Accordingly, experimental wetlands (i.e. small scale wetland set-ups constructed for experimental purpose) represent attractive systems for understanding of pesticide degradation processes. Experimental wetland set-ups provide the complexity of field conditions, while allowing better controls over environmental parameters (e.g. water balances and confounding contaminants) and therefore better interpretation of *in situ* degradation processes.

This PhD thesis attempts to address some of the gaps of knowledge discussed above by investigating the fate of chloroacetanilide herbicides in experimental wetland systems and by answering the following scientific questions:

- How to assess the *in situ* degradation of chloroacetanilide herbicides in wetland systems?

- What is the link between biogeochemical conditions, bacterial communities, and chloroacetanilide degradation in redox-dynamic ecosystems?
- What is the impact of wetland operational and/or environmental parameters on bacterial communities, and on chloroacetanilide degradation?

## 5.2. Research objectives

The overall aim of the PhD thesis is to assess the *in situ* degradation of chloroacetanilide herbicides and characterise the associated bacterial diversity in wetlands. The specific objectives were to:

- Develop and validate a carbon CSIA method for the assessment of chloroacetanilides *in situ* degradation in the environment;
- evaluate the *in situ* degradation of chloroacetanilides in wetlands and its link to biogeochemical conditions;
- follow bacterial communities in chloroacetanilide-contaminated wetlands using molecular tools (e.g. T-RFLP, pyrosequencing, and functional gene analysis);
- evaluate the impact of hydraulic conditions and herbicide exposure mode on wetland biogeochemistry, chloroacetanilide removal, and bacterial communities

We aimed to achieve these objectives by investigating the fate of chloroacetanilide herbicides and their impact on bacterial communities in two experimental wetland set-ups. Lab-scale wetlands were operated under controlled lab-conditions, and used to evaluate dissipation processes of metolachlor, acetochlor and alachlor at oxic/anoxic interfaces in wetlands and their link to water bacterial communities. In a second experiment, we took a step further towards complex field conditions by using larger, less controlled, outdoor wetlands receiving a commercial formulation of *S*-metolachlor (Mercantor®). Outdoor constructed wetlands were used to assess the impact of hydraulic operation of metolachlor-contaminated wetland on metolachlor removal and on wetland bacterial communities. We combined traditional (pesticide analysis, degradation product analysis) and advanced (CSIA and enantiomer analysis) tools to investigate the fate of chloroacetanilides in wetlands. In parallel, analysis of bacterial community composition (T-RFLP and pyrosequencing) were applied to assess their link to wetland hydrogeochemistry and chloroacetanilide exposure.



### 5.3. Thesis layout

This PhD includes 2 refereed publications (Chapter III: section 1 and Chapter IV) for which I am the primary author and 1 submitted publication (Chapter III: section 2) for which I am co-first author. Parts of the work done during this thesis concerning CSIA analysis of chloroacetanilides in constructed wetlands and an agricultural catchment was included in two other manuscripts in preparation (Lutz et al., 2014; Maillard, 2014), for which I am co-author but which are not a part of this thesis. The outline of the following chapters of the thesis is presented below and in Figure I-8.

Chapter II discusses the development, validation and/or testing of methods for the assessment of chloroacetanilide degradation and bacterial community dynamics and function in wetlands, namely CSIA, T-RFLP, and functional genes analysis.

Chapter III investigates the transport and degradation of the chloroacetanilide herbicides metolachlor, acetochlor and alachlor, and the associated bacterial community dynamics in lab-scale wetlands. In section 1, we aim to address the need for new tools for the *in situ* assessment of chloroacetanilide degradation in redox dynamic ecosystems. This is achieved by developing a CSIA method for the analysis of metolachlor, acetochlor and alachlor in wetland water, and applying the method to assess the *in situ* degradation of the three metolachlor, acetochlor and alachlor in vertical-flow lab-scale wetlands having oxic/anoxic interfaces. In section 2, we combine hydrogeochemical analysis, pesticide analysis, degradation product analysis, T-RFLP and pyrosequencing to study the putative degradation processes and on their link with the prevailing biogeochemical conditions, and the dominant bacterial populations in the lab-scale wetlands. In addition, enantiomer analysis is tested and evaluated as a tool for the assessment of the fate of the chiral chloroacetanilide metolachlor in the environment.

In Chapter III, the link between biogeochemical conditions and chloroacetanilide degradation was examined, and a combination of analytical methods were applied for *in situ* assessment of chloroacetanilide degradation. However the impact of wetland hydrology on chloroacetanilide removal and wetland bacterial communities was not explored. In Chapter IV, we investigate the effect of hydraulic operation on metolachlor removal and wetland bacterial communities, by comparing two identical constructed wetlands with different hydraulic operation (batch

versus continuous-flow) in terms of biogeochemical development (hydrogeochemical analysis), removal of *S*-metolachlor (pesticide mass balance and degradation product analysis), and bacterial community dynamics and composition (T-RFLP and pyrosequencing). In addition, the composition of the rhizosphere bacteria in the two wetlands and its putative role in *S*-metolachlor removal is highlighted. In this experiment, we focus on the metolachlor as it is currently the most widely applied chloroacetanilide and we move closer to field conditions by using experimental outdoor constructed wetlands, and the commercial formulation (Mercantor Gold ®).

Chapter V provides a synthetic summary and discussion of the main conclusions of this research, and suggested future studies regarding i) monitoring pesticide degradation in wetlands, ii) the potential of CSIA tools for pesticide assessments and iii) the composition and activity of bacterial communities in pesticide-contaminated wetlands.

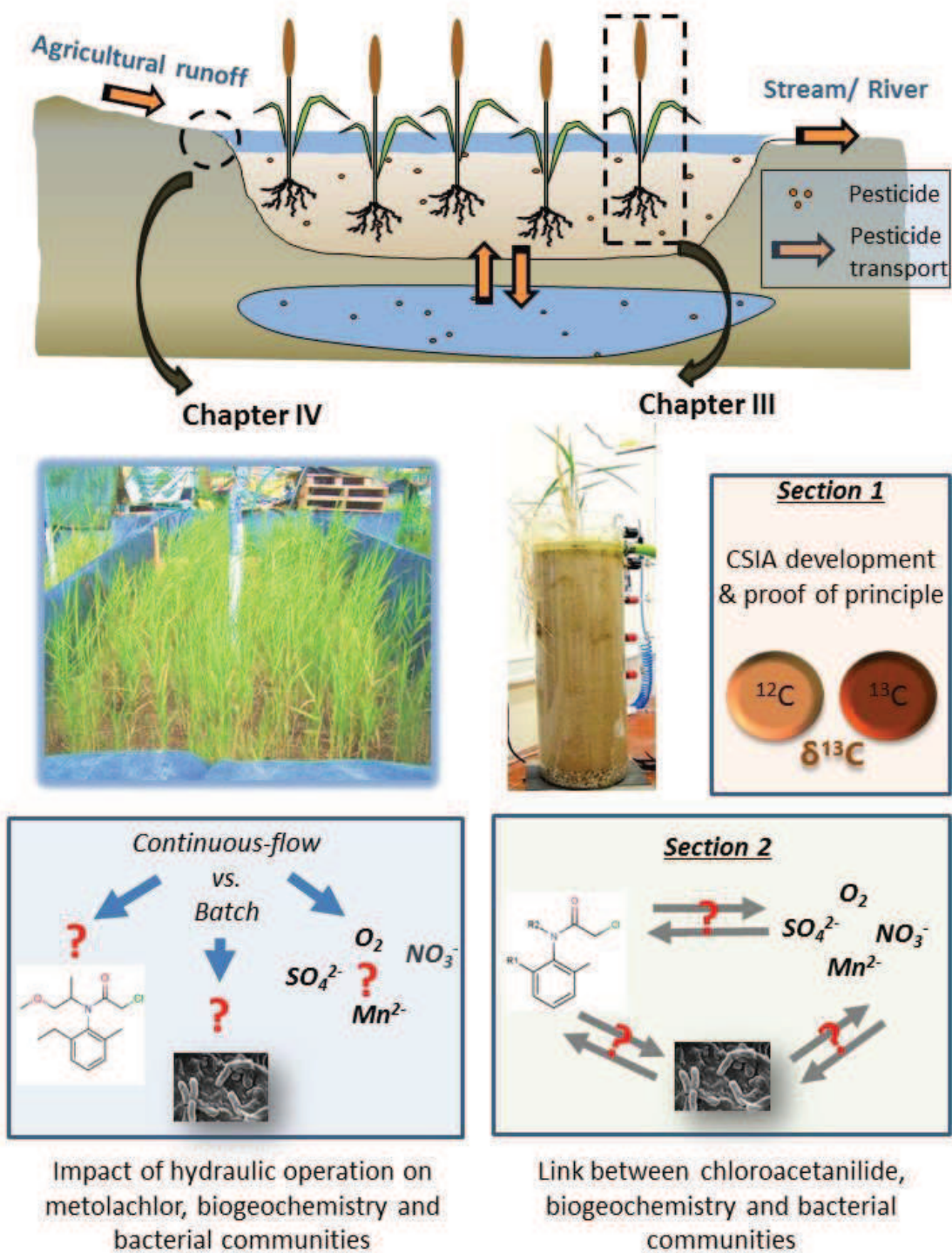


**Figure I-8: Graphical outline representing Chapters III and IV of this PhD thesis.**

Chapter III chloroacetanilides degradation and associated bacterial communities at oxic/anoxic interfaces in vertical-flow lab-scale wetlands. Chapter IV focuses on the impact of hydraulic regime of horizontal-flow constructed wetlands on wetland biogeochemistry, *S*-metolachlor degradation and bacterial communities.

# Chapter II

## Methodology

This chapter presents the development, validation and testing of a subset of the tools that were used in this PhD work to monitor the degradation of chloroacetanilides, and changes in bacterial community composition in two wetland experiments (Chapter III and Chapter IV). First, the development and validation of a CSIA method for the *in situ* assessments of chloroacetanilide degradation in wetland porewater is presented. Then, the development of functional genes assays to evaluate the catabolic potential of wetland bacterial communities to degrade chloroacetanilides *via* GST-mediated dechlorination and N-dealkylation is described. Finally, T-RFLP method is tested on wetland water to confirm its applicability to follow changes in the total bacterial populations in order to i) identify how changes in the composition bacterial communities may reflect changes in chloroacetanilide degradation and/or hydrogeochemical conditions, and ii) study the impact of chloroacetanilide exposure on wetland bacterial communities.

### 1. CSIA to assess *in situ* degradation of chloroacetanilides

Over the past 20 years, theoretical and analytical advances contributed to the growing application of CSIA environmental assessments of the sources and sinks of organic contaminants (McHugh et al., 2011; Braeckevelt et al., 2012). CSIA methods have been developed and applied for a number of organic contaminants, mainly mono-aromatic hydrocarbons (e.g. benzene, toluene, ethyl benzenes and xylene- BTEX) (Feisthauer et al., 2012), short-chained chlorinated hydrocarbons (e.g. chlorinated ethenes and vinyl chloride) (Imfeld et al., 2008), and fuel oxygenates (e.g. methyl *tert*-butyl ether-MTBE) (Rosell et al., 2012).

On the contrary, application of CSIA for emerging micropollutants, such as pesticides and pharmaceuticals, remains scarce. CSIA methods have been developed for a handful of pesticides (see Chapter I, section 3.4 for available methods), and have rarely been applied for the evaluation of pesticide degradation in environmental systems (Milosevic et al., 2013). A number of parameters contribute to this scarcity including i) the dilution of measured isotope effects due to the often larger molecular weight of micropollutants (relevant for carbon and hydrogen isotope analysis), ii) analytical difficulties caused by polar groups in some micropollutant molecules by reducing their volatility and thermal stability thus compromising their analysis by GC-IRMS, and iii) the numerous potential degradation pathways of complex micropollutant molecules, and the lack of corresponding reference enrichment factors limiting the interpretation of fractionation observed in field studies (Spahr et al., 2013; Elsayed et al., 2014b). Therefore, the development of novel CSIA methods for new classes of emerging micropollutants is a challenge that needs to be addressed in order to allow the benefits of CSIA in their environmental assessments.

The analysis of an element's isotope ratios in individual compounds (CSIA) can be achieved through coupling a gas chromatograph (GC) or liquid chromatograph (LC) to an isotope ratio mass spectrometer (IRMS) through a suitable conversion interface that could be a combustion oven (Figure II-1). During the analysis, the compounds are first separated in a gas chromatograph, then they are converted into a measurement gas that is different for every element (e.g. N<sub>2</sub> for nitrogen and H<sub>2</sub> for hydrogen). Conversion interfaces include combustion ovens and reduction reactors and are chosen based on the element to be analysed. In the case of carbon, compounds are converted into CO<sub>2</sub> in a combustion oven. The resulting CO<sub>2</sub> signals,

each corresponding to a separate compound, are introduced into the ion source, where they are ionized. The ionized  $\text{CO}_2$  molecules travel through a magnetic field where they are deflected with a different radius according to their mass/charge ratio and are collected in separate Faraday cups (Elsner et al., 2012). The isotope ratios are measured relative to a reference gas, and are expressed relative to an international standard using the delta ( $\delta$ ) notation in parts per thousand [‰]. The standard for stable carbon isotopes is the Vienna Pee Dee Belemnite (V-PDB) (Meckenstock et al., 2004).

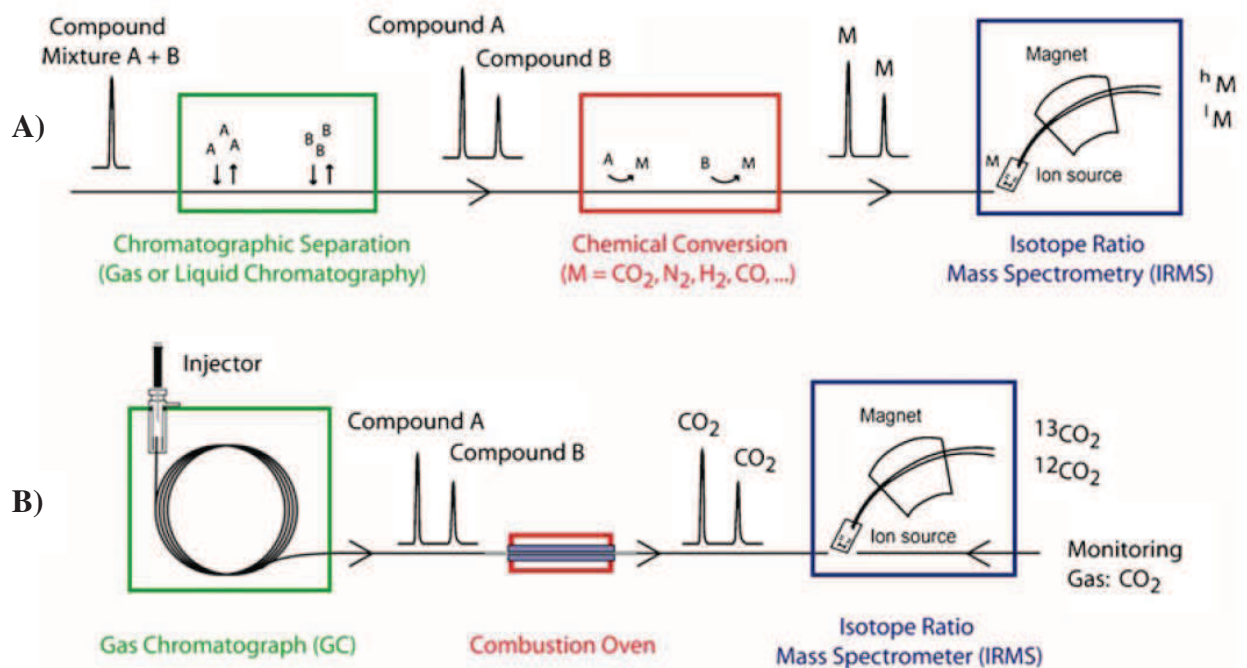


**Figure II-1. The principle (A) and instrumentation (B) of compound-specific isotope analysis by gas chromatography combustion isotope ratio mass spectrometry (GC-C-IRMS) (Elsner et al., 2012)**

Another technique for stable isotope measurements is Elemental analyzer IRMS (EA-IRMS). EA-IRMS is a bulk measurement technique, which provides representative data for the average isotopic signal of the entire sample. In contrast to GC-C-IRMS, EA-IRMS cannot determine  $\delta$  values of separate compounds in the sample and therefore is not used for CSIA measurements of environmental samples. However, EA-IRMS gives more accurate, and precise measurements than GC-C-IRMS. Values obtained by EA-IRMS for a given target compound

are therefore usually used as reference values to control the accuracy of GC-C-IRMS measurements (Hofstetter and Berg, 2011).

In this section, we describe the development and validation of a GC-C-IRMS CSIA method for the analysis of carbon isotope ratios of chloroacetanilide herbicides metolachlor, acetochlor and alachlor in water samples. The analytical methods were evaluated for possible isotope artefacts caused by different steps of the analysis procedure. Possible causes for isotope artefacts include sorption/desorption of the target analyte during solid phase extraction, evaporation during pre-concentration of analyte, incomplete conversion of the analyte in the combustion oven, poor chromatographic performance (e.g. lack of peak separation) and leaks of analyte during split/splitless injection (Blessing et al., 2008).

## 1.1. Materials and Methods

### 1.1.1. *Chemicals*

Physico-chemical properties of metolachlor, alachlor and acetochlor are listed in Table 1. Chloroacetanilides (metolachlor (racemic), alachlor, acetochlor; Pestanal®, analytical grade purity: 97.2, 96.8 and 99.2 respectively) and solvents (dichloromethane and ethyl acetate; HPLC grade purity > 99.9%) were purchased from Sigma-Aldrich (St. Louis, USA). Alachlor- $d_{13}$  and metolachlor- $d_6$  were obtained from Dr. Ehrenstorfer GmbH (Augsburg, Germany). Stock and standard solutions of chloroacetanilides were prepared in dichloromethane and were stored at -20 °C.

### 1.1.2. *Chloroacetanilide extraction from water samples and quantification*

The extraction procedure was adapted from USA EPA method 525.2 using an AutoTrace 280 solid phase extraction (SPE) system (Dionex®, CA, USA) for simultaneous extraction of 6 samples. Extraction cartridges were washed with 5 mL of ethyl acetate, followed by 5 mL of dichloromethane. The cartridges were then sequentially conditioned by 10 mL of methanol and 10 mL of deionised water. Cartridges were then loaded with the samples and dried under nitrogen flux for 10 min. Elution of chloroacetanilides was performed by 5 mL of ethyl acetate followed by 5 mL of dichloromethane. The extract was subsequently concentrated under

nitrogen flux to 1 droplet, and resuspended in dichloromethane for quantification and isotopic composition analyses.

Analysis of chloroacetanilide concentrations was performed by gas chromatography-tandem mass spectrometry (GC-MS/MS, Focus-ITQ 700, Thermo Scientific, Illkirch, France). A mixture of metolachlor- $d_6$  and alachlor- $d_{13}$  was spiked in each sample as internal standard at  $100 \mu\text{g L}^{-1}$ . Pulsed injection ( $3 \mu\text{L}$  at  $3 \text{ mL min}^{-1}$  for 1 min) was done using an AI/AS 3000 autosampler (Thermo Fisher Scientific, USA) in splitless mode. Separation of metolachlor, alachlor and acetochlor was performed using an Optima 5MS column ( $30 \text{ m} \times 0.25 \text{ mm ID}$ ,  $0.25 \text{ mm}$  film thickness; MN, Hoerdt, France), with helium as a carrier gas, at a flow of  $1 \text{ mL min}^{-1}$ . The column was initially held at  $50 \text{ }^\circ\text{C}$  for 2 min, heated at  $30 \text{ }^\circ\text{C min}^{-1}$  to  $150 \text{ }^\circ\text{C}$ , then up to  $250 \text{ }^\circ\text{C}$  at  $5 \text{ }^\circ\text{C min}^{-1}$  and finally heated at  $30 \text{ }^\circ\text{C min}^{-1}$  to  $300 \text{ }^\circ\text{C}$  and held for 5 min. Injector and transfer line temperatures were  $280 \text{ }^\circ\text{C}$  and  $300 \text{ }^\circ\text{C}$ , respectively. Each sample was measured in triplicate to evaluate the reproducibility of measurements. The limit of quantitation was  $10 \mu\text{g L}^{-1}$  with a mean precision of 8%.

### 1.1.3. Carbon isotope analysis of chloroacetanilides

The carbon isotope composition of alachlor, acetochlor and metolachlor was analysed using a GC-C-IRMS system consisting of a gas chromatograph (Agilent 6890) coupled *via* a GC/C III interface to isotope ratio mass spectrometer (Finnigan MAT 252, Thermo Fisher Scientific). The oxidation furnace of the GC/C III interface containing (Pt, Ni, CuO) was set to a temperature of  $980 \text{ }^\circ\text{C}$ . A BPX5 column ( $60 \text{ m} \times 0.32 \text{ mm}$ ,  $0.5 \mu\text{m}$  film thickness, SGE, Ringwood, Australia) was used for chromatographic separation, with helium as the carrier gas at a flow rate of  $2.0 \text{ mL min}^{-1}$ . The column was held at  $50 \text{ }^\circ\text{C}$  for 5 min, heated at a rate of  $20 \text{ }^\circ\text{C min}^{-1}$  to  $150 \text{ }^\circ\text{C}$ , then up to  $250 \text{ }^\circ\text{C}$  at  $5 \text{ }^\circ\text{C min}^{-1}$ , then heated at  $20 \text{ }^\circ\text{C min}^{-1}$  to  $300 \text{ }^\circ\text{C}$  and held for 1 min, and finally heated at  $20 \text{ }^\circ\text{C min}^{-1}$  to  $320 \text{ }^\circ\text{C}$ , where it was held for 5 min. Samples ( $4 \mu\text{L}$  volume) were injected into a split/splitless injector operated in splitless mode and held at  $280 \text{ }^\circ\text{C}$ . A chloroacetanilide standard with known isotopic composition was measured every nine injections to control the quality of the measurements. Reference carbon isotope composition values of standards of alachlor, acetochlor and metolachlor were obtained using an elemental analyser-isotopic ratio mass spectrometer (EA-IRMS, EuroVector, Milan, Italy)



coupled *via* a ConFlo III (open split, Thermo Fisher Scientific, Bremen, Germany) to a MAT 253 isotope ratio mass spectrometer (Thermo Fisher Scientific). The reproducibility of triplicate measurements was  $\leq 0.2\text{‰}$  ( $1\sigma$ ). The  $\delta^{13}\text{C}$  values were calibrated using a two-point calibration against the V-PDB standard.

## 1.2. Results and discussion

### 1.2.1. *Peak separation and optimisation of injection parameters*

Metolachlor retention time was 92 and 112 s longer than retention times of alachlor and acetochlor respectively (Figure II-2), which indicated the possibility of the concomitant measurement of carbon isotope value of metolachlor with either alachlor or acetochlor in the same chromatographic run. On the contrary, alachlor and acetochlor could not be measured in the same chromatographic run due to similar retention times (20 s difference), which hindered peak separation and led to erroneous  $\delta^{13}\text{C}$  values when the two compounds were present in the same sample.

Different injection parameters including split settings and injection volumes were tested to find the optimum injection configuration. Split setting is one of the parameters that could introduce bias in the measured  $\delta^{13}\text{C}$  values (Lollar et al., 2007). Thus, three different split settings were evaluated for their effect on the measured  $\delta^{13}\text{C}$  values: 1:3, 1:1 and splitless injection. The standards used for comparison of split settings were chosen to be in the expected linear range, with peak amplitudes between 1000 and 4000 mV. Standard deviations of  $\delta^{13}\text{C}$  values from different splits were  $\leq 0.1\text{‰}$  for the three chloroacetanilides, which indicates the absence of effects of the chosen split on the measurement of carbon stable isotope ratios. Accordingly, splitless injection was chosen for further analysis in order to maximize the obtained signal amplitudes. Using splitless injection, injection volumes of 2, 4 and 5  $\mu\text{L}$  were tested for their effect on the measured  $\delta^{13}\text{C}$  values. Results showed no effect of the tested injection volumes on the measured  $\delta^{13}\text{C}$  (standard deviations  $\leq 0.3\text{‰}$ ). Therefore, the three injection volumes could be used for further measurements.

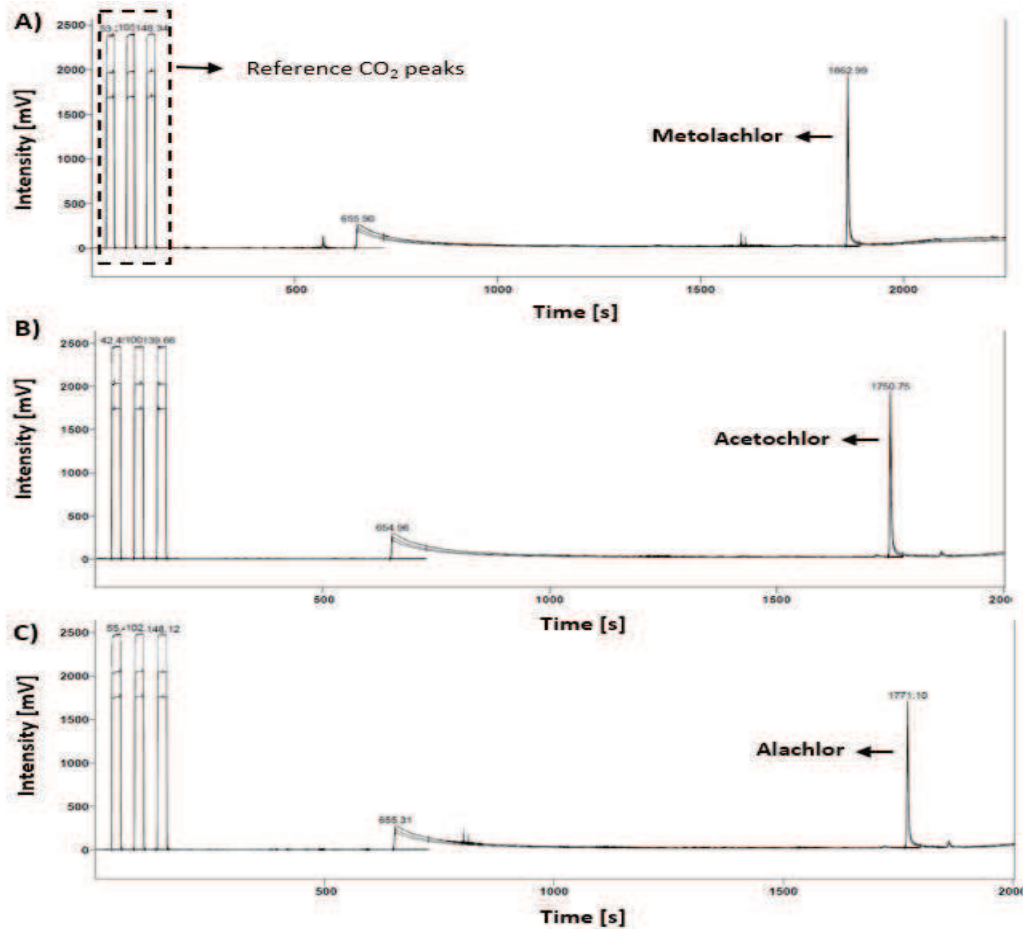


**Figure II-2. Example GC-C-IRMS chromatograms for A) metolachlor, B) acetochlor and C) alachlor**

### 1.2.2. Determination of the linear range

The range in which the measured  $\delta^{13}\text{C}$  values are independent of the amount of compound injected in the GC-C-IRMS, commonly referred to as the linear range, was determined for each of the compounds by monitoring the  $\delta^{13}\text{C}$  values for different amounts of compound injected. A series of standards were dissolved in DCM to concentrations of 2.8, 3.7, 27.8, 37.1 and 92.7  $\mu\text{M}$  for alachlor and acetochlor, and 3.5, 17.6, 26.4, 35.5 and 88.1  $\mu\text{M}$  for metolachlor (corresponding to 2 to 63 ng of carbon injected on column), and measured by GC-C-IRMS. The corresponding range of signal amplitudes was 120 to 7000 mV, 100 to 5600 mV and 150 to 8000 mV for metolachlor, alachlor and acetochlor, respectively. The tested signal range had an acceptable variance in isotopic values compared to the averaged isotopic composition. Despite a lower reproducibility for lower amplitude signals, the obtained values were always within 0.5‰ of the averaged  $\delta^{13}\text{C}$  value for the three compounds (Figure II-3). This indicates

the reliability of the  $\delta^{13}\text{C}$  values measured within the tested ranges of concentrations and signal intensities.

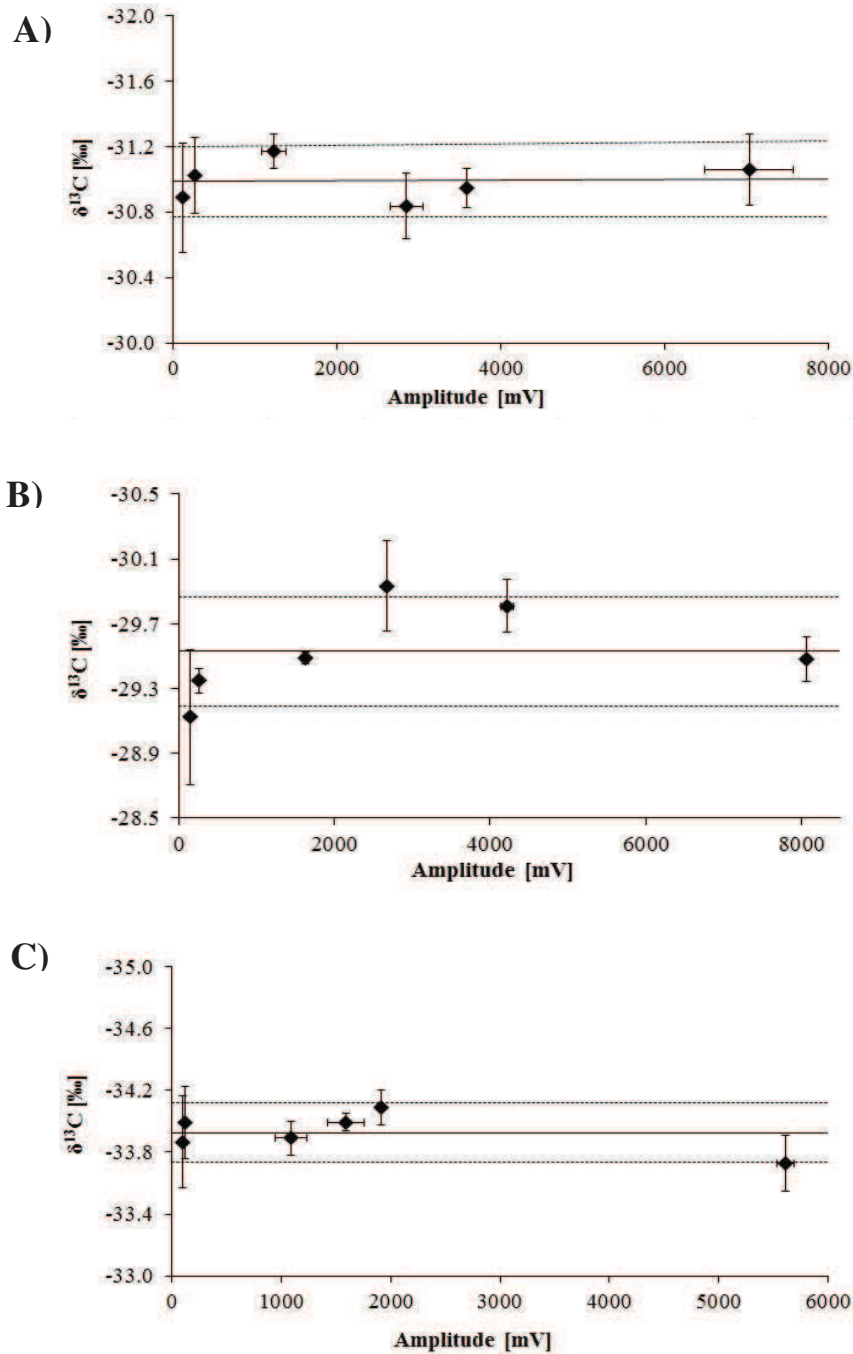


**Figure II-3. Linearity tests for (A) metolachlor, (B) acetochlor and (C) alachlor.** Signal amplitudes correspond to concentrations of 92.7, 37.1, 27.8, 3.7 and 2.8  $\mu\text{M}$  for alachlor and acetochlor, and 88.1, 35.2, 26.4, 17.6 and 3.5  $\mu\text{M}$  for metolachlor. Solid lines represent the means of all measurements; dotted lines represent one standard deviation ( $2\sigma$ ) of all measurements. Error bars represent one standard deviation ( $2\sigma$ ) of triplicate measurements.

### 1.2.3. Accuracy of GC-C-IRMS measurements of $\delta^{13}\text{C}$ values

The isotopic composition of the three compounds obtained by GC-C-IRMS and EA-IRMS were compared to assess the accuracy of the GC-C-IRMS method. GC-C-IRMS and EA-IRMS methods showed a good agreement indicating a good performance of the GC-IRMS method (Table II-1. Comparison between EA-IRMS and GC-C-IRMS  $\delta^{13}\text{C}$  [‰] (mean  $\pm$  standard deviation) values vs. VPDB for standards and GC-C-IRMS values for solid phase extracted standards.). The shift in  $\delta^{13}\text{C}$  values GC-C-IRMS and EA-IRMS was  $\leq 0.3 \pm 0.3\text{‰}$  for alachlor and acetochlor and  $0.8 \pm 0.2\text{‰}$  for metolachlor, which was considered to be acceptable given the high reproducibility of the results obtained.

### 1.2.4. Effect of SPE procedure on measured $\delta^{13}\text{C}$ values

Sample extraction and preparation methods could lead to a significant fractionation of stable isotope in the target compound and in turn introduce bias in the measured  $\delta^{13}\text{C}$  values (Ivdrá et al., 2014). For example, small but significant isotope fractionation could occur during sorption/desorption from solid phase extraction columns or during evaporation of the analyte during pre-concentration (Blessing et al., 2008). Therefore, the effect of SPE procedure on measured  $\delta^{13}\text{C}$  values was evaluated. For this purpose, standards of each of metolachlor, alachlor and acetochlor were spiked into wetland water (i.e. water supplied to the lab-scale wetlands, see Chapter III for details) to give concentrations in the range of 0.9 to 18.5  $\mu\text{M}$ . The prepared spiked water was extracted using the SPE procedure described above. Difference between average  $\delta^{13}\text{C}$  values measured for standards extracted from wetland water and averages of non-extracted standards were  $\leq 0.6 \pm 0.2\text{‰}$  ( $n = 9$ ) (Table 2-1). This indicates the absence of significant fractionation effects for the SPE method used in this study, and thus the suitability of the method for CSIA of chloroacetanilides in wetland water samples.

In conclusion, a novel method for the CSIA analysis of chloroacetanilides in water samples was successfully developed and validated on wetland water samples. This method was later used to assess the *in situ* degradation of chloroacetanilides in lab-scale wetlands (Chapter III), of *S*-metolachlor in constructed outdoors wetlands (Maillard, 2014), and in an agricultural catchment (Lutz et al., 2014).

**Table II-1. Comparison between EA-IRMS and GC-C-IRMS  $\delta^{13}\text{C}$  [‰] (mean  $\pm$  standard deviation) values vs. VPDB for standards and GC-C-IRMS values for solid phase extracted standards.**

Compound	$\delta^{13}\text{C}$ [‰]			$\Delta\delta^{13}\text{C}$ [‰]	
	EA-IRMS (n = 3)	GC-C-IRMS (n = 15)	GC-C-IRMS extracted (n = 9)	$\Delta\delta^{13}\text{C}$ EA-IRMS vs. GC-C-IRMS	$\Delta\delta^{13}\text{C}$ extracted vs. non extracted
Metolachlor	$-30.2 \pm 0.1$	$-31.0 \pm 0.2$	$-30.7 \pm 0.3$	$0.8 \pm 0.2$	$0.3 \pm 0.3$
Alachlor	$-33.8 \pm 0.1$	$-33.9 \pm 0.2$	$-33.9 \pm 0.3$	$0.1 \pm 0.2$	$0.2 \pm 0.2$
Acetochlor	$-29.8 \pm 0.2$	$-29.5 \pm 0.3$	$-30.1 \pm 0.2$	$0.3 \pm 0.3$	$0.6 \pm 0.2$

## 2. Investigation of putative genes for chloroacetanilide biodegradation

Monitoring of genes coding for pesticide-degrading enzymes can provide hints on catabolic potential of pesticide in a given field site (Monard et al., 2013). While assessments of total bacterial diversity can enable to evaluate the responses of bacterial communities to contaminant exposure, such assessments lack direct insight on their functional capabilities. Since the same metabolic genes can be found and exchanged between diverse groups of organisms (e.g. through horizontal gene transfer) (Springael and Top, 2004), the assignment of a function of interest to specific phylogenetic groups is problematic. Therefore, molecular approaches targeting genes of interest can be of interest for environmental assessments of contaminant biodegradation. The potential of *in situ* biodegradation of a contaminant have been previously showed using PCR-based detection and quantification of functional genes from environmental samples (Bers et al., 2012; Dealtry et al., 2014). In addition, studies of the diversity of bacterial populations carrying a functional gene of interest would allow to bridge the gap between a metabolic process and the phylogenetic groups carrying out this process in a contaminated site (Galvao et al., 2005). However, the analysis of functional bacterial genes putatively involved in contaminant degradation requires prior knowledge of the main degradation pathways of the contaminant of interest, and the identification of the catabolic genes involved in these pathways. Catabolic genes have been identified for a number of herbicides including gamma-hexachlorocyclohexane (lindane) (Lal et al., 2013), atrazine (Devers et al., 2007), linuron (Bers et al., 2013), and 2,4-dichlorophenoxyacetic acid (2,4-D) (de Liphay et al., 2001). Yet, for the large majority of pesticides, the genetic basis of their microbial degradation remains poorly understood.

In spite of decades-long worldwide application of chloroacetanilide herbicides, the genes involved in their degradation remain largely unknown. The two main known biodegradation pathways of chloroacetanilides involve thiolytic (glutathione-dependant) dechlorination (Graham et al., 1999), or N-dealkylation (Liu et al., 2012b). Recently, a hydrolase enzyme has been shown to catalyse the hydrolysis of the amide bond of N-dealkylated acetochlor and the corresponding gene (*cmeH*) has been identified in a *Sphingobium* strain (Li et al., 2013). The enzyme responsible for the N-dealkylation step was later identified as CndA, a three component Rieske non-heme oxygenase encoded by the *cndA* gene (Chen et al., 2014b). The proposed pathway of acetochlor degradation by *Sphingobium DC2* is depicted in Figure II-4. The

glutathione *S*-transferase (GST)-mediated degradation of chloroacetanilides have been demonstrated in several studies and is believed to be the principle route of chloroacetanilide degradation in the environment. However, there are no reports in literature of the associated GST genes. Glutathione transferases are an enzyme superfamily involved in cellular detoxification that is widely distributed in both prokaryotes and eukaryotes (Vuilleumier and Pagni, 2002). Bacterial GSTs catalyse the nucleophilic attack of glutathione (GSH) on the electrophilic groups of a wide range of toxic compounds including monocyclic aromatic compounds (e.g. phenol, toluene), chlorinated aliphatic (e.g. dichloromethane) or chlorinated aromatic compounds (e.g. atrazine) (Allocati et al., 2009).

Another enzyme putatively involved in a downstream step of chloroacetanilide degradation is 1,2-catechol dioxygenase. 1,2-catechol dioxygenase catalyses the oxidative ring cleavage of catechol, and thus plays a key role in the biodegradation of a wide class of aromatic organic compounds (El Azhari et al., 2010). The activity of 1,2-catechol dioxygenase enzyme has been shown to increase in response to exposure to butachlor (a chloroacetanilide herbicide) suggesting its involvement in the biodegradation of chloroacetanilides (Zhang et al., 2011).

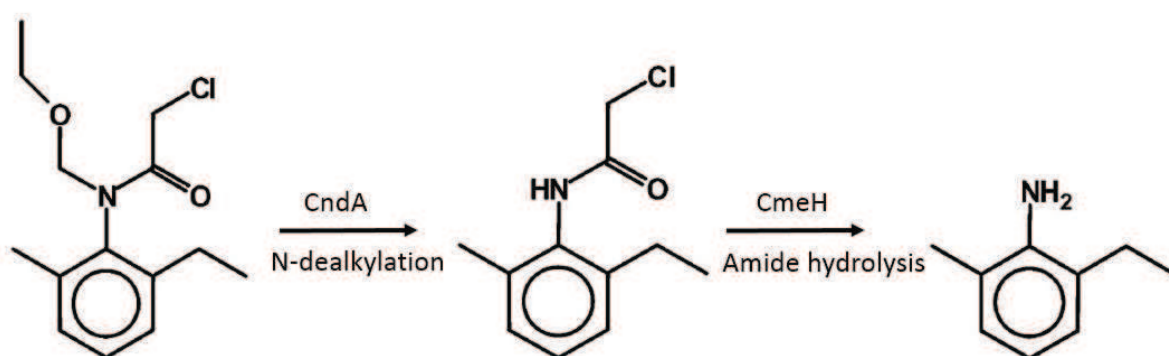


**Figure II-4: Pathway of acetochlor degradation by *Sphingobium DC2*.** A three component Rieske non-heme oxygenase (CndA) catalyses the dealkylation of acetochlor which is followed by the hydrolysis of the amide bond catalysed by a hydrolase (CmeH). (Li et al., 2013; Chen et al., 2014b)

In this section, we describe the design and validation of degenerate primer pairs targeting a set of genes putatively involved in chloroacetanilides degradation, namely GST genes and a hydrolase gene (*cmeH*). The *cndA* acetochlor N-dealkylase was described after this methodological development work was finished, and therefore was not included as a target

gene. In addition, a previously developed primer pair (El Azhari et al., 2010) was used to screen for the presence/absence of 1,2-catechol dioxygenase in wetland samples. The presence/absence of target functional genes in wetland samples was then monitored by PCR.

## 2.1. Materials and methods

### 2.1.1. *Primer design*

Two well characterised representatives of the beta GST class from *Proteus mirabilis* (PmGST) and *Ochrobactrum anthropi* (OaGST) and one representative of Gram positive bacterial GST from the XI class (of the strain *Streptomyces avermitilis* MA-4680; hereafter called StrepGST) were chosen as reference protein sequences for primer design. Primer pairs PmF/PmR, OaF/OaR and StrepF/StrepR were designed to amplify subsets of PmGST, OaGST and StrepGST homologues respectively in bacteria from environmental samples. This aimed to identify a possible role of the target GSTs in bacterial degradation of metolachlor or adaptation to metolachlor exposure. In addition, protein sequence of the amidase gene *cmeH* of *Sphingobium quisquiliarum* that was recently reported to be involved in acetochlor degradation (Li et al., 2013) was used as reference protein sequences for primer design targeting *cmeH* gene and its homologs.

Amino acid sequences sharing 50% amino acid sequence homology with the chosen reference protein sequences (PmGST, OaGST and StrepGST, CmeH; Uniprot accession numbers: P15214, P81065, Q825J4 and S5PLR2 respectively) were obtained from Uniprot protein database. The obtained homologous sequences were aligned using MAFFT within MyHits (<http://myhits.isb-sib.ch/cgi-bin/mafft>) and visualised using the sequence editing software Jalview 2 (<http://www.jalview.org/>) to remove redundant sequences. In the case of the Strep and Pm primer pairs, Jalview was also used to decrease the number of sequences to 58-60 sequences by removing distant sequence branches in a neighbour-joining tree. The resulting amino acid sequence alignments were submitted in Protogene software (<http://www.igs.cnrs-mrs.fr/Tcoffee/tcoffee.cgi/index.cgi?stage1=1&daction=PROTOGENE::Advanced>) to obtain the equivalent alignment of the original gene coding DNA. Duplicate sequences and multiple sequences from same species in the Protogene output coding DNA sequences were removed manually. Coding DNA sequences were then aligned using ClustalX and viewed using



Boxshade within MyHits ([http://myhits.vital-it.ch/cgi-bin/ to boxshade](http://myhits.vital-it.ch/cgi-bin/to_boxshade)). Primers were picked from the Boxshade multiple DNA alignments manually. Mismatches of the chosen primers with the reference sequences were avoided by increasing degeneracy. Primers were designed and tested *in silico* on reference sequences using Primer3 (<http://primer3.ut.ee/>). Primer pairs presenting 1) least degeneracy, 2) PCR product fragments in the size range of 150 to 300 bp (can be later used for quantitative PCR (qPCR) amplification), and 3) good performance on Primer3 with respect to self-complementarity and melting temperatures, were chosen.

### 2.1.2. Primer validation

The designed primer pairs were tested and their amplification by PCR was optimised on DNA from chosen strains (positive control strains). Table II-2 contains a list of the used reference strains, their corresponding target genes and primer sequences. Strains that were used as positive controls were the strains containing the reference protein sequences that were used for primer design in the case of PmGST, OaGST and StrepGST primer pairs. For CmeH primer pair, the reference containing the reference protein sequence was not accessible (*Sphingobium quisquiliarum* DC-2; (Li et al., 2013)), so a strain containing a homologous protein (50% homology) was used. For the CatA primer pair targeting the catechol 1,2-dioxygenase gene (El Azhari et al., 2010), positive control DNA from a *Pseudomonas stutzeri* isolated from an arsenic contaminated environmental sample (DNA kindly provided by Sandrine Koechler, GMGM, Strasbourg) that we expected to contain the 1,2 catechol dioxygenase gene was used.

A range of primer concentrations (final concentration 0.4-2  $\mu$ M), annealing temperatures (50 – 65 °C) and DMSO concentration (1-10% v/v; only for GC- rich positive control strains *S. avermitilis* and *X. flavus*) were tested to achieve optimal conditions for PCR amplification of target gene fragments. The amplification of the *catA* gene was done as previously described (El Azhari et al., 2010). Each PCR reaction contained 0.5 U of Taq polymerase (Q-biogene), 1X PCR buffer (Q-biogene), 200  $\mu$ M each of the four deoxynucleoside triphosphates, 1-2 ng of template DNA and the optimised concentrations of primers and DMSO in a final volume of 10  $\mu$ L. A no template DNA control (no DNA negative control) was prepared with every PCR run. The used PCR program included a 10-min denaturation step at 95°C, followed by 40 cycles of 15 s of denaturation at 95°C and 1 min of annealing/extension at 60°C.

Specificity of each primer pair to the target gene fragment was tested by i) verifying size of the amplified fragment, ii) verifying that each primer pair does not amplify non-target DNA from the five positive control strains listed in Table II-2 (cross-testing), and iii) sequencing of the amplified fragment. Cross-testing was done to check that each primer pair amplified target gene fragments in the positive control strain (known to contain the target gene) and not amplify fragments from other strains (known not to contain the target gene). Amplified gene fragments were sequenced using the same primer pairs used for amplification by primer walking using Dye-Terminator chemistry and an ABI 377 Automated Sequencer or an ABI 310 Genetic Analyser (Applied Biosystems, Darmstadt Germany). Similarity searches against public gene databases were performed using blast.

Table II-2. Target functional genes and their corresponding primer pairs.

Primer name	Primer sequence* (5' to 3')	Degeneracy	Target gene (name)	Product size	Positive control strain	Accession number	Optimised annealing temperature	Optimised primers concentration
PmF	GYTCKCTDTCWCKKAYAT	96X	GST Beta class	136 bp	<i>Proteus Mirabilis</i>	NC_010554	57 °C	2 µM
PmR	GGSSTRAASCYYTTRTGMA	128X	( <i>pmGST</i> )					
OaF	GYGGCWATYCTSCMMTATAT	64X	GST Beta class	268 bp	<i>Ochrobactrum anthropi</i>	NC_009667	57 °C	0.8 µM
OaR	GGCATCYGSYTGVTGAA	48X	( <i>oaGST</i> )					
StrepF	TGGMRYTTCRMYCTSGAYCC	256X	GST Xi class	164 bp	<i>Streptomyces avermitilis MA-4680</i>	NC_003155	52 °C	2 µM
StrepR	AKCKRSKGGWAGTAGTTS GT	128X	( <i>strepGST</i> )					
cmeHF	TSTKCGAYGARTGSSRYC	256X	Amidase	136 bp	<i>Xanthobacter flavus 301</i>	CAD10800	-	-
cmeHR	CCRTGSGTRAASASGATSAC	64X	( <i>cmeH</i> )					
CataF	ACVCCVCGHACCATYGAAGG	54X	catechol 1,2-dioxygenase	470 bp	<i>Pseudomonas stutzeri</i> (S. Kocheler)	AJ617524	58 °C	2 µM
CataR	CGSGTNGCAWANGCAAAGT	16X	( <i>catA</i> )					

\* Nucleotide nomenclature according to the IUPAC degeneracy codes. “-“ failed to amplify under any of the tested conditions.

### 2.1.3. *Target gene detection in environmental samples*

To test the presence of the target genes in wetland samples, the optimised PCR procedure as described above was followed. A set of 33 DNA samples from outdoor constructed wetlands water and rhizosphere were selected to check possible correlations between target functional genes and exposure to *S*-metolachlor (for details on the wetlands set-up see Chapter IV). Amount of template wetland DNA used for the test was 5 ng except for samples for which DNA amount was not sufficient. An inhibition control was prepared for each environmental sample to evaluate the presence/absence of PCR amplification inhibitors that could have been co-extracted with environmental DNA. Presence of PCR inhibitors could potentially lead to false negatives by causing the failure of PCR amplification in samples containing the target gene fragment. Therefore, 40 pg of positive control DNA were added to a replicate of each PCR reaction (PCR inhibition control) to check for inhibition. Absence of amplification in the PCR inhibition control would signify the presence of PCR inhibitors in the environmental DNA.

## 2.2. Results and discussion

### 2.2.1. *Primer validation*

Target *GST* genes were successfully amplified from *P.mirabilis*, *O.anthropi* and *S.avermitilis* and the *cata* gene from *P.stutzeri* using the respective primer pairs. Optimised annealing temperatures and primer concentrations are provided in Table II-2. Sequencing results confirmed that the amplified fragments corresponded to the target fragments of *pmGST*, *oaGST*, *StrepGST*, and *cataA* genes. The amplification of the *cmeH* amidase gene from *X.flavus 301* failed repeatedly despite the range of different PCR conditions tested. The smallest amount of DNA template resulting in visible amplification on the agarose gel (hereafter called the detection limit) was determined for each of the primer pairs. The CataF/CataR primer pair had the lowest detection limit (1.6 pg), followed by OaF/OaR (8 pg) and PmF/PmR (40 pg) primer pairs, whereas the StrepF/StrepR primer pair had the highest detection limit (200 pg).

Cross-testing of each of the four primer pairs on DNA of all positive control strains showed that the PmF/PmR, OaF/OaR and StrepF/StrepR primer pairs were specific as they showed

specific amplification with their respective positive control strains. For example PmF/PmR primer pair gave a visible band only with the *P.mirabilis* DNA but gave when tested on DNA of other strains (i.e. *O.anthropi*, *S.avermitilis*, *P.stutzeri* and *X.flavus*). The CatA primer pair amplified three clear fragments from *O.anthropi*, however the three fragments had larger sizes (700 to > 1000 bp) than the expected *cataA* fragment (470 bp), so this non-specific amplification was not expected to interfere with the visualisation of *cataA* gene fragments amplified from environmental samples. In conclusion, the primer pairs PmF/PmR, OaF/OaR, StrepF/StrepR and CataF/CataR, but not cmeF/cmeR, were successfully used to specifically amplify target gene fragments from positive control strains.

### 2.2.2. Target gene detection in environmental samples

A set of 33 wetland water and rhizosphere DNA samples were chosen to test for the presence/absence of the target genes. Samples were taken from two constructed wetlands (see Chapter IV for details on the set-up) and had different levels of exposure to *S*-metolachlor (for details on *S*-metolachlor concentrations in the samples see Table II-3). Tests of detection of *strepGST* in a subset of 15 wetland water samples using the StrepF/StrepR primer pair resulted in a smear, indicating the non-specific binding of the primer pair to environmental DNA. Although StrepF/StrepR primer pair did not amplify non-specifically in tested strains (cross-testing), the significantly higher diversity of bacterial DNA sequences in environmental samples provided more targets for potential non-specific amplification, of DNA fragments of different sizes leading to the observed smear. Therefore, the screening of the *strepGST* in wetland samples was not possible. OaGST primer pair did not amplify in any of the 33 tested samples, and no inhibition was detected (Table II-3). This indicates that this gene is not present in detectable amounts in wetland samples and is therefore not a suitable target gene for this study.

On the contrary, *cataA* was detected in all samples and *pmGST* in 27 out of the 33 wetland samples regardless of their exposure status to *S*-metolachlor, including samples that were not exposed to *S*-metolachlor. This suggests that the two genes are ubiquitously present in wetland set-ups, and thus lacked the needed selectivity to be suitable targets for assessments of chloroacetanilide exposure and/or degradation by PCR detection. Yet, quantification of the

gene copy numbers using qPCR could reveal a sensitivity of the abundance of the two genes to chloroacetanilide exposure, but this remains to be tested. The observed ubiquity of catechol dioxygenase probably reflects the ubiquity of natural and xenobiotic aromatic organic compounds in environmental samples, the biodegradation of which under aerobic conditions mostly converge through catechol-like intermediates (Fuchs et al., 2011). Results also indicate that the set *pmGST* homologues amplified is probably too broad, underscoring that less degenerate primers targeting a smaller subset of bacterial GSTs may be needed. However such close targeting of specific GSTs require some *a priori* knowledge on the genetic basis of chloroacetanilide degradation by GSTs which is currently not available.

Due to this inability to identify genes that respond to chloroacetanilide exposure, the analysis of functional genes involved in response to chloroacetanilides was not included in investigations of chloroacetanilide degradation in wetlands (Chapters III and IV). Different approaches to the identification of functional genes involved in bacterial response to chloroacetanilides (i.e. RNASeq and metatranscriptomics) is discussed in Chapter V. On the other hand, the high prevalence of *pmGST* and *catA* genes in wetlands make them good candidates for studying bacterial diversity of *pmGST* harbouring, and catechol degrading bacterial communities in wetlands in future studies.

**Table II-3. Detection of target functional genes in constructed wetland samples.** “+” indicates that the gene is detected, “-” indicates that the gene is not detected. \*amount of DNA template used for testing the presence of target genes.

	Sample location	Sampling day	Exposed to S-metolachlor? (conc. $\pm$ stdev)	Amount of DNA (ng)*	Target gene		
					<i>OaGST</i>	<i>PmGST</i>	<i>catA</i>
Continuous-flow wetland	inlet	0	no	5	-	+	+
	2 m	0	no	5	-	-	+
	outlet	0	no	5	-	+	+
	1 m	35	yes (1 $\pm$ 0)	5	-	+	+
	2 m	35	yes (4 $\pm$ 0)	5	-	+	+
	3 m	35	yes (2 $\pm$ 0)	5	-	-	+
	outlet	35	yes (2 $\pm$ 0)	5	-	+	+
	inlet	42	no	1	-	-	+
	1 m	42	yes (124 $\pm$ 5)	5	-	+	+
	2 m	42	yes (113 $\pm$ 6)	1	-	-	+
	3 m	42	yes (117 $\pm$ 3)	5	-	-	+
	outlet	42	yes (107 $\pm$ 6)	5	-	+	+
	1 m	56	yes (42 $\pm$ 1)	5	-	+	+
	2 m	56	yes (73 $\pm$ 5)	5	-	+	+
	3 m	56	yes (48 $\pm$ 1)	5	-	+	+
	outlet	56	yes (39 $\pm$ 1)	5	-	+	+
Batch	inlet	0	no	5	-	+	+
	pooled	0	no	5	-	+	+
	outlet	0	no	5	-	-	+
	pooled	35	yes (181 $\pm$ 6)	5	-	+	+
	outlet	35	yes (112 $\pm$ 1)	5	-	+	+
	inlet	42	no	5	-	+	+
	pooled	42	yes (77 $\pm$ 1)	5	-	+	+
	pooled	56	yes (165 $\pm$ 4)	5	-	+	+
	outlet	56	yes (67 $\pm$ 1)	5	-	+	+
Continuous-flow	<i>Phalaris</i> A		yes	5	-	+	+
	<i>Phragmites</i> A		yes	5	-	+	+
	<i>Phalaris</i> B		yes	5	-	+	+
	<i>Phragmites</i> B		yes	2	-	+	+
	<i>Phalaris</i> A		yes	5	-	+	+
Batch	<i>Phragmites</i> A		yes	4	-	+	+
	<i>Phalaris</i> B		yes	5	-	+	+
	<i>Phragmites</i> B		yes	5	-	+	+

### 3. T-RFLP on lab-scale wetland samples

Terminal restriction fragment length polymorphism (T-RFLP) is a PCR-based DNA fingerprinting technique that allows high-throughput, cost-effective comparison of bacterial community structure of multiple samples. It provides higher resolving power than earlier fingerprinting techniques such as denaturing gradient gel electrophoresis (DGGE) and random amplified polymorphic DNA (RAPD) (Ranjard et al., 2000; Nunan et al., 2005). T-RFLP has been widely used in the last two decades to address questions regarding spatial and temporal variability of bacterial communities in different environmental contexts (Anderson et al., 2010; Giebler et al., 2013). It has also been used in combination with multivariate statistics to study biotic and abiotic drivers of bacterial community structure (Hwang et al., 2012; Valentin-Vargas et al., 2012). T-RFLP is most commonly performed on the 16S-rRNA gene to study total bacterial diversity but it can also be applied on other genes of interest (e.g. nitrous oxide reductase) to target a specific population of interest (e.g. denitrifiers).

The main steps of the T-RFLP procedure are illustrated in Figure II-5. The procedure starts with the PCR-based amplification of the gene of interest using one or two fluorescently labelled primers. The resulting gene fragments are then digested using one or more restriction digestion enzymes that have a four base recognition site. The sizes and relative abundances of the obtained fluorescent terminal fragments are determined using an automated DNA sequencer. Since each peak/T-RF reflects differences in the 16S rRNA gene sequence, each peak in the electropherogram corresponds to a distinct phylogenetic group. Thus, the pattern of obtained T-RFs from a given sample reflects the diversity of the phylogenetically distinct groups present in the sample.

Data treatment is a crucial step in the interpretation of T-RFLP profiles (Schütte et al., 2008). The first step of data treatment is noise cancellation which includes distinguishing the signal ("true" peaks) from electronic noise in a T-RFLP profile. Several approaches for noise cancellation have been developed including fixed threshold (Osborn et al., 2000), proportional threshold (Dunbar et al., 2001; Osborne et al., 2005), and statistical determination of the threshold (Abdo et al., 2006). A second essential step is the alignment of peaks to allow the comparison between different T-RFLP profiles. Run-to-run variability in T-RFLP analysis causes slight differences in the estimated sizes of T-RF fragments from the same bacterial phylotype, therefore fingerprints need to be aligned before further treatment and interpretation



of T-RFLP data. Approaches used for peak alignment by assigning fragment sizes to categories (bins) include nearest integer rounding, manual binning (Blackwood and Paul, 2003), and clustering-based statistical approaches (Smith et al., 2005). The use of statistical approaches is deemed superior to other approaches and is the most widely applied approach because they consist of automated procedures that allow analysis of large data sets with statistical justification (Schütte et al., 2008).

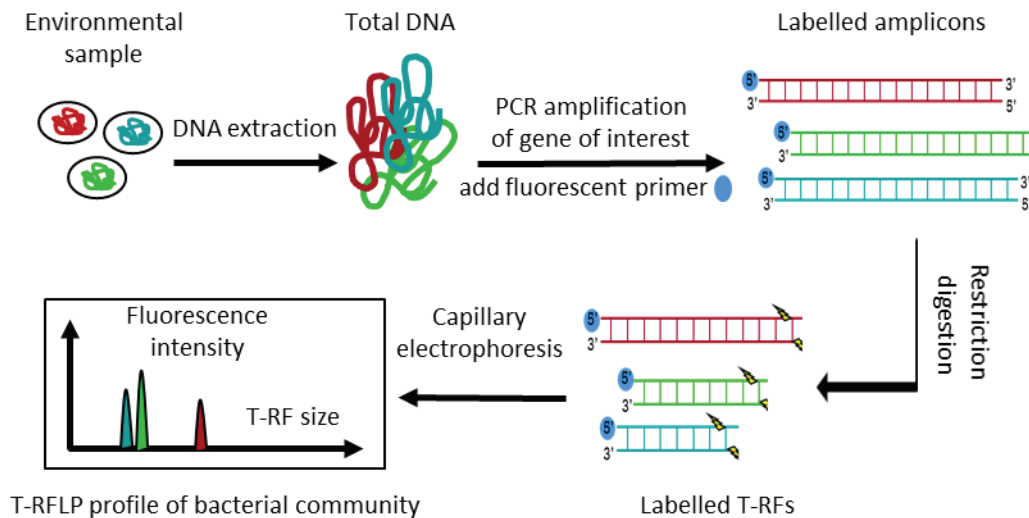


**Figure II-5: Main steps of the T-RFLP procedure.** Modified from (Penny, 2009)

The aim of the methodological development described in this section was to test a 16S rRNA gene-based T-RFLP protocol that was previously established in our team for analysing bacterial diversity in aquifers on wetland water samples (Penny, 2009). The protocol was tested on our target environmental samples (i.e. wetland water) to check if i) enough DNA is extracted to allow T-RFLP procedure, ii) 16S-rRNA gene fragments can be amplified and purified from extracted DNA, and iii) restriction digestion can be successfully applied to differentiate phylotypes by generating TRFs of different sizes. Wetland water samples used here were taken from outlets of experimental lab-scale wetlands (for details of the experimental setup see Chapter III). Two restriction enzymes that were used in the previously established protocol (AluI and HhaI) were compared for their resolution capacity of wetland water diversity (i.e. number of TRFs resulting from restriction digestion). A range of sample volumes (20 – 200 mL) was also tested to check for possible effects of sample volume on obtained DNA yields

and measured bacterial diversity. Finally, two data treatment methods analysis methods for noise cancellation and peak alignment were compared based on their time-effectiveness, error proneness and the level of bacterial diversity they generate.

### 3.1. Materials and methods

#### 3.1.1. *Sampling*

Wetland water samples were taken from lab-scale wetlands (see Chapter III for details on experimental set-up). Outlet water from the four lab-scale wetlands outlets was combined to make one pooled sample. Different volumes (20, 50, 100 and 200 mL) of water samples were sterile-filtered on 0.2 µm mixed cellulose esters filters (Millipore, Molsheim, France). Two replicates were filtered for each sample volume. The filters were placed inside 50 mL sterile tubes and were stored at -20 °C until DNA extraction.

#### 3.1.2. *DNA extraction and T-RFLP procedure*

Total DNA was extracted from water filters using PowerWater® DNA Isolation Kit following manufacturer's instructions (MO BIO, Carlsbad, CA, USA). Concentrations of DNA were determined by spectrometry using Nanodrop (Nanodrop Technologies, Wilmington, DE, USA). T-RFLP was performed according to a previously established protocol (Penny et al., 2010a). Bacterial 16S rRNA gene fragments (0.9 kb) were PCR-amplified using 5' carboxyfluorescein (6-FAM) labelled 27f primer (Edwards et al., 1989) and 927r primer (Muyzer et al., 1995). PCR mixtures (total volume, 50 µL) contained 1X high-fidelity PCR buffer (containing 7.5 mM MgCl<sub>2</sub>) (Bio-Rad, Marnes-la-Coquette, France), 200 µM of each dNTP, primers (0.4 µM each), 1 U iProof high-fidelity polymerase (Bio-Rad), and 0.1 - 1 ng of DNA. PCR amplification involved an initial denaturation at 95°C for 2 min, followed by 30 cycles of denaturation at 94°C for 20 s, annealing at 52 °C for 30 s, extension at 72°C for 30 s, and a final 1 min extension step at 72°C. PCR reactions were carried out in triplicate, pooled and purified from 1% agarose gels using the QIAquick® gel extraction kit (QIAGEN, Stockach, Germany). Purified 16S rRNA gene fragments (50 to 100 ng) were digested at 37°C for 16 h with 20 U of either HhaI or AluI (Fermentas, Les Ulis, France). Digestion products were purified with the QIAquick® nucleotide removal kit (QIAGEN). 5 µl of DNA aliquot (10 to 50 ng) was mixed with 10 µl of Hi-Di formamide (Applied Biosystems,

Darmstadt, Germany) containing 1:20 (vol/vol) carboxy-X-rhodamine (ROX)-labeled MapMarker 1000 (Bioventures), denatured at 95 °C for 5 min, and snap-cooled on ice. Denatured restriction fragments were loaded onto an ABI Prism 3130 XL capillary sequencer (Applied Biosystems) equipped with 50 cm long capillary and POP 7 electrophoresis matrix according to the manufacturer's instructions.

### 3.1.3. *Data treatment*

T-RFLP electropherograms were analysed with PeakScanner V1.0 software (Applied Biosystems). Peaks between 50 bp and 800 bp were included into the data set to avoid uncertainties associated with fragment size determination. Two methods of data treatment (noise cancellation and peak alignment) were compared. Method 1 was the method previously used in our team for treatment of T-RFLP profiles and included noise cancellation using proportional threshold approach (Dunbar et al., 2001), and using hierarchical clustering algorithm for peak alignment *via* the online T-Align software (Smith et al., 2005). Method 2 included noise cancellation by statistical determination of the threshold approach (Abdo et al., 2006) and on hierarchical clustering algorithm for peak alignment (Smith et al., 2005), both steps done using the online software T-REX (Culman et al., 2009).

Method 1: The first tested noise cancellation method was described by (Dunbar et al., 2001). The procedure was performed using Excel spreadsheets (Microsoft, Seattle, WA, USA). The method depends on the standardisation of the sum of peak heights (total fluorescence) between profiles, which they assume corresponds to DNA quantity represented by each profile. The sum of all peak heights is larger or equal to a given “baseline noise threshold value” (e.g. 25 fluorescence units). Total peak height is standardized to the profile with the smallest total peak height by proportionally reducing the height of each peak in larger profiles. To accomplish this, peak heights in each profile were multiplied by a correction factor (total peak height profile/ smallest total peak height), and new total peak height values were calculated for each profile. For example, given two profiles with total fluorescence values of 20,000 and 40,000, respectively, each peak in the latter profile would be multiplied by a correction factor of 0.5. This procedure often eliminated peaks from larger profiles by reducing some peak heights below the baseline noise threshold (25 fluorescence units). Therefore, after the correction factor step, the new sum of peak heights of  $\geq 25$  fluorescence units

was calculated, and the standardisation procedure was repeated until, by iteration, the total peak height (i.e., DNA quantity) of each profile was equal to the total peak height of the smallest profile.

In some cases, the total peak height of one or more profiles cannot be made exactly equal to the total peak height of the smallest profile. In these cases, the total peak heights of the larger profile fluctuate between a value above and a value below the total peak height of the smaller profile in successive iterations of the standardization routine. This occurs when one or more peaks fall below the noise threshold (25 fluorescence units) in one iteration, resulting in a total DNA quantity less than that in the smaller profile, and then rise above the threshold in the next iteration, resulting in a total quantity greater than that in the smaller profile. To solve this problem, a chi square value is calculated for each of the iteration within the first 10 standardisation cycles. This iteration having the highest chi square value (the one resulting in the closest total peak heights for all profiles) is chosen to be the last iteration. For alignment of peaks from different T-RFLP profiles the T-Align software was used (<http://inismor.ucd.ie/~talign/>; (Smith et al., 2005)).

Method 2: Noise cancellation and peak alignment were done using T-REX (<http://trex.biohpc.org>) (Culman et al., 2009). T-REX software uses the same peak alignment algorithm used by T-Align (Smith et al., 2005). However, it applies a statistical noise cancellation methodology described by Abdo et al. (Abdo et al., 2006). The first step of the procedure involves calculation of the relative peak height (or area) for each peak (relative peak height = peak height/total peak height in this particular sample). Then, the standard deviation of this dataset is calculated assuming that the true mean is zero. Peaks with a relative height larger than a given number of standard deviations (e.g. 3) from the mean are identified as ‘true signal’ and are removed. The number of standard deviations, called the ‘multiplier factor’ used can be defined by the user. This process is reiterated until no more ‘true’ peaks are identified.

Richness (number of terminal restriction fragments (TRFs) in a profile), Shannon’s diversity and Jaccard’s similarities indices were calculated using Microsoft Office Excel. Jaccard’s similarity index was calculated as  $J = (A \cap B) / (A \cup B)$ , where  $A \cap B$  is the number of TRFs present in both profiles.  $A \cup B$  is  $A \cap B +$  number of TRFs present in one of the two profiles. Shannon’s diversity index:  $H' = -\sum(P_i \ln[P_i])$ , where  $P_i$  is the relative peak height (peak height/total peak height in a given profile).

### 3.2. Results and discussion

DNA extraction from wetland water samples was successful as evidenced by good DNA yields and amplifiability of 16S-rRNA gene fragments. DNA yields ranged from 128 to 1949 ng, with an average yield of  $619 \pm 525$  ng, and no distinction between yields from different sample volumes. The T-RFLP procedure resulted in exploitable profiles; Figure II-6 shows an example of a profile obtained from a water sample digested by AluI enzyme.

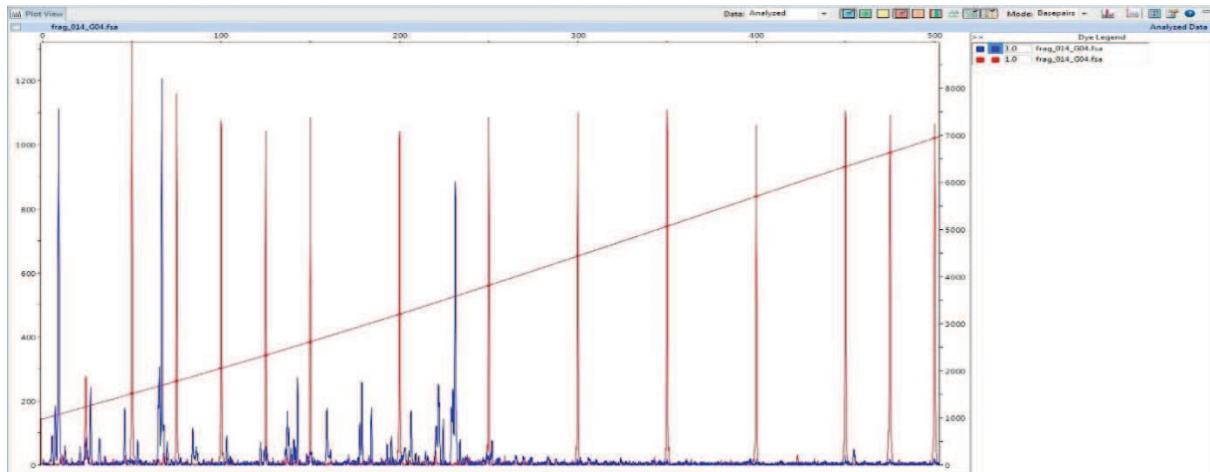


**Figure II-6. Example T-RFLP electropherogram as visualised using PeakScanner software showing sample peaks (blue) and size marker peaks (red).**

Profiles from HhaI restriction enzyme had markedly low number of T-RFs ( $7 \pm 1$ ) in comparison to AluI enzyme profiles ( $20 \pm 5$ ). Consequently, only profiles generated using the AluI restriction enzyme were used for further data interpretation. Initial sample volume did not significantly impact the diversity ( $H'$ ) of the profiles (Kruskal Wallis test,  $p = 0.132$ ), suggesting that volumes in the tested sample volume range were similarly suitable for T-RFLP analysis. Comparison of the two data analysis methods revealed that Method 2 was less time consuming, and resulted in higher average diversities ( $H'$ ) and Jaccard's similarity indices ( $J$ ) between replicate samples. Comparison criteria and results are presented in Table II-4.

**Table II-4. Comparison of the two T-RFLP data treatment methods.**

<b>Criteria</b>	<b>Method 1: Excel standardisation + T-Align</b>	<b>Method 2: T-REX</b>
Noise cancellation methodology	(Dunbar et al., 2001)	(Abdo et al., 2006)
Assumptions	baseline threshold (25 RFUs)	multiplier factor (3)
Alignment method	hierarchical clustering algorithm according to (Smith et al., 2005)	
Time efficiency	slow	fast
Visualisation of profiles	not possible	possible: individual profiles and superimposed profiles
Error proneness	high (during standardisation on Excel)	low
Average number of TRFs	19	27
Average Jaccard's similarity index between replicates (J)	0.5	0.6
Average Shannon's diversity index (H')	2.5	2.8

AluI restriction enzyme proved to have a higher discriminatory power between bacterial phylotypes in our wetland water samples than HhaI and was thus used in further T-RFLP analysis throughout this PhD work. Comparison of the two data analysis methods revealed the advantages of using T-REX software for T-RFLP data treatment. In Chapters III and IV, T-RFLP data interpretation was facilitated by combining T-REX output and chemical analysis data (chloroacetanilide concentrations and hydrochemical parameters) with multivariate statistics and ordination methods. In conclusion, T-RFLP was successfully applied to lab-scale wetland water samples. The results presented here supported the use of any water sample volume in the tested range (20- 200 mL), AluI for restriction digestion and T-REX for T-RFLP

data treatment for wetland water samples. The procedure was consequently followed in Chapters III and IV to follow changes in bacterial community composition in two different wetland experimental set-ups.

## Chapter III

# Degradation of chloroacetanilide herbicides in lab-scale wetlands

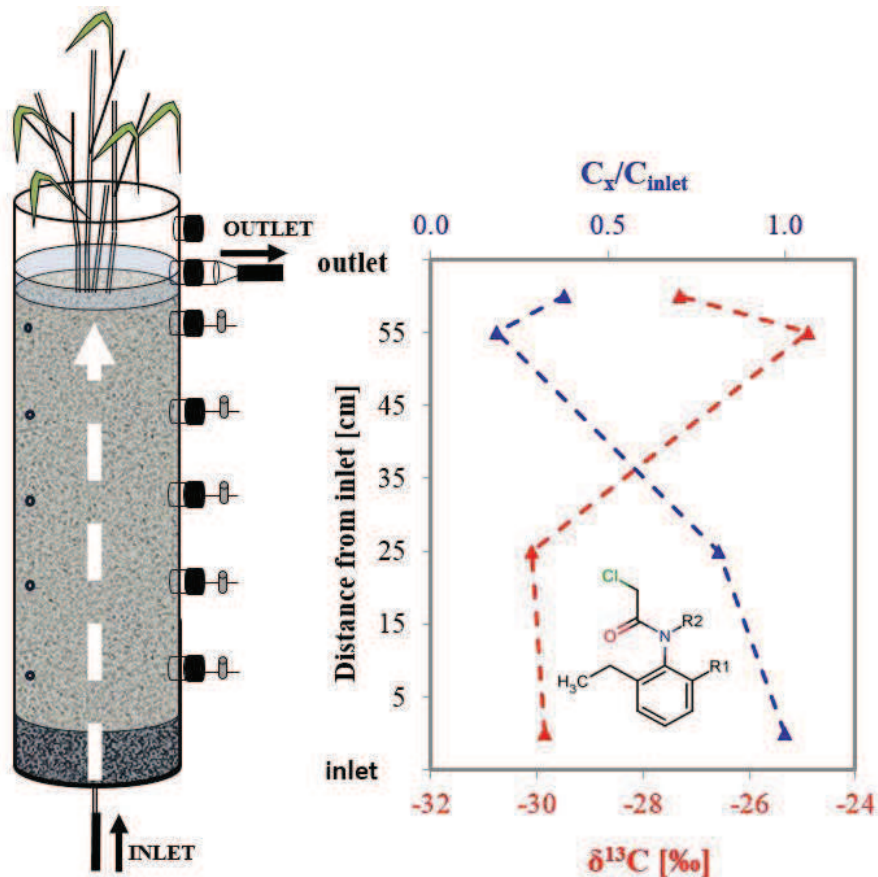
In this experiment, the degradation of metolachlor, acetochlor and metolachlor and their impact on wetland bacterial populations was followed at oxic/anoxic interfaces in lab-scale wetlands. Section 1 describes the application of the newly developed CSIA method [Chapter II] to assess *in situ* degradation of the three chloroacetanilides in wetlands. In Section 2 we investigate in more detail putative degradation pathways of the three chloroacetanilides in the lab-scale wetlands. The applicability of enantiomer analysis to monitor the biodegradation of the chiral chloroacetanilide metolachlor in redox-dynamic ecosystems is evaluated. In addition, the link between biogeochemical conditions, exposure to chloroacetanilides and bacterial composition is explored.



# Section 1. Using compound specific isotope analysis to assess the degradation of chloroacetanilide herbicides in lab-scale wetlands

(modified from: Elsayed, O.F., Maillard, E., Vuilleumier, S., Nijenhuis, I., Richnow, H.H., Imfeld, G., 2014. Using compound-specific isotope analysis to assess the degradation of chloroacetanilide herbicides in lab-scale wetlands. Chemosphere 99, 89-95.)

This section has been modified from the original publication to remove text, figures and tables concerning the development of carbon-CSIA method for chloroacetanilide herbicides in water samples is described in Chapter II of this manuscript.



### Abstract

Compound specific isotope analysis (CSIA) is a promising tool to study the environmental fate of a wide range of contaminants including pesticides. The novel CSIA method for stable carbon isotope measurements of chloroacetanilide herbicides was applied in combination with herbicide concentration and hydrochemical analyses to investigate *in situ* biodegradation of metolachlor, acetochlor and alachlor during their transport in lab-scale wetlands. Two distinct redox zones were identified in the wetlands. Oxidic conditions prevailed in the lower parts close to wetland inlets (oxygen concentration of  $212 \pm 24 \mu\text{M}$ ), and anoxic conditions (oxygen concentrations of  $28 \pm 41 \mu\text{M}$ ) prevailed towards the outlets, where dissipation of herbicides mainly occurred. Removal of acetochlor and alachlor loads from inlet to outlet of wetlands was 56 and 51%, whereas metolachlor was more persistent (23% of load dissipation). CSIA of chloroacetanilides at the wetland inlets and outlets revealed carbon isotope fractionation of alachlor ( $\epsilon_{\text{bulk}} = -2.0 \pm 0.3\text{‰}$ ) and acetochlor ( $\epsilon_{\text{bulk}} = -3.4 \pm 0.5\text{‰}$ ), indicating that biodegradation contributes to the dissipation of both herbicides. This study is a first step towards the application of CSIA to evaluate the transport and degradation of chloroacetanilide herbicides in the environment.

**Keywords:** herbicide; wetland; carbon isotope fractionation; biodegradation

## 1. Introduction

Chloroacetanilide herbicides are used to control annual grasses and broad-leaved weeds on a variety of crops including maize, sugar beet and sunflower. Metolachlor-S and acetochlor are among the ten most commonly used herbicides in the European Union and the United States (EPA, 2011). Alachlor and racemic metolachlor were commonly used in the 1990s (EPA, 1999), until the introduction of metolachlor enriched in the active S isomer in 1996, and banning the use of alachlor in 2006 in the European Union. The extensive use of chloroacetanilide herbicides is reflected in their frequent detection in ground and surface waters, and the concomitant detection of their ionic and neutral degradation products (Steele et al., 2008; Hladik et al., 2005). However, the processes governing transport and biodegradation of chloroacetanilides from agricultural land, passing through reactive zones of the landscape, such as wetlands or ground-surface water interfaces, before they reach other ecosystems, remain poorly understood.

Wetland systems can intercept upward flow of pesticide-contaminated water from shallow aquifers during groundwater discharge (Alewell et al., 2008), and influence key ecosystem services, such as water quality improvement. Several biotic (e.g. biotransformation, plant uptake) and abiotic (e.g. adsorption, volatilisation, photolysis) processes control the transport of organic contaminants in wetlands (Imfeld et al., 2009). Transport of pesticides in wetlands has been mostly evaluated based on assessment of pesticide concentrations and removal efficiencies (Stehle et al., 2011). However, such approach provides no distinction between destructive and non-destructive contaminant attenuation processes, which may lead to inaccurate estimations of the remediation potential of wetland systems. Few studies focused on degradation processes in wetlands through examining the relation between functional genes and observed degradation (Bers et al., 2012), or using microcosms (Runes et al., 2001) and mineralisation experiments to assess degradation kinetics and pathways (Gebremariam and Beutel, 2010). While these studies provide information about the potential of pesticide biodegradation in complex environmental systems, they offer no direct evidence of *in situ* biodegradation processes.

Compound-specific stable isotope analysis (CSIA) provides a valuable tool for the assessment of contaminant transport and fate in the environment (Thullner et al., 2012). CSIA relies on the enrichment of the heavy isotope of an element in the unreacted fraction of a compound during the degradation process. This isotope enrichment occurs due to slight differences in activation

energies required to break bonds involving heavy versus light isotopes (Hofstetter and Berg, 2011). Consequently, the isotopic composition of the contaminants can provide insights about key degradation pathways occurring *in situ*, and in some cases enables measuring the extent of biodegradation (Elsner, 2010). During the last decade, CSIA has been increasingly applied to study several groups of contaminants, most notably chlorinated ethenes (Imfeld et al., 2008), petroleum hydrocarbons (Richnow et al., 2003), and alkanes (Bouchard et al., 2008). Recently, CSIA methods have been developed for a handful of pesticides: lindane (Badea et al., 2009), isoproturon (Penning et al., 2010), atrazine (Meyer et al., 2009), 2,6- dichlorobenzamide (BAM) (Reinnicke et al., 2012), a metabolite of dichlobenil and phenoxy-acid herbicides (Maier et al., 2013). However, CSIA methods have not yet been reported for the evaluation of pesticide biodegradation in complex and dynamic environmental systems.

The aim of this study was to explore the applicability of CSIA as a tool to assess the biodegradation of chloroacetanilide herbicides in wetland systems. A gas chromatography combustion isotope ratio mass spectrometry (GC-C-IRMS) CSIA method was developed for stable carbon isotope analysis of chloroacetanilide herbicides in environmental aqueous samples. The novel method was applied to assess the *in situ* biodegradation of metolachlor, acetochlor and alachlor during transport in vertical-flow lab-scale wetlands, designed to study the upward discharge of pesticide-contaminated water into environments at groundwater/surface-water interfaces. In addition, hydrogeochemical development of the systems was monitored to determine prevailing biogeochemical processes.

## 2. Materials and Methods

### 2.1. Chemicals

Chloroacetanilides (metolachlor (racemic), alachlor, acetochlor; Pestanal®, analytical grade purity: 97.2, 96.8 and 99.2 respectively) and solvents (dichloromethane and ethyl acetate; HPLC grade purity > 99.9%) were purchased from Sigma-Aldrich (St. Louis, USA). Alachlor- $d_{13}$  and metolachlor- $d_6$  were obtained from Dr. Ehrenstorfer GmbH (Augsburg, Germany). Stock and standard solutions of chloroacetanilides were prepared in dichloromethane and were stored at -20 °C.

## 2.2. Chloroacetanilide extraction from water samples and quantification

Solid-phase extraction (SPE) of 10 mL lab-scale wetland water samples was carried out using SolEx C18 cartridges (Dionex®, CA, USA) packed with 100 mg irregular silica particles. The extraction procedure was adapted from USA EPA method 525.2 using an AutoTrace 280 SPE system (Dionex®, CA, USA). The procedure of chloroacetanilides extraction and quantification is described in the Appendix.

## 2.3. Carbon isotope analysis

The carbon isotope composition of alachlor, acetochlor and metolachlor was analysed using a GC-C-IRMS system consisting of a gas chromatograph (Agilent 6890) coupled *via* a GC/C III interface to an isotope ratio mass spectrometer (Finnigan MAT 252, Thermo Fisher Scientific). The oxidation furnace of the GC/C III interface containing (Pt, Ni, CuO) was set to a temperature of 980 °C. A BPX5 column (60 m × 0.32 mm, 0.5 µm film thickness, SGE, Ringwood, Australia) was used for chromatographic separation, with helium as the carrier gas at a flow rate of 2.0 mL min<sup>-1</sup>. The column was held at 50 °C for 5 min, heated at a rate of 20 °C min<sup>-1</sup> to 150 °C, then up to 250 °C at 5 °C min<sup>-1</sup>, then heated at 20 °C min<sup>-1</sup> to 300 °C and held for 1 min, and finally heated at 20 °C min<sup>-1</sup> to 320 °C, where it was held for 5 min. Samples (4 µL volume) were injected into a split/splitless injector operated in splitless mode and held at 280 °C. A chloroacetanilide standard with known isotopic composition was measured every nine injections to control the quality of the measurements.

Reference carbon isotope composition values of standards of alachlor, acetochlor and metolachlor were obtained using an elemental analyser-isotopic ratio mass spectrometer (EA-IRMS, EuroVector, Milan, Italy) coupled *via* a ConFlo III (open split, Thermo Fisher Scientific, Bremen, Germany) to a MAT 253 isotope ratio mass spectrometer (Thermo Fisher Scientific). The reproducibility of triplicate measurements was ≤ 0.2‰ (1σ). The δ<sup>13</sup>C values were calibrated using a two-point calibration against the V-PDB standard.

## 2.4. Lab-scale wetlands characteristics and set-up

The wetlands consisted of four borosilicate glass columns (inner diameter: 15 cm, height: 65 cm), filled with 5 cm of gravel (Ø 1 – 2 mm) and 52 cm of sand (Ø 0.40 – 0.63 mm) and planted

with *Phragmites australis* (Cav.) (Figure III-1). Physical properties and chemical characteristics of the sand and gravel have been described elsewhere (Durst et al., 2013). The wetlands were kept in an air conditioned room at  $20\text{ }^{\circ}\text{C} \pm 0.5\text{ }^{\circ}\text{C}$ , and exposed daily to light from a LED lamp (Greenpower LED lamp, Philips®, Eindhoven, The Netherlands) for 8 hours. All tubing and stoppers in contact with the wetlands matrix was made of Viton® (Rotilabo®, Carl-Roth, Karlsruhe, Germany). Five sampling ports were located at 15, 25, 35, 45 and 55 cm from the inlet point in each column. Dissolved oxygen concentrations were monitored using non-invasive oxygen sensors (Presens®, Germany) facing each of the five sampling points that were mounted inside the columns (Figure III-1). Water used to supply the wetlands was taken monthly from a vegetated ditch (Alteckendorf, France) that collects chloroacetanilide contaminated agricultural runoff from sugar beet and corn catchments. Inlet water composition can be found in the Appendix, Table III-2. The water was continuously pumped to the wetlands inlets at a flow rate of  $0.33\text{ mL min}^{-1}$  using a high precision pump (ISMATEC® IPC model ISM936D, Zürich, Switzerland). Nominal residence time was calculated to be approximately 9.3 days. Lab-scale wetlands were covered with reflective foil to prevent algal growth and photolytic decay of chloroacetanilides.

The lab-scale wetland experiment was carried out over 202 days. The injection of chloroacetanilides in wetlands was preceded by an inoculation period of 104 days, during which the wetlands were supplied with vegetated ditch water without addition of herbicides. Metolachlor, acetochlor and alachlor were dissolved in ultrapure water and stored at  $-20\text{ }^{\circ}\text{C}$  until they were added to the inlet water. Three columns were supplied each with one of the target herbicides metolachlor, acetochlor and alachlor with an initial concentration of  $1.8\text{ }\mu\text{M}$  for metolachlor and  $1.9\text{ }\mu\text{M}$  for acetochlor and alachlor. A fourth column was supplied with vegetated ditch water without addition of herbicide. The supplied water was renewed and herbicides were added biweekly, after each sampling campaign. No significant change in chloroacetanilides concentrations was observed in the inlet tanks during two weeks period between sampling campaigns (nonparametric Wilcoxon test for paired samples,  $p > 0.05$ ).

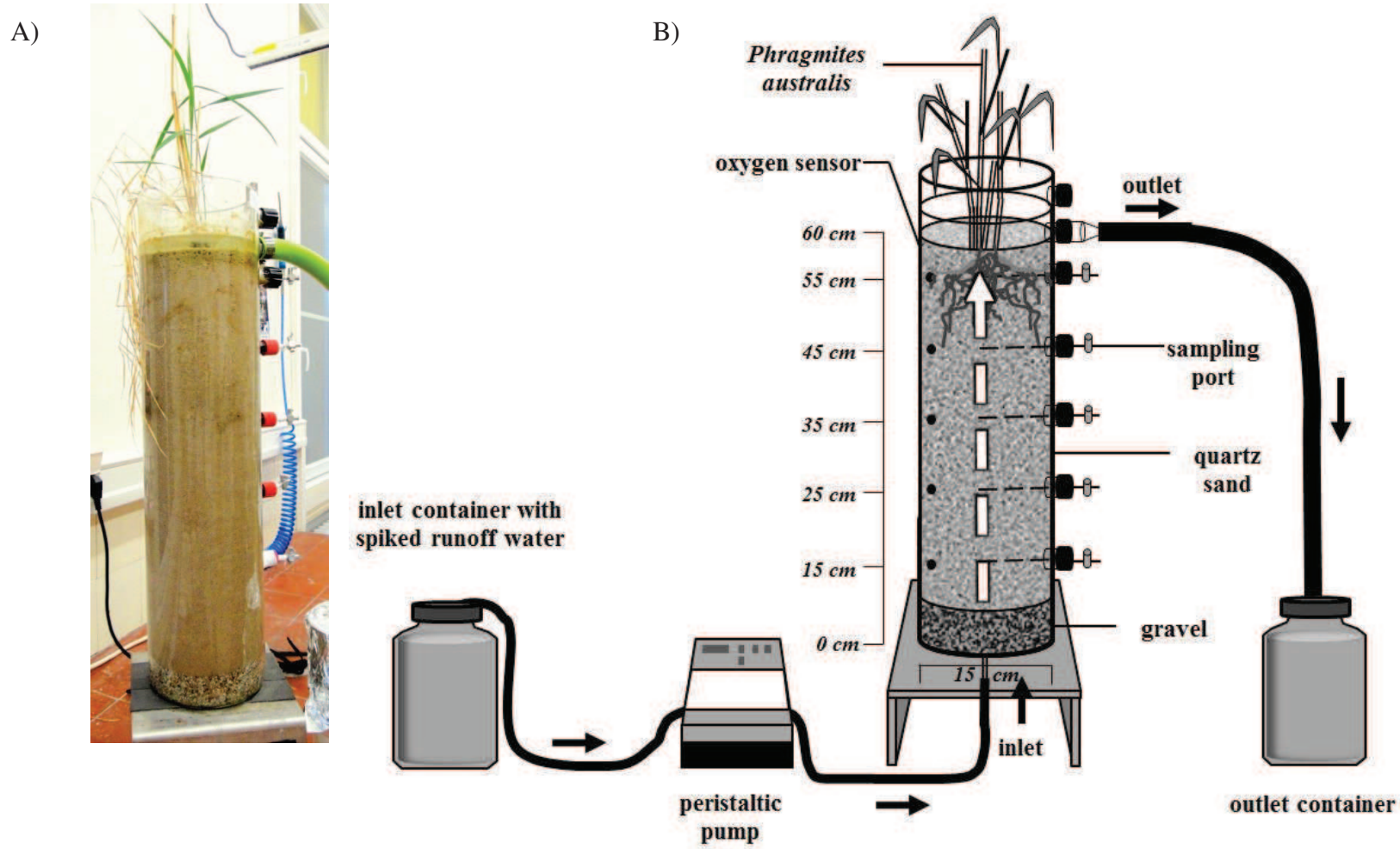


Figure III-1. Picture (A) and schematic representation (B) of the vertical flow lab-scale wetlands. Arrows indicate water flow direction.

### 2.5. Pore water sampling

Sampling campaigns were carried out biweekly at 0, 14, 28, 42, 56, 70, 84 and 98 days where day 0 represents the first day of chloroacetanilide injection. At each sampling campaign, water samples were retrieved with a glass syringe from the previous and the freshly prepared tank with spiked herbicides, the wetland inlet, outlet and from the five sampling ports for hydrochemical (30 mL), herbicide concentration and CSIA analyses (30 mL).

### 2.6. Hydrochemical analysis

Conductivity, pH and dissolved oxygen concentration were directly measured in wetland inlet and outlet water using WTW multi 350i sensors (WTW, Weilheim, Germany). Concentrations of dissolved organic carbon, major ions, total phosphorous, total sulphur and metals were determined by FR EN ISO standards and laboratory procedures.

### 2.7. Data analysis

Inlet hydrochemistry, chloroacetanilide concentration and stable carbon isotope inlet values were calculated as the average values of freshly spiked inlet water and the same inlet water after two weeks, at the time of the sampling. The nonparametric Wilcoxon test for paired samples was applied at a significance level of 0.05 to compare inlets and outlets hydrochemical parameters using the program R (R: Copyright 2005, The R Foundation for Statistical Computing, Version 2.15.1).

Daily chloroacetanilide loadings inflowing and outflowing the wetlands were estimated by interpolating and multiplying chloroacetanilide concentrations between consecutive sampling dates and the corresponding daily flow rate. Loads of chloroacetanilides at a given point between two sampling campaigns was calculated from the integral sum of all the daily load estimates. Mass removal of chloroacetanilides [%] was calculated as the relative decrease of outlet mass ( $mass_{out}$ ) to the inlet mass ( $mass_{in}$ ) for each lab-scale wetland on the same time period.



## 2.8. Carbon isotope notation and calculation

The carbon isotope ratios were reported in  $\delta$  notation in parts per thousand [‰] relative to the international carbon isotope standard Vienna Pee Dee Belemnite (V-PDB), according to the following Eqn. (2):

$$\delta^{13}\text{C}_{\text{sample}} = \frac{(\text{R}_{\text{sample}} - \text{R}_{\text{standard}})}{\text{R}_{\text{standard}}}$$

where  $\text{R}_{\text{sample}}$  and  $\text{R}_{\text{standard}}$  are the ratios  $^{13}\text{C}/^{12}\text{C}$  of sample and standard.

Bulk isotope enrichment factors ( $\epsilon_{\text{bulk}}$ ) were calculated from logarithmic linearization of the Rayleigh equation, Eqn. (3):

$$\ln\left(\frac{\delta^{13}\text{C}_x + 1000}{\delta^{13}\text{C}_{\text{in}} + 1000}\right) = \frac{\epsilon_{\text{bulk}}}{1000} \times \ln\left(\frac{C_x}{C_{\text{in}}}\right)$$

where  $\delta^{13}\text{C}_{\text{in}}$  and  $\delta^{13}\text{C}_x$  are the measured carbon isotope ratios of the substrate at inlet and at a given sampling point, and  $C_{\text{in}}$  and  $C_x$  are the concentrations of the substrate in inlet and at a given sampling point, respectively.

In order to compare observed carbon isotope fractionation with fractionation reported in literature, the apparent kinetic isotope effect (AKIE) values were calculated using Eqn. 4, according to Elsner et al. (Elsner et al., 2005).

$$\text{AKIE} \approx 1/1 + z \times \left(\frac{n}{x}\right) \times \frac{\epsilon_{\text{bulk}}}{1000}$$

where  $n$  is the number of atoms of a given element,  $x$  is the number of indistinguishable reactive positions, and  $z$  is the number of positions in intramolecular competition.

## 3. Results and discussion

### 3.1. Transport and attenuation of chloroacetanilide herbicides

Hydrochemical parameters were monitored to evaluate the evolution of prevailing hydrogeochemical conditions in the wetlands throughout the experiment (see Appendix, Table III-2). pH values ranged from 7.3 to 8.3 for the four wetlands, and did not significantly change between inlets and outlets ( $p > 0.05$ ). A spatial gradient of oxygen concentrations was observed in the four lab-scale wetlands with oxic conditions ( $212 \pm 24 \mu\text{M}$ ) prevailing at the bottom of the wetlands between 15-25 cm, and anoxic conditions between 45-55 cm from inlet points. Oxygen concentrations at the top of the wetlands were lower for acetochlor and alachlor

wetlands ( $2 \pm 10 \mu\text{M}$ ) than for metolachlor and control wetlands ( $52 \pm 44 \mu\text{M}$ ). Nitrate inlet concentration averaged  $484 \pm 38 \mu\text{M}$  and decreased significantly inside the four wetlands ( $p < 0.05$ ). Nitrate dissipation observed in the four wetlands indicates that nitrate reducing conditions prevailed in anoxic zones towards wetlands outlets. Higher nitrate dissipation occurred in wetlands supplied with acetochlor and alachlor (78 and 73% decrease in average  $\text{NO}_3^-$  concentrations respectively) compared to metolachlor and control wetlands (47 and 25% respectively), following the same trend observed for oxygen profiles. Sulphate concentrations did not significantly change between the inlets and outlets ( $537 \pm 24 \mu\text{M}$ ) throughout the experiment except for a significant ( $p = 0.02$ ) but small (9%) decrease in the outlet of the wetland supplied with acetochlor, which indicates the prevalence of stronger reducing conditions in this wetland. Other redox sensitive species, such as manganese and ferrous iron, remained low ( $< 4 \mu\text{M}$ ) over the course of the experiment, and are thus expected to play only a minor role in biodegradation processes in the systems.

The dissipation of chloroacetanilide herbicides in the wetlands was evaluated using a mass-balance approach. Removal of acetochlor and alachlor loads from inlets to outlets from day 24 to day 98 averaged  $56 \pm 6\%$  and  $53 \pm 11\%$  respectively, whereas metolachlor was more persistent with an average mass removal of  $23 \pm 5\%$  (Appendix, Table III-3). Higher removal rates (62- 90% for the three herbicides) observed during the early stages of the experiment gradually decreased and stabilised in the period between day 14 to day 28. This could be explained by chloroacetanilide sorption to sand, glass or plant roots in the wetlands that occurred in the initial phase of chloroacetanilide injection. During this initial phase of the experiment it is likely that equilibrium was established between sorbed and dissolved chloroacetanilide, therefore, effects of sorption on chloroacetanilide removal at later stages of the experiment are expected to be minimal. In a previous study, more than 95% of sorption of metolachlor, alachlor and acetochlor on soil was found to occur within 4 hours (Liu et al., 2000).

Other abiotic processes alone are unlikely to cause the observed removal of acetochlor and alachlor. Photolysis was avoided by the reflective foil used to protect the systems from light. Volatilization of chloroacetanilides from the water phase is unlikely since their volatilization rate is low at  $20^\circ\text{C}$  (see Table I-1). Although biotic removal through plant uptake cannot be excluded, chloroacetanilides have relatively high octanol /water coefficient ( $\text{Log}K_{ow}$  3.1- 4.1) and are thus expected to be retained by the lipids in root epidermis hindering further uptake by plant cells (Trapp, 1995). In a previous study, metolachlor found in plant samples accounted

for maximally 10% of the total measured metolachlor mass in constructed wetlands (Moore et al., 2001). Therefore, microbial degradation is considered to be the main process affecting chloroacetanilide herbicides attenuation in the lab-scale wetlands, as previously suggested in field experiments (Stamper and Tuovinen, 1998; Fenner et al., 2013).

Degradation of chloroacetanilides was previously observed under both aerobic and anaerobic conditions (Graham et al., 2000). In our study, the attenuation of the chloroacetanilides occurred essentially in oxygen depleted zones in the upper parts of the wetlands (Appendix, Figure III-3), suggesting enhanced degradation of chloroacetanilides under anoxic conditions. Biodegradation in the oxygen depleted zones in the upper part of the wetlands may be associated with the root zones where enhanced microbial activity and density is expected (Imfeld et al., 2009), as previously demonstrated for metolachlor (Anderson et al., 1994). Enhanced degradation of chloroacetanilides in predominantly anoxic zones comes in accordance with previous investigation in a mesocosm scale field experiment, where removal of alachlor was larger under anaerobic conditions than under aerobic conditions (Graham et al., 2000). It should be noted that oxygen measurements were taken along the periphery of the column, and thus did not account for micro-redox gradients which could be present in the lab-scale wetlands (Alewell et al., 2008), therefore aerobic degradation may also have contributed to chloroacetanilides removal in the wetland.

The persistence of metolachlor in comparison to other chloroacetanilides observed in our experiment was previously demonstrated in anoxic soil (Konopka, 1994), in oxic water (Graham et al., 1999), and in aerobic microbial cultures (Zhang et al., 2011). The persistence of metolachlor in the wetlands can be explained by the substitution of an amide alkoxyethyl side chain, present in alachlor and acetochlor, with a bulkier alkoxyethyl side chain, present in metolachlor, which may lead to greater steric hindrance around the carbon chlorine bond and lower degradation rates (Zhang et al., 2011).

In order to evaluate the occurrence of *in situ* degradation in the wetlands and to obtain an insight into mechanisms involved in the initial transformation step of chloroacetanilides, CSIA was applied to analyse isotope composition of chloroacetanilides in lab-scale wetland samples.

### 3.2. Chloroacetanilide carbon isotope fractionation

The developed CSIA method was used to evaluate *in situ* biodegradation of chloroacetanilides in the lab-scale wetlands. Samples from inlets, outlets and two points inside the wetlands at 25

and 55 cm from the inlets were collected for carbon isotope analysis at days 42, 70 and 98 (Figure III-2). CSIA of chloroacetanilides at the wetland inlets and outlets revealed similar average carbon isotope enrichment for alachlor ( $\Delta\delta^{13}\text{C}$  of  $2.5 \pm 0.33\text{‰}$ ) and acetochlor ( $\Delta\delta^{13}\text{C}$  of  $2.6 \pm 0.02\text{‰}$ ). In contrast, enrichment in carbon isotope composition of metolachlor from the wetland inlet to the outlet was small ( $\Delta\delta^{13}\text{C} \leq 0.7\text{‰}$ ). Isotope composition values at 25 and 55 cm from the inlet indicate that carbon isotope fractionation occurred in anoxic zones towards the outlets of the wetlands and correlated with the mass dissipation of the herbicides (Figure III-2). The correlation between changes in the carbon isotope composition of chloroacetanilide and their mass removal confirms the occurrence of biodegradation in the wetlands.

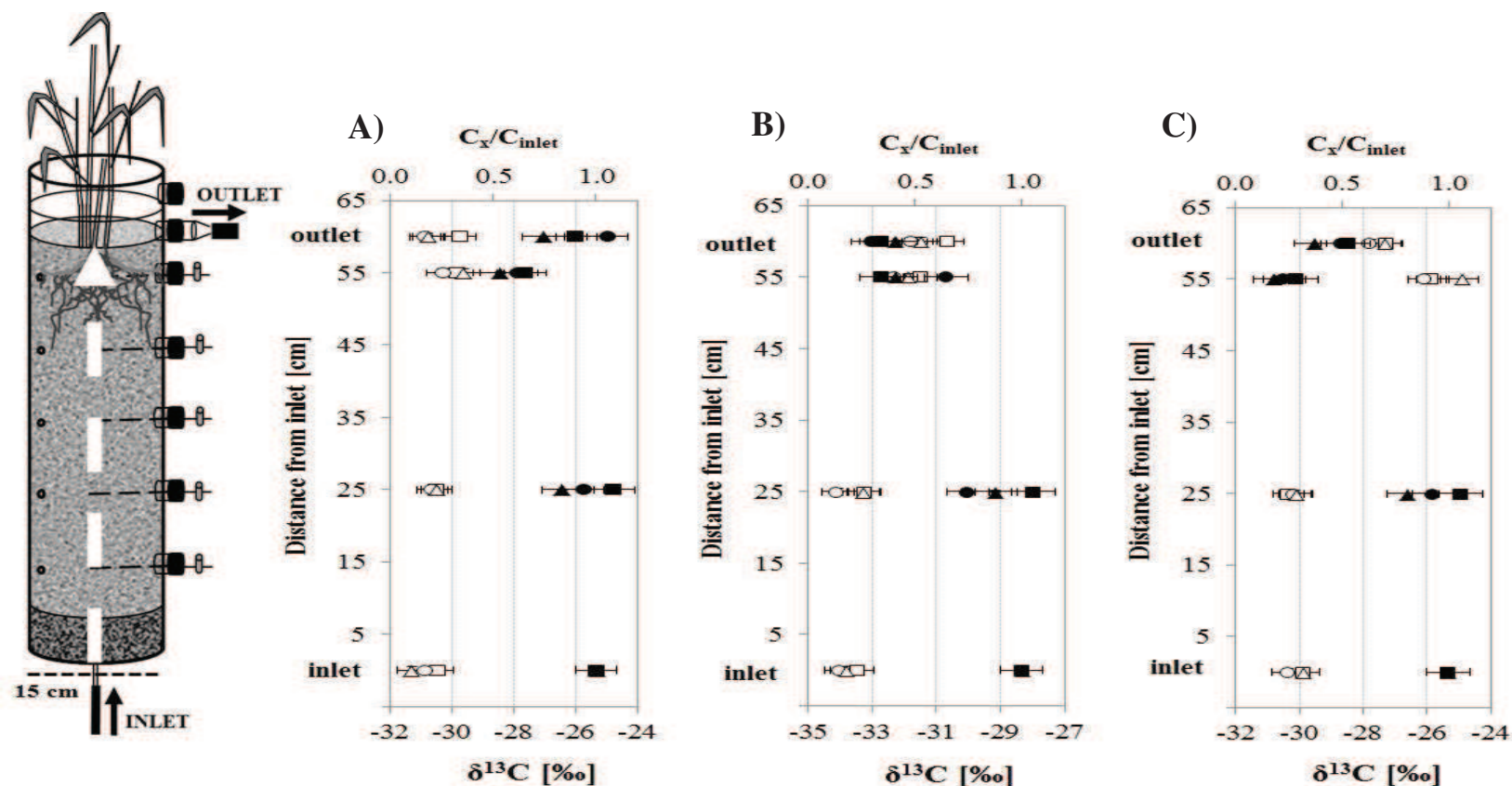


**Figure III-2. Carbon isotope signatures of metolachlor, acetochlor and alachlor in lab-scale wetlands.** Carbon isotope composition represented in  $\delta^{13}C$  notation (open symbols) and ratio of concentration at a given point (x) to inlet concentration (filled symbols) of metolachlor A) alachlor B) and acetochlor C) inside lab-scale wetlands on day 42 (squares), day 70 (circles) and day 98 (triangles). Arrows indicate the direction of water flow. Error bars indicate uncertainty of  $\delta^{13}C$  ( $\pm 0.5\text{‰}$ ), and propagated error of  $C_x/C_{inlet}$  based on standard deviations of concentrations.

Estimates of enrichment factors for alachlor and acetochlor were calculated according to the Rayleigh model (Eqn. 2) for closed systems taking inlet values as initial values of  $\delta^{13}\text{C}$ . Enrichment factors were not calculated for metolachlor because variations in carbon isotopic composition of metolachlor were too small ( $\leq 0.8\text{‰}$ ) to be considered significant given the uncertainty of the method. Separate enrichment factors ( $\epsilon_{\text{bulk}}$ ) were calculated by linear regression for days 42, 70 and 98 to examine the evolution of prevailing degradation pathways through time. Enrichment factors ranged from  $-1.5 \pm 0.9\text{‰}$  to  $-2.1 \pm 0.4\text{‰}$  for alachlor and  $-3.2 \pm 1.2\text{‰}$  to  $-3.6 \pm 1.1\text{‰}$  for acetochlor and were not significantly different taking into account the uncertainty of the calculations (Table III-1). Average enrichment factors calculated using all points from the three sampling dates were  $\epsilon_{\text{bulk}} = -2.0 \pm 0.3\text{‰}$  for alachlor and  $\epsilon_{\text{bulk}} = -3.4 \pm 0.5\text{‰}$  for acetochlor (Appendix, Figure III-4, Table III-1). A potential source of bias contributing to the observed fractionation is the possibility of preferential flow paths in the wetlands. This phenomenon might have led to the mixing of water containing chloroacetanilides coming from different flow paths with different travel times and extent of chloroacetanilide degradation upon reaching of the outlet (Thullner et al., 2012). This mixing effect is evident in the wetland supplied with acetochlor (Figure III-2 C), where concentrations were higher at the outlet than at the sampling port at 55 cm. However, this effect did not change significantly the enrichment factor calculated for acetochlor ( $\epsilon_{\text{bulk}} = -3.2 \pm 0.2\text{‰}$  without the outlet value, and  $-3.4 \pm 0.5\text{‰}$  including the outlet value).

Since this is the first report for chloroacetanilide isotope fractionation, no values of enrichment factors are available for comparison. In order to further interpret the observed fractionation and provide indication of prevailing degradation mechanisms, we calculated AKIE values for alachlor and acetochlor degradation in lab-scale wetlands. AKIE values have the advantage of being associated with isotope effect of the specific bond cleavage, and therefore can be used for comparison of isotope fractionation between different compounds. Different degradation pathways for chloroacetanilide herbicides have been reported including thiolytic (glutathione-dependent) dechlorination (Graham et al., 1999), hydrolytic dechlorination, N-atom dealkylation (Sanyal and Kulshrestha, 2002) and reductive dechlorination (Helbling et al., 2010). Glutathione-dependant dechlorination and N-atom dealkylation have been mainly observed in aerobic systems. No studies could be found in literature investigating chloroacetanilides degradation pathways under anaerobic conditions.

For AKIE calculations, the number of carbon atoms in the reactive position does not vary for different possible reactions, where in all cases  $x$  and  $z$  are equal to one. AKIE values ranged from 1.022 to 1.031 for alachlor, and from 1.046 to 1.053 for acetochlor (Table III-1). Acetochlor AKIE values fit in the range of experimentally derived AKIEs from literature for  $S_N2$  type nucleophilic substitution reactions involving C-N, C-Cl or C-O bonds (1.03- 1.09), whereas they are higher than typical reported values of  $S_N1$  type substitution reactions (1.00-1.03), reductive dechlorination (1.027-1.033), and oxidative N-dealkylation reactions (up to 1.019) (Skarpeli-Liati et al., 2012), suggesting hydrolytic or thiolytic  $S_N2$  type nucleophilic substitution to be the first degradation step for acetochlor in our systems. On the other hand, alachlor AKIE values overlap with reported ranges for both nucleophilic substitution and reductive dechlorination reactions. It should be noted that other rate limiting steps preceding the initial degradation step such as transport across cell membrane and substrate binding to enzyme reactive site can lower observed fractionation leading to lower AKIEs (Nijenhuis et al., 2005).

**Table III-1. Bulk enrichment factors and AKIE values calculated for alachlor and acetochlor for sampling campaigns at days 42, 70 and 98 and for data from the three campaigns combined.** For AKIE calculations  $n = 14$ ,  $z = 1$  and  $x = 1$ .

day	$\epsilon_{\text{bulk}}^{\text{a}}$ [‰]		AKIE <sup>b</sup>	
	Alachlor	Acetochlor	Alachlor	Acetochlor
42	$-2.1 \pm 0.4$	$-3.5 \pm 0.4$	$1.031 \pm 0.006$	$1.052 \pm 0.006$
70	$-1.5 \pm 0.9$	$-3.2 \pm 1.2$	$1.022 \pm 0.013$	$1.046 \pm 0.018$
98	$-2.1 \pm 0.2$	$-3.6 \pm 1.1$	$1.030 \pm 0.003$	$1.053 \pm 0.017$
all	$-2.0 \pm 0.3$	$-3.4 \pm 0.5$	$1.028 \pm 0.004$	$1.051 \pm 0.007$

<sup>a</sup> Standard errors for  $\epsilon_{\text{bulk}}$  were calculated *via* linear regression analysis.

<sup>b</sup> Errors for AKIE values were calculated *via* error propagation based on  $\pm 1$  standard deviation of the  $\epsilon_{\text{bulk}}$  values.

Additional insights on mechanisms of bond cleavage can be obtained using multi-element CSIA of nitrogen, hydrogen or chlorine (Vogt et al., 2008). Unfortunately, the utility of nitrogen and hydrogen isotope analysis is reduced by current detection limits of CSIA. Given

the small contribution of nitrogen and hydrogen to the molar mass of a chloroacetanilide molecule and the amount required of each element for analysis (30 and 42 ng on column for hydrogen and nitrogen respectively), inlet concentrations in the range of 50 to 100  $\mu\text{M}$  would have been needed for CSIA in our experiment. This limitation currently reduces the potential of multi-element CSIA analyses of pesticides at environmental concentrations. Chlorine isotope analysis, on the other hand, would require concentrations in the same range as carbon isotope analysis, but chlorine isotopic analytical methods still need to be developed (Elsner et al., 2012). In addition to CSIA, degradation product analysis can provide important complementary information to help unravel degradation pathways. In the case of chloroacetanilide herbicides, this is not a straightforward task due to the large number of potential degradation products, and the lack of information on extant degradation pathways. Recent developments in high resolution mass spectrometry methods may help develop such investigations in the near future (Fenner et al., 2013).

Our results highlight the applicability of CSIA to study the fate of relatively large organic compounds (containing 14 -15 carbon atoms) in the environment. Based on calculated average enrichment factors, we expect differences in carbon isotopic composition ( $\Delta\delta^{13}\text{C}$ ) of 1.4‰ and 2.4‰ for alachlor and acetochlor respectively at 50% degradation, and 4.6‰ and 7.8‰ respectively at 90% degradation. Given the fact that such differences are detectable within current analytical limitations, the suitability of CSIA to study the fate of larger organic contaminants in the environment is demonstrated, encouraging further development of such methods for a large variety of micropollutants, and most notably pharmaceuticals and pesticides.

#### 4. Conclusion

CSIA is an emerging tool in the study of pesticides transport and transformation in dynamic and complex ecosystems such as wetlands. In this study, moderate mass removal for acetochlor and alachlor of 56 and 51% respectively was observed under denitrifying conditions, in contrast to lower removal for metolachlor of 23%. With a novel CSIA method, a pronounced carbon stable isotope fractionation was measured, indicating *in situ* biodegradation of alachlor ( $\epsilon_{\text{bulk}} = -2.0 \pm 0.3$ ) and acetochlor ( $\epsilon_{\text{bulk}} = -3.4 \pm 0.5$ ) in the lab-scale wetlands. Our results demonstrate the potential of CSIA, combined with traditional approaches, in evaluating the transport of



chloroacetanilide herbicides in biogeochemically dynamic environments such as wetlands. Further laboratory investigations aiming at providing reference enrichment factors and analysis of degradation products under different hydrogeochemical conditions are needed to allow the evaluation of chloroacetanilide transport and degradation in the environment.

## 5. Acknowledgments

This research has been funded by the European Union under the 7th Framework Programme (Marie Curie Initial Training Network CSI:ENVIRONMENT, contract number PITN-GA-2010-264329). The authors wish to thank Ana Cristina Abenza for her contribution in chloroacetanilide quantification. We specially acknowledge Mathias Gehre and Ursula Günther for technical assistance in the isotope laboratory of the UFZ, and Sara Herrero Martin for helpful discussions.

## 6. Appendix Chapter III - section 1

### Chloroacetanilide extraction and quantification

The extraction procedure was adapted from USA EPA method 525.2 using an AutoTrace 280 SPE system (Dionex®, CA, USA) for simultaneous extraction of 6 samples. Extraction cartridges were washed with 5 mL of ethyl acetate, followed by 5 mL of dichloromethane. The cartridges were then sequentially conditioned by 10 mL of methanol and 10 mL of deionised water. Cartridges were then loaded with the samples and dried under nitrogen flux for 10 min. Elution of chloroacetanilides was performed by 5 mL of ethyl acetate followed by 5 mL of dichloromethane. The extract was subsequently concentrated under nitrogen flux to 1 droplet, and resuspended in dichloromethane for quantification and isotopic composition analyses.

Analysis of chloroacetanilide concentrations was performed by gas chromatography-tandem mass spectrometry (GC-MS/MS, Focus-ITQ 700, Thermo Scientific, Illkirch, France). A mixture of metolachlor-*d*<sub>6</sub> and alachlor-*d*<sub>13</sub> was spiked in each sample as internal standard at 100 µg L<sup>-1</sup>. Pulsed injection (3 µL at 3 mL min<sup>-1</sup> for 1 min) was done using an AI/AS 3000 autosampler (Thermo Fisher Scientific, USA) in splitless mode. Separation of metolachlor, alachlor and acetochlor separations was performed on an Optima 5MS column (30 m x 0.25 mm ID, 0.25 mm OD; MN, Hoerd, France), with helium as a carrier gas, at a flow of 1 mL

min<sup>-1</sup>. The column was initially held at 50 °C for 2 min, heated at 30 °C min<sup>-1</sup> to 150 °C, then up to 250 °C at 5 °C min<sup>-1</sup> and finally heated at 30 °C min<sup>-1</sup> to 300 °C and held for 5 min. Injector and transfer line temperatures were 280 °C and 300 °C, respectively. Each sample was measured in triplicate. The limit of quantitation was 10 µg L<sup>-1</sup> with a mean precision of 8%.

**Table III-2. Average values (mean  $\pm$  standard deviation) for hydrochemical parameters of inlets and outlets of lab-scale wetlands from day 0 to day 98. Ranges are indicated between brackets.**

Parameter	Inlet	Outlet metolachlor	Outlet alachlor	Outlet acetochlor	Outlet control
<b>pH</b>	7.7 $\pm$ 0.1 (7.7 - 8.1)	7.7 $\pm$ 0.2 (7.4 - 7.9)	7.7 $\pm$ 0.2 (7.5 - 8.1)	7.8 $\pm$ 0.2 (7.4 - 8.3)	7.8 $\pm$ 0.3 (7.3 - 8.1)
<b>EC</b>	776 $\pm$ 85 (627 - 902)	708 $\pm$ 26 (677 - 754)	678 $\pm$ 33 (630 - 715)	675 $\pm$ 32 (630 - 707)	713 $\pm$ 31 (679 - 749)
<b>DOC</b>	3.8 $\pm$ 1.3 (2.6 - 5.2)	21.8 $\pm$ 8.1 (9.6 - 30.6)	58.6 $\pm$ 63.3 (4.4 - 172.2)	43.5 $\pm$ 79.6 (5.3 - 239.2)	27.7 $\pm$ 21.4 (7.2 - 64.1)
<b>Nitrate [<math>\mu</math>M]</b>	484 $\pm$ 38 (389 - 534)	256 $\pm$ 63 (170 - 345)	132 $\pm$ 91 (37 - 301)	107 $\pm$ 63 (26 - 186)	364 $\pm$ 106 (247 - 488)
<b>Ferrous iron [<math>\mu</math>M]</b>	2 $\pm$ 2 (0 - 8)	1 $\pm$ 1 (0 - 3)	2 $\pm$ 1 (0 - 4)	3 $\pm$ 5 (0 - 13)	1 $\pm$ 1 (0 - 3)
<b>Manganese [<math>\mu</math>M]</b>	< 1	< 1	< 1	< 1	< 1
<b>Sulphate [<math>\mu</math>M]</b>	539 $\pm$ 36 (433 - 591)	555 $\pm$ 62 (429 - 610)	522 $\pm$ 34 (476 - 581)	488 $\pm$ 37 (441 - 553)	570 $\pm$ 54 (481 - 656)
<b>Phosphate [ <math>\mu</math>M]</b>	< 1	$\leq$ 1	$\leq$ 1	< 1	$\leq$ 1
<b>Chloride [mM]</b>	3.0 $\pm$ 1.1 (2.0 - 5.2)	3.0 $\pm$ 2.0 (1.7 - 7.5)	2.9 $\pm$ 1.2 (2.1 - 5.7)	3.0 $\pm$ 1.5 (1.8 - 6.3)	3.0 $\pm$ 2.0 (1.9 - 7.6)
<b>Phosphorus [<math>\mu</math>M]</b>	0 $\pm$ 0 (0 - 1)	1 $\pm$ 0 (0 - 1)	1 $\pm$ 0 (0 - 1)	2 $\pm$ 4 (0 - 8)	0 $\pm$ 0 (0 - 1)
<b>Sulphur [<math>\mu</math>M]</b>	549 $\pm$ 19 (506 - 576)	572 $\pm$ 41 (498 - 605)	539 $\pm$ 40 (490 - 605)	476 $\pm$ 46 (418 - 528)	568 $\pm$ 22 (534 - 597)
<b>Sodium [<math>\mu</math>M]</b>	909 $\pm$ 65 (761 - 1.040)	915 $\pm$ 152 (630 - 1.070)	940 $\pm$ 132 (665 - 1.060)	957 $\pm$ 105 (743 - 1.040)	941 $\pm$ 165 (583 - 1.080)
<b>Magnesium [<math>\mu</math>M]</b>	959 $\pm$ 34 (909 - 1.040)	1,010 $\pm$ 160 (691 - 1.120)	966 $\pm$ 104 (744 - 1.060)	946 $\pm$ 100 (765 - 1.070)	989 $\pm$ 124 (728 - 1.090)
<b>Potassium [ <math>\mu</math>M]</b>	24 $\pm$ 3 (18 - 33)	40 $\pm$ 37 (14 - 113)	30 $\pm$ 14 (20 - 59)	77 $\pm$ 57 (32 - 198)	24 $\pm$ 9 (15 - 37)
<b>Calcium [mM]</b>	3.2 $\pm$ 0.4 (2.2 - 3.6)	2.2 $\pm$ 0.3 (1.8 - 2.5)	2.3 $\pm$ 0.3 (1.9 - 2.7)	2.4 $\pm$ 0.4 (2.0 - 2.9)	2.3 $\pm$ 0.3 (1.8 - 2.7)

**Table III-3. Average mass removal [%] of metolachlor, alachlor and acetochlor between inlets and outlets of lab-scale wetlands between day 28 and 98, and during the three periods of isotope investigation.**

Time period [days]	Mass removal [%]		
	Metolachlor	Alachlor	Acetochlor
28 - 42	24	39	48
56 - 70	27	59	55
84 - 98	20	45	65
28 - 98 (n = 5)	23 ± 5	51 ± 9	56 ± 6

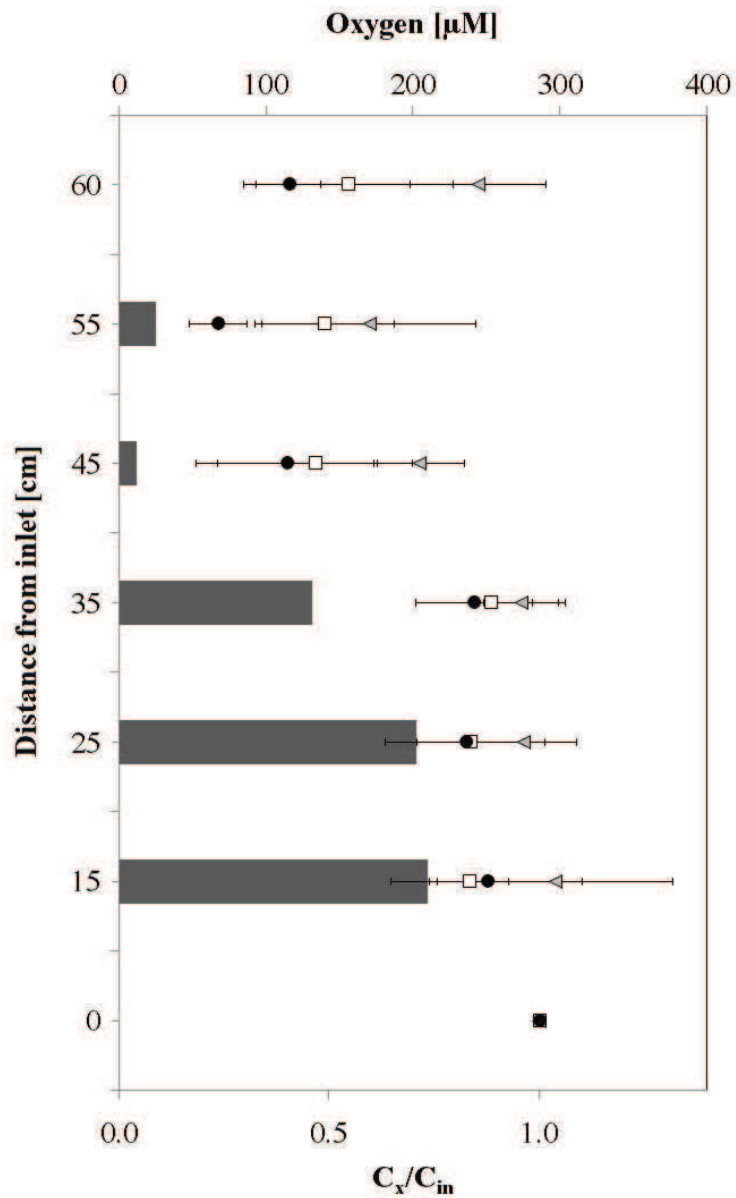


**Figure III-3.** Relative concentrations ( $C_x/C_{in}$  = concentration at point (x) divided by inlet concentration) for metolachlor (triangles), alachlor (squares) and acetochlor (circles) and corresponding average oxygen concentrations at different depths in lab-scale wetlands. Values are averages  $\pm$  standard deviations of samplings at day 14, 28, 42, 56, 70, 84 and 98.

**Table III-4. Mean and standard deviations of stable carbon isotope ( $\delta^{13}\text{C}$ ) triplicate measurements for two weeks old inlets (two weeks inlet), freshly spiked inlets (fresh inlet) and outlets at days 42, 70 and 98. Propagated errors for average inlet values are indicated in brackets.**

		day 42	day 70	day 98
<b>Metolachlor</b>	two weeks inlet	$-30.5 \pm 0.10$	$-30.6 \pm 0.27$	$-31.2 \pm 0.18$
	fresh inlet	$-30.3 \pm 0.05$	$-31.1 \pm 0.14$	$-31.3 \pm 0.07$
	average inlet	$-30.4 (0.06)$	$-30.9 (0.15)$	$-31.3 (0.09)$
	Outlet	$-29.7 \pm 0.26$	$-30.8 \pm 0.08$	$-30.8 \pm 0.10$
<b>Alachlor</b>	two weeks inlet	$-33.3 \pm 0.10$	$-33.9 \pm 0.36$	$-33.8 \pm 0.06$
	fresh inlet	$-33.6 \pm 0.23$	$-34.1 \pm 0.17$	$-33.8 \pm 0.14$
	average inlet	$-33.5 (0.13)$	$-34.0 (0.20)$	$-33.8 (0.08)$
	Outlet	$-30.6 \pm 0.03$	$-31.8 \pm 0.33$	$-31.5 \pm 0.26$
<b>Acetochlor</b>	two weeks inlet	$-29.3 \pm 0.08$	$-29.8 \pm 0.11$	$-29.3 \pm 0.18$
	fresh inlet	$-29.4 \pm 0.22$	$-29.9 \pm 0.18$	$-29.4 \pm 0.26$
	average inlet	$-29.4 (0.12)$	$-29.8 (0.11)$	$-29.4 (0.16)$
	Outlet	$-26.8 \pm 0.12$	$-27.2 \pm 0.23$	$-26.8 \pm 0.12$

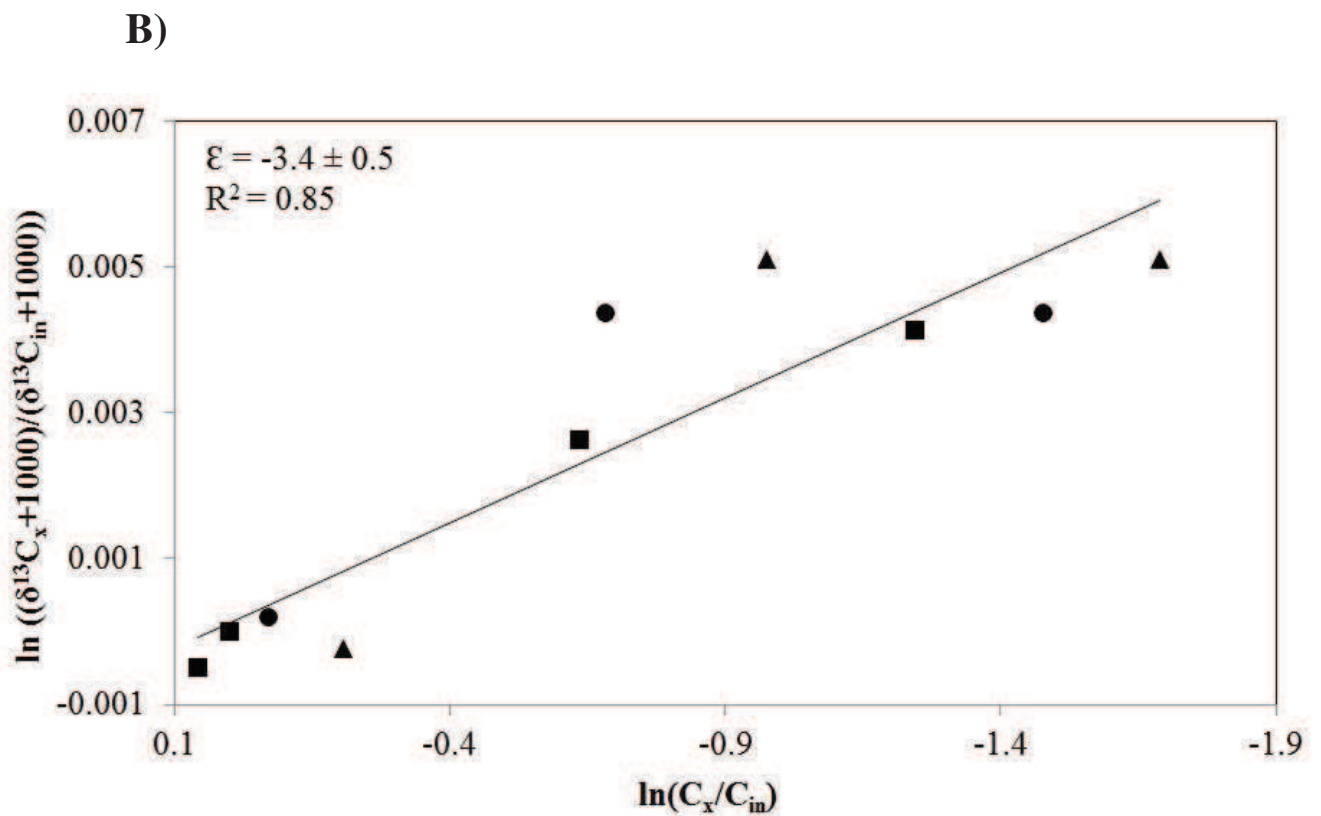
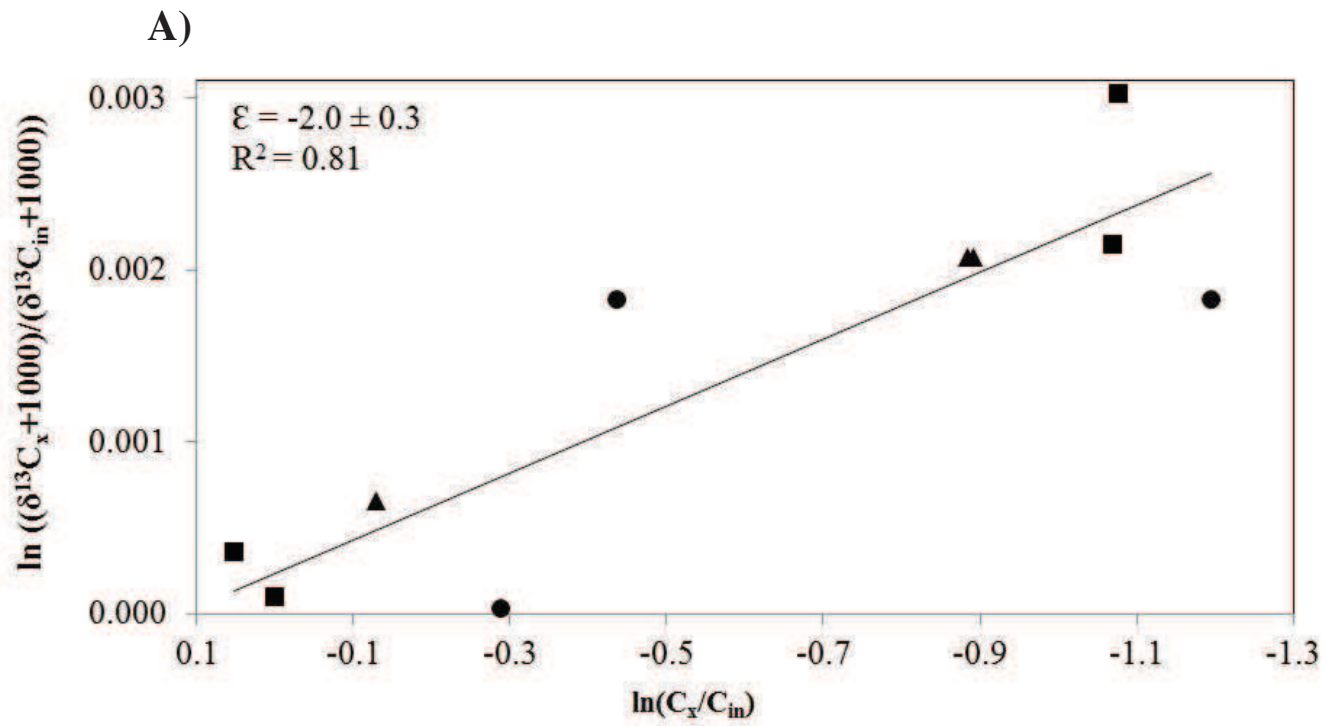


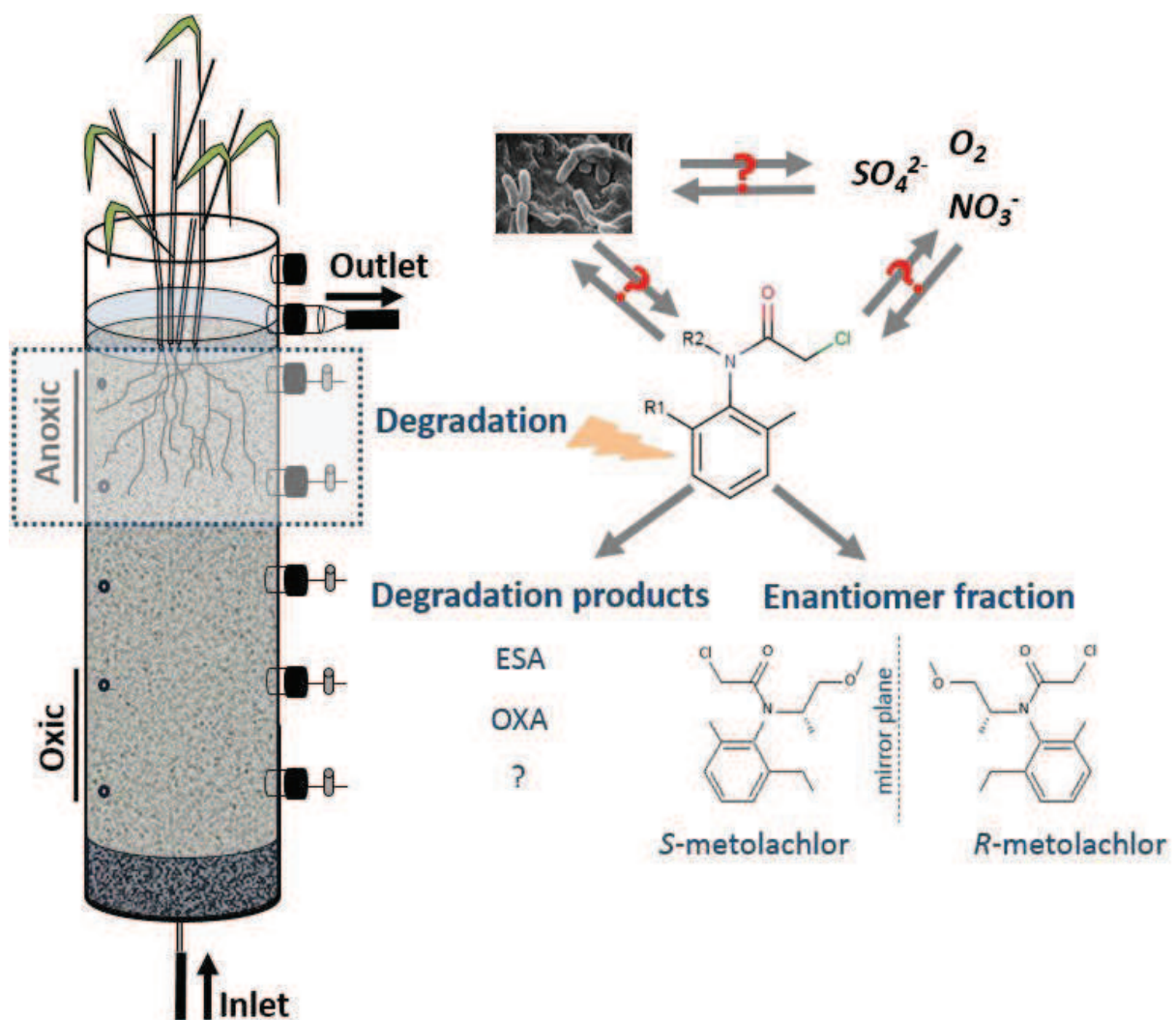
**Figure III-4. Linearized Rayleigh plots for alachlor A) and acetochlor B).** Data from day 42 (squares), day 70 (circles) and day 98 (triangles) are shown.

# Section 2. Degradation of chloroacetanilide herbicides and bacterial community composition in lab-scale wetlands

Omnia Fawzy Elsayed\*, Elodie Maillard\*, Stéphane Vuilleumier, Maurice Millet and Gwenaël Imfeld.

\* Both authors contributed equally to this work.

To be submitted to Science of the Total Environment





## Abstract

Degradation of chloroacetanilide herbicides *rac*-metolachlor, acetochlor, and alachlor, as well as associated bacterial populations, were evaluated in vertical upflow laboratory columns using a combination of hydrochemical and herbicide analyses, and DNA-based approaches. Mass dissipation of chloroacetanilides, continuously supplied at 1.8 – 1.9  $\mu\text{M}$  for 112 days, mainly occurred in the rhizosphere zone under nitrate and sulfate-reducing conditions, and averaged  $61 \pm 14\%$ ,  $52 \pm 12\%$  and  $29 \pm 19\%$  of the total in columns injected with acetochlor, alachlor or *rac*-metolachlor, respectively. Metolachlor enantiomer fractions of  $0.494 \pm 0.006$  in the oxic zone and  $0.480 \pm 0.005$  in the rhizosphere zone indicated preferential biodegradation of the *S*-enantiomer. Well-known chloroacetanilide ethane sulfonic acid and oxanilic acid degradates were detected at very low concentrations only ( $< 0.5$  nM), suggesting extensive degradation and the operation of as yet unknown pathways for chloroacetanilide degradation. Hydrochemical parameters and oxygen concentration were major drivers of wetland bacterial composition, whereas exposure to chloroacetanilides had no detectable impact. Taken together, the obtained results underline the importance of anaerobic degradation of chloroacetanilides in wetlands, and highlight the potential of complementary chemical and biological approaches to characterise the processes involved in dissipation of chloroacetanilides in the environment.

**Keywords:** Chloroacetanilides, chiral pesticides, wetlands, biodegradation, bacterial diversity

## 1. Introduction

Wetlands are reactive zones of the landscape that can intercept pesticide-contaminated surface runoff or groundwater. Wetland systems support a variety of biological, chemical and physical processes that make them “hotspots” for pesticide attenuation (Maillard et al., 2011; Imfeld et al., 2013). Transport and transformation pathways of pesticides depend on biogeochemical processes occurring in wetlands (Borch et al., 2010b) and on the associated microbial flora. Both the structure of a microbial community and the functions it performs may be influenced by pesticide exposure (Imfeld and Vuilleumier, 2012). DNA fingerprinting techniques and advances in high-throughput sequencing technologies now enable detailed DNA-based investigations of the microbial response to contaminants in wetland systems (Weber et al., 2011; Fahrenfeld et al., 2014), thereby encouraging the application of DNA-based bioindicators to assess wetland pesticide contamination status (Sims et al., 2013).

Chloroacetanilide herbicides are used worldwide for pre-emergence control of annual grasses and broad-leaved weeds for a variety of crops, including maize, sugar beet and sunflower (Pereira et al., 2009). Together with their degradation products, notably ethane sulfonic acids (ESA) and oxanilic acids (OXA), they are easily transported to non-target water bodies and are frequently detected in both ground and surface waters (Gadagbui et al., 2010; Baran and Gourcy, 2013a). Chloroacetanilide herbicides acetochlor, alachlor and metolachlor share the same 2-chloroacetanilide core structure (Table I-1) (Liu et al., 2001; Saha et al., 2012). Metolachlor is a chiral compound consisting of four diastereoisomers (i.e. two pairs of *S*- and *R*-enantiomers) (Ma et al., 2006). Alachlor and racemic metolachlor (*rac*-metolachlor) were extensively used until the mid-1990s, and were subsequently replaced by respectively acetochlor and *S*-metolachlor, which is enriched in the herbicidally more active 1'*S*-enantiomer (Müller et al., 2000; Xu et al., 2010a). Abiotic degradation and transport processes are essentially unaffected by stereo configuration, so preferential degradation of specific stereoisomeric forms can serve as a clear indication of *in situ* biodegradation (Wong et al., 2002; Milosevic et al., 2013).

Microbially-mediated degradation appears to be the major mode of dissipation of chloroacetanilide herbicides in wetlands (Gadagbui et al., 2010), but little is yet known about transport and modes of degradation of chloroacetanilides, and the associated bacterial diversity in contaminated redox-dynamic wetland environments. Using compound-specific isotope analysis (CSIA), we recently demonstrated *in situ* biodegradation of acetochlor and alachlor in vertical-flow laboratory wetlands designed to study the upward discharge of contaminated water into groundwater/surface-water interface ecosystems, and the processes leading to

dissipation of chloroacetanilide contaminants (Elsayed et al., 2014a). However, this study also brought up new questions. Was metolachlor, which was dissipated to a lesser extent than acetochlor and alachlor, actually degraded biologically, or was it only dissipated through non-degradative processes in such wetlands? What is the relationship between prevailing biogeochemical conditions and degradation of chloroacetanilides? How are bacterial communities affected by changes in biogeochemical conditions and chloroacetanilide exposure? In the present study, hydrochemical conditions, concentrations of *rac*-metolachlor, acetochlor and alachlor, of their ethane sulfonic acid (ESA) and oxanilic acid (OXA) degradates, and enantiomeric fractions of metolachlor in lab-scale wetlands, were determined, and their relation to bacterial composition and taxonomic diversity was explored using terminal restriction fragment length polymorphism (T-RFLP) and 454 pyrosequencing of the 16S rRNA bacterial gene amplified by PCR from DNA extracted from the wetlands.

## 2. Material and methods

### 2.1. Chemicals

Chloroacetanilides (*rac*-metolachlor, acetochlor, alachlor; Pestanal®, analytical grade purity: 97.2, 96.8 and 99.2 respectively) and solvents (methylene chloride, methanol and ethyl acetate; HPLC grade purity > 99.9%) were purchased from Sigma-Aldrich (St. Louis, MO, USA). Alachlor-*d*<sub>13</sub> and metolachlor-*d*<sub>6</sub> (Dr. Ehrenstorfer GmbH, Augsburg, Germany) were used as internal standards. Reference and stock solutions of chloroacetanilides were prepared in dichloromethane and stored at -20 °C.

### 2.2. Lab-scale wetlands

Wetlands consisted of four borosilicate glass columns (inner diameter: 15 cm, height: 65 cm), filled with 5 cm of gravel (Ø 1 – 2 mm) and 52 cm of sand (Ø 0.40 – 0.63 mm), and planted with *Phragmites australis* (Cav.) Trin. Ex Steud (Figure III-1 B). Physical properties and chemical characteristics of sand and gravel were described elsewhere (Durst et al., 2013) (Table III-5). Wetlands were kept at 20 ± 0.5 °C, and exposed daily to light from a LED lamp (Greenpower LED lamp, Philips®, Eindhoven, The Netherlands) for 8 hours. All tubings and stoppers in contact with the wetland matrix were Viton® (Rotilabo®, Carl-Roth, Karlsruhe, Germany). Five sampling ports were positioned at 15, 25, 35, 45 and 55 cm from the inlet point in each column. Water supply (renewed monthly) was from a vegetated ditch (Alteckendorf, France) collecting chloroacetanilide contaminated runoff from sugar beet and corn catchments. After addition of chloroacetanilides (described in the next section), water was continuously pumped to column inlets at a flow rate of 0.33 mL min<sup>-1</sup> using a high precision pump (ISMATEC® IPC model ISM936D, Zürich, Switzerland). Nominal residence time in wetland columns was 9.3 days. Columns were covered with reflective foil to prevent algal growth and photolytic decay of chloroacetanilides. Column wetland set-up and sampling procedure

Column wetlands were first incubated for 104 days with vegetated ditch water without addition of herbicides before amendment with herbicides. Three columns were then each continuously supplied for 112 days with one of the target herbicides supplied at an initial concentration of 1.8 µM for *rac*-metolachlor, and of 1.9 µM for acetochlor and alachlor. Chloroacetanilides were dissolved in ultrapure water to obtain stock solutions of 360 µM for *rac*-metolachlor, and of 380 µM for acetochlor and alachlor that were stored at -20 °C before addition to inlet water. A fourth column was supplied with vegetated ditch water without herbicide addition. Supplied water was

renewed and herbicides added every two weeks, i.e. after each sampling. No significant change in chloroacetanilide concentrations were observed in inlet tanks between sampling campaigns (nonparametric Wilcoxon test for paired samples,  $p > 0.05$ ).

Sampling was carried out at 0, 14, 28, 42, 56, 70, 84 and 98 and 112 days after beginning chloroacetanilide application. Water samples were retrieved using glass syringes from wetland inlet, wetland outlet and the five sampling ports, for hydrochemical (30 mL), chloroacetanilide, degradation product, and enantiomeric analyses (30 mL), and for DNA extraction (50 mL). Between sampling points, syringes were thoroughly flushed successively with 10% hydrochloric acid, 70% ethanol, and autoclave-sterilised ultrapure water. For DNA extraction, water samples were filtered through sterile 0.2  $\mu\text{m}$  cellulose filters (Millipore, Billerica, MA, USA), which were then stored in sterile 50 mL plastic Falcon tubes at  $-20^{\circ}\text{C}$  until further processing.

### 2.3. Hydrogeochemical analysis

Hydrogeochemical parameters were analysed every two weeks at inlet, outlet and at the 5 sampling ports. Concentrations of total organic carbon (TOC) and dissolved organic carbon (DOC) were measured at the inlet and outlet only. Carbon and major ion concentrations were determined according to standard (FR EN ISO) laboratory procedures. Electrical conductivity, pH and dissolved oxygen were directly measured in wetland inlet and outlet water using WTW multi 350i sensors (WTW, Weilheim, Germany). Dissolved oxygen concentrations were measured using non-invasive oxygen sensors (Presens, Regensburg, Germany), mounted inside the columns and facing each of the five sampling points (Figure III-1 B).

### 2.4. Quantification of chloroacetanilides and degradation products

Chloroacetanilide herbicides and their ethane sulfonic (ESA) and oxanilic acid (OXA) degradation products were extracted from water samples by solid-phase extraction (SPE) using SolEx C18 cartridges (Dionex®, Sunnyvale, CA, USA) and an AutoTrace 280 SPE system (Dionex®) as described previously (Elsayed et al., 2014a). Quantification was performed by GC-MS/MS (Chloroacetanilides) and by LC-MS (ESA and OXA). Detailed protocols for extraction and quantification of chloroacetanilides in water, sand and plant, and of ESA and OXA degradation products of metolachlor (MESA and MOXA), acetochlor (AcESA and AcOXA) and alachlor (AIESA and AIOXA) in outlet water, are provided as SI. Detection limits were 6.3, 2.0 and 2.5 nM, and quantification limits were 7.4, 18.5, 7.0 nM for acetochlor,

alachlor and *rac*-metolachlor, respectively. For degradates, detection limits were 0.2, 0.1, 0.1, 0.3, 0.2 and 0.1 nM, and quantification limits 0.4, 0.1, 0.2, 0.5, 0.4 and 0.2 nM for AcOXA, AcESA, AIOXA, AIESA, MOXA and MESA, respectively. *Rac*-metolachlor enantiomer analysis was carried out with a Trace GC 2000 series GC-MS apparatus (Thermo Fisher Scientific, Waltham, MA, USA) as detailed in the Appendix.

## 2.5. Molecular analysis

### 2.5.1. *DNA extraction*

Total DNA was extracted from filters with the PowerWater® DNA Isolation Kit (MO BIO, Carlsbad, CA, USA) following manufacturer's instructions. Concentrations of DNA were determined using the Quant-it PicoGreen dsDNA assay kit (Invitrogen, Carlsbad, CA, USA).

### 2.5.2. *T-RFLP analysis*

Bacterial 16S rRNA gene fragments (0.9 kb) were PCR-amplified using 5'carboxyfluorescein (6-FAM) labelled 27f and 927r primers as described previously (Penny et al., 2010a) (see SI for details). T-RFLP electrophoregrams were analysed with PeakScanner V1.0 (Applied Biosystems, Carlsbad, CA, USA). Noise cancellation, peak alignment and matrix (samples × T-RFs) generation was performed using T-REX (<http://trex.biohpc.org>) (Culman et al., 2009). Peak heights were normalized to the same total fluorescence units per sample, and resulting data matrices were used for statistical analysis (see SI).

### 2.5.3. *Pyrosequencing*

Universal 16S bacterial primers 28F (5'-TTTGATCNTGGCTCAG-3') and 519r (5'-GTNTTACNGCGGCKGCTG-3') (Andreotti et al., 2011) were used to amplify an approximately 500 bp fragment of the 16S rRNA gene spanning the hypervariable region V1-V3 which was then used for bacterial tag-encoded FLX amplicon pyrosequencing (Acosta-Martinez et al., 2008). Sequences were generated by PCR according to established methods (Andreotti et al., 2011). Sequencing was performed at Research and Testing Laboratory (Lubbock, TX, USA), on a Roche 454 FLX instrument following the manufacturer's protocols (Roche, Basel, Switzerland).

## 2.6. Data analysis

### 2.6.1. *Mass balance of herbicides and hydrochemical parameters*

Daily chloroacetanilide and hydrochemical species loadings flowing through the wetlands were estimated by interpolation, multiplying chloroacetanilide concentrations between consecutive sampling dates with the corresponding flow rates. Loads of chloroacetanilides and hydrochemical parameters at a given point between two sampling campaigns were calculated from the integral sum of all daily load estimates. Mass removal [%] was calculated as the relative decrease of outlet mass ( $mass_{out}$ ) to the inlet mass ( $mass_{in}$ ) for each lab-scale wetland during a given time period. Remaining fractions of chloroacetanilides ( $C_x/C_{in}$ ) are defined as the ratio between the concentration measured at each sampling point along the flow path ( $C_x$ ) and at the inlet ( $C_{in}$ ).

### 2.6.2. *Enantiomer fraction determination*

Metolachlor is a sterically hindered tertiary amine with two elements of chirality: a chiral axis formed by the obstruction to the free rotation about the phenyl-nitrogen bond and a stereogenic carbon centre located at the carbon atom C 1' in the 1'-methyl-2'-methoxyethyl group.

The enantiomer fraction (EF) was used to describe enantiomer composition in the column wetlands, and is defined as the ratio of the S-enantiomer concentration to the sum total enantiomer concentration (Harner et al., 2000), as defined by eq. 1:

$$EF = \frac{S\text{-enantiomers}}{S\text{-enantiomers}+R\text{-enantiomers}} = \frac{aS1'S+aR1'S}{aS1'S+aR1'S+aS1'R+aR1'R} \quad (1)$$

where S-enantiomers stand for the peak areas of  $\alpha S1'S$  and  $\alpha R1'S$  atropoisomers, and the R-enantiomers for the peak areas of  $\alpha R1'R$  and  $\alpha S1'R$  atropoisomers. Pure enantiomers have EFs of 0 (R-) or 1 (S-), while racemic mixtures have an EF of 0.5. (2)

### 2.6.3. *Processing of pyrosequencing data*

Denoising, chimera checking, generation of OTUs and taxonomic classification were performed using a custom-scripted bioinformatics pipeline ((Handl et al., 2011). Obtained matrices of taxonomic data were used for further statistical analysis, except for calculation of diversity and richness indices (see SI for details).

#### 2.6.4. *Statistical analysis*

Statistical analysis was carried out within R ([www.r-project.org](http://www.r-project.org)), with *p*-values set at 0.05. Hydrochemical data were compared using the paired non-parametric Wilcoxon signed rank test. Two-dimensional nonmetric multidimensional scaling (NMDS) based on Bray-Curtis dissimilarities of Hellinger transformed data (square root transformation of relative abundances) was used to visualize dissimilarities in bacterial community structures. The relationship between community profiles and hydrogeochemical variables was investigated by fitting environmental vectors *a posteriori* onto the NMDS, and their significance was assessed by conducting a Monte-Carlo permutation test with 1000 permutation steps. Analysis of similarities (ANOSIM) based on Bray-Curtis dissimilarities was used to infer statistical differences between groups. Statistically significant differences in T-RFLP-based diversity metrics were assessed using an ANOVA with Tukey's post hoc pairwise comparison.

### 3. Results

#### 3.1. Biogeochemical evolution and chloroacetanilide dissipation

Oxic conditions prevailed at the bottom of the four column wetlands (15- 25 cm from inlet), but anoxic conditions developed in the rhizosphere zone, near the top of the columns (45 – 55 cm from inlet) (Figure III-5). Organic carbon was released by plant roots, as evidenced by an increase in DOC at wetland outlets (average DOC load at the inlet and outlet of  $5.7 \pm 5.0$  and  $16.3 \pm 16.7$  mg/day, respectively). Reduction of nitrate and sulfate occurred in the anoxic zone of all four wetlands (Figure III-5). Average nitrate mass dissipation was  $58 \pm 11\%$ ,  $80 \pm 9\%$ ,  $61 \pm 15\%$  and  $36 \pm 19\%$  in wetlands receiving *rac*-metolachlor, acetochlor, alachlor and in the control wetland, respectively, indicating nitrate reduction. Sulfate reduction also occurred albeit to a lower extent, with average sulfate mass dissipation  $16 \pm 10\%$ ,  $21 \pm 12\%$ ,  $8 \pm 4\%$  and  $9 \pm 6\%$  in wetlands receiving *rac*-metolachlor, acetochlor, alachlor and the control wetland, respectively. Other redox sensitive species such as manganese and iron remained low ( $< 4 \mu\text{M}$ ) over the course of the experiment.



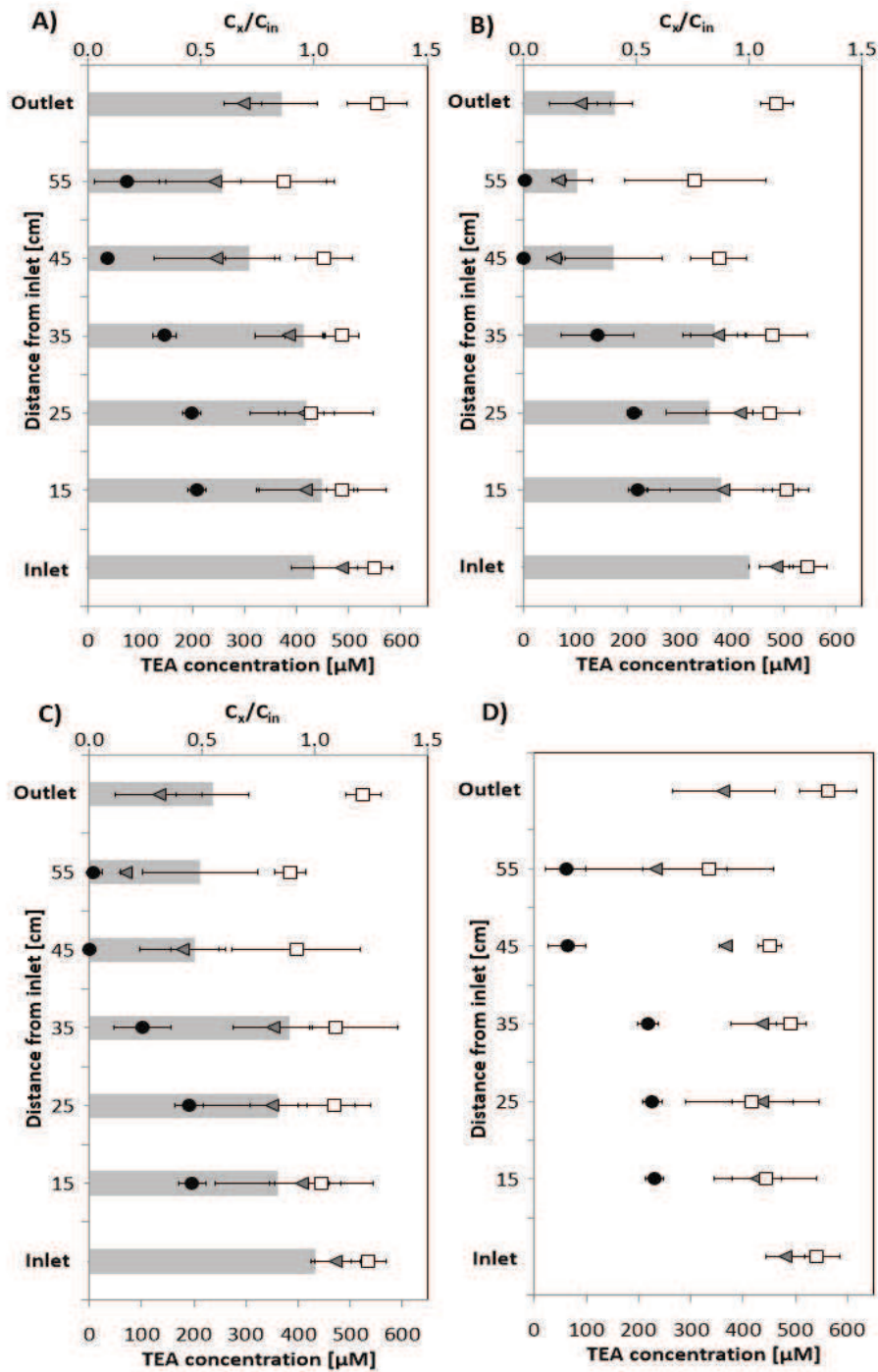


**Figure III-5.** Concentrations of terminal electron acceptors (TEAs) oxygen (black circles), nitrate (grey triangles) and sulphate (white squares) in column wetlands experimentally contaminated with metolachlor (A), acetochlor (B), and alachlor (C). (D), ditch water control. Relative concentrations of chloroacetanilides ( $C_x/C_{in}$  = concentration at point (x) divided by inlet concentration) at different depths in lab-scale wetlands are indicated by grey bars, as the average  $\pm$  standard deviation of all values obtained at the corresponding column position throughout the experiment.

Crucially, chloroacetanilide dissipation mainly occurred together with nitrate and sulfate reduction in the rhizosphere zone. Mean mass removal of *rac*-metolachlor, acetochlor, and alachlor was  $29 \pm 19\%$ ,  $61 \pm 14\%$ , and  $52 \pm 12\%$  respectively. Dissipation varied over time and ranged from 8 to 70%, from 56 to 90%, from 32 to 64% for metolachlor, acetochlor, and alachlor, respectively (Figure III-12). Extent of dissipation increased at the beginning of the experiment between day 0 and day 28, and did not significantly change thereafter ( $p > 0.05$ ). Concentrations of chloroacetanilides, nitrate and sulfate were larger at the outlet than at the 55 cm sampling port, likely due to preferential flow paths (Bundt et al., 2001) and root channelling in the top part of the columns.

### 3.2. Detection of ESA and OXA degradation products in the wetlands

ESA and OXA degradation products of chloroacetanilides were both detected, although mostly below the quantification limit (Figure III-12). ESA degradates of acetochlor and alachlor were the most frequently found degradation products, and were detected at the column outlet on days 70, 84 and 112. The alachlor ESA was also detected on day 98. OXA degradates were only detected once each for metolachlor (day 14) and alachlor (day 70).

### 3.3. Enantiomer analysis of *rac*-metolachlor

Enantiomer analysis of metolachlor was used to identify the biodegradation of the chiral chloroacetanilide metolachlor (Figure III-6). Average enantiomer fraction (EF) was significantly lower in the rhizosphere zone ( $EF = 0.480 \pm 0.005$ ) than in the oxic zone ( $EF = 0.494 \pm 0.006$ ). Moreover, lower *rac*-metolachlor concentrations significantly correlated with lower EF values (Spearman's  $\rho = 0.39$ ,  $p = 0.006$ ; data not shown), confirming the occurrence of enantioselective metolachlor degradation.

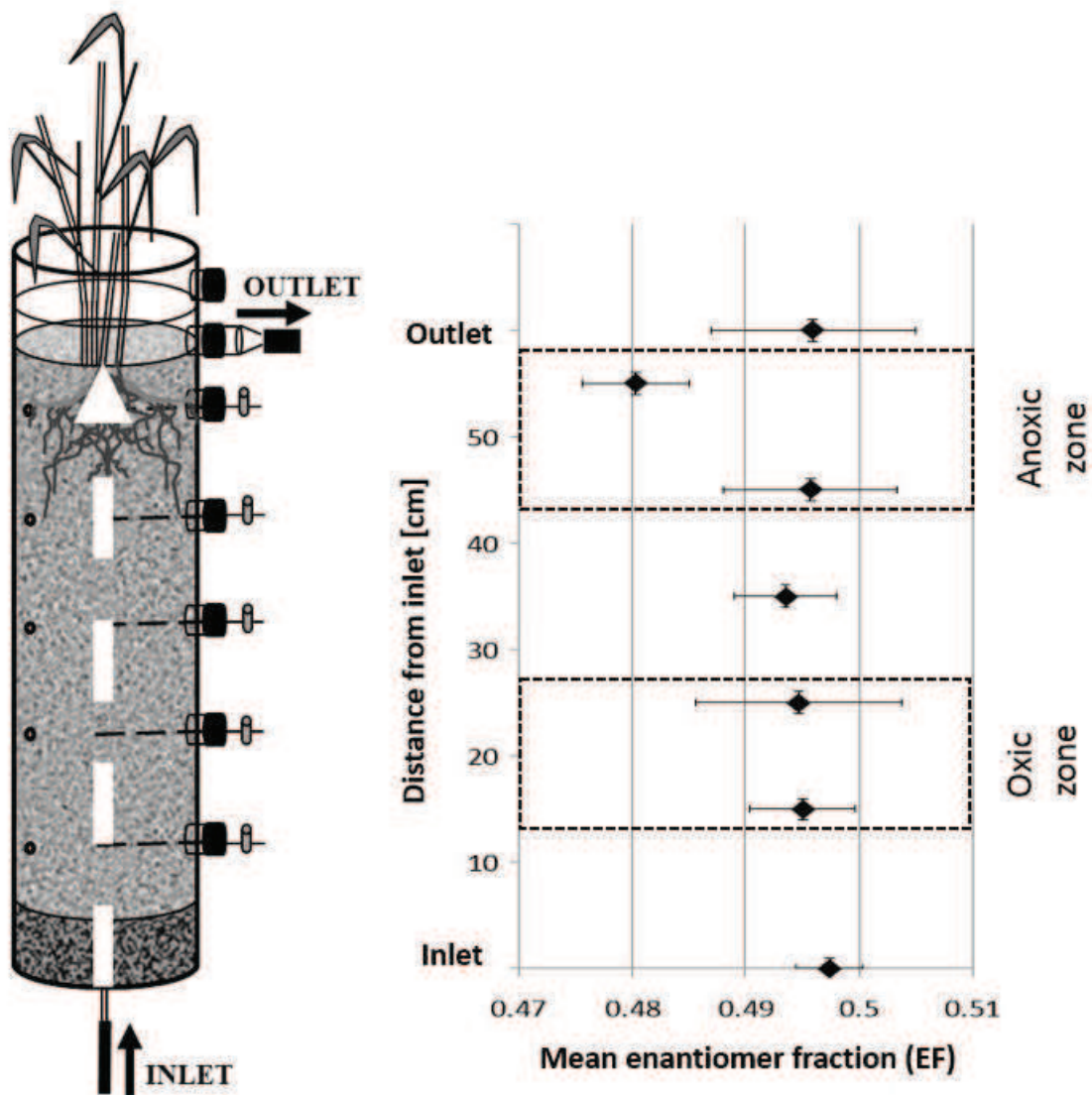


**Figure III-6. Mean enantiomer fraction ( $\pm$  SD) of metolachlor along the flow path for the period between day 0 and day 112.**

### 3.4. Composition of water bacterial communities

Terminal restriction fragment length polymorphism (T-RFLP) analysis was performed on DNA extracted from water samples on days 0, 14, 70 and 98 of the experiment to follow temporal evolution of water bacterial composition in column wetlands. The number of samples successfully analysed by T-RFLP ranged between 9 (day 98) and 22 (day 70). PCR amplification and subsequent T-RFLP analysis was difficult for some samples, likely because of a combination of PCR inhibitor presence and low DNA concentrations. Comparisons between bacterial populations were visualised using NMDS ordination of T-RFLP data (Figure III-7 A). Anoxic zone samples showed significantly higher diversity than samples from oxic

zones or outlets (Tukey's test,  $p < 0.05$ ). A *posteriori* fitting of environmental parameters onto the NMDS ordination showed that bacterial composition correlated best with changes in oxygen concentrations ( $p = 0.004$ ) (Figure III-7 B), followed by changes in magnesium ( $p = 0.007$ ), sulfate ( $p = 0.036$ ) and manganese ( $p = 0.049$ ). No significant distinction was detected between the four wetlands (ANOSIM  $R = 0.01$ ,  $p = 0.366$ ), and diversity metrics (number of OTUs Shannon and Simpson diversity) did not differ between the four wetlands ( $p > 0.05$ ). Moreover, no correlation was found between wetland bacterial composition and chloroacetanilide concentrations.

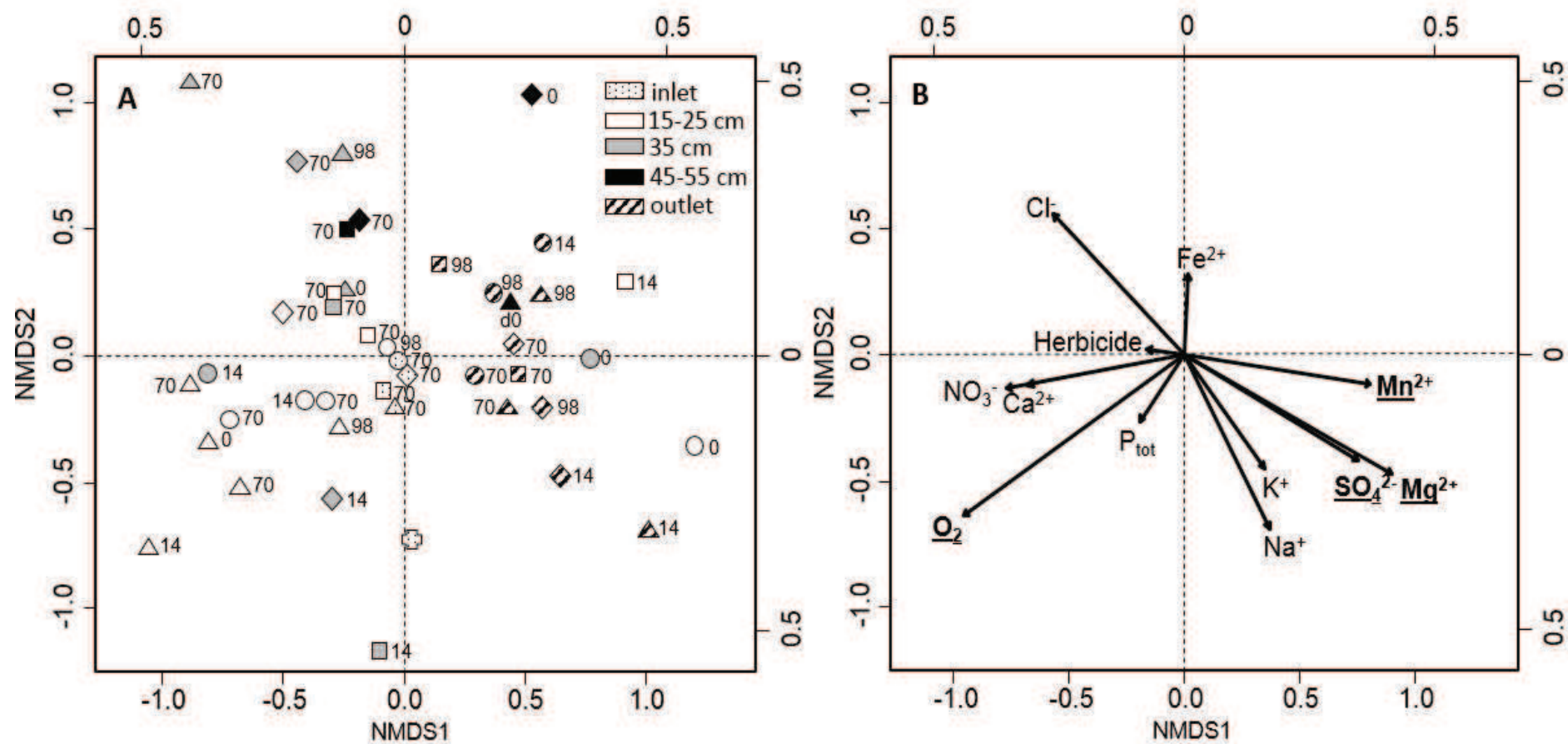


**Figure III-7. 2D-NMDS ordination of T-RFLP bacterial profiles (A) and *a posteriori* fitting of environmental parameters (B).** Symbols represent samples from metolachlor (squares), acetochlor (triangles), alachlor (diamonds) –contaminated and control (circles) lab-scale wetlands, and vegetated-ditch water (cross). Symbols are labelled with corresponding sampling days (days 0, 14, 70 and 98). Vector arrows in part B are fitted to the NMDS ordination and indicate the direction and magnitude of the change of the variable value. The significance of fitted vectors was calculated by *a posteriori* permutation of variables at  $p < 0.05$ . Parameters significantly correlated with bacterial composition are underlined. Plot stress = 0.2%.

To investigate bacterial composition in wetlands in more taxonomic detail, DNA extracted from outlet water samples at days 0 and 70 was analysed by 454 pyrosequencing of PCR products of the variable V1-V3 region of the 16S ribosomal RNA gene. Outlet samples from day 0 and day 70 were chosen so as to provide an integrative view of bacterial composition in each wetland, and of its evolution with time. In addition, day 70 samples from the anoxic zone (at 45 cm from the inlet) were also sequenced in order to characterise communities present in the reactive anoxic zones of the three chloroacetanilide-contaminated wetlands.

Simpson diversity values obtained by pyrosequencing and T-RFLP were significantly correlated for all samples (Spearman  $\rho = 0.93$ ,  $p = 0.0001$ ), except one (outlet sample of metolachlor-contaminated wetland at day 0, for which only few OTUs were recovered by sequencing, unlike by T-RFLP, see Table III-7). Moreover, ordination of bacterial profiles based on 454 pyrosequencing and corresponding T-RFLP-based profiles clearly showed similar trends (Figure III-8). In particular, anoxic samples formed distinct clusters, whereas outlet samples converged from different initial bacterial compositions at day 0 towards a similar composition at day 70.

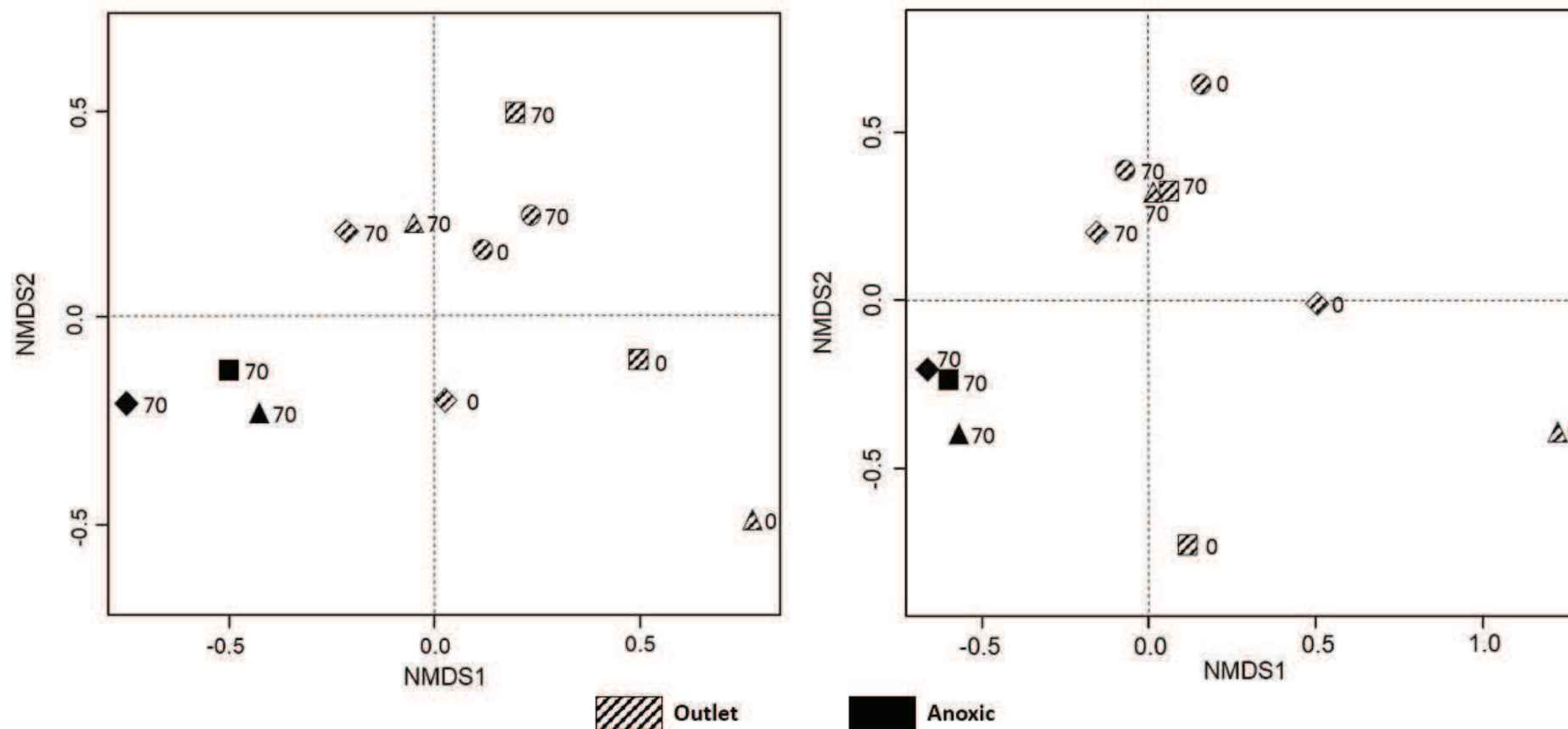


**Figure III-8. 2D-NMDS ordination of A) pyrosequencing (97% sequence identity) and B) corresponding T-RFLP bacterial community profiles of sequenced lab-scale wetland samples.** Symbols represent samples from metolachlor (squares), acetochlor (triangles), alachlor (diamonds) –contaminated and control (circles) lab-scale wetlands. Sample symbols are labelled with corresponding sampling days (days 0 and 70). Plot stress for A) and B) = 0.1.

Outlet bacterial communities of the four wetlands showed similar dominant phylotype, with classes *Flavobacteriia*, *Alphaproteobacteria*, *Betaproteobacteria* and *Cyanobacteria* representing 80% of total bacterial abundance in all outlet samples (Figure III-9). Changes in relative abundances of the dominant bacterial classes in wetland outlets were more pronounced between day 0 and day 70 in chloroacetanilide-contaminated wetlands than in the control wetland. *Flavobacteriia* decreased from 53 and 73% to 6 and 38% abundance in *rac*-metolachlor and acetochlor-contaminated wetlands, respectively. *Betaproteobacteria* decreased from 17-33% to 2-4% in outlets of the chloroacetanilide-contaminated wetlands, but increased slightly from 4 to 8% in the control wetland. Conversely, abundances of *Alphaproteobacteria* and photosynthetic *Cyanobacteria* increased from 1-8% and 0-1% to 14-43% and 6-27% in outlets of the three chloroacetanilide-contaminated wetlands, respectively, but did not change in the control wetland outlet.

Bacterial communities in the anoxic zones of chloroacetanilide-contaminated wetlands were mainly composed of *Clostridia*, *Actinobacteria* and *Proteobacteria*. *Clostridia* largely dominated anoxic zone communities, representing 21-64% of total bacterial abundance, with the genus *Clostridium* the most abundant (14-52% of total). *Actinobacteria* was the second most abundant class in anoxic zones (3-13% of total). Several phylotypes tentatively assigned to sulfate-reducing bacteria were also detected in anoxic zones, including genera *Desulfotomaculum* and *Desulfosporosinus* from the clostridial *Peptococcaceae* family, as well as *Desulfobacteraceae*, *Desulfovibrionaceae* and *Desulfobulbaceae* families. In total, sulfate-reducing genera represented 2.6-3.9% of total bacterial genera in anoxic samples, compared to less than 1.4% in outlet samples.



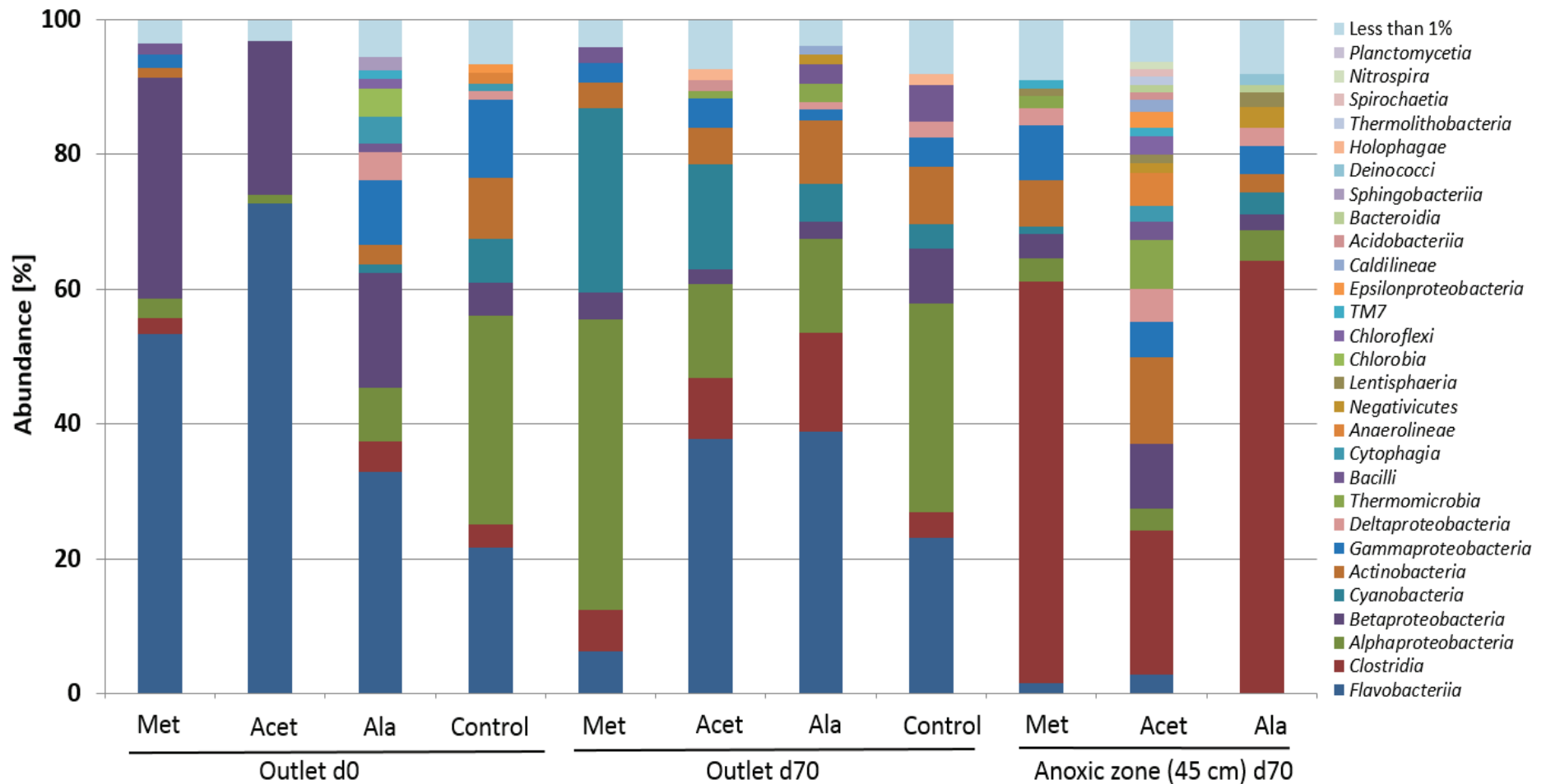


**Figure III-9. Relative abundance [%] of bacterial classes (defined at 80% sequence identity) in lab-scale wetland outlets on day 0 and day 70, and in the anoxic zone (at 45 cm from inlets) of wetlands contaminated with metolachlor (Met), acetochlor (Acet) and alachlor (Ala) on day 70. In total, 114,986 quality reads were obtained, corresponding to 5,873- 16,995 reads per sample (mean = 11,236 reads).**

## 4. Discussion

### 4.1. Biogeochemical conditions and chloroacetanilide degradation

Our laboratory column wetland designs allowed to conclusively demonstrate that degradation of chloroacetanilides occurred concomitantly with reduction of microbial terminal electron acceptors oxygen, nitrate and sulfate in a reactive, predominantly anoxic rhizosphere zone in the upper part of the columns (Figure III-5), implying high microbial activity, and associated degradation of xenobiotics (Briceño et al., 2007; Dennis et al., 2010) under such conditions. Indeed, the enhanced degradation of chloroacetanilides in the rhizosphere zone observed here (Figure III-5) was also noted previously (Anhalt et al., 2000; Bai et al., 2013). Ready availability of a variety of carbon sources from decaying plant material and root exudates in the rhizosphere may also contribute to explain the significant decrease in oxygen concentration ( $p < 0.001$ ). Therefore, aerobic degradation of chloroacetanilides cannot be completely excluded, especially given that heterogeneity of redox conditions in the rhizosphere may exist at the microscopic scale. Indeed, wetland plants are known to release some oxygen from the atmosphere through their roots following transport through plant tissues into the root system (Laanbroek, 2010), and that this also could occur in our set-up was suggested by the observation of reddish brown iron oxide precipitates along the periphery of plant roots (Figure III-11).

Dissipation of chloroacetanilides was largest initially (before day 28), and this could be attributed to sorption of herbicides on organic matter from plant roots or derived from plant decay, and also to dilution (Liu et al., 2000; Si et al., 2009). However, chloroacetanilide concentrations at wetland outlets did not correlate with DOC or TOC ( $p > 0.05$ ) (data not shown), suggesting that DOC-related sorption and transport of chloroacetanilides played only a minor role in chloroacetanilide dissipation throughout the experiment. Moreover, chloroacetanilide concentrations extracted from sand and plant roots collected 2 months after the end of the experiment were mostly below the quantification limits. This suggests that sorption and plant uptake, as already shown previously for volatilization and photolysis (Elsayed et al., 2014a), did not significantly contribute to chloroacetanilide dissipation in our experiments. Microbially-mediated processes are therefore expected to be a major dissipation route of chloroacetanilides in the investigated wetlands, and are discussed further in the following.

#### 4.2. Enantioselective degradation of metolachlor

Changes in isotopic composition of metolachlor carbon were not sufficient to decide on the occurrence of *in situ* degradation of metolachlor in the column wetlands investigated here (Elsayed et al., 2014a). In the present study, enantiomer analysis revealed preferential degradation of the *S*-enantiomer in the anoxic rhizosphere zone (Figure III-6), despite low mass dissipation of *rac*-metolachlor in compared to acetochlor and alachlor (Elsayed et al., 2014a). Enantiomer analysis thus appears to be a more sensitive probe to monitor metolachlor biodegradation under anaerobic conditions. Preferential degradation of the *S*-enantiomer of metolachlor was already noted previously in soil (Ma et al., 2006), although in another study, enantioselectivity was not observed (Klein et al., 2006).

The enantioselective microbial degradation observed here (Figure III-6) could be due to preferential transformation by stereoselective enzymes, as previously shown for phenoxyacid herbicides (Müller et al., 2006), and/or to preferential uptake by transporter proteins (Wang et al., 2013a). Alternatively, enantioselective uptake of metolachlor by plants (White et al., 2002; Zhang et al., 2013a) is also possible. However, plant uptake of *S*-metolachlor is expected to be limited, since metolachlor could not be detected here in plant roots (data not shown).

#### 4.3. Putative degradation pathways of chloroacetanilides in the rhizosphere

Several degradation pathways may be envisaged for chloroacetanilides (Hladik et al., 2005), and given the heterogeneity of redox conditions observed here, different degradation pathways may co-exist in column wetlands. The most commonly detected degradation intermediates of chloroacetanilides (ESA and OXA) were monitored at column outlets. ESA and OXA degradates were not mostly mostly below the limit of quantification ( $< 0.5$  nM) (Figure III-12). ESA and OXA formation are putatively mediated by a glutathione-S-transferase (GST) dependent pathway (Graham et al., 1999), but no GST enzyme specific for chloroacetanilides has yet been described. ESA and OXA are expected to be more persistent than their parent compounds (Huntscha et al., 2008), so the low concentrations found in lab-scale wetlands would be explained only in part by rapid degradation. Accordingly, alternative and as yet unknown biological degradation pathways that do not feature OXA and ESA as intermediates may also operate.

In addition, the occurrence of abiotic reactions involving chloroacetanilides and their degradates is also a possibility. Interestingly, such abiotic processes may nevertheless find their origin in microbial metabolism. For instance, the occurrence of microbial sulfate reduction

concomitantly with chloroacetanilide degradation was noted in the rhizosphere zone (Figure III-5). Abiotic transformation of chloroacetanilides by reduced sulfur species such as sulfide, bisulfite, polysulfides, all possible intermediates of redox processes involving sulfur species (Brunner, 2005). The reactions of chloroacetanilides with bisulfide and polysulfides have been shown to give rise to mercaptoacetanilides under sulfate reducing conditions in prairie pothole water (Zeng et al., 2011). In laboratory studies, the reaction of chloroacetanilides with sulfide, bisulfite and thiosulfate led to the formation of ESA and thiosulfonic acid degradates (Stamper and Tuovinen, 1998; Cai et al., 2007; Bai et al., 2013). With the information available so far, however, the respective importance and roles of abiotic and biotic dechlorination of chloroacetanilides, and the nature and origin of subsequent degradation steps could not be teased apart. High-resolution mass spectrometry may be helpful in this respect, by allowing the detection and quantification of a large number of potential chloroacetanilide degradation products (Reemtsma et al., 2013). In addition, carbon or sulfur isotope analysis of ESA degradates may allow to distinguish between biotically and abiotically formed ESA, although most such methods remain to be developed. Summing up, however, hydrochemical, pesticide and degradation product analysis clearly indicated the role of microorganisms in biogeochemical cycling and chloroacetanilide degradation in laboratory wetlands. Therefore, we examined bacterial communities in our wetland columns, to explore the major parameters influencing wetland water bacterial communities, and the relationship between bacterial communities and biogeochemical and degradation processes.

#### 4.4. Influence of hydrogeochemical conditions and contamination on wetland bacterial populations

Microbial communities were likely responsible for the observed reduction of terminal electron acceptors, as well as for chloroacetanilide degradation (Figure III-5). As first explored by T-RFLP genotyping (Figure III-7) bacterial composition of column wetlands was mainly influenced by prevailing biogeochemical conditions, and primarily by concentrations of dissolved oxygen. Indeed, bacterial communities of the anoxic rhizosphere zones were more diverse than those at the oxic inlet (ANOSIM  $R = 0.413$ ,  $p = 0.001$ ) and showed different profiles (Figure III-7 A, Figure III-13). On the other hand, no evidence of an impact of chloroacetanilide exposure on bacterial diversity metrics (number of OTUs, Shannon and Simpson diversity, Table III-7) could be found, although effects of herbicide exposure on soil bacterial community structure and function had previously been documented in several studies

(Lo, 2010). In particular, metolachlor exposure was shown to impact overall bacterial community structure in agricultural soils at doses of 2 to 5 mg kg<sup>-1</sup> (Seghers et al., 2003b; Vryzas et al., 2012), as well as the development of specific bacterial functional groups such as methanotrophs (Seghers et al., 2003b; Vryzas et al., 2012). Likewise, alachlor exposure (120 mg/l, 445 µM) was shown to impact bacterial community structure in anoxic slurries (Lauga et al., 2013). Also, the effect of acetochlor on freshwater bacterial communities was evidenced by DGGE analysis at concentrations similar to those used in our study (50 - 500 µg/l, 0.19 - 1.9 µM) in water microcosms (Foley et al., 2008). The observed discrepancy between previous results and those of our study is possibly due to differences in experimental set-up. For example, the complexity of the lab-scale wetland matrix (e.g. nutrient cycling, organic matter dependent herbicide partitioning and bioavailability, water flow) compared to freshwater systems may be associated with lesser exposure, and thus lesser impact, of herbicides in column wetlands, as noted previously for acetochlor (Perucci et al., 2000; Villeneuve et al., 2011).

#### 4.5. Bacterial taxonomic structure in wetland water

Knowledge about bacterial populations in anoxic zones of herbicide-contaminated wetlands is still particularly scarce. Using high-throughput sequencing, we were able to identify and to compare dominant bacterial populations in the reactive anoxic rhizosphere zone and in the outlets of column wetlands. As in T-RFLP analysis, no differences in bacterial composition were apparent between chloroacetanilide-contaminated wetlands and the control wetland (Figure III-7, Figure III-8). In addition, bacterial taxonomic composition in the different columns converged towards more similar bacterial compositions with time, probably owing to similar hydraulic and other operational parameters (e.g. temperature, light exposure) (Figure III-7). Such similar observations using T-RFLP and pyrosequencing supported the validity of the T-RFLP approach to study wetland water bacterial community composition despite its lower level of resolution, as also noted previously (Elsayed et al., 2014b) .

The wealth of information which can be derived from high-throughput sequencing, however, allowed to demonstrate how taxonomically different to that of the outlet the bacterial composition of the anoxic reactive zone was, thereby confirming its distinctive role in wetlands (Figure III-9). Gram-positive bacteria strongly dominated anoxic rhizosphere zones. *Clostridia*, the most abundant bacterial class in the anoxic rhizosphere zone, are Gram-positive, spore-forming, obligate anaerobes with versatile metabolic capacities, including acetogenesis,

carbohydrate and organic contaminant degradation (Paredes et al., 2005). With regard to certain taxa, however, rRNA 16S sequence information may provide more specific functional information relevant to chloroacetanilide degradation processes in wetlands. In particular, the abundance and localisation in the anoxic reactive zone of taxa known to be strongly associated with sulfate reduction, i.e. *Deltaproteobacteria* (*Desulfobacteraceae*, *Desulfovibrionaceae*, and *Desulfobulbaceae*), and *Clostridia* (*Peptococcaceae*), was in good agreement with the observed reduction of sulfate. Notably, strains of the *Desulfotomaculum* and *Desulfosporosinus* genera from the clostridial *Peptococcaceae* family were previously shown to couple sulfate reduction and toluene degradation (Winderl et al., 2010). More generally, *Clostridia* members have often been found to be associated with the degradation of chlorinated pesticides under anaerobic conditions. For example, the degradation of alachlor was previously observed in anoxic slurries dominated by *Clostridia* (Lauga et al., 2013), although actual degradation of chloroacetanilides by *Clostridia* was not yet been directly demonstrated. *Clostridium* strains were also found to degrade gamma-hexachlorocyclohexane (lindane), to mediate the abiotic dechlorination of DDT by reduced sulfur species in anaerobic paddy soils (Ohisa and Yamaguchi, 1979) (Bao et al., 2012), as well as of chlorinated alkanes such as tetrachloromethane (Penny et al., 2010b). In the same context, *Actinobacteria*, the second most abundant class in anoxic rhizosphere zones in the laboratory wetlands investigated here, include both aerobes and facultative anaerobes known to degrade several chlorinated pesticides (Fuentesa et al., 2010), and their numbers were also previously shown to increase in response to alachlor exposure in anoxic soil slurries (Lauga et al., 2013). Similarly, representatives of the actinobacterial genus *Streptomyces* detected in anoxic samples were also noted in previous studies to degrade metolachlor and alachlor (Liu et al., 1999; Sette et al., 2005b).

Despite such abundant circumstantial evidence, however, an active role of *Clostridia* and *Actinobacteria* in the degradation of chloroacetanilides in wetlands remains to be demonstrated. Nevertheless, our results provide further evidence to suggest the metabolic importance of Gram-positive bacterial populations in anoxic zones in redox-dynamic environments. Identification of chloroacetanilide degraders will likely require other approaches aiming at highlighting metabolically active subpopulations, such as stable isotope probing (Uhlik et al., 2013), as well as technical innovations for *in situ* work (Schurig et al., 2014).

## 5. Conclusions

In this study, chloroacetanilides were shown to be mainly degraded in the rhizosphere zone, where nitrate and sulfate reducing conditions prevailed. The observed preferential degradation of the *S*-enantiomer of metolachlor highlighted the usefulness of enantiomer analyses as an indicator of the degradation of chiral pesticides in the environment. In addition, the observed low concentrations of well-known ESA and OXA degradation products of chloroacetanilides suggested that other as yet unknown degradation pathways not involving the formation of ESA and OXA may be operating in wetlands. We consider our study as the starting point for coupling hydrochemical, analytical chemical and microbiological approaches to evaluate and predict the fate of widely used chloroacetanilides in receptor aquatic environments.

## 6. Acknowledgements

This work was funded by CNRS (INSU Research Program EC2CO) and the European INTERREG IV program Upper Rhine (PhytoRET project C.21). Support from REALISE, the Network of Laboratories in Engineering and Science for the Environment in the Alsace Region (<http://realise.unistra.fr>) is also gratefully acknowledged. Omniea F. Elsayed was supported by a fellowship of the European Union under the 7<sup>th</sup> Framework Programme (Marie Curie Initial Training Network CSI:Environment, Contract Number PITN-GA-2010-264329), and Elodie Maillard was supported by a PhD fellowship from Région Alsace. The authors thank Carole Lutz, Sophie Gangloff, Marie-Pierre Ottermatte, Eric Pernin, René Boutin, Benoit Guyot for their help with chemical analyses, as well as Renata Martins Pacheco and Ana Cristina Abenza for analytical support.

## 7. Appendix Chapter III- section 2

### Detailed materials and methods

#### Preparation and extraction of chloroacetanilides from sand and plant samples

The same protocol was applied for the extraction of sand and plant samples. Briefly, 5 g of sample (sand or plant) were extracted with 4 mL of ACN/pure water (v:v 60/40), shaken for 1 min (vortex), incubated for 30 min at 115°C, shaken for 1 min, centrifuged during 10 min at 3500 rpm. The supernatant was then collected and a second extraction was carried out, using the same protocol. 0.1% H<sub>3</sub>PO<sub>4</sub> were added to the sample for the second extraction. The 8 mL-sample was then filtered using a 0.2 µm PTFE filter and evaporated. 50 mL of pure water were added to the sample and were extracted by solid-phase extraction (see below).

#### Solid phase extraction

Solid-phase extraction was carried out with 10 mL water samples using SolEx C18 cartridges (Dionex®, CA, USA) packed with 100 mg bonded silica. AutoTrace 280 SPE system was used for simultaneous extraction of 6 samples. The extraction cartridges were washed with 5 ml of ethyl acetate, followed by 5 mL of methylene chloride and sequentially conditioned by 10 mL of methanol and 10 mL of deionised water. Cartridges were then loaded with the samples and dried with nitrogen for 10 min. Elution of the chloroacetanilide herbicides and their degradation products was performed by 3 mL followed by 2 mL of ethyl acetate and methylene chloride respectively. Finally, the extract was concentrated under nitrogen flux to 1 droplet, and 2 mL of methylene chloride were added.

#### Analysis of alachlor, metolachlor and acetochlor

Chloroacetanilide herbicides were quantified using a Focus-ITQ 700 model GC-MS/MS apparatus from Thermo Fisher Scientific (Waltham, MA, USA) and Xcalibur (version 2.0.7) for data acquisition. Metolachlor, acetochlor and alachlor separations were conducted on a, 30 m x 0.25 mm ID, 0.25 µm film thickness OPTIMA 5MS (5% phenyl - 95% dimethylpolysiloxane) fused-silica capillary column (Macherey Nagel, Düren, Germany), with helium as a carrier gas, at a flow rate of 1 mL min<sup>-1</sup>. The oven was held at 50°C for 2 min, ramped at 30°C min<sup>-1</sup> to 150°C, then up to 250°C at 5°C min<sup>-1</sup> and finally ramped at 30°C min<sup>-1</sup> to 300°C and held for 5 min. A volume of 3 µL of sample was injected on a split/splitless injector (pulsed splitless at 2.5 mL min<sup>-1</sup> for 1 min) using an AI/AS 3000 autosampler (Thermo Fisher Scientific). The injector temperature and transfer line were set at 280°C and 300°C. The



mass spectrometer was operated in the electron ionization mode (EI, 70 eV). The ion source temperature was maintained at 210°C. For GC-MS/MS analysis, 10 µL of internal standards (final concentration 100 µg L<sup>-1</sup>) were added to 190 µL of water samples. Retention times, selected ions used for identification and recovery are detailed in Table III-6.

#### Enantiomer analysis of metolachlor

Metolachlor enantiomer analysis was carried out with a Trace GC 2000 series GC-MS apparatus (Thermo Fisher Scientific, Waltham, MA, USA) using a 30 m × 0.25 mm ID, 0.25 µm film 20% tert-butyldimethylsilyl-β-cyclodextrin dissolved in 15% phenyl-, 85% methylpolysiloxane column (BGB Analytik, Boeckten, Switzerland) with helium as a carrier gas at a flow rate of 1.0 mL min<sup>-1</sup>. The column was held at 50°C for 3 min, ramped at 15°C min<sup>-1</sup> to 150°C, and finally ramped at 0.5°C min<sup>-1</sup> to 190°C and held for 5 min. A volume of 3 µL of sample was injected on a split/splitless injector (pulsed splitless flow for 1 min). The injector, the transfer line and ion source temperatures were maintained at 250°C, 250°C and 230°C, respectively. The mass spectrometer was operated in the electron ionization mode (EI+, 70 eV). The quantification was based on the parent ions 238 and 242 and the daughter ions 162 and 166 for respectively metolachlor and metolachlor-*d*<sub>6</sub>. The stereoisomer elution was *aS1'S*; *aS1'R*; *aR1'S*; *aR1'R* (see Appendix, Figure III-10)

#### Analysis of ESA and OXA degradation products

Ethane sulfonic (ESA) and oxanilic acids (OXA) degradation products of metolachlor (MESA and MOXA), alachlor (AIESA and AIOXA) and acetochlor (AcESA and AcOXA) were analysed using a TSQ Quantum ACCESS LC/MS equipped with a Thermo Fisher Scientific Accela autosampler with a temperature-controlled sample tray (15°C). Xcalibur (version 2.1.0) was used for data acquisition. Injection volume was 20 µL. The mobile phase consisted of 0.1% formic acid/high-purity water (A) and 0.1% formic acid/acetonitrile (B). The gradient program started with 35% B held for 5 min, then B increased from 35% to 95% for 16 min, 95% B was held for 5 min, then B decreased from 95% to 35% for 1 min and held at 35% for 5 min. The flow rate was 0.3 mL min<sup>-1</sup>. The analytical column was a EC 150/3 Nucleodur Polar Tec (particle size 3µm, length 150 mm, internal diameter 3 mm) and a precolumn EC 4/3 Polar Tec, 30 mm (Macherey Nagel). Column oven temperature was set at 60°C to achieve better separation and peak shapes. The mass spectrometer (MS) was a Thermo TSQ Quantum triple

quadrupole mass spectrometer (Thermo Fisher Scientific) operated using a heated electrospray ionization (HESI) source. The mass spectra were recorded in the negative ion mode (spray voltage: 3500 V) for the 6 degradation products and in the positive mode (spray voltage: 4250 V) for the internal standard Alachlor-d13. The vaporiser temperature was 300°C, sheath gas N2 pressure 10 (arbitrary units), auxiliary gas pressure 20 (arbitrary units), ion sweep gas pressure 0 and the ion transfer capillary temperature 300°C. The best sensitivity in multiple reaction monitoring operation was achieved through the acquisition of selected reaction monitoring (SRM) transitions with MRM mode. For identification of the studied compounds, two SRM transitions and a correct ratio between the abundances of the two optimized SRM transitions (SRM1/SRM2) were used along with retention time matching. Information about SRM transitions and analytical uncertainties are provided in Table III-6.

#### Processing of pyrosequencing data

Short reads of < 250 bp were removed, and denoising and chimera checking were accomplished using the UCLUST and UCHIIME algorithms (Edgar, 2010; Edgar et al., 2011). In total, 114,986 quality reads were obtained starting from 150,886 raw reads, corresponding to 5,873-16,995 reads per sample (mean = 11,236 reads). To determine the taxonomic affiliation of remaining sequences, the sequences were clustered into operational taxonomic units (OTUs). For each cluster, the seed sequence was put into a FASTA formatted sequence file. This file was then queried against a highly curated database compiled by Research and Testing Laboratory and originating from NCBI (<http://ncbi.nlm.nih.gov>), and bacterial taxa were identified using Krakenblast (<http://www.krakenblast.com>). Based upon BLASTn derived sequence identity percentage, the sequences were classified at the appropriate taxonomic level, according to the following criteria. Sequences with identity scores to known or well-characterized 16S sequences >97% identity (<3% divergence) were resolved at the species level, between 95% and 97% at the genus level, between 90% and 95% at the family level, between 80% and 90% at the order level, between 80 and 85% at the class level, and between 77% – 80% at the phylum level. Any match below this level of identity was not used in taxonomical analysis. Obtained matrices of taxonomic data were used for further statistical analysis, except for calculation of diversity and richness indices (see below).

### Measurements of bacterial diversity

Shannon's and Simpson's diversity indices and number of OTUs from T-RFLP data were calculated using R version 3.0.1 (<http://www.r-project.org>). For pyrosequencing data, sequence datasets were reanalysed using MOTHUR version 1.32.1 (<http://www.mothur.org>) starting from denoised and chimera checked sequences, aligned, and clustered to define OTUs at 97% sequence identity. A subsample of sequences was then randomly selected to obtain equally sized datasets according to the standard operating procedure ([http://www.mothur.org/wiki/454\\_SOP](http://www.mothur.org/wiki/454_SOP), Schloss et al., 2011). Resulting datasets were used for calculation of diversity indices using R, and for rarefaction analysis. Shannon's diversity index ( $H'$ ) was calculated as  $H' = -\sum p_i \ln p_i$  and Simpson's diversity index ( $S$ ) was calculated as  $S = 1 - D$  with  $D = \sum p_i^2$ , where  $p_i$  is the relative abundance of species  $i$ . Chao1 richness estimate was calculated as  $S_{chao1} = S_{obs} + \frac{f_1^2}{2 \times f_2}$ , where  $S_{obs}$  is total number of OTUs in a sample,  $f_1$  is the number of OTUs with only one sequence (i.e. "singletons") and  $f_2$  the number of OTUs with only two sequences (i.e. "doubletons").

**Table III-5. Physicochemical properties of the filling materials used for the lab-scale wetlands.**

	<b>Parameters</b>	<b>Units</b>	<b>Fine gravel</b>	<b>Medium sand</b>
<b>Physical properties</b>	<b>Grain size</b>	[mm]	1 - 2	0.4 - 0.63
	<b>Porosity</b>	[vol %]	41.9 ± 0.1	43.9 ± 0.8
	<b>Bulk density</b>	[g cm <sup>-3</sup> ]	0.69 ± 0.02	0.72 ± 0.01
	<b>Hydraulic conductivity</b>	[m s <sup>-1</sup> ]	1.3 10 <sup>-3</sup> ± 3.8 10 <sup>-5</sup>	1.04 10 <sup>-3</sup> ± 1.5 10 <sup>-4</sup>
<b>Chemical composition</b>	<b>Organic carbon</b>		0.15 ± 0.05	0.31 ± 0.08
	<b>SiO<sub>2</sub></b>		91.2	98.5
	<b>Al<sub>2</sub>O<sub>3</sub></b>		4.2	1.0
	<b>MgO</b>		0.1	-
	<b>CaO</b>		0.2	-
	<b>Fe<sub>2</sub>O<sub>3</sub></b>	[m%]	0.5	0.1
	<b>MnO</b>		-	-
	<b>TiO<sub>2</sub></b>		-	-
	<b>Na<sub>2</sub>O</b>		0.4	-
	<b>K<sub>2</sub>O</b>		2.5	0.4
<b>P<sub>2</sub>O<sub>5</sub></b>		0.1	-	

**Table III-6. Analytical data of the GC-MS/MS quantification of metolachlor, alachlor and acetochlor and the LC-MS quantification of their ESA and OXA degradation products.**

		Quantification	Identification	Retention time	Recovery (%)	SD (%)	
		daughter ion 1	daughter ion 2 (m/z)	(min)			
		(m/z)	(m/z)				
<b>GC-MS/MS</b>	<b>Chloroacetanilide herbicides</b>	<b>Acetochlor</b>	146	131	15.3	43	8
		<b>Alachlor</b>	188	160	15.47	82	8
		<b>Metolachlor</b>	162	133	16.78	96	8
	<b>Internal standard</b>	<b>Alachlor-<i>d</i><sub>13</sub></b>	172		15.3	-	-
		<b>Metolachlor-<i>d</i><sub>6</sub></b>	134		16.71	-	-
<b>LC-MS</b>	<b>Degradation products</b>	<b>Acetochlor OXA</b>	146	144	10	0.6	0.35
		<b>Acetochlor ESA</b>	144	162	10.5	10.69	3.82
		<b>Alachlor OXA</b>	160	158	9.7	1.32	1.16
		<b>Alachlor ESA</b>	160	176	10.1	5.11	6.46
		<b>Metolachlor OXA</b>	206	172	11.36	3.28	3.97
		<b>Metolachlor ESA</b>	121	192	9.9	0.58	0.42
		<b>Internal standard</b>	<b>Alachlor-<i>d</i><sub>13</sub></b>	251	175	18.3	-

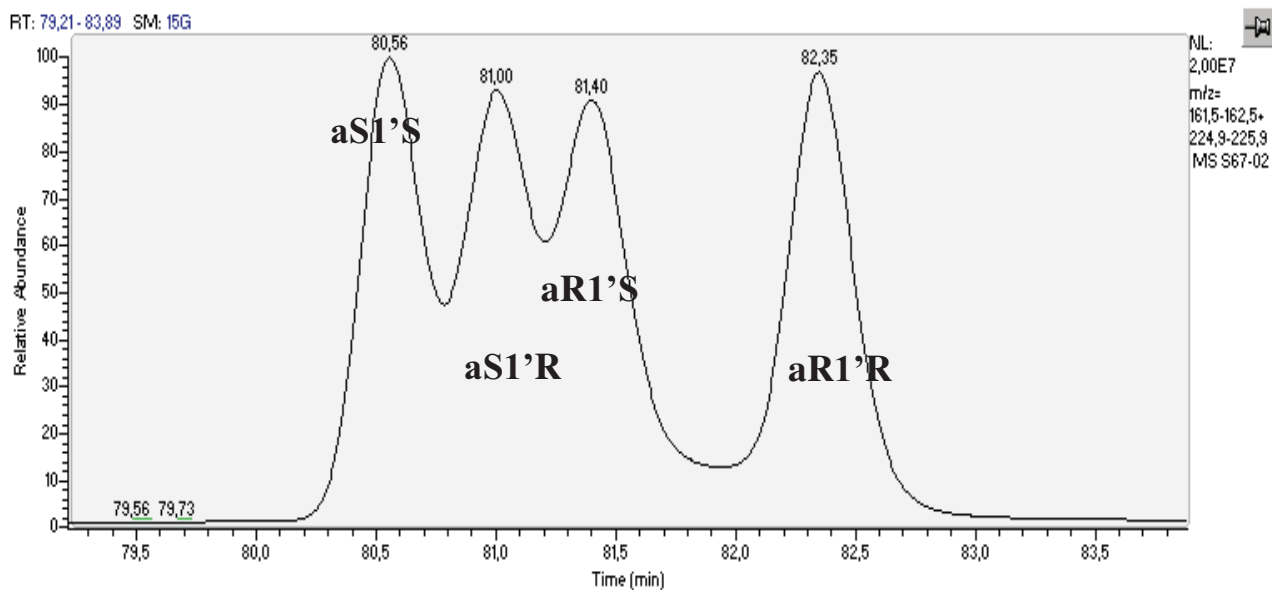


**Figure III-10 Chromatogram of metolachlor diastereoisomers obtained with chiral GC-MS analysis.**



**Figure III-11. Reddish-brown ferric iron oxide precipitates along *Phragmites australis* root periphery in a lab-scale wetland.**

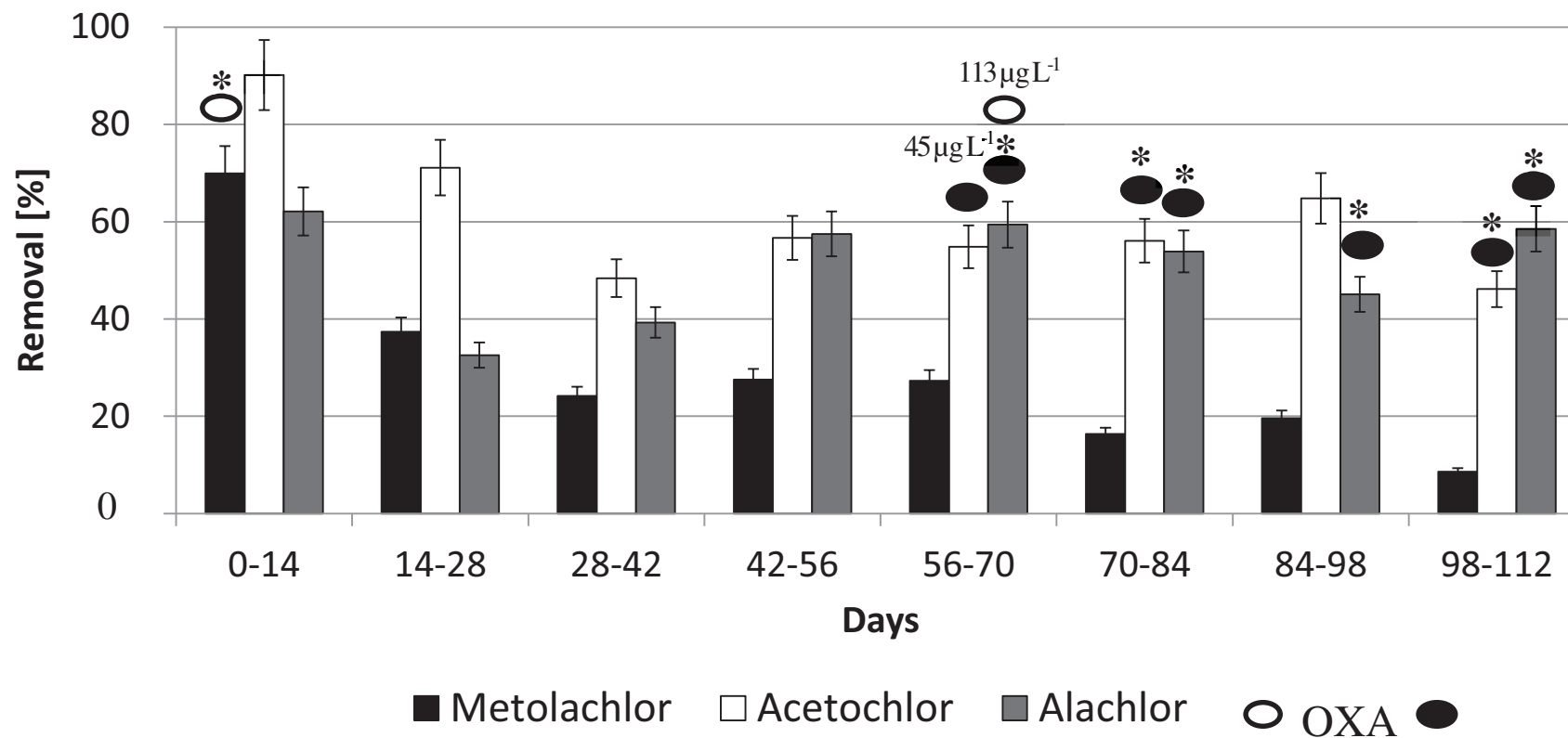


**Figure III-12. Load removal of metolachlor, alachlor and acetochlor between two sampling campaigns from day 0 to day 112.**

Circles placed above the bars represent the presence of the respective oxanilic acid (OXA) (empty circles), or ethanesulfonic acid (ESA) (solid circles) degradation products of the corresponding chloroacetanilide herbicide. The concentration of degradation products is mentioned above their respective circles. \*indicates a concentration below the limit of quantification. Error bars correspond to the analytical uncertainty.

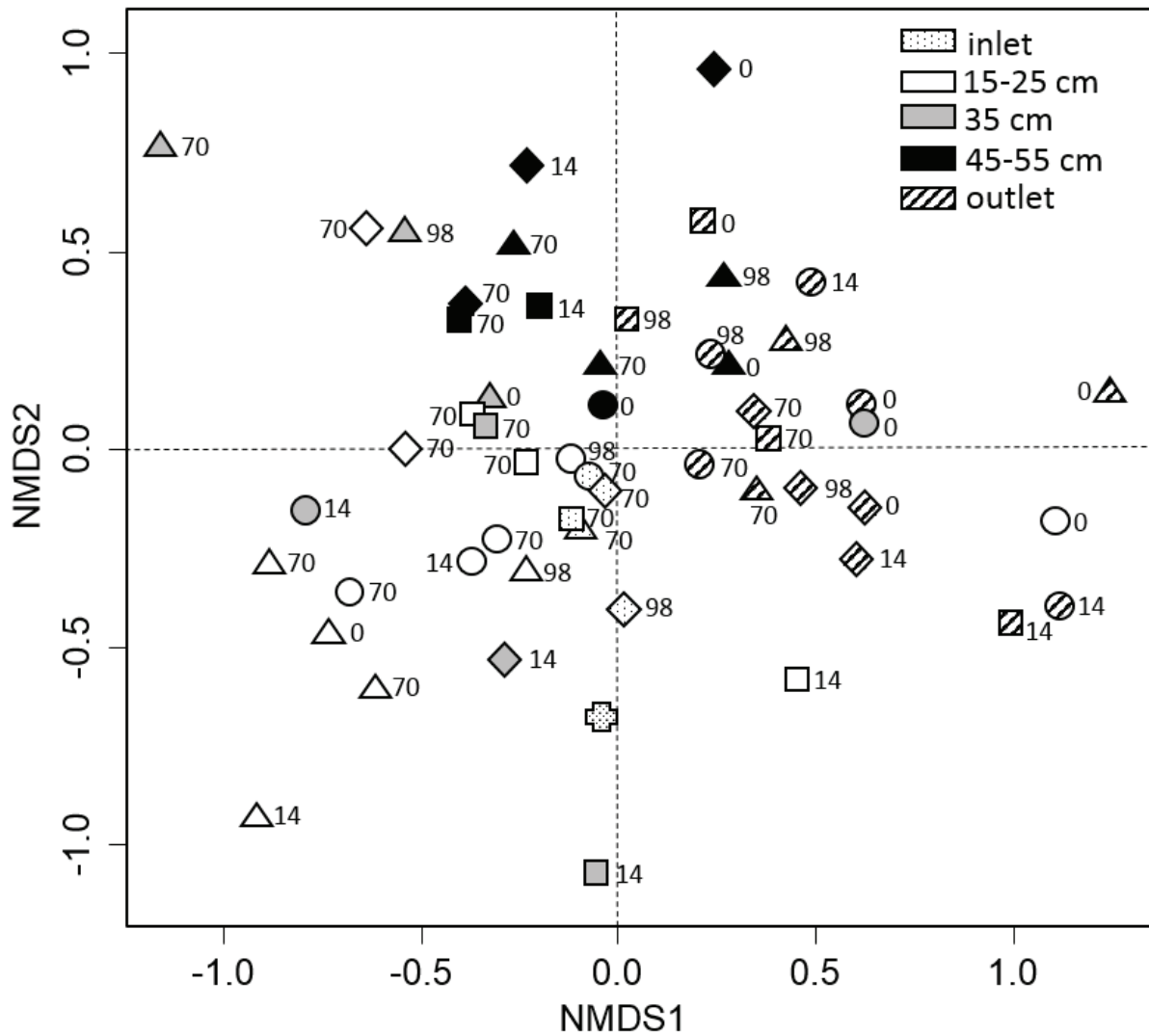


**Figure III-13. 2D-NMDS ordination of T-RFLP bacterial community profiles.**

Symbols represent samples from metolachlor (squares), acetochlor (triangles), alachlor (diamonds) –contaminated and control (circles) lab-scale wetlands, and vegetated-ditch water (cross). Sample symbols are labelled with corresponding sampling days (days 0, 14, 70 and 98). 55 samples are represented. Plot stress = 0.2%.



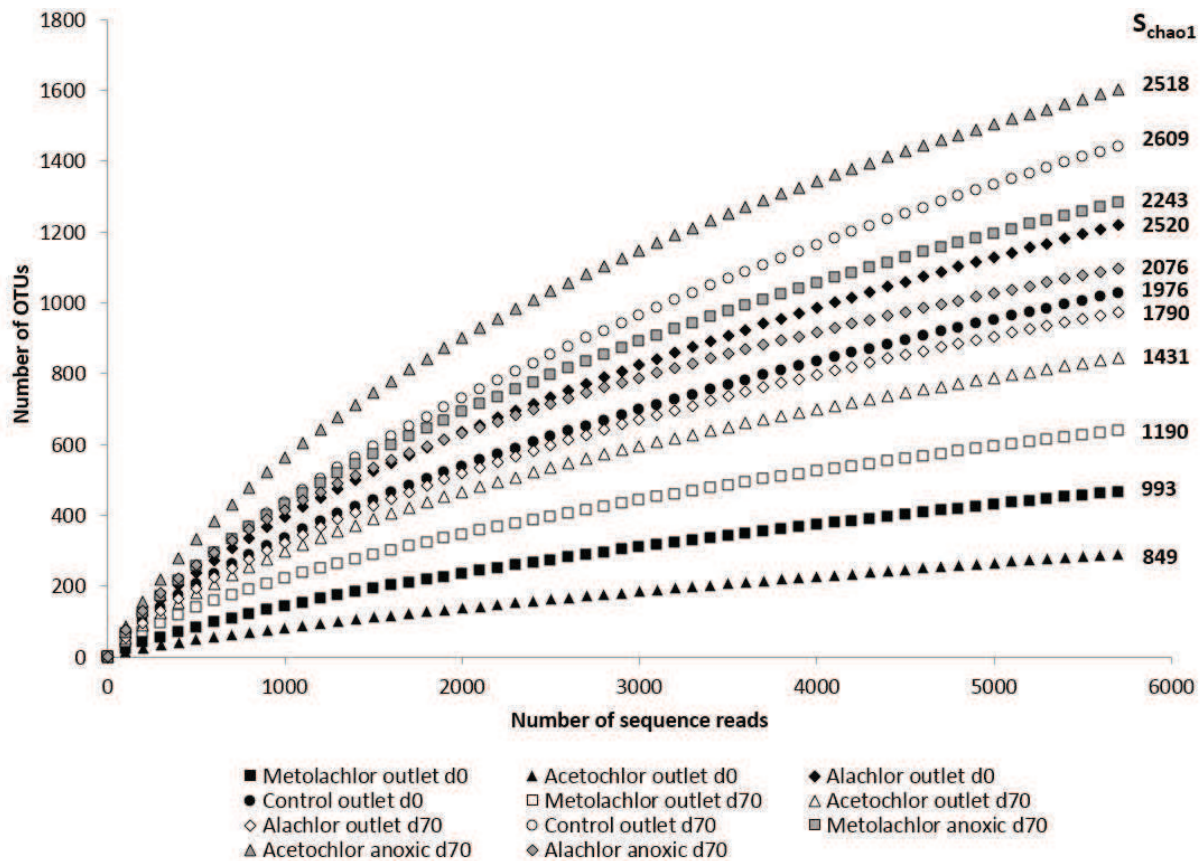


**Figure III-14. Rarefaction curves for bacterial OTUs, clustering at 97% sequence identity.**

Curves are shown for lab-scale wetland outlet samples on day 0 and day 70, and anoxic zone samples of chloroacetanilide-contaminated lab-scale wetlands (at 45 cm from inlets) on day 70. Corresponding  $S_{\text{chao1}}$  richness estimates (97% sequence identity) are represented in bold.

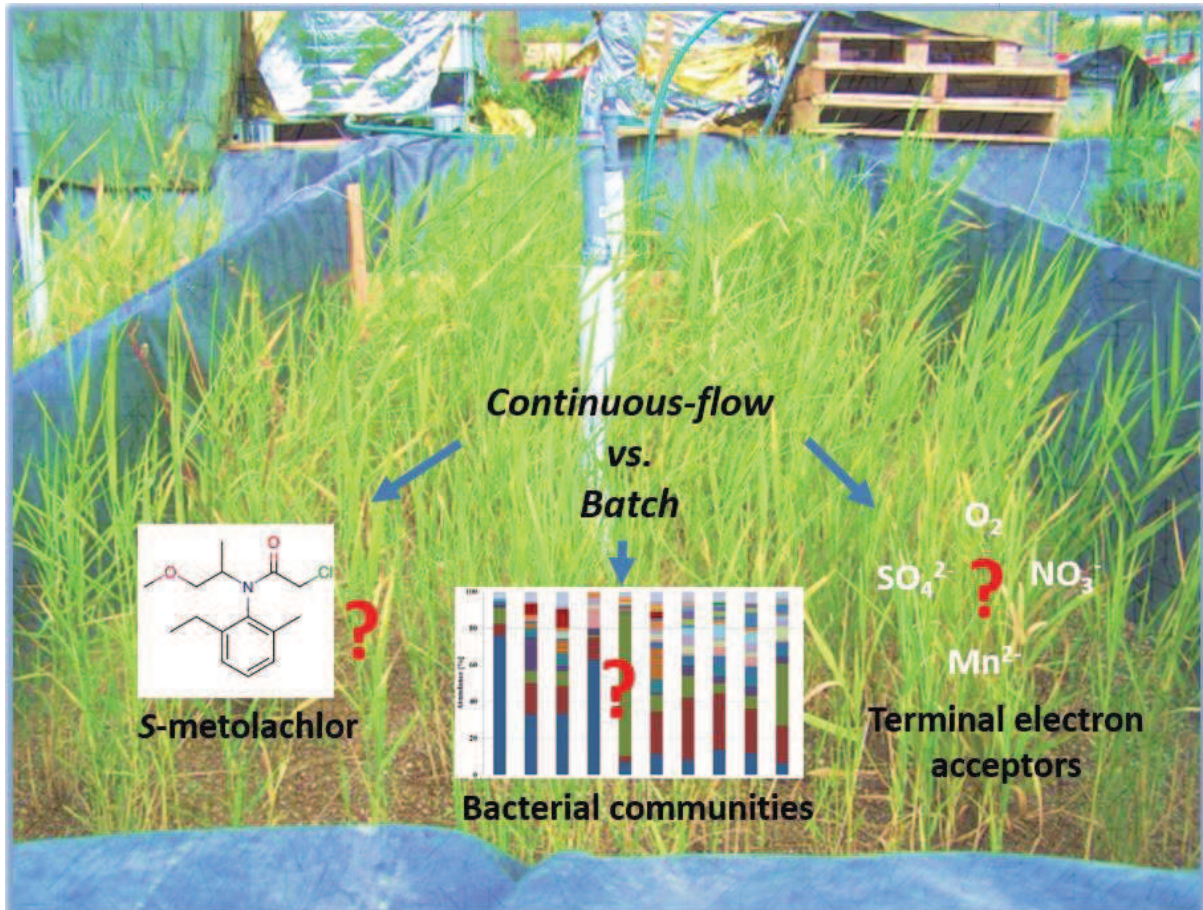
**Table III-7. Diversity and richness indices calculated for lab-scale wetland water samples by T-RFLP and by 454 pyrosequencing (OTUs at 97% sequence identity) for days 0, 14, 70 and 98. “-”, samples not sequenced.**

Wetland	Day	Sample	T-RFLP			Sequencing		
			Shannon	Simpson	OTUs	Shannon	Simpson	OTUs
Metolachlor	d0	outlet	3.2	0.95	33	2.4	0.71	467
Acetochlor	d0	15 cm	1.9	0.66	35	-	-	-
Acetochlor	d0	35 cm	3.5	0.96	52	-	-	-
Acetochlor	d0	55 cm	3.8	0.96	77	-	-	-
Acetochlor	d0	outlet	1.5	0.66	18	1.8	0.62	291
Alachlor	d0	55 cm	2.9	0.93	23	-	-	-
Alachlor	d0	outlet	2.9	0.90	50	5.4	0.97	1219
Control	d0	15 cm	1.3	0.55	30	-	-	-
Control	d0	35 cm	2.7	0.86	67	-	-	-
Control	d0	55 cm	3.7	0.96	67	-	-	-
Control	d0	outlet	2.4	0.83	27	4.9	0.95	1027
Metolachlor	d14	15 cm	2.6	0.86	43	-	-	-
Metolachlor	d14	35 cm	2.8	0.92	22	-	-	-
Metolachlor	d14	55 cm	3.4	0.96	40	-	-	-
Metolachlor	d14	outlet	1.0	0.38	25	-	-	-
Acetochlor	d14	15 cm	1.5	0.57	35	-	-	-
Acetochlor	d14	outlet	1.4	0.53	21	-	-	-
Alachlor	d14	35 cm	3.3	0.95	38	-	-	-
Alachlor	d14	45 cm	2.7	0.90	22	-	-	-
Alachlor	d14	outlet	2.0	0.69	37	-	-	-
Control	d14	25 cm	3.2	0.91	51	-	-	-
Control	d14	35 cm	2.1	0.76	20	-	-	-
Control	d14	outlet	2.5	0.86	31	-	-	-
Alteckendorf	d28	vegetated	3.0	0.91	40	-	-	-
Metolachlor	d70	inlet	3.4	0.95	55	-	-	-
Metolachlor	d70	15 cm	3.7	0.96	71	-	-	-
Metolachlor	d70	25 cm	3.7	0.96	64	-	-	-
Metolachlor	d70	35 cm	3.8	0.97	74	-	-	-
Metolachlor	d70	45 cm	2.8	0.90	40	5.6	0.98	1283
Metolachlor	d70	outlet	2.6	0.83	55	3.7	0.87	639
Acetochlor	d70	inlet	3.3	0.94	51	-	-	-
Acetochlor	d70	15 cm	1.3	0.46	24	-	-	-
Acetochlor	d70	25 cm	1.4	0.51	24	-	-	-
Acetochlor	d70	35 cm	1.9	0.82	9	-	-	-
Acetochlor	d70	45 cm	3.3	0.96	33	5.8	0.99	1097
Acetochlor	d70	55 cm	3.5	0.95	57	-	-	-
Acetochlor	d70	outlet	2.7	0.82	57	4.6	0.95	844
Alachlor	d70	inlet	3.3	0.94	43	-	-	-
Alachlor	d70	25 cm	3.4	0.95	46	-	-	-
Alachlor	d70	35 cm	3.1	0.94	38	-	-	-
Alachlor	d70	45 cm	3.2	0.94	56	5.8	0.99	1097
Alachlor	d70	outlet	3.0	0.86	90	4.5	0.91	975
Control	d70	inlet	3.4	0.92	70	-	-	-
Control	d70	15 cm	1.5	0.57	18	-	-	-
Control	d70	25 cm	2.5	0.74	47	-	-	-
Control	d70	outlet	3.3	0.93	68	5.6	0.98	1441
Metolachlor	d98	outlet	3.5	0.95	53	-	-	-
Acetochlor	d98	15 cm	3.0	0.84	60	-	-	-
Acetochlor	d98	35 cm	3.0	0.92	31	-	-	-
Acetochlor	d98	55 cm	3.9	0.97	83	-	-	-
Acetochlor	d98	outlet	2.0	0.64	45	-	-	-
Alachlor	d98	inlet	3.3	0.94	68	-	-	-
Alachlor	d98	outlet	2.8	0.83	67	-	-	-
Control	d98	15 cm	3.4	0.94	51	-	-	-
Control	d98	outlet	3.5	0.95	52	-	-	-

# Chapter IV

## Bacterial communities in batch and continuous-flow wetlands treating *S*-metolachlor

Elsayed, O.F., Maillard, E., Vuilleumier, S., Imfeld, G., 2014. Bacterial communities in batch and continuous-flow wetlands treating the herbicide *S*-metolachlor. *Science of the Total Environment* 499, 327-335.



**Abstract**

Knowledge of wetland bacterial communities in the context of pesticide contamination and hydrological regime is scarce. We investigated the bacterial composition in constructed wetlands receiving Mercantor Gold<sup>®</sup> contaminated water (960 g L<sup>-1</sup> of the herbicide *S*-metolachlor, >80% of the *S*-enantiomer) operated under continuous-flow or batch modes to evaluate the impact of the hydraulic regime. In the continuous-flow wetland, *S*-metolachlor mass removal was >40%, whereas in the batch wetland, almost complete removal of *S*-metolachlor (93-97%) was observed. Detection of ethanesulfonic and oxanilic acid degradation products further indicated *S*-metolachlor biodegradation in the two wetlands. The dominant bacterial populations were characterized by terminal restriction fragment length polymorphism (T-RFLP) and 454 pyrosequencing. The bacterial profiles evolved during the first 35 days of the experiment, starting from a composition similar to that of inlet water, with the use of nitrate and to a lesser extent sulphate and manganese as terminal electron acceptors for microbial metabolism. *Proteobacteria* were the most abundant phylum, with *Beta*-, *Alpha*- and *Gammaproteobacteria* representing 26%, 19% and 17% respectively of total bacterial abundance. Bacterial composition in wetland water changed gradually over time in continuous-flow wetland and more abruptly in the batch wetland. Differences in overall bacterial water structure in the two systems were modest but significant ( $p = 0.008$ ), and *S*-metolachlor, nitrate, and total inorganic carbon concentrations correlated with changes in the bacterial profiles. Together, the results highlight that bacterial composition profiles and their dynamics may be used as bioindicators of herbicide exposure and hydraulic disturbances in wetland systems.

**Keywords:** pesticide degradation, chloroacetanilides, wetland hydrology, wetland biogeochemistry

## 1. Introduction

Wetlands are dynamic ecosystems with properties resulting from interactions between water, soil and biota. They provide essential ecological functions including flood control, wildlife habitat, biogeochemical cycling, and water quality improvement by pollution reduction (Hansson et al., 2005). Wetlands are thus finding increasing application for water treatment, particularly in the case of waters contaminated with pesticides from agricultural use (Grégoire et al., 2009).

Microbial communities are major drivers of wetland functions, supporting elemental cycling and biodegradation of organic contaminants such as pesticides. Microbial communities and pesticide biodegradation in wetlands are strongly impacted by hydraulic and hydrochemical conditions (Carleton et al., 2001; Truu et al., 2009). Fluctuations of the water table level shape wetland redox conditions by controlling oxygen transfer into wetland sediments (Rezanezhad et al., 2014; Williams and Oostrom, 2010). In turn, redox conditions influence availability of terminal electron acceptors for microbial metabolism, which may eventually affect pollutant removal (Borch et al., 2010). Several studies have documented the impact of hydraulic regime on biogeochemical cycling and organic contaminant degradation, including pharmaceuticals, in natural and constructed wetlands (Avila et al., 2013; Burgin et al., 2011; Rezanezhad et al., 2014; Zhang et al., 2012). In contrast, knowledge on the influence of hydrological conditions on microbial communities in wetlands degrading pesticides is still very scarce.

Exposure to pesticides, transient or chronic, may affect the composition and functioning of the microbial compartment of a given environment, both quantitatively and qualitatively (Imfeld and Vuilleumier, 2012). DNA fingerprinting and sequencing techniques have proven particularly useful in elucidating the relationship between degradation of organic contaminants, biogeochemical processes and bacterial community dynamics in wetland systems (Adrados et al., 2014; Imfeld et al., 2010; Imfeld et al., 2009; Weber et al., 2011). Ongoing advances in high-throughput sequencing techniques are boosting the exploration of microbial taxonomic diversity in wetlands (Hartman et al., 2008; Ligi et al., 2013; Serkebaeva et al., 2013). Characteristics of wetland microbial communities may represent potential indicators to assess their biological status (Imfeld & Vuilleumier, 2012), and aid in the design and operation of constructed wetlands for pollution treatment (Sims et al., 2013).

In this context, we embarked on a study to characterise the dynamics and composition of bacterial communities receiving a commercial formulation of the chloroacetanilide herbicide *S*-metolachlor (i.e., Mercantor Gold®). *S*-metolachlor is widely applied to control annual weeds for a variety of crops including corn and sugar beet. The polar character of *S*-metolachlor and its application as a pre-emergence herbicide (i.e. before the development of a vegetal cover), may favor its transport to non-target environmental compartments (Tran et al., 2007). *S*-metolachlor is frequently detected in both ground and surface water (Hladik et al., 2005; Steele et al., 2008). Biological degradation of chloroacetanilides was repeatedly evidenced by detection of the corresponding ethanesulfonic and oxanilic acid metabolites (e.g. (Baran and Gourcy, 2013)), by enrichment cultures capable of degrading other chloroacetanilide herbicides, such as propachlor, acetochlor and alachlor (Liu et al., 2012; Xu et al., 2006; Zheng et al., 2012) and by the isolation of two bacterial strains capable of degrading metolachlor (Wang et al., 2008; Zhang et al., 2011). However, the influence on wetland microbial communities of *S*-metolachlor exposure, and in particular its commercial formulation, remains largely unexplored.

The aim of the present study is to evaluate the influence of hydraulic and hydrochemical conditions on bacterial communities in two pilot subsurface horizontal flow wetlands treating *S*-metolachlor contaminated water. The two identical subsurface horizontal flow wetlands were operated with different hydraulic regimes to mimic conditions of either continuous low-level (continuous-flow wetland) or acute transient exposure to *S*-metolachlor (batch wetland). The continuous-flow wetland was continuously supplied with water, reproducing conditions occurring in flooded wetland systems that intercept water fluxes with background levels of pesticide contamination. The batch wetland was exposed to successive dry-wet cycles, as in wetlands that punctually received high loads of pesticides in runoff water. Hydrochemical analysis and quantification of *S*-metolachlor and its ethanesulfonic and oxanilic acid degradation products were used to evaluate prevailing wetland conditions as well as *S*-metolachlor degradation, and wetland bacterial communities were evaluated by terminal restriction fragment length polymorphism (T-RFLP) and 454 pyrosequencing.

## 2. Materials and methods

### 2.1. Experimental design

Two identical outdoor subsurface-flow constructed wetlands (48°4'54"N, 7°21'20"E, Colmar, Alsace, France) of 4 m length, 1.8 m width and 52 cm depth, filled with sand (grain size 0-4 mm) and a bottom layer of gravel (grain size 4-8 mm) were used (Figure IV-1 A). Sand had a porosity of 32 and 35%, and a saturated hydraulic conductivity of  $6.9 \times 10^{-5} \text{ m s}^{-1}$  and  $9.7 \times 10^{-5} \text{ m s}^{-1}$  for the continuous-flow and batch wetlands respectively. Three species of commonly used macrophytes, i.e. *Phragmites australis* (Cav.) Trin. ex Steud. (20 plants  $\text{m}^{-2}$ ), *Phalaris arundinacea* L. (3 plants  $\text{m}^{-2}$ ) and *Glyceria maxima* (Hartm.) Holmb. (2 plants  $\text{m}^{-2}$ ) were planted together to combine their potential effect on the dissipation of herbicide-contaminated water in constructed wetlands. Three piezometers (1.05 m in length and 5.5 cm in diameter) embedded in the sand layer along the middle of each bed at successive one meter intervals from the inlet served to monitor water levels and for water sampling. The wetlands were filled with tap water three months and again one week before the start of the experiment.

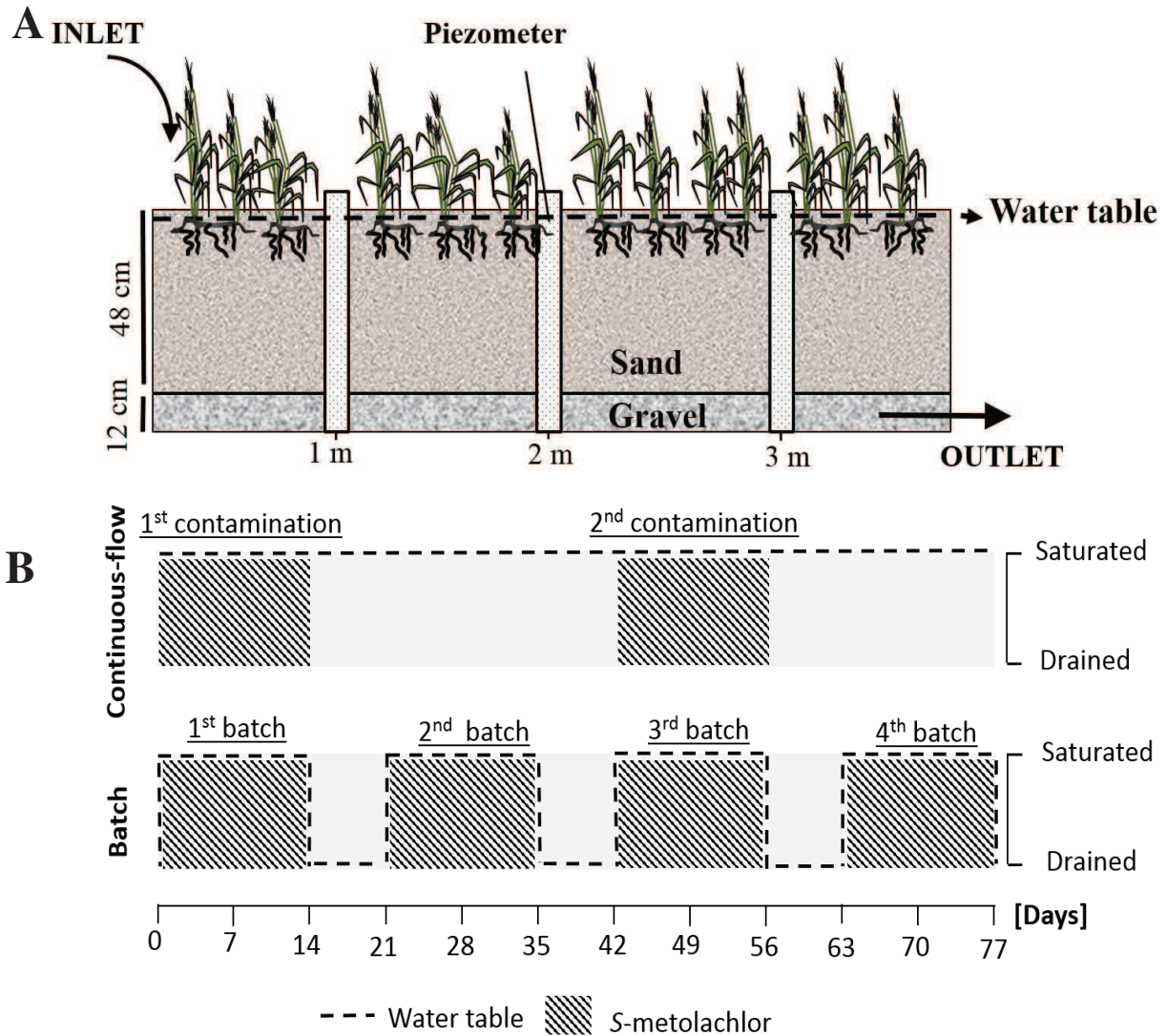


**Figure IV-1. Schematic representation of (A) subsurface-flow constructed wetlands investigated in this study (B) hydraulic operation and contamination for the two wetlands.**

In the continuous wetland, two 14-day periods of continuous supply of water contaminated with *S*-metolachlor were carried out (Figure IV-1B). The mean inlet flow rate was 5.0 L h<sup>-1</sup> and mean residence time was about 6.0 days. Initial continuous exposure with *S*-metolachlor contaminated water was performed from May 24 to June 7, 2012 (i.e. from day 0 to day 14), and the second continuous exposure was done from July 5 to July 19, 2012 (i.e. from day 42 to day 56). After each exposure, the wetland was continuously supplied with uncontaminated water using a screw pump to maintain flooded conditions throughout the experiment (Figure IV-1 B). In the batch wetland, 4 flood-drain cycles were carried out. Each cycle consisted of 14 days of saturated conditions (water residence time of 14 days) of water contaminated with



*S*-metolachlor (prepared as described below), followed by a drained period of 7 days (Figure IV-1 B).

The two wetlands were exposed to the same pesticide load in each contamination cycle to facilitate comparison. Hydrochemistry of supplied tap water, water volumes, and associated *S*-metolachlor concentrations and masses supplied to the wetlands are described in Table IV-1 and Table IV-2 of the Appendix. Mercantor Gold® (960 g L<sup>-1</sup> of *S*-metolachlor, 87.4 ± 1.1% of the *S*-enantiomer, Syngenta, Basel, Switzerland) was dissolved in methanol (Chromasolv® Plus, analytical grade purity > 99.9%; Sigma Aldrich, St. Louis, MO, USA) to obtain a stock solution of 30 g L<sup>-1</sup> of *S*-metolachlor. 10 mL of this solution was added to 1L of ultrapure water and stirred overnight to allow methanol evaporation. For the continuous-flow wetland, contaminated inlet water was prepared with tap water to yield a final concentration of 178 µg L<sup>-1</sup>, thereby supplying 300 mg of *S*-metolachlor to the wetland over each two-week contamination phase. The same total amount of 300 mg *S*-metolachlor, dissolved in a tap water volume that varied from one batch operation to another depending on the initial volume of rainwater in the wetland prior to the batch operation, was provided to the batch wetland in each batch cycle. Initial concentration of *S*-metolachlor in the batch wetland was approximately 500 µg L<sup>-1</sup>.

## 2.2. Sampling

Water samples were collected at the inlet, outlet and at the three piezometers for *S*-metolachlor (1 L), hydrochemical (0.8 L) and microbiological (1 L) analyses. Hydrochemical and pesticide analyses were carried out weekly through the experiment to establish mass balances and evaluate *S*-metolachlor dissipation in the wetlands. Water sub-samples collected from the three piezometers (Figure IV-1 A) were pooled into a single composite sample for the batch wetland, and processed separately for the continuous-flow wetland to evaluate spatial changes in bacterial composition from inlet to outlet.

Samples for DNA extraction were collected through the experiment (on days 0, 35, 42, 56 and 77), and more regularly between day 35 and 56, about 1 month following the establishment of the distinct hydraulic regimes. Sampling of batch wetland water was carried out at the end of every two-week flooding period to ensure that bacterial composition is representative of the

prevailing wetland hydrogeochemical conditions. Samples for DNA extraction were collected in sterile 1 L glass bottles, immediately placed in an ice-cooled container, transported to the laboratory and filtered on sterile 0.2  $\mu\text{m}$  cellulose filters (Millipore, Billerica, MA, USA) on the same day. Filters were placed in sterile 50 mL plastic Falcon tubes and stored at  $-20^{\circ}\text{C}$  until further processing.

Two plants each of *Phragmites australis* and *Phalaris arundinacea* (the dominant plants by the end of the experiment) and bulk sand samples were sampled on the last day of the experiment (day 77 and day 84 for batch and continuous-flow wetlands, respectively) to investigate rhizosphere bacterial composition. Coarse stones and vegetal debris were removed from sampled plants, non-adhering sand separated by shaking, and sand and plant samples stored at  $-20^{\circ}\text{C}$  until further processing.

### 2.3. Hydrochemical and pesticide analysis

Electrical conductivity, pH, dissolved oxygen concentration and redox potential were measured weekly at the inlets, outlets and piezometers using a Hanna Instrument multi-parameters probe HI9828 (Tanneres, France). These physico-chemical parameters were continuously monitored between samplings at the outlet of the continuous-flow and in the middle piezometer (2m from inlet) of the batch wetland. Concentrations of carbon and major ions were determined according to FR EN ISO standard procedures. *S*-metolachlor and its ethanesulfonic acid (ESA) and oxanilic acid (OXA) metabolites were extracted from water samples by solid-phase extraction (SPE) using SolEx C18 cartridges (Dionex®, Sunnyvale, CA, USA) and an AutoTrace 280 SPE system (Dionex®). Quantification was performed by GC-MS/MS (*S*-metolachlor) and by LC-MS (ESA and OXA; see Appendix for details of extraction and quantification procedures and Table IV-3). Detection and quantification limits were 0.7, 0.04, and  $0.06 \mu\text{g L}^{-1}$  and 2, 0.10 and  $0.06 \mu\text{g L}^{-1}$  for *S*-metolachlor, ESA and OXA, respectively.

### 2.4. DNA extraction

For water samples, total DNA was extracted from filters using the PowerWater® DNA kit following the manufacturer's instructions (MO BIO). For rhizosphere samples, DNA was extracted from 0.25 g rhizosphere sand using the PowerSoil® DNA kit (MO BIO, Carlsbad, CA, USA) according to the manufacturer's instructions with minor modifications (see Appendix for details). DNA was extracted from 0.25 g and 10 g bulk sand samples using

PowerSoil® and PowerMax® DNA kits (MO BIO), respectively. DNA concentrations were determined using the Quant-iT dsDNA HS assay kit and the Qubit fluorimeter (Invitrogen, Carlsbad, CA, USA).

### 2.5. T-RFLP analysis

Bacterial 16S rRNA gene fragments (0.9 kb) were PCR-amplified using 5' carboxyfluorescein (6-FAM) labelled 27f primer and 927r primer as described previously (Penny et al., 2010) (see Appendix for details). T-RFLP electropherograms were analysed with the PeakScanner V1.0 software (Applied Biosystems, Carlsbad, CA, USA). Noise cancellation, peak alignment and creation of (samples × T-RFs) matrices was performed using T-REX (<http://trex.biohpc.org>) (Culman et al., 2009). Peak heights were normalized to total fluorescence units per sample, and the resulting data matrices were used for statistical analysis (see SI).

### 2.6. 454 pyrosequencing

Universal 16S bacterial primers 28F (5'-TTTGATCNTGGCTCAG-3') and 519r (5'-GTNTTACNGCGGCKGCTG-3') (Andreotti et al., 2011) were used to amplify an approx. 500 bp fragment of the 16S rRNA gene spanning the hypervariable region V1-V3 for subsequent bacterial tag-encoded FLX amplicon pyrosequencing (Acosta-Martinez et al., 2008). Sequences were generated in a one-step PCR with amplicons originating and extending from the 28F primer according to established methods (Andreotti et al., 2011). Sequencing was performed at Research and Testing Laboratory (Lubbock, TX, USA), on a Roche 454 FLX instrument following the manufacturer's protocols (Roche, Basel, Switzerland).

### 2.7. Data analysis

#### 1.1.1. Processing of pyrosequencing data

Denosing, chimera checking, generation of OTUs and taxonomic classification were performed using a custom scripted bioinformatics pipeline (Handl et al., 2011), see Appendix). Obtained matrices of taxonomic data were used for further statistical analysis, except for calculation of diversity and richness indices (see below).

#### 1.1.2. Measurements of bacterial diversity

Shannon diversity and richness indices from T-RFLP data were calculated using R version 3.0.1 (<http://www.r-project.org>). For pyrosequencing data, sequence datasets were reanalysed using MOTHUR version 1.32.1 (<http://www.mothur.org>) starting from denoised and chimera checked sequences, aligned, and clustered to define OTUs at 97% sequence identity. A subsample of sequences was then randomly selected to obtain equally sized datasets according to the standard operating procedure ([http://www.mothur.org/wiki/454\\_SOP](http://www.mothur.org/wiki/454_SOP), Schloss et al., 2011). Resulting datasets were used for calculation of Shannon diversity and richness indices using R, and for rarefaction analysis.

#### 1.1.3. Statistical analysis

Statistical analysis was carried out with R. Hydrochemical data were compared using the paired non-parametric Wilcoxon signed rank test with *p*-values set at 0.05. Two-dimensional nonmetric multidimensional scaling (NMDS) based on Bray-Curtis dissimilarities of Hellinger transformed data (square root transformation of relative abundances) was used to visualize dissimilarities in bacterial community structures. The relationship between community profiles and hydrogeochemical variables was investigated by fitting environmental vectors *a posteriori* onto the NMDS, and their significance was assessed by conducting a Monte-Carlo permutation test with 1000 permutation steps. Analysis of similarities ANOSIM based on Bray-Curtis dissimilarities was used to infer statistical differences between groups.

### 3. Results and discussion

#### 3.1. Biogeochemical evolution

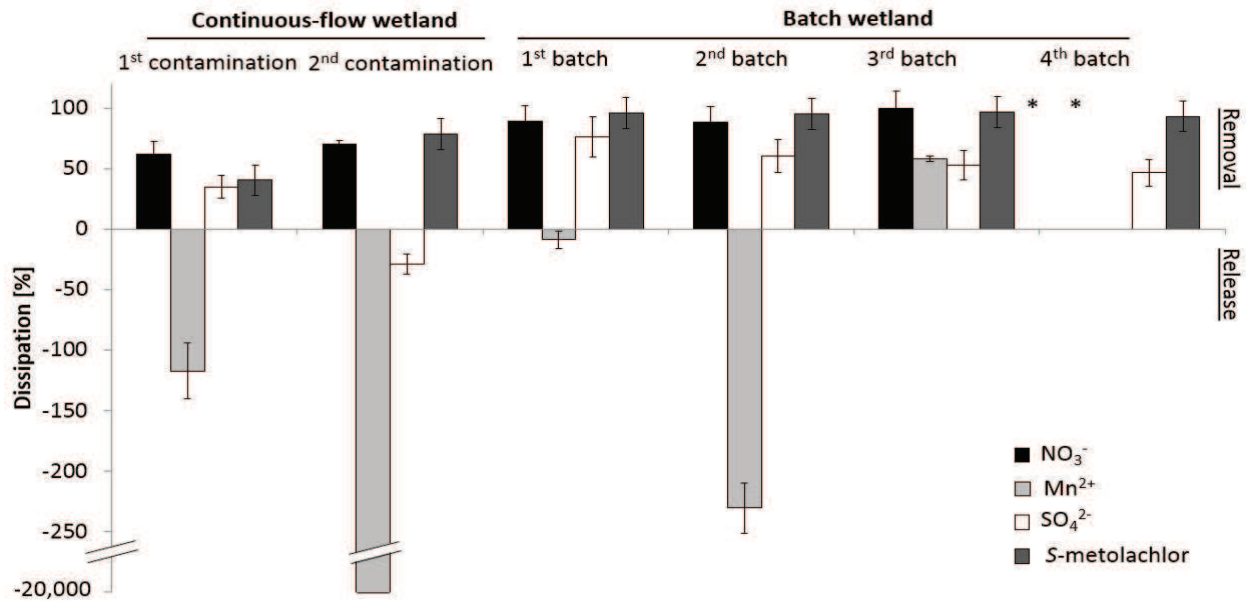
The experiment was conducted from May 24 to August 9, 2012 (spring and summer), which corresponded to the period of macrophyte development and microbial activity, thus enabling the investigation of the influence of hydraulic and hydrochemical conditions on bacterial communities in the wetlands. Outdoor subsurface-flow constructed wetlands were chosen because of (i) their widespread use in the treatment of various types of wastewaters, (ii) their simplicity to operate and implement a mass-balance approach to evaluate contaminant dissipation, and to implement different hydraulic regimes.

The two wetlands showed markedly different oxygen and redox conditions, reflecting the corresponding distinct hydraulic regimes that were chosen. Permanent flooding in the continuous-flow wetland was associated with low values of oxygen and redox potential. Dissolved oxygen concentration dropped from 4.2 mg L<sup>-1</sup> at the beginning of the experiment

to  $< 0.02 \text{ mg L}^{-1}$  from day 7 onwards, and redox potentials ranged from -190 to -400 mV. The batch system featured alternating redox (320 to -400 mV) and oxygen cycles, following the flood-drain cycle. Mean dissolved oxygen concentration was  $3.1 \pm 1.8 \text{ mg L}^{-1}$ , systematically dropping below  $0.02 \text{ mg L}^{-1}$  at the end of every two-week flooding period.

Biogeochemical activity as evidenced by reduction of terminal electron acceptors was observed in both wetlands, but was generally more pronounced in the batch wetland (Figure IV-2 A). Nitrate load reduction between wetland inlet and outlet ranged between 62 and 70% in the continuous-flow wetland, and between 89 and 100% in the batch wetland. Likewise, reduction of sulphate was higher in the batch wetland (47- 76%) than in the continuous-flow wetland (35% reduction during the first contamination period; 29% sulphate release during the second contamination period). Manganese reduction was evidenced by the release of  $\text{Mn}^{2+}$  in both wetlands, except in the third flood-drain cycle of the batch wetland. Given the occurrence of sulphate and manganese reduction. Inlet ferrous and ferric iron concentrations remained low throughout the experiment ( $\leq 0.07 \text{ mg L}^{-1}$ ) (Appendix, Table IV-2). These findings are in keeping with results from previous studies (Adav et al., 2009; Fan et al., 2013; Kishida et al., 2006; Stein et al., 2003), in which higher biogeochemical activity was observed in systems with alternating oxic/anoxic conditions than in systems with either oxic or anoxic conditions alone.

A)



B)

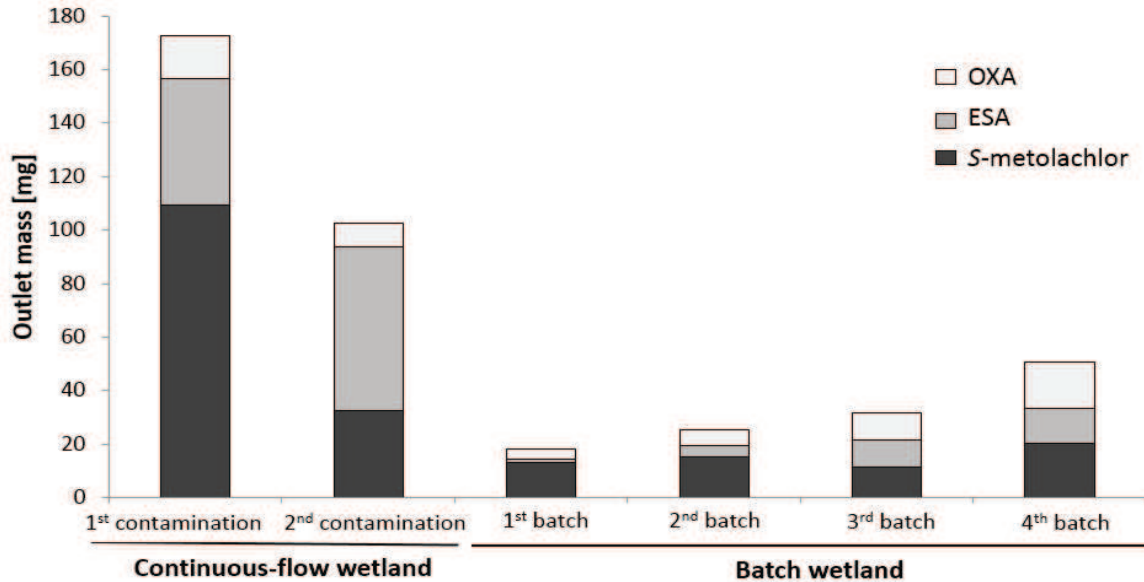


**Figure IV-2. Biogeochemical processes and metolachlor degradation in the two wetlands.** (A) Dissipation (%) of terminal electron acceptors and *S*-metolachlor loads between inlets and outlets. Error bars indicate the propagated errors. (\*) Calculation of dissipation % was not possible because inlet concentrations were below the detection limits. (B) Mass load of *S*-metolachlor and its oxanilic (OXA) and ethane sulfonic (ESA) degradates in wetland outlets. Analytical uncertainties on calculated masses were 8, 38 and 28% for *S*-metolachlor, OXA and ESA, respectively.

### 3.2. *S*-metolachlor dissipation

Removal of *S*-metolachlor loads markedly differed in the two wetlands. In the continuous-flow wetland, *S*-metolachlor mass removal was 40% in the first contamination phase and increased

to 79% in the second contamination phase Figure IV-2. In the batch wetland, in contrast, almost complete removal of *S*-metolachlor (93-97%) was observed for the four batch loads of contaminated water. Most importantly, detection of ESA and OXA indicated the occurrence of *S*-metolachlor biodegradation in the two wetlands (Figure IV-2 B). Higher mass removal of *S*-metolachlor in the batch system may reflect faster aerobic degradation favoured by oxygen replenishment during the dry period of batch operation. Constructed wetlands with alternating phases of saturation and unsaturation and higher redox values (batch wetlands) were shown to better remove several organic contaminants, mostly pharmaceuticals, in comparison to permanently saturated wetlands operating at low redox potential (Avila et al., 2013; Zhang et al., 2012). Interestingly, higher amounts of ESA and OXA were found in the outlet of the continuous-flow wetland (Figure IV-2 B), suggesting either that the pathway involving ESA and OXA as intermediates contributed more towards *S*-metolachlor dissipation under continuous-flow conditions, or that complete degradation of *S*-metolachlor was more prominent in the batch wetland.

### 3.3. T-RFLP analysis of hydraulic regime effects on bacterial communities

Observed differences in the two wetlands in terms of redox conditions, biogeochemical activity and *S*-metolachlor dissipation were reflected in the composition of bacterial communities as revealed by T-RFLP. Complex bacterial profiles were observed in pore-water samples of both wetlands. On average,  $43 \pm 14$  major terminal restriction fragments (T-RFs; range 18 - 73 T-RFs per sample) were obtained per sample. For both wetlands, initial bacterial profiles at day 0 were similar to that in inlet water bacterial communities (Appendix, Figure IV-5). NMDS ordination analysis ( Figure IV-3 A) revealed a significant shift in bacterial composition in the first 35 days of the experiment, as also confirmed by ANOSIM analysis of day 0 samples and samples from later dates ( $p = 0.001$ ). This shift likely reflects adaptation of bacterial communities to the wetland conditions generated after onset of hydraulic operations and *S*-metolachlor exposure during the initial phase. In contrast, samples from day 35 to day 77 were clustered closer together on the ordination plot, indicating that dominant bacterial types did not change significantly after the first 35 days of the experiment.

Differences in bacterial structure of water samples from the two wetlands were small but significant ( $p = 0.008$ ). The batch wetland samples (with the exception of day 0 samples) formed a loose cluster in the ordination plot, but overlapped with continuous-flow wetland

samples ( Figure IV-3 A). Previous studies on the impact of hydraulic conditions on bacterial communities were mainly performed on soil communities (Kim et al., 2008; Mentzer et al., 2006; Rezanezhad et al., 2014). Knowledge on the effect of hydraulic functioning on wetland water communities is scarce, but significant effects of hydraulic functioning on bacterial community structures in wetland sediments were not observed (Ishida et al., 2006). The lack of marked differences in bacterial community structure in water from the two wetlands may be explained by the fact that sampling of batch wetland water was carried out at the end of every two-week flooding period, when the system was oxygen depleted ( $0 - 0.6 \text{ mg L}^{-1}$ ) and showed low redox potential ( $< 0 \text{ mV}$ ) similar to the continuous-flow wetland.



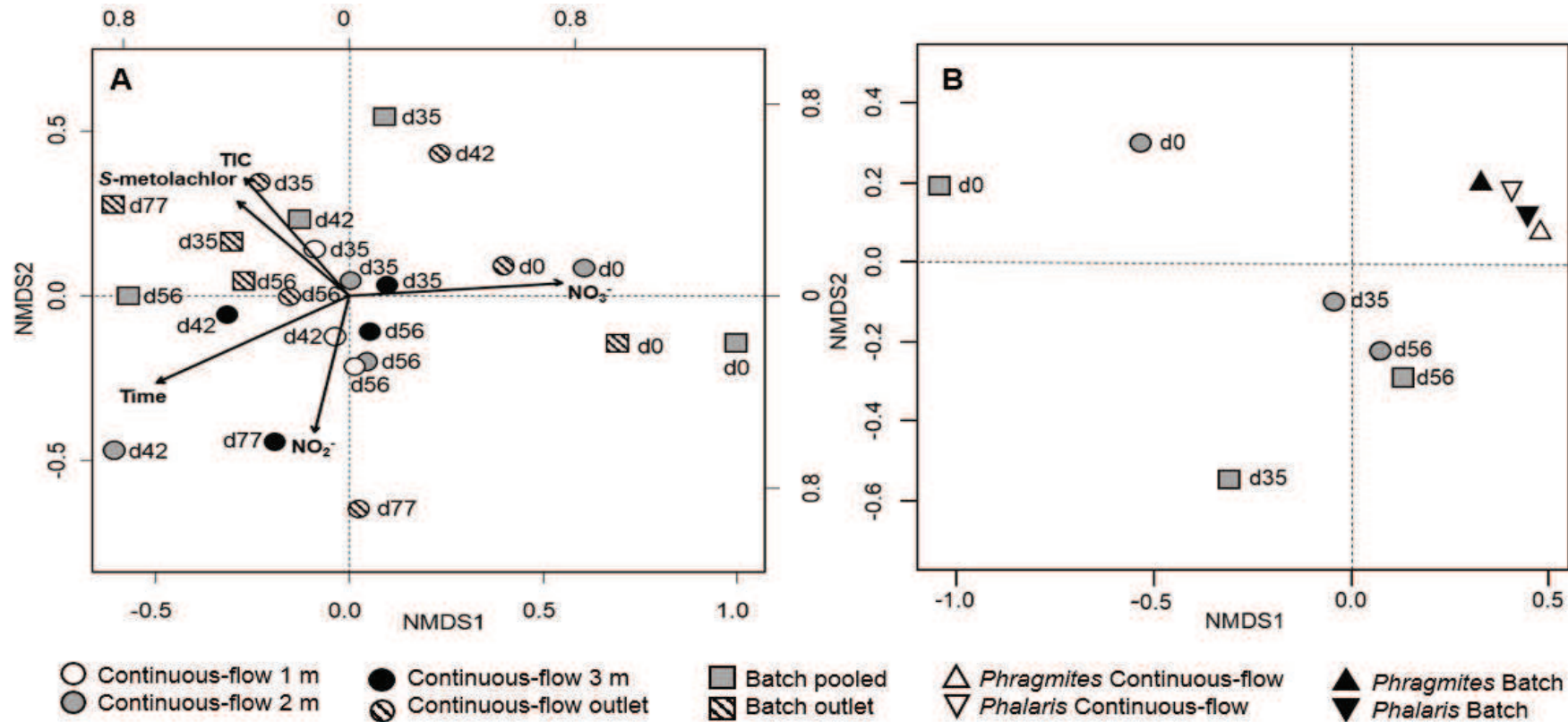


**Figure IV-3.** 2D-NMDS ordination of bacterial community profiles based on (A) T-RFLP and (B) pyrosequencing of the V1-V3 hypervariable region of the 16S rRNA gene in total DNA from wetland water and rhizosphere samples. Sample symbols are labelled according to sampling days (days 0, 35, 42, 56 and 77). 1m, 2m, 3m: 1, 2 and 3 meters from inlet, respectively. In (A), vectors correspond to variables significantly correlated with bacterial community structure are shown (time, *S*-metolachlor, nitrate, nitrite and total inorganic carbon). The significance of fitted vectors was calculated by *a posteriori* permutation of variables at  $p < 0.05$ . Vector arrows were fitted to the NMDS ordination depicting the direction and magnitude of change of the variable. Plot stress (A) 0.18%, (B) 0.04%.

*A posteriori* fitting of environmental parameters onto the NMDS ordination showed that parameters time, total inorganic carbon (TIC), *S*-metolachlor, nitrate and nitrite concentrations all correlated significantly with T-RFLP profiles ( Figure IV-3 A). For example, nitrate was associated with day 0 samples, while nitrite was associated with continuous-flow wetland samples in later stages of the experiment (days 42 -77), in good agreement with the observed shift towards more anoxic conditions accompanied by nitrate reduction. *S*-metolachlor was associated with batch wetland samples, which reflected the higher concentrations of *S*-metolachlor in this wetland. Changes in bacterial community structures due to pesticide exposure may occur through changes in abundances of degrading and pesticide-tolerant populations (Imfeld and Vuilleumier, 2012). The impact of acetochlor, another chloroacetanilide herbicide, on freshwater bacterial communities at concentrations of 50-100  $\mu\text{g L}^{-1}$  was noted previously (Foley et al., 2008), but studies of the impact of metolachlor on bacteria are still rare. Racemic metolachlor at a dose of 2-5  $\text{mg kg}^{-1}$  was shown to impact agricultural soil bacterial community structure based on phospholipid ester-linked fatty acid (PFLA) profiles (Vryzas et al., 2012). An ecotoxicological study with the bacterial reporter *Vibrio fischeri* reported  $\text{IC}_{50}$  values of 174-178  $\text{mg L}^{-1}$  for both pure compound *S*-metolachlor and DualGold Safeneur® (95% *S*-metolachlor and 5% benoxacor) (Joly et al., 2013). However, metolachlor concentrations used in these studies were 1 to 3 orders of magnitude higher than the concentrations used here (max. 500  $\mu\text{g L}^{-1}$ ), which was targeted because it is in the range of highest environmental-relevant concentrations that may impact microorganisms. Worthy of note, the commercial product Mercantor Gold® used in this study contains 13.5% (w/w) additives, which include a mixture of aromatic hydrocarbons, the surfactant calcium dodecylbenzene sulphonate and isobutanol. Surfactants were previously observed to alter soil bacterial community phospholipid fatty acid profiles in combination with herbicides (Banks et al., 2014), probably by increasing their solubility and bioavailability (Giesy et al., 2000; Tsui and Chu, 2004). Hence, additives may also have contributed to the observed impact of the *S*-metolachlor commercial product on bacterial communities in our wetland systems.

#### 3.4. Comparison of T-RFLP and 454 pyrosequencing approaches

To further investigate the temporal evolution of bacterial composition in the two wetlands, total DNA extracted from the composite piezometer water sample in the batch wetland, the middle piezometer water sample (2m from inlet) in the continuous-flow wetland at day 0, day 35 and

day 56, and also from two rhizosphere samples associated to *Phragmites australis* and to *Phalaris arundinacea* plants at the end of the experiment, were analysed by 454 pyrosequencing of PCR products of the 16S gene hypervariable region V1-V3 of the 16S ribosomal RNA gene. Data ordination gave similar results to T-RFLP (Figure IV-3 B), with a clear separation between day 0 samples and later samples. Notably, pyrosequencing provided higher diversity estimates (Shannon index  $H'$  of 2.7 to 7.0) than T-RFLP ( $H'$ : 2.4 to 3.6), because the number of OTUs was 1 to 2 orders of magnitude larger (362 – 2087 OTUs per sample at 97% sequence identity) compared to the number of T-RFs obtained by T-RFLP (see Appendix, Table IV-4. However,  $H'$  diversity indices of the same sample investigated by T-RFLP and pyrosequencing approaches were significantly correlated (Spearman's  $\rho = 0.83$ ,  $p = 0.003$ ; data not shown). This suggests that T-RFLP was able to capture the major trends of bacterial community changes in wetlands despite its lower resolution compared to pyrosequencing. Good overall agreement between T-RFLP and pyrosequencing approaches has been noted in a growing number of studies (e.g., Lee et al., 2011; Mao et al., 2011; Piloni et al., 2012; Yang et al., 2014).

### 3.5. Bacterial composition of wetland water

The pyrosequencing dataset also enabled detailed analysis of the taxonomic composition of bacteria in wetlands and the impact of hydraulic regime. Bacterial composition of wetland water evolved over time from a composition at day 0 close to that of inlet water (Appendix, Figure IV-5) to more diverse communities, including taxa typically involved in the cycling of various terminal electron acceptors and the degradation of organic contaminants. *Proteobacteria* were the most abundant phylum, with *Beta*-, *Alpha*- and *Gammaproteobacteria* representing 26%, 19% and 17% respectively of total bacterial abundance on average for all samples. *Betaproteobacteria*, a classical taxon of freshwaters (Eichler et al., 2006; Lindström et al., 2005), dominated at day 0, representing 63–76% of total abundance at the start of the experiment (Figure IV-4). Abundance of *Betaproteobacteria* subsequently decreased to 33% in continuous-flow wetland water samples, and to 7-11% in batch wetland water samples, and similarly to 7-14% in all rhizosphere samples (7-14%). Within *Betaproteobacteria*, however, abundance of *Rhodocyclales* increased through time. Many representatives of this bacterial order are known to thrive under oligotrophic conditions and to have diverse metabolic and

ecosystemic functions, including anaerobic nitrate reduction and transformation of aromatic pollutants (Hesselsoe et al., 2009).

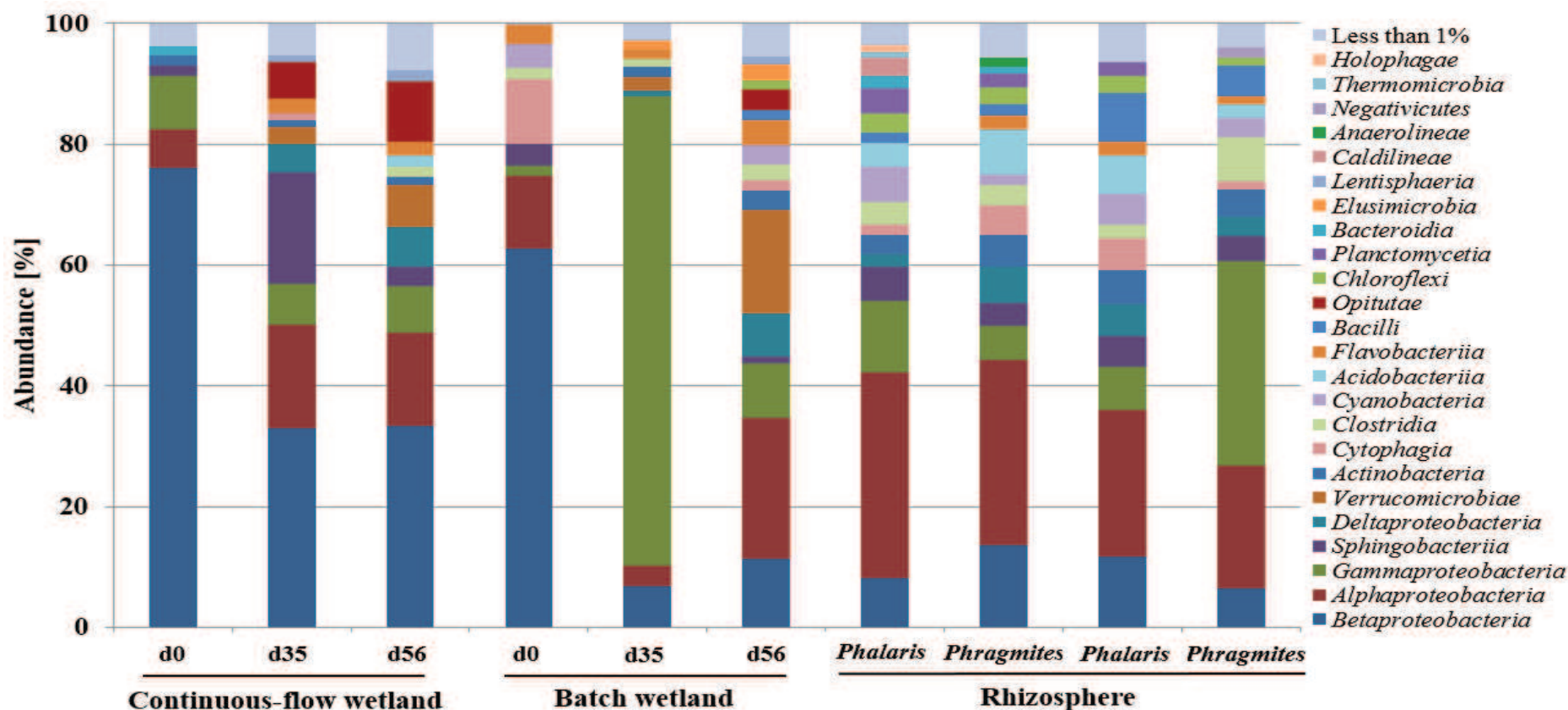


**Figure IV-4. Relative abundance [%] of dominant bacterial classes (80% sequence identity threshold) in the wetland water samples on different sampling days (days 0, 35 and 56) and in the rhizosphere samples.** Continuous-flow wetland pore-water samples represented were at 2 m from inlet. In total, 163,318 raw reads, 114,986 quality reads were obtained, corresponding to 5871–15,897 reads per sample (mean = 11,499 reads).

Another indication of a shift towards more biogeochemically active bacterial populations through time in the investigated wetlands was the increase of *Deltaproteobacteria*, which include many anaerobic sulphate and sulphur reducers. This increase coincided with that of *Chloroflexales* and *Rhodospirillales*, which are typically photosynthetic, and may reflect adaptation to higher sunlight exposure in the wetlands. Also worthy of note, the *Verrucomicrobia* phylum was not significantly detected in day 0 samples but gradually reached 17- 20% abundance in water samples of both wetlands at day 56. *Verrucomicrobia* have been repeatedly detected in wetlands and in particular in acidic peatlands, although little is known about their metabolic capacities and ecological functions (Serkebaeva et al., 2013).

In addition to previously mentioned differences in abundance of *Betaproteobacteria*, two classes showed different abundances in the two wetlands (Figure IV-4): *Sphingobacteria* were more abundant in the continuous-flow wetland (10.8% in average in continuous-flow and 0.8% in batch), whereas *Elusimicrobia* were more abundant in the batch wetland (0.7% in average in continuous-flow and 2.0% in batch). Both classes had previously been noted in wetlands, yet their ecological roles remain poorly understood (Bouali et al., 2014; Serkebaeva et al., 2013). Although bacterial composition in the two wetlands evolved towards relatively diverse but globally similar communities, some differences are worth mentioning. The day 35 water sample of the batch wetland presented a distinctive, low diversity profile, with *Gammaproteobacteria* and mainly *Pseudomonadales* amounting to 78% of the total bacterial abundance (Figure IV-4). The apparently smoother evolution of bacterial composition in the continuous-flow wetland over time was also detectable in the NMDS ordination plot for the T-RFLP and 454 pyrosequencing approaches (Figure IV-2). As noted above, such differences may reflect the different hydraulic regimes and *S*-metolachlor exposure in the two wetlands, with conditions in the continuous-flow wetland gradually evolving from oxic to anoxic during the first 7 days, whereas the batch wetland was subject to sudden fill and drain and oxic/anoxic cycles, with a large load of *S*-metolachlor applied at the onset of each flooding period.

### 3.6. Bacterial composition of the wetland rhizosphere

Rhizosphere-specific communities have been identified in agricultural, grassland, forest and wetland soils (e.g., Lu et al., 2006; Singh et al., 2007; Uroz et al., 2010), and rhizosphere bacteria can play an important role in the degradation of organic contaminants in general, and herbicides in particular (Singh et al., 2004; Yu et al., 2003), and already suggested for *S*-

metolachlor (Anhalt et al., 2000). Rhizodeposits and the redox microenvironment surrounding the root zone result in bacterial communities distinct from those of adjacent water and sediment environments (Dennis et al., 2010), and a strong “rhizosphere effect” was indeed observed in the present study. Rhizosphere communities were markedly different from water communities (Figure IV-2 B), but bacterial composition of the rhizosphere of the two wetlands did not differ significantly (Figure IV-2 B, Figure IV-4). Rhizosphere communities of different samples were  $57 \pm 7\%$  similar to each other on average (Bray Curtis similarity), compared to only  $32 \pm 7\%$  similar in water samples (unfortunately, the very low DNA amounts extracted from bulk sand ( $<0.1$  ng per g) did not allow comparative analysis of the bulk sand bacterial microflora). Taken together, this suggested that hydraulic functioning did not affect the overall composition of the rhizosphere in the two wetlands investigated here.

Rhizosphere samples also displayed a higher average diversity compared to the water samples, basing on Shannon indices (Appendix, Table IV-4) and rarefaction analysis (Appendix, Figure IV-6). Rhizosphere samples shared dominant taxonomic groups with water samples, but relative abundances differed. *Alphaproteobacteria* (20-34%) was the most dominant taxon in both sample types. However, *Rhizobiales* order represented 10-25% of bacteria in rhizosphere samples, but only 1-5% in water samples. Many *Rhizobiales* bacterial types are involved in symbiotic associations with plant roots because of their nitrogen fixing ability (Andreote et al., 2009). *Acidobacteria*, *Bacilli*, *Chloroflexi* and *Planctomycetia* were also more abundant in rhizosphere samples in comparison to water samples. *Gammaproteobacteria* were present in higher abundance (20.5%) in the rhizosphere of the batch wetland compared to the continuous-flow wetland (8.7%). In particular, *Pseudomonadales* represented 14.8% of total rhizosphere genera abundances in the batch wetland and only 1.1% in the continuous-flow wetland. *Pseudomonadales* are often associated with degradation of chlorinated organic compounds. In particular, some *Pseudomonas* strains were found to degrade the chloroacetanilide herbicide acetochlor (Xu et al., 2006), and may have contributed to the higher degradation of *S*-metolachlor observed in the batch wetland.

### 3.7. Towards identification of *S*-metolachlor degraders

The experimental design of our study did not aim to specifically identify *S*-metolachlor degraders, e.g. by comparison with bacterial composition in wetlands that were not exposed to *S*-metolachlor. Thus, the effect of metolachlor exposure on bacterial community composition

could not be explicitly distinguished from that of the hydraulic regime, since changes in these parameters coincided. Only two studies so far identified strains capable of degrading metolachlor, which were affiliated to the genera *Paracoccus* and *Bacillus* (Wang et al., 2008; Zhang et al., 2011). In our study, both *Bacillus* and *Paracoccus* genera were present at very low abundance ( $\leq 0.3\%$ ) in wetland water samples. In rhizosphere samples, *Bacillus* were enriched 1 - 45 fold, while *Paracoccus* were enriched 3 – 17 fold, underlining the interest of further exploration of the bacterial microflora associated with wetland vegetation.

Taxonomic inventories such as performed here are rather poorly suited for identification of *S*-metolachlor-degrading bacteria under the operating conditions of constructed wetlands. First, *S*-metolachlor degradation may be mainly a co-metabolic process and as such not conducive to increase in numbers of degrading bacteria. Second, the amount of nutrients supplied by *S*-metolachlor under the operating conditions of the wetlands is low compared to total available nutrients, making the detection of specific bacteria growing with *S*-metolachlor as a nutrient source very unlikely. Hopefully, the development of approaches to detect and identify specific metabolically active bacteria in complex environments (Uhlik et al., 2013), together with the isolation of further bacteria capable of degrading *S*-metolachlor, will be helpful in this respect.

To summarize, our exploratory study showed that different hydraulic regimes in batch and continuous-flow wetlands led to distinct biogeochemical conditions, and thereby impacted *S*-metolachlor degradation efficiency in the two wetlands. The use of DNA-based approaches to monitor wetland performance was benchmarked by T-RFLP genotyping and 454 pyrosequencing approaches, yielding results in good agreement. Bacterial composition in wetland water mostly changed during the set-up phase, potentially evolving towards more metabolically active communities. Future studies unravelling the impacts of hydraulic functioning and *S*-metolachlor exposure on wetland microbial communities could lead to the development of bioindicators to assess herbicide contamination in wetlands, and to guide the design and management of wetlands treating herbicides.

#### **4. Acknowledgments**

Omnia F. Elsayed was supported by a fellowship of the European Union under the 7<sup>th</sup> Framework Programme (Marie Curie Initial Training Network CSI:Environment, Contract Number PITN-GA-2010-264329). This research was funded by the INTERREG IV Upper Rhine Program to project



PhytoRET (C.21). Elodie Maillard was supported by a PhD fellowship of Région Alsace. Support from REALISE, the Network of Laboratories in Engineering and Science for the Environment in the Alsace Region (<http://realise.unistra.fr>) to both teams of this project is also gratefully acknowledged. The authors thank Julie Brand, Sophie Gangloff, Marie-Pierre Ottermatte, Eric Pernin, René Boutin, Benoit Guyot, Jeanne Dollinger, and Yannis Risacher for analytical support, and Georges Reeb (Atelier REEB, Alsace) and Nicolas Thévenin (RITTMO, Colmar) for advice and help with experimental design.

## 5. Appendix Chapter IV

### Extraction of *S*-metolachlor and degradation products

Solid-phase extraction of water samples was carried out using SolEx C18 cartridges (Dionex®, Sunnyvale, CA, USA) packed with 100 mg bonded silica. An autoTrace 280 SPE system (Dionex) was used for simultaneous extraction of 6 samples. Extraction cartridges were washed with 5 ml of ethyl acetate followed by 5 mL of methylene chloride, and conditioned by sequential elution of 10 mL of methanol and 10 mL of deionised water. Cartridges were then loaded with water samples (10 mL) and dried with nitrogen for 10 min. Elution of chloroacetanilide herbicides and their degradation products was performed with 3 mL followed by 2 mL each of ethyl acetate and methylene chloride respectively. The extract was finally concentrated under nitrogen flux to 1 droplet, and 2 mL of methylene chloride were added.

### *S*-metolachlor quantification

*S*-metolachlor was quantified by GC-MS/MS (Focus-ITQ 700; Thermo Fisher Scientific, Waltham, MA, USA) with Xcalibur (version 2.0.7) for data acquisition, using a 30 m x 0.25 mm ID 0.25 µm film thickness OPTIMA 5MS (5% phenyl-95% dimethylpolysiloxane) fused-silica capillary column (Macherey Nagel GmbH, Düren, Germany), with helium as carrier, at a flow rate of 1 mL min<sup>-1</sup>. The oven was held at 50°C for 2 min, ramped at 30°C min<sup>-1</sup> to 150°C, then up to 250°C at 5°C min<sup>-1</sup> and finally ramped at 30°C min<sup>-1</sup> to 300°C and held for 5 min. A volume of 3 µL of sample was injected on a split/splitless injector (pulsed splitless at 2.5 mL min<sup>-1</sup> for 1 min) using an AI/AS 3000 autosampler (Thermo Fisher Scientific). Injector temperature and transfer line were set at 280°C and 300°C respectively. The mass spectrometer

was operated in electron ionization mode (70 eV) on a mass spectrometer in Selected Ion Mode (SIM). Ion source temperature was maintained at 210°C. For GC-MS/MS analysis, 10 µL of internal standard (final concentration 100 µg L<sup>-1</sup>) were added to 190 µL of water samples. Detection limit was 0.7 µg L<sup>-1</sup> and quantification limit was 2 µg L<sup>-1</sup>. Quantification of *S*-metolachlor was based on the daughter ion 162 and qualification on the daughter ion 133.

#### Analysis of ESA and OXA degradation products

Ethane sulfonic (ESA) and oxanilic acids (OXA) degradation products of metolachlor were analysed using a TSQ Quantum ACCESS LC/MS equipped with an Accela autosampler (Thermo Fisher Scientific) fitted with a temperature-controlled sample tray (15°C). Xcalibur (version 2.1.0) was used for data acquisition. Injection volume was 20 µL. The analytical column was an EC 150/3 Nucleodur Polar Tec (particle size 3µm, length 150 mm, internal diameter 3 mm) fitted with a precolumn EC 4/3 Polar Tec, 30 mm (Macherey Nagel). The mobile phase consisted of 0.1% formic acid/high-purity water (A) and 0.1% formic acid/acetonitrile (B). The program (flow rate 0.3 mL min<sup>-1</sup>) included an initial step at 35% B (5 min) followed by a gradient of 35% to 95% B in 16 min and then 5 min at 95%B, prior to column regeneration (95%-35% B (1 min), 35% B (5 min)). Column oven temperature was set at 60°C. The mass spectrometer (MS) was a TSQ Quantum triple quadrupole mass spectrometer (Thermo Scientific) operated using a heated electrospray ionization (HESI) source. Mass spectra were recorded in the negative ion mode (spray voltage: 3500 V) for the 2 degradation products, and in the positive mode (spray voltage: 4250 V) for the internal standard Alachlor-d<sup>13</sup>. The vaporiser temperature was 300°C, with sheath gas N<sub>2</sub> pressure setting 10 (arbitrary units), auxiliary gas pressure 20, ion sweep gas pressure 0; and ion transfer capillary temperature 300°C. Best sensitivity in multiple reaction monitoring operation (MRM) mode was achieved through acquisition of selected reaction monitoring (SRM) transitions. For compound identification, two SRM transitions and a correct ratio between the abundances of two optimized SRM transitions (SRM1/SRM2) were required along with retention time matching. Limits of detection for OXA and ESA were 0.06 and 0.04 µg L<sup>-1</sup>, and limits of quantification 0.10 and 0.06 µg L<sup>-1</sup>, respectively.

#### Rhizosphere separation from plants

For rhizosphere DNA analysis, frozen plants were fully thawed and roots were separated from aerial parts with a sterile knife. Rhizosphere was defined as the sand adhering to roots after gentle shaking by hand for 20 seconds. Roots were immersed into 50 mL of sterile phosphate buffer saline solution (8 g L<sup>-1</sup> NaCl, 1.44 g L<sup>-1</sup> Na<sub>2</sub>HPO<sub>4</sub>, 0.24 g L<sup>-1</sup> KH<sub>2</sub>PO<sub>4</sub> ; pH 7.2) and incubated on a shaking incubator at 100 rpm for 5 min at room temperature to separate the root-adhering rhizosphere sand from the roots. Washed roots were removed, and the resulting sand suspension was centrifuged at 4000 g for 10 min. DNA was extracted from 0.25 g of the resulting pellet using the PowerSoil® DNA Isolation Kit (MO BIO, Carlsbad, CA, USA) following the manufacturer's instructions and stored at -20°C.

#### Details of T-RFLP analysis

PCR mixtures (total volume, 50 µL) contained 1X high-fidelity PCR buffer (containing 7.5 mM MgCl<sub>2</sub>) (Bio-Rad, Hercules, CA, USA), 200 µM of each dNTP, primers (0.4 µM each), 1U iProof high-fidelity polymerase (Bio-Rad), and 1 ng of total DNA. PCR amplification involved an initial denaturation at 95°C for 2 min, followed by 30 cycles of denaturation at 94°C for 20 s, annealing at 52°C for 30 s, extension at 72°C for 30 s, and a final 1 min extension step at 72°C. PCR reactions were carried out in triplicate, pooled and purified from 1% agarose gels using the QIAquick® gel extraction kit (QIAGEN, Venlo, The Netherlands). Purified 16S rRNA gene fragments (50 to 100 ng) were digested at 37°C for 4 h with 10 U AluI (Thermo Scientific). Digestion products were purified with the QIAquick® nucleotide removal kit (QIAGEN). 5 µl of DNA aliquot (10 to 50 ng) was mixed with 10 µl of Hi-Di formamide (Applied Biosystems) containing 1:20 (vol/vol) carboxy-X-rhodamine (ROX)-labeled MapMarker 1000 (Bioventures, Murfreesboro, TN, USA), denatured at 95°C for 5 min, and snap-cooled on ice. Denatured restriction fragments were loaded onto an ABI Prism 3130 XL capillary sequencer (Applied Biosystems) equipped with 50 cm long capillary and POP 7 electrophoresis matrix according to the manufacturer's instructions. Peaks between 50 bp and 800 bp were analysed. T-RFLP profiles were analysed using T-REX (<http://trex.biohpc.org>) (Culman et al., 2009). T-REX software uses the methodology described by Abdo et al. (Abdo et al., 2006) and Smith et al. (Smith et al., 2005) to identify and align peaks, respectively. Peaks of a minimum height of 10 RFU and higher than 3 standard deviations from the baseline were

considered in further analysis. A clustering threshold of 0.5 was used to align terminal restriction fragments (T-RFs).

#### Details of 454 pyrosequencing analysis

Short reads of < 250 bp were removed, and denoising and chimera checking were accomplished using the UCLUST and UCHIIME algorithms (Edgar, 2010; Edgar et al., 2011). Sequences were clustered into operational taxonomic units (OTUs) at different levels of sequence identity. A seed sequence was defined for each cluster and included in a FASTA formatted file. This file was then queried against a highly curated database compiled by Research and Testing Laboratory and originating from NCBI (<http://ncbi.nlm.nih.gov>), and bacterial taxa were identified using Krakenblast (<http://www.krakenblast.com>). Based upon BLASTn derived sequence identity percentage, sequences were classified at the appropriate taxonomic level, according to the following criteria. Sequences with identity scores to known or well-characterized 16S sequences >97% identity (<3% divergence) were resolved at the species level, between 95% and 97% at the genus level, between 90% and 95% at the family level, between 80% and 90% at the order level, between 80 and 85% at the class level, and between 77% – 80% at the phylum level. Any match below this level of identity was not used in taxonomical analysis.

**Table IV-1. Inlet water volumes and injected *S*-metolachlor concentrations and masses in both studied wetlands.**

Days	Continuous-flow wetland			Batch wetland				
	Water volume supplied (inlet tank)	<i>S</i> -Metolachlor concentration in the inlet tank	<i>S</i> -Metolachlor mass supplied to the wetland	Residual (rainfall) water volume in wetland	Added water volume (inlet tank)	<i>S</i> -Metolachlor concentration in the inlet tank	<i>S</i> -Metolachlor mass supplied to the wetland	
	[L]	[ $\mu\text{g L}^{-1}$ ]	[mg]	[L]	[L]	[ $\mu\text{g L}^{-1}$ ]	[mg]	
0 - 7	923	178	164	Batch 1	0	600	500	300
7 - 14	826	178	147					
14-21	837	-	-					
21 - 28	865	-	-					
28 - 35	1221	-	-	Batch 2	490	110	2727	300
35 - 42	1243	-	-					
42 - 49	194	178	35					
49 - 56	994	178	177	Batch 3	495	105	2857	300
56 - 63	1300	-	-					
63 - 70	400	-	-					
70 - 77	474	-	-	Batch 4	250	350	857	300
77 - 84	773	-	-					

**Table IV-2. Hydrochemical parameters of water samples from the inlet (tap water), outlet and piezometers of the continuous and the batch wetlands.** Values are provided as mean  $\pm 2\sigma$  throughout the investigation period (weekly sampling from May 24, 2012 (day 0) to August 9, 2012 (day 77)).

Parameter	Unit	Continuous-flow wetland			Batch wetland		
		Inlet	Piezometers	Outlet	Inlet	Piezometers	Outlet
Fe <sup>2+</sup>	[mg L <sup>-1</sup> ]	0.01 $\pm$ 0.02	0.01 $\pm$ 0.02	0.01 $\pm$ 0.02	0.04 $\pm$ 0.04	0.02 $\pm$ 0.03	0.05 $\pm$ 0.09
Fe <sup>3+</sup>	[mg L <sup>-1</sup> ]	0.01 $\pm$ 0.01	0.06 $\pm$ 0.23	0.03 $\pm$ 0.05	0.03 $\pm$ 0.03	0.14 $\pm$ 0.42	0.24 $\pm$ 0.48
TOC	[mg L <sup>-1</sup> ]	4.8 $\pm$ 3.0	3.1 $\pm$ 3.3	4.7 $\pm$ 5.6	24.6 $\pm$ 12.0	7.5 $\pm$ 7.6	11.6 $\pm$ 12.6
TIC	[mg L <sup>-1</sup> ]	27.3 $\pm$ 13.9	35.7 $\pm$ 9.0	39.1 $\pm$ 12.0	25.8 $\pm$ 14.8	42.6 $\pm$ 16.4	49.9 $\pm$ 13.2
DOC	[mg L <sup>-1</sup> ]	4.8 $\pm$ 2.8	6.7 $\pm$ 15.2	5.6 $\pm$ 8.4	23.6 $\pm$ 11.5	23.1 $\pm$ 60.4	17.0 $\pm$ 15.0
DIC	[mg L <sup>-1</sup> ]	26.7 $\pm$ 14.0	31.5 $\pm$ 8.6	34.8 $\pm$ 10.7	23.0 $\pm$ 16.1	39.8 $\pm$ 13.9	39.2 $\pm$ 21.2
Cl <sup>-</sup>	[mg L <sup>-1</sup> ]	136.1 $\pm$ 44.6	163.6 $\pm$ 57.8	152.6 $\pm$ 55.7	215.8 $\pm$ 161.6	166.8 $\pm$ 123.1	91.8 $\pm$ 96.1
SO <sub>4</sub> <sup>2-</sup>	[mg L <sup>-1</sup> ]	39.3 $\pm$ 3.1	42.5 $\pm$ 12.8	43.1 $\pm$ 16.1	39.3 $\pm$ 3.0	44.0 $\pm$ 6.7	79.0 $\pm$ 74.0
Total P	[mg L <sup>-1</sup> ]	0.2 $\pm$ 0.3	0.1 $\pm$ 0.2	0.2 $\pm$ 0.3	0.3 $\pm$ 0.3	0.1 $\pm$ 0.2	0.2 $\pm$ 0.3
NH <sub>4</sub> <sup>+</sup>	[mg N L <sup>-1</sup> ]	0.2 $\pm$ 0.4	0.1 $\pm$ 0.2	0.1 $\pm$ 0.1	0.2 $\pm$ 0.2	0.1 $\pm$ 0.1	0.1 $\pm$ 0.2
NO <sub>2</sub> <sup>-</sup>	[mg N L <sup>-1</sup> ]	0.2 $\pm$ 0.2	0.1 $\pm$ 0.2	0.1 $\pm$ 0.1	0.9 $\pm$ 1.9	0.1 $\pm$ 0.1	0.0 $\pm$ 0.0
NO <sub>3</sub> <sup>-</sup>	[mg N L <sup>-1</sup> ]	20.9 $\pm$ 10.6	12.2 $\pm$ 10.9	8.0 $\pm$ 8.4	11.9 $\pm$ 13.7	7.03 $\pm$ 8.0	5.0 $\pm$ 5.4
PO <sub>4</sub> <sup>3-</sup>	[mg P L <sup>-1</sup> ]	0.4 $\pm$ 0.2	0.3 $\pm$ 0.2	0.3 $\pm$ 0.1	0.22 $\pm$ 0.21	0.3 $\pm$ 0.1	0.4 $\pm$ 0.1
Mn <sup>2+</sup>	[mg L <sup>-1</sup> ]	3.1 $\pm$ 3.9	68.4 $\pm$ 92.2	48.3 $\pm$ 67.8	4.8 $\pm$ 3.9	34.3 $\pm$ 33.4	344.5 $\pm$ 295.1

**Table IV-3. Daughter ions and transition SRM used for GC-MS/MS quantification of *S*-metolachlor and LC-MS/MS quantification of its ionic degradation products ESA and OXA.**

	Molecules	Quantification	Identification	
		daughter ion 1 m/z	daughter ion 2 m/z	
GC-MS/MS	Parent compound	Metolachlor	162	133
	Internal standard	Metolachlor- <i>d</i> <sub>6</sub>	134	
LC-MS/MS			Transition SRM1	Transition SRM2
	Degradation products	Metolachlor OXA	206	172
		Metolachlor ESA	121	192
	Internal standard	Alachlor- <i>d</i> <sub>13</sub>	251	175

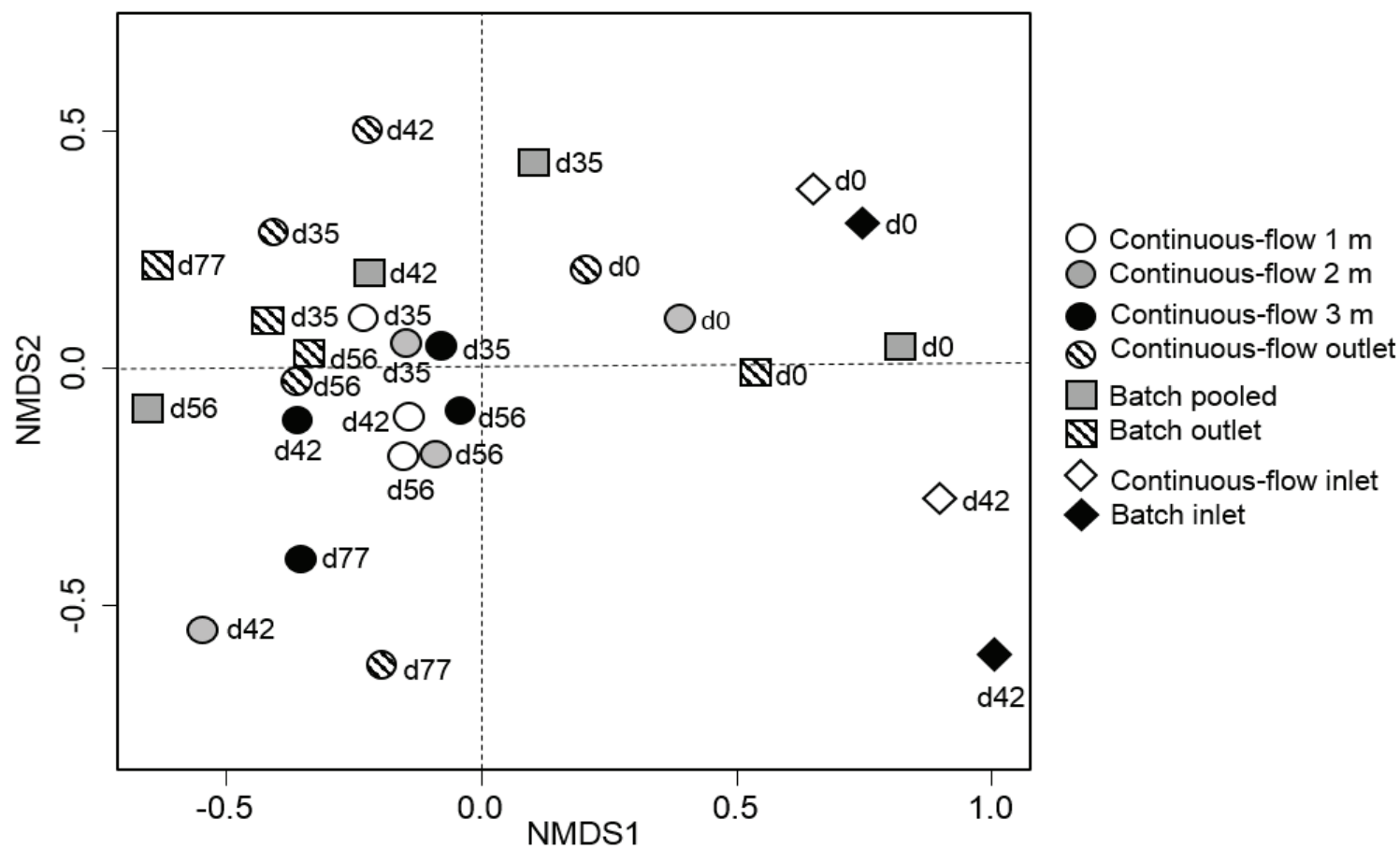


**Figure IV-5. 2D-NMDS ordination of bacterial profiles based on T-RFLP of the 16S rRNA gene from wetland inlet, outlet and piezometer samples.** Samples symbols are labelled with their corresponding sampling days (day 0, 35, 42, 56 and 77). Plot stress = 0.17%.



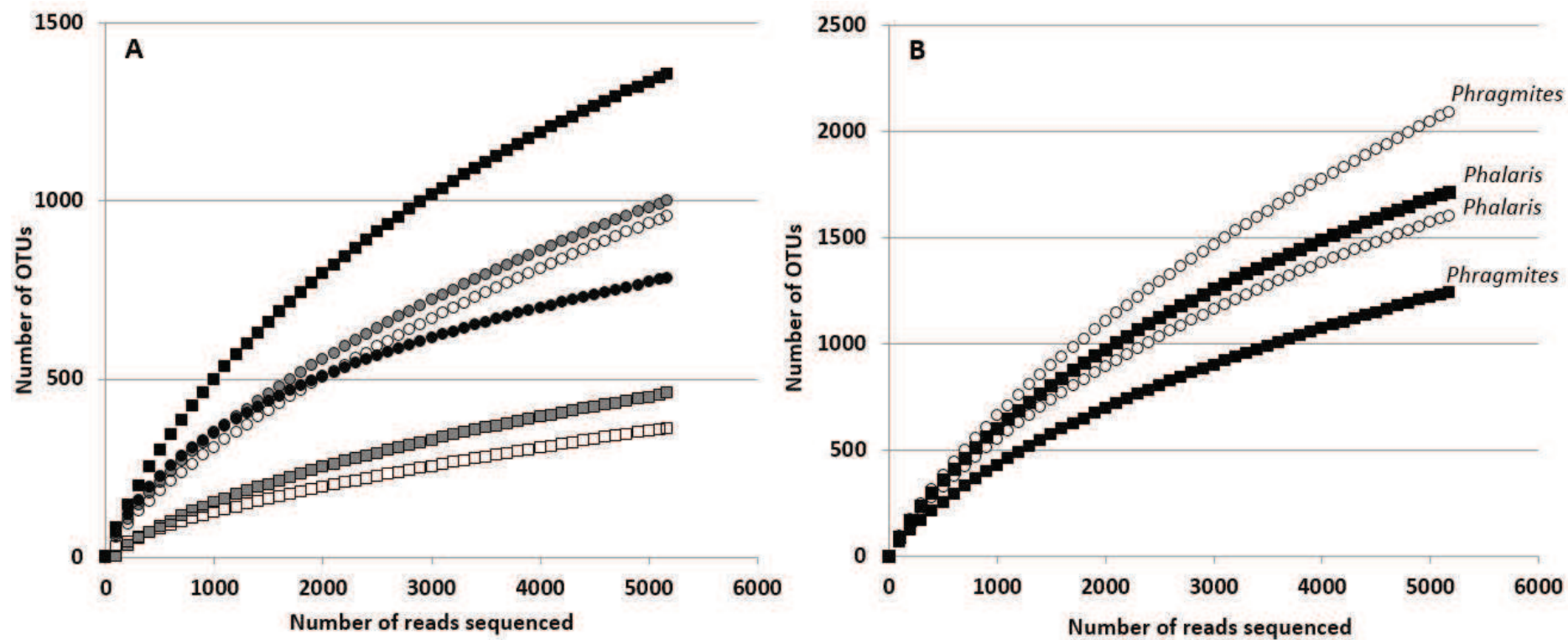


**Figure IV-6. Rarefaction curves for bacterial sequences of the V1-V3 hypervariable region of the 16S rRNA gene with OTUs defined at 97% sequence identity.** Symbols represent samples from continuous-flow wetland (circles) and batch wetland (squares). (A) Water samples from different sampling days: d0 (white symbols), d35 (grey symbols), d56 (black symbols). (B) Rhizosphere samples of plants sampled at the end of the experiment.

**Table IV-4. Shannon diversity index  $H'$  and number of OTUs calculated for wetland samples by T-RFLP (T-RFs) and by 454 pyrosequencing (97% sequence identity), and for rhizosphere samples. “-“, samples not sequenced. A and B refer to duplicates.**

		Sample		T-RFLP		Sequencing	
		Location	Sampling day	$H'$	OTUs	$H'$	OTUs
Continuous-flow		2 m	d0	2.7	35	4.8	957
		outlet	d0	2.7	41	-	-
		1 m	d35	3.3	59	-	-
		2 m	d35	3.2	49	5.1	1001
		3 m	d35	2.7	43	-	-
		outlet	d35	3.2	54	-	-
		1 m	d42	2.8	59	-	-
		2 m	d42	2.6	19	-	-
		3 m	d42	3.3	43	-	-
		outlet	d42	3	62	-	-
		1 m	d56	3.4	59	-	-
		2 m	d56	3.5	73	5.4	783
		3 m	d56	3.6	64	-	-
		outlet	d56	3.1	63	-	-
		3 m	d77	2.7	45	-	-
	outlet	d77	1.8	24	-	-	
Batch		pooled	d0	2.4	30	3.1	362
		outlet	d0	2.5	33	-	-
		pooled	d35	2.6	45	2.7	463
		outlet	d35	3.4	58	-	-
		pooled	d42	3.4	56	-	-
		pooled	d56	3.5	45	6.2	1598
		outlet	d56	3.1	40	-	-
		outlet	d77	2.7	36	-	-
Rhizosphere	Continuous-flow	<i>Phragmites</i> A		3.6	45	7	2087
		<i>Phragmites</i> B		3.2	41	-	-
		<i>Phalaris</i> A		3.3	40	6.4	1598
		<i>Phalaris</i> B		3.4	45	-	-
	Batch	<i>Phragmites</i> A		2.7	48	5.3	1240
		<i>Phragmites</i> B		2.6	18	-	-
		<i>Phalaris</i> A		3.2	32	6.7	1713
		<i>Phalaris</i> B		3.3	34	-	-

## Chapter V

### General discussion and perspectives

One of the major challenges of the 21<sup>st</sup> century is to understand and control the risks that ubiquitous manufactured chemicals pose to the environment. Pesticides represent a major source of diffuse organic contamination of soil, atmosphere and water ecosystems, thereby causing detrimental impacts on flora, fauna and human health. Therefore, understanding pesticide transport and degradation under environmental conditions is required to quantify and if possible to predict pesticide exposure, with the objective of reducing sources and improve design and application of pesticide remediation technologies. Degradation is of particular importance in this respect since it is the only process that leads to effective mass removal of pesticides from environmental compartments.

Despite a multitude of studies on pesticide removal in soil and water, most investigations depend on monitoring pesticide dissipation, and fail to provide insight on degradation processes and the contribution of individual processes to the observed bulk removal (Fenner et al., 2013). Detailed understanding of pesticide degradation processes and the environmental conditions (e.g. redox, availability of TEAs) under which each process takes place is essential to interpret and quantitatively predict pesticide degradation under given environmental conditions. Therefore, approaches that allow assessments of *in situ* pesticide degradation processes under different conditions in key receptor ecosystems are needed.

Pesticides applied on agricultural catchments can reach receptor ecosystems through runoff, aerial deposition and discharge of pesticide-contaminated ground water during flood periods. Among receptor ecosystems, wetlands are ubiquitous and can accommodate a variety of physical, chemical and biological pesticide removal processes, which in turn act as sinks for pesticide contamination before it reaches downstream aquatic ecosystems. Their pesticide sink properties and increasing use for treatment of pesticide-contaminated water made wetlands relevant model ecosystems to study pesticide degradation in redox-dynamic environments in general.

Microorganisms are key players in wetland biogeochemical and organic contaminant, including pesticide, removal functions (Faulwetter et al., 2009). Moreover, microbial

communities can be impacted by pesticide exposure at different levels (i.e., functional, communities) and may therefore provide potential bioindicators of stresses affecting pesticide-contaminated environments (Imfeld and Vuilleumier, 2012; Sims et al., 2013). Yet knowledge of bacterial communities in pesticide-contaminated wetlands, and of their response to environmental and operational disturbances is scarce.

Target pesticides of this PhD work are chloroacetanilide herbicides (metolachlor, acetochlor and alachlor). Their wide use, frequent detection as water contaminants, and the scarcity of knowledge regarding their degradation in redox-dynamic ecosystems made them compounds of choice for this PhD work on pesticide degradation in wetlands.

In this context, the aim of this PhD work was to improve our understanding of *in situ* degradation of chloroacetanilide herbicides taking wetlands as model systems to study pesticide degradation in redox-dynamic ecosystems. Wetland bacterial composition and its environmental (e.g. concentration of TEAs) and operational drivers (e.g. hydraulic regime) were also studied. We used experimental wetlands which have the merit of preserving the complexity of sediment/plant/water interactions while allowing higher level of control of operational parameters (e.g. water flow, input water quality) compared to field studies. A combination of chemical (hydrochemical analysis, pesticide analysis, CSIA, enantiomer analysis) was used to tackle different aspects of chloroacetanilide degradation in wetlands: link with biogeochemical conditions, evidence of *in situ* degradation and identification of prevailing degradation pathways. In parallel, biomolecular (T-RFLP and pyrosequencing) methods enabled the investigation of bacterial community composition.

The main conclusions and impact of this work as well as perspectives for future research are represented in the following section. The discussion is structured around three transversal points i) the utility of combining tools to investigate pesticide degradation in wetlands, ii) the potential and development of CSIA methods to follow and quantify pesticide degradation in the environment, and iii) factors driving bacterial composition and activity in pesticide-contaminated wetlands. Figure V-1 is a schematic representation of the three proposed main routes of future research and techniques to follow them.

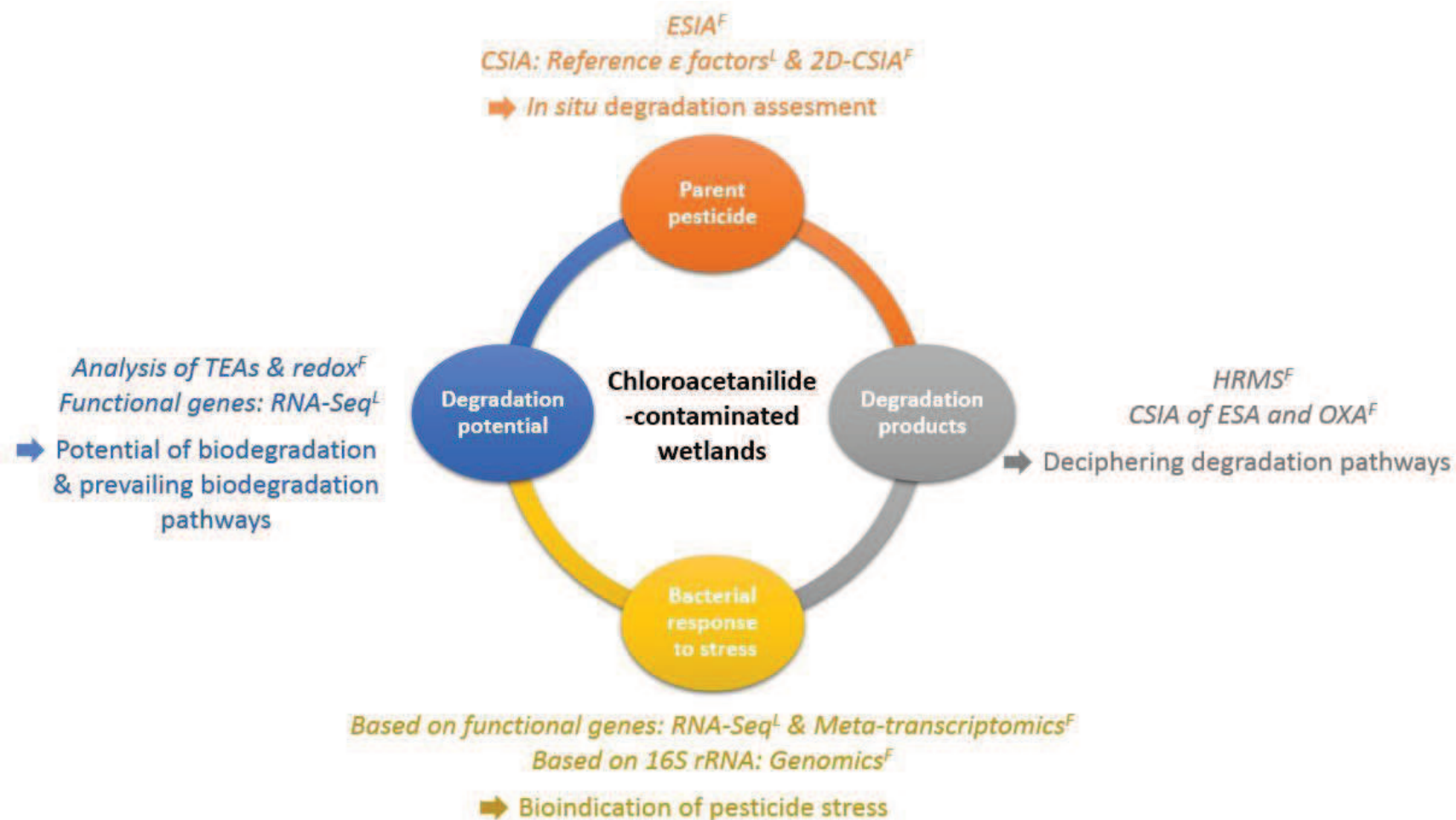


**Figure V-1. Proposed approaches for improving assessments of chloroacetanilide-contaminated wetlands.** Evidence based on parent pesticide, degradation products, degradation potential and bacterial response to pesticides can be combined for better assessments of chloroacetanilide contaminated wetlands. The outcome of each set of methods is indicated by an arrow. The scale at which each method is best applied is indicated by <sup>F</sup> for field-scale and <sup>L</sup> for laboratory-scale.

### 1. Monitoring pesticide degradation in wetlands

Constructed wetlands have attracted interest for being environment-friendly and cost-effective alternatives to physical and chemical treatment methods of urban and agricultural water contaminants. Traditionally, assessments of wetland efficiency in the removal of pesticides are done based on concentration analysis and inlet-outlet mass balances of parent pesticides (Stehle et al., 2011; Tournebize et al., 2013). This approach represents wetlands as a black box providing no understanding of removal processes and failing to show direct evidence of effective mass removal (i.e. degradation) of pesticides from the environment. In this thesis, we addressed this gap by using a combination of methods to tackle different aspects of chloroacetanilide degradation in wetlands, namely evidence of occurrence of degradation, link with biogeochemical conditions and identification of prevailing degradation pathways. Novel approaches used in this PhD work (i.e. CSIA and enantiomer analysis) provided direct evidence of *in situ* degradation of chloroacetanilides independently of the detection of degradation products [Chapter III]. These results demonstrate that CSIA and enantiomer analysis are valuable additions to the toolbox of pesticide fate monitoring in wetlands. These tools can be used to distinguish between pesticide degradation and retention processes in treatment wetlands, a distinction not achievable by ‘traditional approaches’ depending on pesticide concentration analysis.

In addition to its utility as indicator of biodegradation, enantiomer analysis can show the degradation of one enantiomer and the persistence of the other with the implications that this may have on their respective environmental risk (Liu et al., 2005; Ye et al., 2010). Given the significant share of chiral pesticides in total pesticides currently commercialised, and the dearth of knowledge on the fate of separate pesticide enantiomers (Celis et al., 2013), enantiomer analysis is expected to be increasingly used in the evaluation of chiral pesticide degradation in wetlands, and in agroecosystems in general. A solid understanding of enantiomer enrichment patterns associated with different biodegradation processes of chiral pesticides, and of potential confounding processes (e.g. abiotic racemization) can be achieved in benchmark studies (Li et al., 2011; Li et al., 2012; Qiu et al., 2014). This improved understanding of enantiomer patterns can expand the scope of information gained by enantiomer analysis to include the distinction of prevailing biodegradation processes as previously shown for pharmaceuticals in constructed wetlands (Matamoros et al., 2009; Hijosa-Valsero et al., 2010).

The combination of tools used in this study also enabled us to relate biogeochemical conditions and degradation processes, which is necessary to predict the fate of pesticides under different conditions (Borch et al., 2010a). Hydrochemical analysis (analysis of TEAs and redox) was used to identify prevailing redox conditions and corresponding biogeochemical processes in each of the studied wetlands. Chloroacetanilide degradation is mostly studied in fully aerobic systems (Wang et al., 2008; Chen et al., 2014b), and to a lesser extent in fully anaerobic systems (Lauga et al., 2013), whereas effects of changes in redox conditions over space and time on chloroacetanilide degradation are not known. In lab-scale wetlands, acetochlor, alachlor and to a lower extent metolachlor were degraded in the predominantly anoxic rhizosphere zones under nitrate and sulphate reducing conditions [Chapter III, section 2]. Our results show that anaerobic degradation processes play an important role in the dissipation of metolachlor, acetochlor and alachlor in wetlands. Anaerobic processes are also widespread in other predominantly anoxic environments such as aquifers, lake and river sediments and in microniches in agricultural soils and may therefore affect the fate of pesticides in these environments (Zhang and Bennett, 2005; Zeng et al., 2011a; Li et al., 2012). This highlights a need to decipher the yet unknown chloroacetanilide anaerobic degradation pathways to better understand and predict their behaviour under anaerobic conditions in the environment.

In constructed wetlands [Chapter IV], hydrochemical analysis revealed different wetland-scale processes in the two studied wetlands (batch and continuous-flow). Higher dissipation of *S*-metolachlor took place in the batch wetland featuring alternating oxic and anoxic cycles [Chapter IV]. From a remediation viewpoint, this indicates that batch operations resulting in changing redox conditions should be the hydraulic regimen of choice for wetland treating effluents contaminated with *S*-metolachlor.

Few insights on degradation pathways were obtained by the analysis of ionic degradation products ESA and OXA. We chose to screen for ESA and OXA degradation products of chloroacetanilides due to their frequent detection in surface and groundwater reported in previous studies (Hladik et al., 2008a; Baran and Gourcy, 2013b). ESA and OXA were detected in very small amounts in lab-scale wetlands. A possible explanation would be that faster rates of degradation of ESA and OXA than their parent compounds prevented their accumulation in the systems. However this is unlikely given that they are generally considered to be more persistent than their parent compounds (Kalkhoff et al., 2003; Rebich et al., 2004; Huntscha et al., 2008). A more probable explanation to the low detection of ESA and OXA in lab-scale

wetlands is the contribution of different degradation pathways that do not involve the formation of ESA and OXA degradation products in the anaerobic degradation of chloroacetanilides in these systems [Chapter III, section II]. This reflects the findings of a previous study showing that metolachlor ESA and OXA were not substantially formed in anaerobic wetland soils (Seybold et al., 2001). In contrast, *S*-metolachlor ESA and OXA degradation products dominated in predominantly anoxic continuous-flow wetland in comparison to batch wetland [Chapter IV]. Although the degradation of *S*-metolachlor could have occurred in the presence of oxygen in mm scale redox niches in the continuous-flow wetland, we cannot not verify this hypotheses based on our data. Further laboratory studies identifying bacterial populations that degrade chloroacetanilides using the GST pathway, characterising underlying genetic basis and biochemical pathways can shed light on redox conditions under which this degradation reaction is feasible. Our results also point to the limitation of screening for few selected degradation products of pesticides (in this case ESA and OXA) to investigate degradation pathways of pesticides that have many potential degradation products like chloroacetanilides. However, target analysis of other known degradation products of chloroacetanilides products is limited by the absence of corresponding analytical standards. Approaches allowing the non-target screening of wide range of pesticide degradation products can prove more useful to identify degradation pathways in complex environments as highlighted in the following section.

Overall, the results of this work demonstrate the benefit of combining different methods including hydrochemical analysis, pesticide and degradation product analysis, enantiomer analysis and CSIA for evaluating pesticide degradation in wetlands. From this discussion, several avenues of future research arise, which are described below.

### Perspectives

This work represents a first attempt to evaluate chloroacetanilide degradation in redox-dynamic ecosystems. Additional approaches can be applied to elucidate chloroacetanilide degradation pathways, focusing on anaerobic chloroacetanilide degradation, with the aim of improving our understanding and ability to predict chloroacetanilide degradation in different environments. In parallel, unravelling the genetic basis of chloroacetanilide biodegradation would provide new indicators of the potential of biodegradation in chloroacetanilide-contaminated sites.



A first task for future research is the identification of chloroacetanilide biodegradation pathways under different redox conditions with the final aim of improving interpretation and prediction of chloroacetanilide degradation in wetlands. This can be done in small-scale studies using degrading bacterial cultures and larger-scale experimental wetland columns similar to those investigated in Chapter III of this thesis using high-resolution mass spectrometry (HRMS) methods such as Q-TOF and Orbitrap® to screen for all potential chloroacetanilide degradation products (Reemtsma et al., 2013). HRMS methods can be used for non-target screening and post-run identification of unknown degradation products, and therefore overcome the limitation of the scarcity of analytical standards for pesticide degradation products (Padilla-Sanchez et al., 2012; Lopez et al., 2014).

For bacterial culture degradation studies, the isolation of new bacterial degrading strains or consortia will be helpful to identify unknown chloroacetanilide biodegradation pathways. Previously identified chloroacetanilide degraders degraded acetochlor and alachlor aerobically mainly through N-dealkylation (Sette et al., 2004; Liu et al., 2012b; Chen et al., 2014b). Strains degrading chloroacetanilides *via* the GST pathway have not been reported. Moreover, pathways of metolachlor biodegradation have not been described and a very limited number of metolachlor microbial degraders were identified (Munoz et al., 2011). Similarly, no anaerobic chloroacetanilide degraders were identified and anaerobic biodegradation pathways of chloroacetanilides remain completely unknown. Chloroacetanilide-degrading bacterial strains or consortia can be isolated from chloroacetanilide-contaminated agricultural soil, or wetland sediment under aerobic, nitrate and sulphate-reducing conditions.

In experimental wetlands, high resolution mass spectrometry coupled with hydrochemical analysis will allow the identification and elucidation of ongoing degradation processes. This could be done in set-ups similar to those used in Chapter III of this thesis work. Sampling needs to be done with as high spatial resolution as possible (few cm between sampling points) in particular in the metabolically active rhizosphere zone to unravel heterogeneities in redox conditions and corresponding changes in chloroacetanilide degradation pathways. Fine-scale characterisation of hydrogeochemical heterogeneities can be achieved *in situ* using non-invasive redox, oxygen and pH microelectrodes (Wang et al., 2013b).

Another research need is to identify catabolic genes involved in chloroacetanilide degradation which remain mostly unknown. Analysis of catabolic genes can enhance field assessments of pesticide degradation by providing biomarkers of *in situ* biodegradation potential (Nyssonen

et al., 2009), allow the identification of biodegradation hotspots in heterogeneous field sites (Winderl et al., 2008) and provide an additional line of evidence, along with chemical methods (e.g. degradation product analysis and CSIA), on prevailing biodegradation pathways (Callaghan, 2013). In this work, an attempt was made to identify functional genes involved in chloroacetanilide degradation, mainly GSTs, but was unsuccessful [Chapter II]. The absence of any specific knowledge in literature about the type of bacterial GSTs involved in chloroacetanilide biodegradation to guide our choice of GST target DNA sequences potentially contributed to this result. Targeting bacterial GSTs was a particularly challenging task since bacterial GSTs are a part of a protein super-family with members involved in a variety of functions (mostly xenobiotic degradation and protection against chemical and oxidative stress) making it hard to identify a target enzyme (Allocati et al., 2009; Fenner et al., 2013a). Further attempts can be done following the same approach used in this thesis [Chapter II] and targeting the recently described acetochlor N-dealkylase and its putative homologues in *Rhodococcus* and *Streptomyces* strains that were shown also to degrade acetochlor and alachlor *via* N-dealkylation (Sette et al., 2004; Liu et al., 2012b; Chen et al., 2014b).

Identifying chloroacetanilide catabolic genes can be tackled differently using transcriptomic and meta-transcriptomic approaches (Desai et al., 2010). (Meta-)transcriptomics can be applied to identify the genetic basis of microbial response to pesticide exposure without *a priori* knowledge of target catabolic genes as they do not involve targeting particular genes (Mutz et al., 2013). The possible benefit of applying (meta-)transcriptomic approaches to improve monitoring of pesticide-contaminated ecosystems is twofold; first they can lead to identification of pesticide metabolic pathways, second they can be used to identify potential biomarker genes that respond to pesticide stress (bioindicator).

Applications of these approaches to identify microbial responses to xenobiotic and natural organic compounds in the environment are rapidly rising (Jennings et al., 2009; Vila-Costa et al., 2010; Scheublin et al., 2014), but no reports of their application to characterise bacterial response to pesticides could be found in literature. (Meta-)transcriptomic approaches require the following basic steps; i) extraction and enrichment of the total mRNA, ii) reverse transcription of mRNA into complementary cDNA, iii) high throughput sequencing of the complete cDNA transcriptome, and iv) mapping sequence reads to a known sequences in databases, or assembled *de novo* without the genomic sequence to produce a transcription map that consists of both the transcriptional structure and/or level of expression for each gene

(Carvalhais et al., 2012; Sharma and Vogel, 2014). RNASeq transcriptomic technique can be applied on cultures of chloroacetanilide degrading strains to investigate the adaptive response of this specific strain to chloroacetanilide exposure, possibly giving insight on chloroacetanilide metabolic pathways. On the other hand, meta-transcriptomics can be applied on environmental samples (e.g. wetland sediment sample) to investigate the integrative functional response of whole microbial communities to chloroacetanilides and provide insight into *in situ* biodegradation (Vilchez-Vargas et al., 2010). In spite of several technical bottlenecks including extraction of high quality RNA from environmental matrices and rapid changes in transcriptional profiles between sampling and RNA preservation (Carvalhais and Schenk, 2013), continuing methodological developments allowed the successful application of meta-transcriptomics to evaluate microbial response to organic contaminants (phenanthrene and benzalkonium chlorides) in soil and river sediment samples (de Menezes et al., 2012; Oh et al., 2014), encouraging their application in wetlands. A limitation of this approach is the high concentration of chloroacetanilides probably needed to elicit significant detectable changes of bacterial expression profiles. For example, 60 mg L<sup>-1</sup> of benzalkonium chloride were used to detect its impact on river sediment bacteria (de Menezes et al., 2012). The implication of the choice of concentration on data interpretation and resulting conclusions should be carefully considered.

## 2. Following pesticide degradation in wetlands using CSIA

CSIA has been widely used to study the fate of priority organic pollutants including chlorinated ethenes and aromatic hydrocarbons but only recently began to be applied to investigate micropollutants (Badea et al., 2009; Milosevic et al., 2013; Wu et al., 2014). In this context, a novel GC-C-IRMS-based CSIA tool was developed to measure stable carbon isotope ratios to assess the degradation of metolachlor, acetochlor and alachlor in wetland water samples [Chapter II]. The minimum amount of pure compound (analytical standard) needed for accurate analysis was relatively low (2 ng of carbon on-column) considering that most CSIA methods require a minimum of 1.2 – 60 ng of carbon on-column for accurate measurements (Schmidt and Jochmann, 2012). This highlighted the method's potential for analyse carbon stable isotope ratios of chloroacetanilide from water samples with environmentally relevant concentrations of chloroacetanilides (few micrograms per litre) [Chapter II].

The relevance of the method to assess chloroacetanilide degradation *in situ* was confirmed in the lab-scale wetlands [Chapter III], where a significant isotope shift of approximately 2.5‰ corresponding to > 50% mass dissipation indicated degradation of acetochlor and alachlor. Yet, for the less degraded metolachlor (23% mass dissipation), the isotopic shift was too small ( $\leq 0.8\text{‰}$ ) to be considered significant given the uncertainty of the method. The extent of degradation that is required to produce a significant isotopic shift depends on the fractionation factor (therefore on the degradation mechanism) and on the extent of dilution of the isotopic fractionation by non-reacting atoms of the target element (in this case carbon). Chloroacetanilides, like most micropollutants, contain many carbon atoms (14-15 for chloroacetanilides), therefore changes in carbon isotopic signature of the carbon atom at the reactive site are diluted to a large extent, which contributes to low fractionation measured at low extents of degradation (Elsner et al., 2005). These findings suggest that the CSIA method will be mostly useful in field assessments of chloroacetanilide degradation when considerable degradation ( $\geq 50\%$ ) takes place. The method was also applied to indicate the occurrence of *in situ* degradation of *S*-metolachlor in constructed wetlands (same experimental set-up as Chapter IV) (Maillard, 2014), and in an agricultural catchment (Lutz et al., 2014). This novel CSIA method proved to be promising to monitor chloroacetanilide degradation in dynamic environments including wetlands and agricultural catchments. Further studies estimating reference fractionation factors for different chloroacetanilide degradation processes are needed to complement the developed CSIA method in order to expand its utility beyond the indication of *in situ* degradation. Other analytical developments of new stable isotope methods will also contribute to improved evaluations of chloroacetanilide environmental fate as outlined in the next section.

### Perspectives

Further developments in the field of stable isotope analysis of chloroacetanilides can allow the distinction between different degradation pathways, quantification of the extent of degradation and tracking the fate of separate enantiomers of metolachlor in the environment.

The CSIA method developed here proved to be useful to indicate *in situ* chloroacetanilide degradation but in order to determine degradation pathways and quantify degradation benchmark isotope fractionation studies are needed. Laboratory-driven reference enrichment

factors ( $\epsilon$ ) need to be obtained for known degradation reactions (e.g. biotic GST-dependant dechlorination, biotic N-dealkylation, abiotic dechlorination by reduced sulphur species). This involves setting up degradation experiments and following up the evolution of chloroacetanilide concentrations and their corresponding stable carbon isotope composition according to previously established protocols (Badea et al., 2009; Zhang et al., 2014). Since no strains that degrade chloroacetanilides have been reported to use GSTs for this purpose, the isolation of bacterial strains or consortia that degrade chloroacetanilides using GSTs from contaminated agricultural soil and wetlands would have to precede investigations of associated stable isotope fractionation. N-dealkylation biodegradation experiments can be done using bacterial strains previously shown to degrade acetochlor and alachlor including *Rhodococcus*, *Sphingobium* and *Streptomyces* strains (Sette et al., 2004; Liu et al., 2012b; Chen et al., 2014b). Abiotic dechlorination by reduced sulphur species experiments can be done using sulphate rich water (in mM range) under highly reducing conditions similar to set-ups previously described (Zeng et al., 2011). Although volatilization and sorption for most organic contaminants is often assumed to result in low isotope fractionation, experiments could be set-up to evaluate isotope effect they may cause (Imfeld et al., 2014). The obtained reference enrichment factors could then be used to distinguish and quantify, the respective contribution of individual degradation processes occurring during pesticide attenuation. In addition to in assessments of pesticide fate, estimates of enrichment factors for a given degradation pathway can provide insight on bond cleavage mechanisms of the first step of degradation as previously shown for other pesticides including atrazine (Meyer et al., 2009), and isoproturon (Penning et al., 2010).

Additional stable isotope methods can be developed and used to complement information obtained from the developed stable carbon isotope CSIA method for chloroacetanilides. For example two dimensional (2D)-CSIA based on carbon and chlorine stable isotope measurements can enhance the ability of CSIA to distinguish between different degradation mechanisms of chloroacetanilides (Abe et al., 2009; Wiegert et al., 2012). One reason for this is that the extent of Cl fractionation can give additional information about degradation pathways. For example, we would expect changes in the isotopic composition of both carbon and Cl for degradation reactions involving substitution of Cl, whereas for N-dealkylation reactions no changes in Cl isotopic composition are expected. 2D-CSIA also overcomes the limitation of lowering or “masking” observed fractionation by non-fractionating rate-limiting steps. Since the isotopic fractionation of both elements is equally affected by masking the ratio

between carbon and chlorine fractionation as represented in the slope of 2D-CSIA graphs remains the same and “masking” effects are cancelled out (Rosell et al., 2012). Chlorine isotope methods are currently available mainly for chlorinated aliphatic hydrocarbons (Wiegert et al., 2012), but continuing analytical advances encourage the expansion of chlorine CSIA to other classes of organic contaminants. On the other hand, methods for nitrogen and hydrogen stable isotope analysis of chloroacetanilides will have probably limited applicability in field studies since they require approximately 25 - 50 × higher concentrations of chloroacetanilides than carbon and chlorine CSIA methods as discussed in Chapter III, section 1. Nitrogen CSIA would be more suited for pesticides containing several nitrogen atoms such as oryzalin (4-(Dipropylamino)-3,5-dinitrobenzenesulfonamide) and primicarb (2-Dimethylamino-5,6-dimethylpyrimidin-4-yl) *N,N*-dimethylcarbamate.

Another methodological development is carbon CSIA of ESA and OXA chloroacetanilide degradation products. The high mobility and persistence of ESA and OXA chloroacetanilides results in their detection in ground and surface water in concentrations usually higher than their parent compounds (Postigo and Barcelo, 2014). Meanwhile, knowledge about their further degradation is lacking. Isotopic composition of pesticide degradation products can provide hints both on their formation (based on parent compound isotopic signature and degradation pathway) and on their degradation (Reinnicke et al., 2012; Meyer and Elsner, 2013). During the transformation of chloroacetanilides to ESA and OXA chloroacetanilides, the isotopic composition of ESA and OXA chloroacetanilides is expected to be  $^{13}\text{C}$  depleted in comparison to that of the parent compounds at the start of the reaction. ESA and OXA degradation products then become progressively more  $^{13}\text{C}$  enriched as the reaction progresses, until reaching the same isotopic composition value as the parent compound if all chloroacetanilide molecules are transformed into ESA and/or OXA to satisfy isotopic mass balance (Stelzer et al., 2009; Aeppli et al., 2010). It should be taken into account that an additional bond breaking step is involved in the formation of OXA, which should lead to higher  $^{13}\text{C}$  enrichment in OXA in comparison to ESA. CSIA of ESA/OXA can indicate if ESA and/or OXA are the only degradation products resulting from the degradation of chloroacetanilides in a given system. In parallel, further degradation of ESA and OXA could lead to further  $^{13}\text{C}$  enrichment which can indicate their further degradation. Yet, the application of chloroacetanilide ESA and OXA CSIA would require availability of microbial strains and/or consortia that degrade chloroacetanilides *via* the GST pathway to allow investigations of isotopic compositions during these reactions. Also,

given their high polarity, LC- based IRMS methods will be needed for carbon isotope measurements of ESA and OXA chloroacetanilides (Gilevska et al., 2014). LC- IRMS methods remain less well established than GC-IRMS methods, but constant analytical developments are fuelled by a need for CSIA methods for polar organic contaminants, in particular pharmaceuticals, pesticides and their degradation products (Elsner et al., 2012; Reinnicke et al., 2012; Gilevska et al., 2014).

Finally, enantiomer-specific stable carbon isotope analysis (ESIA) is another methodological advancement that could benefit environmental assessments of chiral pesticides such as metolachlor or the acetanilide herbicide metalaxyl (Maier et al., 2013). While enantiomer analysis was useful in indicating the occurrence of *in situ* biodegradation of metolachlor in wetlands [Chapter III, section 2], it fails if biodegradation is not enantiospecific, or if enzymes preferentially degrading *S*- and *R*- enantiomers are simultaneously present at the field site causing enantiomer enrichment to be cancelled out. ESIA combines the advantages of enantiomer analysis and CSIA: gas chromatographic enantiomer separation and online isotope measurement, and therefore enables the isotope analysis of individual enantiomers allowing the tracing of their degradation in the environment as separate contaminants. ESIA methods have been developed for a few pesticides (Maier et al., 2013; Zhang et al., 2014), but this innovative technique holds promise for better understanding of the transformation of individual enantiomers of chiral pesticides in the environment, and in turn to better evaluate the their respective environmental risks.

### 3. Bacterial composition and activity in chloroacetanilide-contaminated wetlands

While microbial communities play a key role in the geochemical cycling of nutrients and the degradation of organic contaminants in wetlands, their composition and the factors influencing it are poorly understood (Truu et al., 2009). This holds particularly true in wetlands treating pesticide-contaminated water. Increasing awareness of the role of microbial communities in ecosystem functions and services, and the advent of high throughput sequencing technologies for the analysis of microbial diversity in ecosystems are fuelling the interest in deciphering relationships between wetland microbial composition, environmental or operational parameters, and eventually their impact on wetland functions (Arroyo et al., 2014).

Chemical parameters (e.g. pH, nutrient availability) are known drivers of bacterial composition in soil and in aquatic ecosystems (Griffiths et al., 2011; Jankowski et al., 2014). A growing

body of literature explores the impacts of wetland hydrochemistry (Imfeld et al., 2010; Peralta et al., 2013b), and hydrology (Foulquier et al., 2013; Ligi et al., 2013) on bacterial composition of natural and constructed wetlands. In this PhD work, the impact of hydrochemistry and hydraulic operations on chloroacetanilide-contaminated wetland bacterial composition were evident. Redox conditions significantly influence bacterial composition as indicated by the correlation of the terminal electron acceptors with changes of bacterial communities in wetland water [Chapter III, section 2 and Chapter IV]. Hydraulic operation (continuous-flow *vs.* batch), being the main determinant of wetland redox conditions, also had a small but significant effect on bacterial composition in wetland water. Our results suggest that bacterial composition profiles can act as bioindicators of hydraulic disturbances and redox changes in pesticide-contaminated wetlands.

Pesticides have been shown in a large number of studies to affect the composition and functions of bacterial communities (Lo, 2010). Pesticide effects can be due to sensitivity of certain bacterial subpopulations to the pesticide (toxicity), or to overall adaptation of bacterial community by selection for pesticide-resistant subpopulations and genetic change (e.g. horizontal gene transfer) (Imfeld and Vuilleumier, 2012). Few studies demonstrated the impact of pesticides on wetland bacterial community composition and activity (Milenkovski et al., 2010; San Miguel et al., 2014). In this work, the impact of chloroacetanilides on wetland bacterial communities could not be directly observed. No impact of chloroacetanilide exposure ( $500 \mu\text{g L}^{-1}$ ) could be distinguished in lab-scale wetlands [Chapter III, section 2]. In contrast, *S*-metolachlor concentrations ( $\leq 500 \mu\text{g L}^{-1}$ ) correlated with bacterial composition profiles in constructed wetlands [Chapter IV]. However, different exposure modes to *S*-metolachlor in constructed wetlands coincided with different hydraulic regimes hindering the distinction between the impact of *S*-metolachlor exposure and that of hydraulic regime. Further possible investigations of changes in bacterial composition in response to chloroacetanilide stress are highlighted in the perspectives section below.

A final highlight of this PhD work was the evident impact of plant rhizosphere on bacterial composition and metabolic activity. Rhizosphere bacterial communities in constructed wetlands were different and more diverse than water bacterial communities [Chapter IV]. Similarly, water bacterial communities in the rhizosphere zone of lab-scale wetlands had distinct composition and were more diverse than bacterial communities from other locations of the wetlands [Chapter III, section 2]. Several previous studies showed little differences in



bacterial composition between interstitial water and soils/sediments of planted and unplanted experimental wetlands (Ahn et al., 2007; Baptista Jde et al., 2008). In these studies, fine-scale heterogeneities in bacterial composition around plant roots may have been overlooked due to sampling strategies that did not specifically target rhizosphere zones. In Chapter III, metabolically active zones in the lab-scale wetlands where consumption of TEAs and chloroacetanilide degradation took place corresponded to rhizosphere zones. Enhanced organic contaminant degradation in the plant rhizosphere can be attributed to the metabolic versatility of fungal and bacterial populations associated with the rhizosphere, as well as root exudates which provide a variety of carbon sources that support cometabolic aerobic and anaerobic degradation processes (Fester et al., 2014; Qin et al., 2015). While some studies reported no influence of plants on contaminant removal (Lee and Scholz, 2007; Cardinal et al., 2014), our results support the more widely accepted notion that plants, and in particular plant rhizosphere, play important roles in biogeochemical cycling and organic contaminant removal processes in wetlands (Vymazal, 2011b; Chen et al., 2012; Carranza-Diaz et al., 2014; Fester et al., 2014; Qin et al., 2015).

### Perspectives

Knowledge of bacterial diversity and functions in different ecosystems is increasing at an exponential level owing to continuing advances in high-throughput sequencing techniques. These techniques have allowed detailed surveys of bacterial diversity and their relationships to different environmental parameters in a variety of ecosystems including freshwater, marine and agro-ecosystems (Nacke et al., 2011; Gilbert et al., 2012; Logue et al., 2012). Their application to study bacterial diversity in wetlands is still limited to a few recent studies (Ligi et al., 2013; Nolvak et al., 2013; Peralta et al., 2013b; Arroyo et al., 2014). Future research can improve our understanding of parameters influencing wetland bacterial community composition and activity, and lead to the development of a set of bacterial indicators for assessment of wetland biological integrity (i.e. oligotrophic conditions, xenobiotic contamination, etc.). Traditional wetland health indicators include physical (e.g. water depth and land use), chemical (total P and N), and biological (e.g. composition and abundance of plant species and macroinvertebrates) (Favas et al., 2012; Rooney and Bayley, 2012). Microorganisms perform key ecological functions in wetlands and are characterised by their fast response to disturbances (Wessén and Hallin, 2011). Therefore, the addition of bacterial indicators to the existing

toolbox of wetland health indicators provides a rich topic for further research (Sims et al., 2013). Current sequencing techniques may allow the identification of bacterial DNA-based indicators of pesticide contamination and hydraulic disturbances in wetlands. Bacterial indicators to pesticide-stress based on functional genes were discussed earlier under section 1.2 of this chapter, below we describe future research aiming to identify 16S rRNA gene based indicators of pesticide and hydraulic stress.

A microcosm-scale study can be envisaged where the effect of a range of environmentally relevant pesticide concentrations (e.g. 1 - 500  $\mu\text{g L}^{-1}$ ) and high range concentrations representing acute pesticide exposure (e.g. 1 - 50  $\text{mg L}^{-1}$ ) are tested on wetland water and soil/sediment bacteria. Pesticide can be added to flasks (volume < 1L) containing wetland water or wetland sediment/soil. High throughput sequencing of 16S rRNA genes can be used to identify significant increases or decreases in relative abundances of responsive bacterial taxa. Changes in terminal electron acceptors concentrations should be monitored and taken into account to distinguish between their impacts and pesticide impacts on bacterial communities. Certain aspects of abundance of responsive taxa such as their ratios relative to one another can be proposed as potential bioindicators (Hartman et al., 2008). In previous studies, ratio of ammonia oxidizing bacteria to ammonia oxidising archaea was proposed as an indicator of oligotrophic conditions in wetlands whereas ratio of *Proteobacteria* to *Acidobacteria* was proposed as indicator of wetland trophic status (Smit et al., 2001; Sims et al., 2012). Validation of the choice of indicators can be done in larger-scale studies on constructed and natural wetlands by monitoring their response to varying fluxes of pesticide contamination. Other changes in operational (input water quality, hydraulic regime) or environmental parameters (temperature, redox) should also be measured and taken into consideration for interpretation. High throughput sequencing of a large number of samples can be interpreted along with hydrochemical data to find correlations between pesticide concentrations, hydrochemical parameters and specific bacterial taxa. In these field studies, the use of Illumina platform for high throughput sequencing is already increasingly favoured over 454 pyrosequencing. Illumina sequencing has the advantages of being more cost-effective and of providing larger number of sequence reads which improves the identification of rare phylotypes and is especially useful for environmental samples with high bacterial diversity (Werner et al., 2012). In the meantime, new protocols for Illumina sequencing are being developed and applied to

overcome the limitation of shorter sequence reads generated by the Illumina platform, and its effect on accurate phylogenetic assignment (Ong et al., 2013; Logares et al., 2014).

On the contrary to pesticide bacterial indicators, identification of bacterial indicators to hydraulic changes cannot be done using closed microcosm-scale flasks. For this purpose, experimental wetlands will be needed where controlled water inflow regimes can be varied. An acclimation phase of 1-2 months using the same hydraulic regime (e.g. continuous-flow) should precede the start of the experiment to allow the establishment of plants, similar biogeochemical conditions and microbial communities. Different hydraulic regimes can then be used to operate each wetland and responsive taxa to hydraulic changes can be identified.

Bacterial indicators can also be useful in monitoring the impact of chronic contamination by pesticides and its effect on wetland functioning. Most studies on pesticide impacts on bacterial community investigate the effects of acute short-term exposure, whereas studies of chronic low-level exposure are more representative of diffuse non-point source contamination such as agricultural pesticide contamination (Seghers et al., 2003a; Seghers et al., 2003b). Long-term experiments investigating the impact of chronic exposure pesticide mixtures on wetland bacterial communities are therefore needed. Such investigations can make use of the pollution-induced community tolerance (PICT) approach which is suited to identify subtle community-level, rather than population level, composition changes caused by pollutant exposure (Pesce et al., 2010; Imfeld and Vuilleumier, 2012). Determining the effects of long-term exposure to pesticide mixtures on wetland bacterial communities and their implications on wetland functions would give an insight on the sustainability of using constructed wetlands to treat agricultural runoff on the long-term.

In conclusion, this PhD work contributes to improving assessments of pesticide-contaminated wetlands and associated processes. The benefits of using complementary chemical and biomolecular approaches to tackle different aspects of pesticide degradation in redox-dynamic ecosystems were demonstrated. Novel tools for *in situ* assessment of pesticide degradation were developed and their utility confirmed in wetland set-ups. Finally, parameters driving wetland bacterial composition were identified paving the way to the identification of bacterial DNA-based bioindicators to pesticide and hydraulic disturbances in wetlands. Overall, the results of this work will contribute to improving evaluations of pesticide degradation and pesticide impact on redox-dynamic environments and thereby, in the longer term, allow better prediction of the environmental fate and risk assessment of pesticides.

## References

- Abdo, Z., Schüette, U.M., Bent, S.J., Williams, C.J., Forney, L.J., Joyce, P., 2006. Statistical methods for characterizing diversity of microbial communities by analysis of terminal restriction fragment length polymorphisms of 16S rRNA genes. *Environmental Microbiology* 8, 929–938.
- Abe, Y., Aravena, R., Zopfi, J., Shouakar-Stash, O., Cox, E., Roberts, J.D., Hunkeler, D., 2009. Carbon and chlorine isotope fractionation during aerobic oxidation and reductive dechlorination of vinyl chloride and cis-1,2-dichloroethene. *Environmental Science & Technology* 43, 101-107.
- Acosta-Martinez, V., Dowd, S., Sun, Y., Allen, V., 2008. Tag-encoded pyrosequencing analysis of bacterial diversity in a single soil type as affected by management and land use. *Soil Biology and Biochemistry* 40, 2762–2770.
- Adrian, L., Hansen, S.K., Fung, J.M., Gorisch, H., Zinder, S.H., 2007. Growth of *Dehalococcoides* strains with chlorophenols as electron acceptors. *Environmental Science & Technology* 41, 2318-2323.
- Aeppli, C., Hofstetter, T.B., Amaral, H.I., Kipfer, R., Schwarzenbach, R.P., Berg, M., 2010. Quantifying in situ transformation rates of chlorinated ethenes by combining compound-specific stable isotope analysis, groundwater dating, and carbon isotope mass balances. *Environmental Science & Technology* 44, 3705-3711.
- Aga, D.S., Thurman, E.M., Yockel, M.E., Zimmerman, L.R., Williams, T.D., 1996. Identification of a new sulfonic acid metabolite of metolachlor in soil. *Environmental Science & Technology* 30, 592-597.
- Ahmadian, A., Ehn, M., Hober, S., 2006. Pyrosequencing: history, biochemistry and future. *Clinica Chimica Acta* 363, 83-94.
- Ahn, C., Gillevet, P.M., Sikaroodi, M., 2007. Molecular characterization of microbial communities in treatment microcosm wetlands as influenced by macrophytes and phosphorus loading. *Ecological Indicators* 7, 852-863.
- Alewell, C., Paul, S., Lischeid, G., Storck, F.R., 2008. Co-regulation of redox processes in freshwater wetlands as a function of organic matter availability? *Science of the Total Environment* 404, 335–342.
- Allocati, N., Federici, L., Masulli, M., Di Ilio, C., 2009. Glutathione transferases in bacteria. *FEBS journal* 276, 58-75.
- Amalric, L., Baran, N., Coureau, C., Maingot, L., Buron, F., Routier, S., 2013. Analytical developments for 47 pesticides: First identification of neutral chloroacetanilide derivatives in French groundwater. *International Journal of Environmental Analytical Chemistry* 93, 1660-1675.
- Amaral, M.J., Bicho, R.C., Carretero, M.A., Sanchez-Hernandez, J.C., Faustino, A.M., Soares, A.M., Mann, R.M., 2012. The use of a lacertid lizard as a model for reptile ecotoxicology studies: part 2--biomarkers of exposure and toxicity among pesticide exposed lizards. *Chemosphere* 87, 765-774.
- Anderson, S.A., Northcote, P.T., Page, M.J., 2010. Spatial and temporal variability of the bacterial community in different chemotypes of the New Zealand marine sponge *Mycale hentscheli*. *FEMS Microbiology Ecology* 72, 328-342.
- Anderson, T.A., Kruger, E.L., Coats, J.R., 1994. Enhanced degradation of a mixture of three herbicides in the rhizosphere of a herbicide-tolerant plant. *Chemosphere* 28, 1551–1557.
- Andreotti, R., Pérez de León, A.A., Dowd, S.E., Guerrero, F.D., Bendele, K.G., Scoles, G.A., 2011. Assessment of bacterial diversity in the cattle tick *Rhipicephalus (Boophilus) microplus* through tag-encoded pyrosequencing. *BMC Microbiology* 11, 6.

- Andresen, L.C., Nothlev, J., Kristensen, K., Navntoft, S., Johnsen, I., 2012. The wild flora biodiversity in pesticide free bufferzones along old hedgerows. *Journal of Environmental Biology* 33, 565-572.
- Andreu, V., Picó, Y., 2004. Determination of pesticides and their degradation products in soil: critical review and comparison of methods. *TrAC Trends in Analytical Chemistry* 23, 772-789.
- Anhalt, J.C., Arthur, E.L., Anderson, T.A., Coats, J.R., 2000. Degradation of atrazine, metolachlor, and pendimethalin in pesticide-contaminated soils: effects of aged residues on soil respiration and plant survival. *Journal of Environmental Science and Health B* 35, 417-438.
- Arroyo, P., Saenz de Miera, L.E., Ansola, G., 2014. Influence of environmental variables on the structure and composition of soil bacterial communities in natural and constructed wetlands. *Science of the Total Environment* 506-507c, 380-390.
- Avila, C., Reyes, C., Bayona, J.M., Garcia, J., 2013. Emerging organic contaminant removal depending on primary treatment and operational strategy in horizontal subsurface flow constructed wetlands: influence of redox. *Water Research* 47, 315-325.
- Baczynski, T.P., Grotenhuis, T., Knipscheer, P., 2004. The dechlorination of cyclodiene pesticides by methanogenic granular sludge. *Chemosphere* 55, 653-659.
- Badea, S., Vogt, C., Weber, S., Danet, A., Richnow, H.H., 2009. Stable isotope fractionation of  $\gamma$ -hexachlorocyclohexane (lindane) during reductive dechlorination by two strains of sulfate-reducing bacteria. *Environmental Science & Technology* 43, 3155–3161.
- Bai, Z., Xu, H.-J., He, H.-B., Zheng, L.-C., Zhang, X.-D., 2013. Alterations of microbial populations and composition in the rhizosphere and bulk soil as affected by residual acetochlor. *Environmental Science and Pollution Research* 20, 369-379.
- Bao, P., Hu, Z.Y., Wang, X.J., Chen, J., Ba, Y.X., Hua, J., Zhu, C.Y., Zhong, M., Wu, C.Y., 2012. Dechlorination of p,p'-DDTs coupled with sulfate reduction by novel sulfate-reducing bacterium *Clostridium sp. BXM*. *Environmental Pollution* 162, 303-310.
- Baptista Jde, C., Davenport, R.J., Donnelly, T., Curtis, T.P., 2008. The microbial diversity of laboratory-scale wetlands appears to be randomly assembled. *Water Research* 42, 3182-3190.
- Baran, N., Gourcy, L., 2013a. Sorption and mineralization of S-metolachlor and its ionic metabolites in soils and vadose zone solids: Consequences on groundwater quality in an alluvial aquifer (Ain Plain, France). *Journal of Contaminant Hydrology* 154, 20-28.
- Baran, N., Gourcy, L., 2013b. Sorption and mineralization of S-metolachlor and its ionic metabolites in soils and vadose zone solids: consequences on groundwater quality in an alluvial aquifer (Ain Plain, France). *Journal of Contaminant Hydrology* 154, 20-28.
- Barbash, J.E., 2014. 11.15 - The Geochemistry of Pesticides. in: Holland, H.D., Turekian, K.K. (Eds.). *Treatise on Geochemistry (Second Edition)*. Elsevier, Oxford, pp. 535-572.
- Barry, K.H., Koutros, S., Andreotti, G., Sandler, D.P., Burdette, L.A., Yeager, M., Beane Freeman, L.E., Lubin, J.H., Ma, X., Zheng, T., Alavanja, M.C., Berndt, S.I., 2012. Genetic variation in nucleotide excision repair pathway genes, pesticide exposure and prostate cancer risk. *Carcinogenesis* 33, 331-337.

- Bers, K., Batisson, I., Proost, P., Wattiez, R., De Mot, R., Springael, D., 2013. HylA, an alternative hydrolase for initiation of catabolism of the phenylurea herbicide linuron in *Variovorax sp.* strains. *Applied and Environmental Microbiology* 79, 5258-5263.
- Bers, K., Sniegowski, K., De Mot, R., Springael, D., 2012. Dynamics of the linuron hydrolase *libA* gene pool size in response to linuron application and environmental perturbations in agricultural soil and on-farm biopurification systems. *Applied and Environmental Microbiology* 78, 2783-2789.
- Bian, H., Chen, J., Cai, X., Liu, P., Wang, Y., Huang, L., Qiao, X., Hao, C., 2009. Dechlorination of chloroacetanilide herbicides by plant growth regulator sodium bisulfite. *Water Research* 43, 3566-3574.
- Bidleman, T.F., Jantunen, L.M., Binnur Kurt-Karakus, P., Wong, F., Hung, H., Ma, J., Stern, G., Rosenberg, B., 2013. Chiral chemicals as tracers of atmospheric sources and fate processes in a world of changing climate. *Mass Spectrometry (Tokyo)* 2.
- Blackwood, C.B., Paul, E.A., 2003. Eubacterial community structure and population size within the soil light fraction, rhizosphere, and heavy fraction of several agricultural systems. *Soil Biology and Biochemistry* 35, 1245-1255.
- Blessing, M., Jochmann, M.A., Schmidt, T.C., 2008. Pitfalls in compound-specific isotope analysis of environmental samples. *Analytical and Bioanalytical Chemistry* 390, 591-603.
- Bois, P., Huguenot, D., Jezequel, K., Lollier, M., Cornu, J.Y., Lebeau, T., 2013. Herbicide mitigation in microcosms simulating stormwater basins subject to polluted water inputs. *Water Research* 47, 1123-1135.
- Bombach, P., Richnow, H.H., Kastner, M., Fischer, A., 2010. Current approaches for the assessment of *in situ* biodegradation. *Applied Microbiology and Biotechnology* 86, 839-852.
- Boparai, H.K., Shea, P.J., Comfort, S.D., Snow, D.D., 2006. Dechlorinating chloroacetanilide herbicides by dithionite-treated aquifer sediment and surface soil. *Environmental Science & Technology* 40, 3043-3049.
- Borch, T., Kretzschmar, R., Kappler, A., Cappellen, P.V., Ginder-Vogel, M., Voegelin, A., Campbell, K., 2010. Biogeochemical redox processes and their impact on contaminant dynamics. *Environmental Science & Technology* 44, 15-23.
- Botta, F., Fauchon, N., Blanchoud, H., Chevreuil, M., Guery, B., 2012. Phyt'Eaux Cites: application and validation of a programme to reduce surface water contamination with urban pesticides. *Chemosphere* 86, 166-176.
- Bouchard, D., Hunkeler, D., Höhener, P., 2008. Carbon isotope fractionation during aerobic biodegradation of n-alkanes and aromatic compounds in unsaturated sand. *Organic Geochemistry* 39, 23-33.
- Bowen, J.L., Ward, B.B., Morrison, H.G., Hobbie, J.E., Valiela, I., Deegan, L.A., Sogin, M.L., 2011. Microbial community composition in sediments resists perturbation by nutrient enrichment. *Isme j* 5, 1540-1548.
- Braeckevelt, M., Fischer, A., Kästner, M., 2012. Field applicability of Compound-Specific Isotope Analysis (CSIA) for characterization and quantification of *in situ* contaminant degradation in aquifers. *Applied Microbiology and Biotechnology* 94, 1401-1421.
- Briceño, G., Palma, G., Durán, N., 2007. Influence of Organic Amendment on the Biodegradation and Movement of Pesticides. *Critical Reviews in Environmental Science and Technology* 37, 233-271.

- Budd, R., O'Geen, A., Goh, K.S., Bondarenko, S., Gan, J., 2011. Removal mechanisms and fate of insecticides in constructed wetlands. *Chemosphere* 83, 1581–1587.
- Bundt, M., Widmer, F., Pesaro, M., Zeyer, J., Blaser, P., 2001. Preferential flow paths: biological 'hot spots' in soils. *Soil Biology and Biochemistry* 33, 729-738.
- Burgin, A.J., Yang, W.H., Hamilton, S.K., Silver, W.L., 2011. Beyond carbon and nitrogen: how the microbial energy economy couples elemental cycles in diverse ecosystems. *Frontiers in Ecology and the Environment* 9, 44-52.
- Buttigieg, P.L., Ramette, A., 2014. A guide to statistical analysis in microbial ecology: a community-focused, living review of multivariate data analyses. *FEMS Microbiology Ecology*.
- Cai, X., Sheng, G., Liu, W., 2007. Degradation and detoxification of acetochlor in soils treated by organic and thiosulfate amendments. *Chemosphere* 66, 286–292.
- Callaghan, A.V., 2013. Metabolomic investigations of anaerobic hydrocarbon-impacted environments. *Current Opinion in Biotechnology* 24, 506-515.
- Caquet, T., Lagadic, L., Sheffield, S., 2000. Mesocosms in Ecotoxicology (1): Outdoor Aquatic Systems. in: Ware, G. (Ed.). *Reviews of Environmental Contamination and Toxicology*. Springer New York, pp. 1-38.
- Cardinal, P., Anderson, J.C., Carlson, J.C., Low, J.E., Challis, J.K., Beattie, S.A., Bartel, C.N., Elliott, A.D., Montero, O.F., Lokesh, S., Favreau, A., Kozlova, T.A., Knapp, C.W., Hanson, M.L., Wong, C.S., 2014. Macrophytes may not contribute significantly to removal of nutrients, pharmaceuticals, and antibiotic resistance in model surface constructed wetlands. *Science of the Total Environment* 482-483, 294-304.
- Carlson, D.L., Than, K.D., Roberts, A.L., 2006. Acid- and base-catalyzed hydrolysis of chloroacetamide herbicides. *Journal of Agriculture and Food Chemistry* 54, 4740-4750.
- Carranza-Diaz, O., Schultze-Nobre, L., Moeder, M., Nivala, J., Kusch, P., Koeser, H., 2014. Removal of selected organic micropollutants in planted and unplanted pilot-scale horizontal flow constructed wetlands under conditions of high organic load. *Ecological Engineering* 71, 234-245.
- Carvalhais, L.C., Dennis, P.G., Tyson, G.W., Schenk, P.M., 2012. Application of metatranscriptomics to soil environments. *Journal of Microbiological Methods* 91, 246-251.
- Carvalhais, L.C., Schenk, P.M., 2013. Sample processing and cDNA preparation for microbial metatranscriptomics in complex soil communities. *Methods in Enzymology* 531, 251-267.
- Cederlund, H., Börjesson, E., Öneby, K., Stenström, J., 2007. Metabolic and cometabolic degradation of herbicides in the fine material of railway ballast. *Soil Biology and Biochemistry* 39, 473-484.
- Celis, R., Gamiz, B., Adelino, M.A., Hermosin, M.C., Cornejo, J., 2013. Environmental behavior of the enantiomers of the chiral fungicide metalaxyl in Mediterranean agricultural soils. *Science of the Total Environment* 444, 288-297.
- Chen, C., Yang, K., Yu, C., Huang, R., Chen, X., Tang, X., Shen, C., Hashmi, M.Z., Shi, H., 2014a. Influence of redox conditions on the microbial degradation of polychlorinated biphenyls in different niches of rice paddy fields. *Soil Biology and Biochemistry* 78, 307-315.

- Chen, Q., Wang, C.H., Deng, S.K., Wu, Y.D., Li, Y., Yao, L., Jiang, J.D., Yan, X., He, J., Li, S.P., 2014b. Novel three-component Rieske non-heme iron oxygenase system catalyzing the N-dealkylation of chloroacetanilide herbicides in *shingomonads* DC-6 and DC-2. *Applied and Environmental Microbiology* 80, 5078-5085.
- Chen, Z., Wu, S., Braeckevelt, M., Paschke, H., Kastner, M., Koser, H., Kusch, P., 2012. Effect of vegetation in pilot-scale horizontal subsurface flow constructed wetlands treating sulphate rich groundwater contaminated with a low and high chlorinated hydrocarbon. *Chemosphere* 89, 724-731.
- Culman, S.W., Bukowski, R., Gauch, H.G., Cadillo-Quiroz, H., Buckley, D.H., 2009. T-REX: software for the processing and analysis of T-RFLP data. *BMC Bioinformatics* 10, 171.
- Cupples, A.M., Sims, G.K., 2007. Identification of *in situ* 2,4-dichlorophenoxyacetic acid-degrading soil microorganisms using DNA-stable isotope probing. *Soil Biology and Biochemistry* 39, 232-238.
- Darko, G., Akoto, O., Oppong, C., 2008. Persistent organochlorine pesticide residues in fish, sediments and water from Lake Bosomtwi, Ghana. *Chemosphere* 72, 21-24.
- Dawson, A.H., Eddleston, M., Senarathna, L., Mohamed, F., Gawarammana, I., Bowe, S.J., Manuweera, G., Buckley, N.A., 2010. Acute human lethal toxicity of agricultural pesticides: a prospective cohort study. *PLoS Medicine* 7, e1000357.
- de Boer, T.E., Tas, N., Braster, M., Temminghoff, E.J., Roling, W.F., Roelofs, D., 2012. The influence of long-term copper contaminated agricultural soil at different pH levels on microbial communities and springtail transcriptional regulation. *Environmental Science & Technology* 46, 60-68.
- de Liphay, J.R., Barkay, T., Sorensen, S.J., 2001. Enhanced degradation of phenoxyacetic acid in soil by horizontal transfer of the *tfdA* gene encoding a 2,4-dichlorophenoxyacetic acid dioxygenase. *FEMS Microbiology Ecology* 35, 75-84.
- de Menezes, A., Clipson, N., Doyle, E., 2012. Comparative metatranscriptomics reveals widespread community responses during phenanthrene degradation in soil. *Environmental Microbiology* 14, 2577-2588.
- De Wilde, T., Spanoghe, P., Ryckeboer, J., Jaeken, P., Springael, D., 2009. Sorption characteristics of pesticides on matrix substrates used in biopurification systems. *Chemosphere* 75, 100-108.
- Dealtry, S., Holmsgaard, P.N., Dunon, V., Jechalke, S., Ding, G.C., Krogerrecklenfort, E., Heuer, H., Hansen, L.H., Springael, D., Zuhlke, S., Sorensen, S.J., Smalla, K., 2014. Shifts in abundance and diversity of mobile genetic elements after the introduction of diverse pesticides into an on-farm biopurification system over the course of a year. *Applied and environmental microbiology* 80, 4012-4020.
- DeLorenzo, M.E., Scott, G.I., Ross, P.E., 2001. Toxicity of pesticides to aquatic microorganisms: a review. *Environmental Toxicology and Chemistry* 20, 84-98.
- Dennis, P.G., Miller, A.J., Hirsch, P.R., 2010. Are root exudates more important than other sources of rhizodeposits in structuring rhizosphere bacterial communities? *FEMS Microbiology Ecology* 72, 313-327.
- Desai, C., Pathak, H., Madamwar, D., 2010. Advances in molecular and "-omics" technologies to gauge microbial communities and bioremediation at xenobiotic/anthropogen contaminated sites. *Bioresource Technology* 101, 1558-1569.
- Devers, M., El Azhari, N., Kolic, N.U., Martin-Laurent, F., 2007. Detection and organization of atrazine-degrading genetic potential of seventeen bacterial isolates belonging to divergent taxa indicate a recent common origin of their catabolic functions. *FEMS Microbiology Letters* 273, 78-86.



- Diao, J., Xu, P., Wang, P., Lu, D., Lu, Y., Zhou, Z., 2010. Enantioselective degradation in sediment and aquatic toxicity to *Daphnia magna* of the herbicide lactofen enantiomers. *Journal of Agricultural and Food Chemistry* 58, 2439-2445.
- dos Santos, H.F., Cury, J.C., do Carmo, F.L., dos Santos, A.L., Tiedje, J., van Elsas, J.D., Rosado, A.S., Peixoto, R.S., 2011. Mangrove bacterial diversity and the impact of oil contamination revealed by pyrosequencing: bacterial proxies for oil pollution. *PLoS One* 6, e16943.
- Dunbar, J., Ticknor, L.O., Kuske, C.R., 2001. Phylogenetic specificity and reproducibility and new method for analysis of terminal restriction fragment profiles of 16S rRNA genes from bacterial communities. *Applied and Environmental Microbiology* 67, 190-197.
- Durst, R., Imfeld, G., Lange, J., 2013. Transport of pesticides and artificial tracers in vertical-flow lab-scale wetlands. *Water Resources Research* 49, 554-564
- Edgar, R.C., 2010. Search and clustering orders of magnitude faster than BLAST. *Bioinformatics* 26, 2460-2461.
- Edgar, R.C., Haas, B.J., J.C., C., Quince, C., Knight, R., 2011. UCHIIME improves sensitivity and speed of chimera detection. *Bioinformatics* 27, 2194-2200.
- Edwards, U., Rogall, T., Blöcker, H., Emde, M., Böttger, E.C., 1989. Isolation and direct complete nucleotide determination of entire genes. Characterization of a gene coding for 16S ribosomal RNA. *Nucleic Acids Research* 17, 7843-7853.
- El Azhari, N., Devers-Lamrani, M., Chatagnier, G., Rouard, N., Martin-Laurent, F., 2010. Molecular analysis of the catechol-degrading bacterial community in a coal wasteland heavily contaminated with PAHs. *Journal of Hazardous materials* 177, 593–601.
- Eljarrat, E., Guerra, P., Barceló, D., 2008. Enantiomeric determination of chiral persistent organic pollutants and their metabolites. *TrAC Trends in Analytical Chemistry* 27, 847-861.
- Elsayed, O.F., Maillard, E., Vuilleumier, S., Nijenhuis, I., Richnow, H.H., Imfeld, G., 2014a. Using compound-specific isotope analysis to assess the degradation of chloroacetanilide herbicides in lab-scale wetlands. *Chemosphere* 99, 89-95.
- Elsayed, O.F., Maillard, E., Vuilleumier, S., Imfeld, G., 2014b. Bacterial communities in batch and continuous-flow wetlands treating the herbicide *S*-metolachlor. *Science of the Total Environment* 499, 327-335.
- Elsner, M., 2010. Stable isotope fractionation to investigate natural transformation mechanisms of organic contaminants: principles, prospects and limitations. *Journal of Environmental Monitoring* 12, 2005–2031.
- Elsner, M., Jochmann, M.A., Hofstetter, T.B., Hunkeler, D., Bernstein, A., Schmidt, T.C., Schimmelmann, A., 2012. Current challenges in compound-specific stable isotope analysis of environmental organic contaminants. *Analytical and Bioanalytical Chemistry* 403, 2471-2491.
- Elsner, M., Zwank, L., Hunkeler, D., Schwarzenbach, R.P., 2005. A New Concept Linking Observable Stable Isotope Fractionation to Transformation Pathways of Organic Pollutants. *Environmental Science & Technology* 39, 6896–6916.
- EPA, 1999. Pesticide industry sales and usage: 1996 and 1997 market estimates. U.S. Environmental Protection Agency, Washington, DC.

EPA, 2011. Pesticide industry sales and usage: 2006 and 2007 market estimates. U.S. Environmental Protection Agency, Washington, DC.

Escher, B.I., Fenner, K., 2011. Recent advances in environmental risk assessment of transformation products. *Environmental Science & Technology* 45, 3835-3847.

EU, 2014. EU pesticides database. The European Commission. [http://ec.europa.eu/sanco\\_pesticides/public](http://ec.europa.eu/sanco_pesticides/public). Retrieved September, 03 2014

European food safety authority, 2011. Conclusion on the peer review of the pesticide risk assessment of the active substance acetochlor. *EFSA journal*.

Eykholt, G.R., Davenport, D.T., 1998. Dechlorination of the chloroacetanilide herbicides alachlor and metolachlor by iron metal. *Environmental Science & Technology* 32, 1482-1487.

Fahrenfeld, N., Cozzarelli, I.M., Bailey, Z., Pruden, A., 2014. Insights into biodegradation Through depth-resolved microbial community functional and structural profiling of a Crude-oil contaminant plume. *Microbial ecology*.

Farlin, J., Gallé, T., Bayerle, M., Pittois, D., Braun, C., El Khabbaz, H., Lallement, C., Leopold, U., Vanderborght, J., Weihermueller, L., 2013. Using the long-term memory effect of pesticide and metabolite soil residues to estimate field degradation half-life and test leaching predictions. *Geoderma* 207–208, 15-24.

Faulwetter, J.L., Gagnon, V., Sundberg, C., Chazarenc, F., Burr, M.D., Brisson, J., Camper, A.K., Stein, O.R., 2009. Microbial processes influencing performance of treatment wetlands: A review. *Ecological Engineering* 35, 987-1004.

Favas, P.J., Pratas, J., Prasad, M.N., 2012. Accumulation of arsenic by aquatic plants in large-scale field conditions: opportunities for phytoremediation and bioindication. *Science of the Total Environment* 433, 390-397.

Feisthauer, S., Seidel, M., Bombach, P., Traube, S., Knoller, K., Wange, M., Fachmann, S., Richnow, H.H., 2012. Characterization of the relationship between microbial degradation processes at a hydrocarbon contaminated site using isotopic methods. *Journal of Contaminant Hydrology* 133, 17-29.

Fenner, K., Canonica, S., Wackett, L.P., Elsner, M., 2013. Evaluating pesticide degradation in the environment: Blind spots and emerging opportunities. *Science* 341, 752-758.

Fester, T., Giebler, J., Wick, L.Y., Schlosser, D., Kastner, M., 2014. Plant-microbe interactions as drivers of ecosystem functions relevant for the biodegradation of organic contaminants. *Current Opinion in Biotechnology* 27, 168-175.

Foley, M.E., Sigler, V., Gruden, C.L., 2008. A multiphasic characterization of the impact of the herbicide acetochlor on freshwater bacterial communities. *The ISME journal* 2, 56–66.

Fortes, C., Mastroeni, S., Melchi, F., Pilla, M.A., Alotto, M., Antonelli, G., Camaione, D., Bolli, S., Luchetti, E., Pasquini, P., 2007. The association between residential pesticide use and cutaneous melanoma. *European Journal of Cancer* 43, 1066-1075.

Foulquier, A., Volat, B., Neyra, M., Bornette, G., Montuelle, B., 2013. Long-term impact of hydrological regime on structure and functions of microbial communities in riverine wetland sediments. *FEMS Microbiology Ecology* 85, 211-226.

- Fuchs, G., Boll, M., Heider, J., 2011. Microbial degradation of aromatic compounds - from one strategy to four. *Nature reviews Microbiology* 9, 803-816.
- Fuentesa, M.S., Benimelia, C.S., Cuozzoa, S.A., Amoroso, M.J., 2010. Isolation of pesticide-degrading actinomycetes from a contaminated site: Bacterial growth, removal and dechlorination of organochlorine pesticides. *International Biodeterioration & Biodegradation* 64, 434–441.
- Gadagbui, B., Maier, A., Dourson, M., Parker, A., Willis, A., Christopher, J.P., Hicks, L., Ramasamy, S., Roberts, S.M., 2010. Derived Reference Doses (RfDs) for the environmental degradates of the herbicides alachlor and acetochlor: Results of an independent expert panel deliberation. *Regulatory Toxicology and Pharmacology* 57, 220-234.
- Galvao, T.C., Mohn, W.W., de Lorenzo, V., 2005. Exploring the microbial biodegradation and biotransformation gene pool. *Trends in Biotechnology* 23, 497-506.
- Gebremariam, S.Y., Beutel, M.W., 2010. Effects of drain-fill cycling on chlorpyrifos mineralization in wetland sediment–water microcosms. *Chemosphere* 78, 1337-1341
- Ghafoor, A., Jarvis, N.J., Thierfelder, T., Stenstrom, J., 2011. Measurements and modeling of pesticide persistence in soil at the catchment scale. *Science of the Total Environment* 409, 1900-1908.
- Giebler, J., Wick, L.Y., Chatzinotas, A., Harms, H., 2013. Alkane-degrading bacteria at the soil-litter interface: comparing isolates with T-RFLP-based community profiles. *FEMS Microbiology Ecology* 86, 45-58.
- Gilbert, J.A., Steele, J.A., Caporaso, J.G., Steinbruck, L., Reeder, J., Temperton, B., Huse, S., McHardy, A.C., Knight, R., Joint, I., Somerfield, P., Fuhrman, J.A., Field, D., 2012. Defining seasonal marine microbial community dynamics. *The ISME journal* 6, 298-308.
- Gilevska, T., Gehre, M., Richnow, H.H., 2014. Performance of the wet oxidation unit of the HPLC isotope ratio mass spectrometry system for halogenated compounds. *Analytical Chemistry* 86, 7252-7257.
- Gonod, L.V., Martin-Laurent, F., Chenu, C., 2006. 2,4-D impact on bacterial communities, and the activity and genetic potential of 2,4-D degrading communities in soil. *FEMS Microbiology Ecology* 58, 529-537.
- Gotz, T., Boger, P., 2004. The very-long-chain fatty acid synthase is inhibited by chloroacetamides. *Zeitschrift für Naturforschung C* 59, 549-553.
- Graham, D.W., Miley, M.K., deNoyelles, F., Smith, V.H., Thurman, E.M., Carter, R., 2000. Alachlor transformation patterns in aquatic field mesocosms under variable oxygen and nutrient conditions. *Water Research* 34, 4054–4062.
- Graham, W.H., Graham, D.W., deNoyelles, F., Jr., Smith, V.H., Larive, C.K., Thurman, E.M., 1999. Metolachlor and alachlor breakdown product formation patterns in aquatic field mesocosms. *Environmental Science & Technology* 33, 4471–4476.
- Griffiths, R.I., Thomson, B.C., James, P., Bell, T., Bailey, M., Whiteley, A.S., 2011. The bacterial biogeography of British soils. *Environmental Microbiology* 13, 1642-1654.
- Groner, M.L., Relyea, R.A., 2011. A tale of two pesticides: how common insecticides affect aquatic communities. *Freshwater Biology* 56, 2391-2404.
- Grégoire, C., Elsaesser, D., Huguenot, D., Lange, J., Lebeau, T., Merli, A., Mose, R., Passeport, E., Payraudeau, S., Schütz, T., Schulz, R., Tapia-Padilla, G., Tournebize, J., Trevisan, M., Wanko, A., 2009. Mitigation of

agricultural nonpoint-source pesticide pollution in artificial wetland ecosystems. *Environmental Chemistry Letters* 7, 205-231.

Hagblom, M.M., Knight, V.K., Kerkhof, L.J., 2000. Anaerobic decomposition of halogenated aromatic compounds. *Environmental Pollution* 107, 199-207.

Handl, S., Dowd, S.E., Garcia-Mazcorro, J.F., Steiner, J.M., Suchodolski, J.S., 2011. Massive parallel 16S rRNA gene pyrosequencing reveals highly diverse fecal bacterial and fungal communities in healthy dogs and cats. *FEMS Microbiology Ecology* 76, 301-310.

Harner, T., Wiberg, K., Norstrom, R., 2000. Enantiomer fractions are preferred to enantiomer ratios for describing chiral signatures in environmental analysis. *Environmental Science & Technology* 34, 218-220.

Hartman, W.H., Richardson, C.J., Vilgalys, R., Bruland, G.L., 2008. Environmental and anthropogenic controls over bacterial communities in wetland soils. *Proceedings of the National Academy of Sciences of the United States of America* 105, 17842–17847.

Hatzinger, P.B., Bohlke, J.K., Sturchio, N.C., 2013. Application of stable isotope ratio analysis for biodegradation monitoring in groundwater. *Current Opinion in Biotechnology* 24, 542-549.

Haws, N.W., Ball, W.P., Bouwer, E.J., 2006. Modeling and interpreting bioavailability of organic contaminant mixtures in subsurface environments. *Journal of Contaminant Hydrology* 82, 255-292.

Hefting, M., Clément, J.C., Dowrick, D., Cosandey, A.C., Bernal, S., Cimpian, C., Tatur, A., Burt, T.P., Pinay, G., 2004. Water table elevation controls on soil nitrogen cycling in riparian wetlands along a European climatic gradient. *Biogeochemistry* 67, 113-134.

Hegeman, W.J., Laane, R.W., 2002. Enantiomeric enrichment of chiral pesticides in the environment. *Reviews of Environmental Contamination and Toxicology* 173, 85-116.

Helbling, D.E., Hollender, J., Kohler, H.P., Fenner, K., 2010. Structure-based interpretation of biotransformation pathways of amide-containing compounds in sludge-seeded bioreactors. *Environmental Science & Technology* 1, 6628-6635.

Helbling, D.E., Johnson, D.R., Honti, M., Fenner, K., 2012. Micropollutant biotransformation kinetics associate with WWTP process parameters and microbial community characteristics. *Environmental Science & Technology* 46, 10579-10588.

Hernandez, F., Sancho, J.V., Ibanez, M., Abad, E., Portoles, T., Mattioli, L., 2012. Current use of high-resolution mass spectrometry in the environmental sciences. *Analytical and Bioanalytical Chemistry* 403, 1251-1264.

Heydens, W.F., Wilson, A.G., Kier, L.D., Lau, H., Thake, D.C., Martens, M.A., 1999. An evaluation of the carcinogenic potential of the herbicide alachlor to man. *Human Experimental Toxicology* 18, 363-391.

Hijosa-Valsero, M., Matamoros, V., Martin-Villacorta, J., Becares, E., Bayona, J.M., 2010. Assessment of full-scale natural systems for the removal of PPCPs from wastewater in small communities. *Water Research* 44, 1429-1439.

Hladik, M.L., Bouwer, E.J., Roberts, A.L., 2008a. Neutral chloroacetamide herbicide degradates and related compounds in Midwestern United States drinking water sources. *Science of the Total Environment* 390, 155-165.

Hladik, M.L., Bouwer, E.J., Roberts, A.L., 2008b. Neutral degradates of chloroacetamide herbicides: Occurrence in drinking water and removal during conventional water treatment. *Water Research* 42, 4905–4914.

- Hladik, M.L., Hsiao, J.J., Roberts, A.L., 2005. Are neutral chloroacetamide herbicide degradates of potential environmental concern? Analysis and occurrence in the upper Chesapeake Bay. *Environmental Science & Technology* 39, 6561–6574.
- Hofstetter, T.B., Berg, M., 2011. Assessing transformation processes of organic contaminants by compound-specific stable isotope analysis. *Trends in Analytical Chemistry* 30, 618–627.
- Hofstetter, T.B., Spain, J.C., Nishino, S.F., Bolotin, J., Schwarzenbach, R.P., 2008. Identifying competing aerobic nitrobenzene biodegradation pathways by compound-specific isotope analysis. *Environmental Science & Technology* 42, 4764–4770.
- Huntscha, S., Singer, H., Canonica, S., Schwarzenbach, R.P., Fenner, K., 2008. Input dynamics and fate in surface water of the herbicide metolachlor and of its highly mobile transformation product metolachlor ESA. *Environmental Science & Technology* 42, 5507–5513.
- Hwang, C., Ling, F., Andersen, G.L., LeChevallier, M.W., Liu, W.T., 2012. Microbial community dynamics of an urban drinking water distribution system subjected to phases of chloramination and chlorination treatments. *Applied and Environmental Microbiology* 78, 7856–7865.
- Imfeld, G., Aragonés, C.E., Zeiger, S., Vitzthum von Eckstädt, C., Paschke, H., Trabitzzsch, R., Weiss, H., Richnow, H.H., 2008. Tracking *in situ* biodegradation of 1,2-dichloroethenes in a model wetland. *Environmental Science & Technology* 42, 7924–7930.
- Imfeld, G., Aragonés, C.E., Fetzer, I., Mészáros, E., Zeiger, S., Nijenhuis, I., Nikolausz, M., Delerce, S., Richnow, H.H., 2010. Characterization of microbial communities in the aqueous phase of a constructed model wetland treating 1,2-dichloroethene-contaminated groundwater. *FEMS Microbiology Ecology* 72, 74–88.
- Imfeld, G., Braeckevelt, M., Kusch, P., Richnow, H.H., 2009. Review: Monitoring and assessing processes of organic chemicals removal in constructed wetlands. *Chemosphere* 74, 349–362.
- Imfeld, G., Kopinke, F.D., Fischer, A., Richnow, H.H., 2014. Carbon and hydrogen isotope fractionation of benzene and toluene during hydrophobic sorption in multistep batch experiments. *Chemosphere* 107, 454–461.
- Imfeld, G., Lefrancq, M., Maillard, E., Payraudeau, S., 2013. Transport and attenuation of dissolved glyphosate and AMPA in a stormwater wetland. *Chemosphere* 90, 1333–1339.
- Imfeld, G., Vuilleumier, S., 2012. Measuring the effects of pesticides on bacterial communities in soil: A critical review. *European Journal of Soil Biology* 49, 22–30.
- Ishida, C.K., Kelly, J.J., Gray, K.A., 2006. Effects of variable hydroperiods and water level fluctuations on denitrification capacity, nitrate removal, and benthic-microbial community structure in constructed wetlands. *Ecological Engineering* 22, 363–373.
- Ivdrá, N., Herrero-Martin, S., Fischer, A., 2014. Validation of user- and environmentally friendly extraction and clean-up methods for compound-specific stable carbon isotope analysis of organochlorine pesticides and their metabolites in soils. *Journal of Chromatography A* 1355, 36–45.
- Jablonowski, N.D., Schaffer, A., Burauel, P., 2011. Still present after all these years: persistence plus potential toxicity raise questions about the use of atrazine. *Environmental Science and Pollution Research* 18, 328–331.
- Jankowski, K., Schindler, D.E., Horner-Devine, M.C., 2014. Resource availability and spatial heterogeneity control bacterial community response to nutrient enrichment in lakes. *PLoS One* 9, e86991.

- Jennings, L.K., Chartrand, M.M., Lacrampe-Couloume, G., Lollar, B.S., Spain, J.C., Gossett, J.M., 2009. Proteomic and transcriptomic analyses reveal genes upregulated by cis-dichloroethene in *Polaromonas sp.* strain JS666. *Applied and Environmental Microbiology* 75, 3733-3744.
- Johnsen, K., Jacobsen, C., Torsvik, V., Sørensen, J., 2001. Pesticide effects on bacterial diversity in agricultural soils – a review. *Biology and Fertility of Soils* 33, 443-453.
- Junk, W., An, S., Finlayson, C.M., Gopal, B., Květ, J., Mitchell, S., Mitsch, W., Robarts, R., 2013. Current state of knowledge regarding the world's wetlands and their future under global climate change: a synthesis. *Aquatic Sciences* 75, 151-167.
- Kah, M., Hofmann, T., 2014. Nanopesticide research: current trends and future priorities. *Environment International* 63, 224-235.
- Kalkhoff, S.J., Lee, K.E., Porter, S.D., Terrio, P.J., Thurman, E.M., 2003. Herbicides and herbicide degradation products in Upper Midwest agricultural streams during August base-flow conditions. *Journal of Environmental Quality* 32, 1025-1035.
- Kato, D., Yoshida, H., Takeo, M., Negoro, S., Ohta, H., 2010. Purification and gene cloning of an enantioselective thioesterification enzyme from *Brevibacterium ketoglutamicum* KU1073, a deracemization bacterium of 2-(4-chlorophenoxy)propanoic acid. *Bioscience, Biotechnology, and Biochemistry* 74, 2405-2412.
- Keddy, P.A., 2010. *Wetland ecology: Principles and conservation*. Cambridge university press, Cambridge.
- Kidmose, J., Dahl, M., Engesgaard, P., Nilsson, B., Christensen, B.S.B., Andersen, S., Hoffmann, C.C., 2010. Experimental and numerical study of the relation between flow paths and fate of a pesticide in a riparian wetland. *Journal of Hydrology* 386, 67-79.
- Kinney, C.A., Mandernack, K.W., Mosier, A.R., 2005. Laboratory investigations into the effects of the pesticides mancozeb, chlorothalonil, and prosulfuron on nitrous oxide and nitric oxide production in fertilized soil. *Soil Biology and Biochemistry* 37, 837-850.
- Kirk, G., 2004. *The Biogeochemistry of Submerged Soils*. John Wiley & Sons, West Sussex.
- Klein, C., Schneider, R.J., Meyer, M.T., Aga, D.S., 2006. Enantiomeric separation of metolachlor and its metabolites using LC-MS and CZE. *Chemosphere* 62, 1591-1599.
- Knabel, A., Stehle, S., Schafer, R.B., Schulz, R., 2012. Regulatory FOCUS surface water models fail to predict insecticide concentrations in the field. *Environmental Science & Technology* 46, 8397-8404.
- Kohler, H.R., Triebkorn, R., 2013. Wildlife ecotoxicology of pesticides: can we track effects to the population level and beyond? *Science* 341, 759-765.
- Konopka, A., 1994. Anaerobic degradation of chloroacetanilide herbicides. *Applied Microbiology and Biotechnology* 42, 440-445.
- Kookana, R.S., Boxall, A.B., Reeves, P.T., Ashauer, R., Beulke, S., Chaudhry, Q., Cornelis, G., Fernandes, T.F., Gan, J., Kah, M., Lynch, I., Ranville, J., Sinclair, C., Spurgeon, D., Tiede, K., Van den Brink, P.J., 2014. Nanopesticides: guiding principles for regulatory evaluation of environmental risks. *Journal of Agriculture and Food Chemistry* 62, 4227-4240.
- Krone-Davis, P., Watson, F., Los Huertos, M., Starner, K., 2013. Assessing pesticide reduction in constructed wetlands using a tanks-in-series model within a Bayesian framework. *Ecological Engineering* 57, 342-352.

- Kuhlmann, B., Kaczmarczyk, B., 1995. Biodegradation of the herbicides 2,4-dichlorophenoxyacetic acid, 2,4,5-trichlorophenoxyacetic acid, and 2-methyl-4-chlorophenoxyacetic acid in a sulfate-reducing aquifer. *Environmental Toxicology and Water Quality* 10, 119-125.
- Kuramae, E.E., Yergeau, E., Wong, L.C., Pijl, A.S., van Veen, J.A., Kowalchuk, G.A., 2012. Soil characteristics more strongly influence soil bacterial communities than land-use type. *FEMS Microbiology Ecology* 79, 12-24.
- Kurt-Karakus, P.B., Bidleman, T.F., Staebler, R.M., Jones, K.C., 2006. Measurement of DDT fluxes from a historically treated agricultural soil in Canada. *Environmental Science & Technology* 40, 4578-4585.
- Laanbroek, H.J., 2010. Methane emission from natural wetlands: interplay between emergent macrophytes and soil microbial processes. A mini-review. *Annals of Botany* 105, 141-153.
- Lal, D., Jindal, S., Kumari, H., Jit, S., Nigam, A., Sharma, P., Kumari, K., Lal, R., 2013. Bacterial diversity and real-time PCR based assessment of *linA* and *linB* gene distribution at hexachlorocyclohexane contaminated sites. *Journal of Basic Microbiology*.
- Larentis, M., Hoermann, K., Lueders, T., 2013. Fine-scale degrader community profiling over an aerobic/anaerobic redox gradient in a toluene-contaminated aquifer. *Environmental Microbiology Reports* 5, 225-234.
- Lauga, B., Girardin, N., Karama, S., Le Ménach, K., Budzinski, H., R, D., 2013. Removal of alachlor in anoxic soil slurries and related alteration of the active communities. *Environmental Science and Pollution Research International* 20, 1089-1105.
- Lee, B.-H., Scholz, M., 2007. What is the role of *Phragmites australis* in experimental constructed wetland filters treating urban runoff? *Ecological Engineering* 29, 87-95.
- Lefrancq, M., Imfeld, G., Payraudeau, S., Millet, M., 2013. Kresoxim methyl deposition, drift and runoff in a vineyard catchment. *Science of the Total Environment* 442, 503-508.
- Legendre, P., Fortin, M.-J., 2010. Comparison of the Mantel test and alternative approaches for detecting complex multivariate relationships in the spatial analysis of genetic data. *Molecular Ecology Resources* 10, 831-844.
- Li, Y., Chen, Q., Wang, C.H., Cai, S., He, J., Huang, X., Li, S.P., 2013. Degradation of acetochlor by consortium of two bacterial strains and cloning of a novel amidase gene involved in acetochlor-degrading pathway. *Bioresource Technology* 148, 628-631.
- Li, Y., Dong, F., Liu, X., Xu, J., Li, J., Kong, Z., Chen, X., Zheng, Y., 2012. Environmental behavior of the chiral triazole fungicide fenbuconazole and its chiral metabolites: enantioselective transformation and degradation in soils. *Environmental Science & Technology* 46, 2675-2683.
- Li, Z., Zhang, Y., Li, Q., Wang, W., Li, J., 2011. Enantioselective degradation, abiotic racemization, and chiral transformation of triadimefon in soils. *Environment Science & Technology* 45, 2797-2803.
- Ligi, T., Oopkaup, K., Truu, M., Preem, J.-K., Nõlvak, H., Mitsch, W.J., Mander, Ü., Truu, J., 2013. Characterization of bacterial communities in soil and sediment of a created riverine wetland complex using high-throughput 16S rRNA amplicon sequencing. *Ecological Engineering*.
- Lin, X., Green, S., Tfaily, M.M., Prakash, O., Konstantinidis, K.T., Corbett, J.E., Chanton, J.P., Cooper, W.T., Kostka, J.E., 2012. Microbial community structure and activity linked to contrasting biogeochemical gradients in bog and fen environments of the Glacial Lake Agassiz Peatland. *Applied and Environmental Microbiology* 78, 7023-7031.

- Liu, H., Huang, R., Xie, F., Zhang, S., Shi, J., 2012a. Enantioselective phytotoxicity of metolachlor against maize and rice roots. *Journal of Hazardous Materials* 217-218, 330-337.
- Liu, H., Xiong, M., 2009. Comparative toxicity of racemic metolachlor and S-metolachlor to *Chlorella pyrenoidosa*. *Aquatic Toxicology* 93, 100-106.
- Liu, H.M., Cao, L., Lu, P., Ni, H., Li, Y.X., Yan, X., Hong, Q., Li, S.P., 2012b. Biodegradation of butachlor by *Rhodococcus* sp. strain B1 and purification of its hydrolase (ChlH) responsible for N-dealkylation of chloroacetamide herbicides. *Journal of Agricultural and Food Chemistry* 60, 12238-12244.
- Liu, S.-Y., Lu, M.-H., Bollag, J.-M., 1999. Transformation of metolachlor in soil inoculated with a *Streptomyces* sp. *Biodegradation* 1, 9-17.
- Liu, W., Gan, J., Papiernik, S.K., Yates, S.R., 2000. Structural influences in relative sorptivity of chloroacetanilide herbicides on soil. *Journal of Agriculture & Food Chemistry* 48, 4320-4325.
- Liu, W., Gan, J., Schlenk, D., Jury, W.A., 2005. Enantioselectivity in environmental safety of current chiral insecticides. *Proceedings of the National Academy of Sciences*, 102: 701–706.
- Liu, W.P., Liu, H.J., Zheng, W., Lu, J.H., 2001. Adsorption of chloroacetanilide herbicides on soil. Structural influence of chloroacetanilide herbicide for their adsorption on soils and its components. *Journal of Environmental Sciences (China)* 13, 37-45.
- Lo, C.C., 2010. Effect of pesticides on soil microbial community. *Journal of Environmental Science and Health Part B* 45, 348-359.
- Logares, R., Sunagawa, S., Salazar, G., Cornejo-Castillo, F.M., Ferrera, I., Sarmiento, H., Hingamp, P., Ogata, H., de Vargas, C., Lima-Mendez, G., Raes, J., Poulain, J., Jaillon, O., Wincker, P., Kandels-Lewis, S., Karsenti, E., Bork, P., Acinas, S.G., 2014. Metagenomic 16S rDNA Illumina tags are a powerful alternative to amplicon sequencing to explore diversity and structure of microbial communities. *Environmental Microbiology* 16, 2659-2671.
- Logue, J.B., Langenheder, S., Andersson, A.F., Bertilsson, S., Drakare, S., Lanzen, A., Lindstrom, E.S., 2012. Freshwater bacterioplankton richness in oligotrophic lakes depends on nutrient availability rather than on species-area relationships. *The ISME journal* 6, 1127-1136.
- Lollar, B.S., Hirschorn, S.K., Chartrand, M.M., Lacrampe-Couloume, G., 2007. An approach for assessing total instrumental uncertainty in compound-specific carbon isotope analysis: implications for environmental remediation studies. *Analytical Chemistry* 79, 3469-3475.
- Loman, N.J., Constantinidou, C., Chan, J.Z., Halachev, M., Sergeant, M., Penn, C.W., Robinson, E.R., Pallen, M.J., 2012. High-throughput bacterial genome sequencing: an embarrassment of choice, a world of opportunity. *Nature Reviews Microbiology* 10, 599-606.
- Loos, R., Locoro, G., Comero, S., Contini, S., Schwesig, D., Werres, F., Balsaa, P., Gans, O., Weiss, S., Blaha, L., Bolchi, M., Gawlik, B.M., 2010. Pan-European survey on the occurrence of selected polar organic persistent pollutants in ground water. *Water Research* 44, 4115-4126.
- Lopez, S.H., Ulaszewska, M.M., Hernando, M.D., Bueno, M.J., Gomez, M.J., Fernandez-Alba, A.R., 2014. Post-acquisition data processing for the screening of transformation products of different organic contaminants. Two-year monitoring of river water using LC-ESI-QTOF-MS and GCxGC-EI-TOF-MS. *Environmental Science and Pollution Research International*.



- Luo, W., Zhao, Y., Ding, H., Lin, X., Zheng, H., 2008. Co-metabolic degradation of bensulfuron-methyl in laboratory conditions. *Journal of Hazardous Materials* 158, 208-214.
- Lutz, S., Van der Velde, Y., Elsayed, O., Imfeld, G., Lefrancq, M., Payraudeau, S., Van Breukelen, B., 2014. Compound-specific stable isotope analysis of herbicides in stream water: a combined monitoring and modeling approach to assess pollutant degradation at catchment scale. Paper presented at the EGU General Assembly 2014, Vienna, Austria.
- Lutz, S.R., van Meerveld, H.J., Waterloo, M.J., Broers, H.P., van Breukelen, B.M., 2013. A model-based assessment of the potential use of compound-specific stable isotope analysis in river monitoring of diffuse pesticide pollution. *Hydrology and Earth System Sciences* 17, 4505-4524.
- Ma, Y., Liu, W.-P., Wen, Y.-Z., 2006. Enantioselective degradation of *rac*-metolachlor and *S*-metolachlor in soil. *Pedosphere* 16, 489-494.
- Maier, M.P., Qiu, S., Elsner, M., 2013. Enantioselective stable isotope analysis (ESIA) of polar herbicides. *Analytical and Bioanalytical Chemistry* 405, 2825-2831.
- Maillard, E., 2014. Transport and degradation of pesticides in wetland systems: A downscaling approach. University of Strasbourg, Strasbourg.
- Maillard, E., Imfeld, G., 2014. Pesticide mass budget in a stormwater wetland. *Environmental Science & Technology* 48, 8603-8611.
- Maillard, E., Payraudeau, S., Faivre, E., Grégoire, C., Gangloff, S., Imfeld, G., 2011. Removal of pesticide mixtures in a stormwater wetland collecting runoff from a vineyard catchment. *Science of the Total Environment* 409, 2317-2324.
- Malaj, E., von der Ohe, P.C., Grote, M., Kuhne, R., Mondy, C.P., Usseglio-Polatera, P., Brack, W., Schafer, R.B., 2014. Organic chemicals jeopardize the health of freshwater ecosystems on the continental scale. *Proceedings of the National Academy of Sciences* 111, 9549-9554.
- Martinez-Lavanchy, P.M., Dohrmann, A.B., Imfeld, G., Trescher, K., Tebbe, C.C., Richnow, H.H., Nijenhuis, I., 2011. Detection of monochlorobenzene metabolizing bacteria under anoxic conditions by DNA-stable isotope probing. *Biodegradation* 22, 973-982.
- Matamoros, V., Hijosa, M., Bayona, J.M., 2009. Assessment of the pharmaceutical active compounds removal in wastewater treatment systems at enantiomeric level. Ibuprofen and naproxen. *Chemosphere* 75, 200-205.
- McHugh, T., Kuder, T., Fiorenza, S., Gorder, K., Dettenmaier, E., Philp, P., 2011. Application of CSIA to distinguish between vapor intrusion and indoor sources of VOCs. *Environmental Science & Technology* 45, 5952-5958.
- Meckenstock, R.U., Morasch, B., Griebler, C., Richnow, H.H., 2004. Stable isotope fractionation analysis as a tool to monitor biodegradation in contaminated aquifers. *Journal of Contaminant Hydrology* 75, 215-255.
- Menon, R., Jackson, C., Holland, M., 2013. The Influence of Vegetation on Microbial Enzyme Activity and Bacterial Community Structure in Freshwater Constructed Wetland Sediments. *Wetlands* 33, 365-378.
- Meyer, A.H., Elsner, M., 2013.  $^{13}\text{C}/^{12}\text{C}$  and  $^{15}\text{N}/^{14}\text{N}$  isotope analysis to characterize degradation of atrazine: evidence from parent and daughter compound values. *Environmental Science & Technology* 47, 6884-6891.

- Meyer, A.H., Penning, H., Elsner, M., 2009. C and N isotope fractionation suggests similar mechanisms of microbial atrazine transformation despite involvement of different enzymes (AtzA and TrzN). *Environmental science & technology* 43, 8079-8085.
- Meyer, A.H., Penning, H., Lowag, H., Elsner, M., 2008. Precise and accurate compound specific carbon and nitrogen isotope analysis of atrazine: critical role of combustion oven conditions. *Environmental Science & Technology* 42, 7757–7763.
- Milenkovski, S., Baath, E., Lindgren, P.E., Berglund, O., 2010. Toxicity of fungicides to natural bacterial communities in wetland water and sediment measured using leucine incorporation and potential denitrification. *Ecotoxicology* 19, 285-294.
- Miller, P.L., Chin, Y.P., 2005. Indirect photolysis promoted by natural and engineered wetland water constituents: processes leading to alachlor degradation. *Environmental Science & Technology* 39, 4454-4462.
- Milligan, P.W., Häggblom, M.M., 1999. Biodegradation and biotransformation of dicamba under different reducing conditions. *Environmental Science & Technology* 33, 1224-1229.
- Mills, D.K., Entry, J.A., Voss, J.D., Gillevet, P.M., Mathee, K., 2006. An assessment of the hypervariable domains of the 16S rRNA genes for their value in determining microbial community diversity: the paradox of traditional ecological indices. *FEMS Microbiology Ecology* 57, 496-503.
- Milosevic, N., Qiu, S., Elsner, M., Einsiedl, F., Maier, M.P., Bensch, H.K., Albrechtsen, H.J., Bjerg, P.L., 2013. Combined isotope and enantiomer analysis to assess the fate of phenoxy acids in a heterogeneous geologic setting at an old landfill. *Water Research* 47, 637-649.
- Monard, C., Martin-Laurent, F., Lima, O., Devers-Lamrani, M., Binet, F., 2013. Estimating the biodegradation of pesticide in soils by monitoring pesticide-degrading gene expression. *Biodegradation* 24, 203-213.
- Moore, M.T., Rodgers, J.H., Smith, S., Cooper, C.M., 2001. Mitigation of metolachlor-associated agricultural runoff using constructed wetlands in Mississippi, USA. *Agriculture, Ecosystems & Environment* 84, 169–176.
- Morissette, J.L., Kardynal, K.J., Bayne, E.M., Hobson, K.A., 2013. Comparing bird community composition among boreal wetlands: Is wetland classification a missing piece of the habitat puzzle? *Wetlands* 33, 653-665.
- Mostafalou, S., Abdollahi, M., 2013. Pesticides and human chronic diseases: evidences, mechanisms, and perspectives. *Toxicology and Applied Pharmacology* 268, 157-177.
- Mueller, J.F., Harden, F., Toms, L.M., Symons, R., Furst, P., 2008. Persistent organochlorine pesticides in human milk samples from Australia. *Chemosphere* 70, 712-720.
- Muller, M.D., Poiger, T., Buser, H., 2001. Isolation and identification of the metolachlor stereoisomers using high-performance liquid chromatography, polarimetric measurements, and enantioselective gas chromatography. *Journal of Agriculture & Food Chemistry* 49, 42-49.
- Munoz, A., Koskinen, W.C., Cox, L., Sadowsky, M.J., 2011. Biodegradation and mineralization of metolachlor and alachlor by *Candida xestobii*. *Journal of Agriculture & Food Chemistry* 59, 619-627.
- Murray, K.E., Thomas, S.M., Bodour, A.A., 2010. Prioritizing research for trace pollutants and emerging contaminants in the freshwater environment. *Environmental Pollution* 158, 3462-3471.
- Mutz, K.O., Heilkenbrinker, A., Lonne, M., Walter, J.G., Stahl, F., 2013. Transcriptome analysis using next-generation sequencing. *Current Opinion in Biotechnology* 24, 22-30.

- Muyzer, G., Teske, A., Wirsen, C.O., Jannasch, H.W., 1995. Phylogenetic relationships of *Thiomicrospira* species and their identification in deep-sea hydrothermal vent samples by denaturing gradient gel electrophoresis of 16S rDNA fragments. *Archives of Microbiology* 164, 165-172.
- Müller, M.D., Poiger, T., Buser, H.-R., 2000. Isolation and identification of the metolachlor stereoisomers using high-performance liquid chromatography, polarimetric measurements, and enantioselective gas chromatography. *Journal of Agriculture & Food Chemistry* 49, 42-49.
- Müller, T.A., Fleischmann, T., van der Meer, J.R., Kohler, H.P., 2006. Purification and characterization of two enantioselective alpha-ketoglutarate-dependent dioxygenases, RdpA and SdpA, from *Sphingomonas herbicidovorans* MH. *Applied and Environmental Microbiology* 72, 4853-4861.
- Nacke, H., Thurmer, A., Wollherr, A., Will, C., Hodac, L., Herold, N., Schoning, I., Schrupf, M., Daniel, R., 2011. Pyrosequencing-based assessment of bacterial community structure along different management types in German forest and grassland soils. *PLoS One* 6, e17000.
- Neubauer, S.C., Givler, K., Valentine, S., Megonigal, J.P., 2005. Seasonal patterns and plant-mediated controls of subsurface wetland biogeochemistry. *Ecology* 86, 3334-3344.
- Nijenhuis, I., Andert, J., Beck, K., Kästner, M., Diekert, G., Richnow, H.H., 2005. Stable isotope fractionation of tetrachloroethene during reductive dechlorination by *Sulfurospirillum multivorans* and *Desulfitobacterium* sp. strain PCE-S and abiotic reactions with cyanocobalamin. *Applied and Environmental Microbiology* 71, 3413-3419.
- Nolvak, H., Truu, M., Tiirik, K., Oopkaup, K., Sildvee, T., Kaasik, A., Mander, U., Truu, J., 2013. Dynamics of antibiotic resistance genes and their relationships with system treatment efficiency in a horizontal subsurface flow constructed wetland. *Science of the Total Environment* 461-462, 636-644.
- Nunan, N., Daniell, T.J., Singh, B.K., Papert, A., McNicol, J.W., Prosser, J.I., 2005. Links between plant and rhizoplane bacterial communities in grassland soils, characterized using molecular techniques. *Applied and Environmental Microbiology* 71, 6784-6792.
- Nyyssonen, M., Kapanen, A., Piskonen, R., Lukkari, T., Itavaara, M., 2009. Functional genes reveal the intrinsic PAH biodegradation potential in creosote-contaminated groundwater following *in situ* biostimulation. *Applied Microbiology and Biotechnology* 84, 169-182.
- Oh, S., Kurt, Z., Tsementzi, D., Weigand, M.R., Kim, M., Hatt, J.K., Tandukar, M., Pavlostathis, S.G., Spain, J.C., Konstantinidis, K.T., 2014. Microbial community degradation of widely used quaternary ammonium disinfectants. *Applied and Environmental Microbiology* 80, 5892-5900.
- Ohisa, N., Yamaguchi, M., 1979. *Clostridium* species and  $\gamma$ -BHC degradation in paddy soil. *Soil Biology and Biochemistry* 11, 645-649.
- Oliver-Rodríguez, B., Zafra-Gómez, A., Camino-Sánchez, F.J., Conde-González, J.E., Pérez-Trujillo, J.P., Vílchez, J.L., 2013. Multi-residue method for the analysis of commonly used commercial surfactants, homologues and ethoxymers, in marine sediments by liquid chromatography-electrospray mass spectrometry. *Microchemical Journal* 110, 158-168.
- Ong, S.H., Kukkillaya, V.U., Wilm, A., Lay, C., Ho, E.X., Low, L., Hibberd, M.L., Nagarajan, N., 2013. Species identification and profiling of complex microbial communities using shotgun Illumina sequencing of 16S rRNA amplicon sequences. *PLoS One* 8, e60811.

- Osborn, A.M., Moore, E.R.B., Timmis, K.N., 2000. An evaluation of terminal-restriction fragment length polymorphism (T-RFLP) analysis for the study of microbial community structure and dynamics. *Environmental Microbiology* 2, 39-50.
- Osborne, C.A., Galic, M., Sangwan, P., Janssen, P.H., 2005. PCR-generated artefact from 16S rRNA gene-specific primers. *FEMS Microbiology Letters* 248, 183-187.
- Padilla-Sanchez, J.A., Michael Thurman, E., Plaza-Bolanos, P., Ferrer, I., 2012. Identification of pesticide transformation products in agricultural soils using liquid chromatography/quadrupole-time-of-flight mass spectrometry. *Rapid Communications in Mass Spectrometry* 26, 1091-1099.
- Paredes, C.J., Alsaker, K.V., Papoutsakis, E.T., 2005. A comparative genomic view of clostridial sporulation and physiology. *Nature Reviews Microbiology* 3, 969-978.
- Pareja, L., Perez-Parada, A., Aguera, A., Cesio, V., Heinzen, H., Fernandez-Alba, A.R., 2012. Photolytic and photocatalytic degradation of quinclorac in ultrapure and paddy field water: identification of transformation products and pathways. *Chemosphere* 87, 838-844.
- Parron, T., Requena, M., Hernandez, A.F., Alarcon, R., 2011. Association between environmental exposure to pesticides and neurodegenerative diseases. *Toxicology and Applied Pharmacology* 256, 379-385.
- Passeport, E., Benoit, P., Bergheaud, V., Coquet, Y., Tournebize, J., 2011. Selected pesticides adsorption and desorption in substrates from artificial wetland and forest buffer. *Environmental Toxicology and Chemistry* 30, 1669-1676.
- Patterson, D.G., Jr., Wong, L.Y., Turner, W.E., Caudill, S.P., Dipietro, E.S., McClure, P.C., Cash, T.P., Osterloh, J.D., Pirkle, J.L., Sampson, E.J., Needham, L.L., 2009. Levels in the U.S. population of those persistent organic pollutants (2003-2004) included in the Stockholm Convention or in other long range transboundary air pollution agreements. *Environmental Science & Technology* 43, 1211-1218.
- Penning, H., Sørensen, S.R., Meyer, A.H., Aamand, J., Elsner, M., 2010. C, N, and H isotope fractionation of the herbicide isoproturon reflects different microbial transformation pathways. *Environmental Science & Technology* 44, 2372-2378.
- Penny, C., 2009. Réponses microbiennes au tétrachlorure de carbone. Univeristy of Strasbourg, Strasbourg.
- Penny, C., Nadalig, T., Alioua, M., Gruffaz, C., Vuilleumier, S., Bringel, F., 2010a. Coupling of denaturing high-performance liquid chromatography and terminal restriction fragment length polymorphism with precise fragment sizing for microbial community profiling and characterization. *Applied and Environment Microbiology* 76, 648-651.
- Penny, C., Vuilleumier, S., Bringel, F., 2010b. Microbial degradation of tetrachloromethane: mechanisms and perspectives for bioremediation. *FEMS Microbiology Ecology* 74, 257-275.
- Peralta, R.M., Ahn, C., Gillevet, P.M., 2013. Characterization of soil bacterial community structure and physicochemical properties in created and natural wetlands. *Science of the Total Environment* 443, 725-732.
- Pereira, S.P., Fernandes, M.A.S., Martins, J.D., Santos, M.S., Moreno, A.J.M., Vicente, J.A.F., Videira, R.A., Jurado, A.S., 2009. Toxicity assessment of the herbicide metolachlor comparative effects on bacterial and mitochondrial model systems. *Toxicology in Vitro* 23, 1585-1590.
- Perucci, P., Dumontet, S., Bufo, S.A., Mazzatura, A., Casucci, C., 2000. Effects of organic amendment and herbicide treatment on soil microbial biomass. *Biology and Fertility of Soils* 32, 17-23.

- Pesce, S., Margoum, C., Montuelle, B., 2010. *In situ* relationships between spatio-temporal variations in diuron concentrations and phototrophic biofilm tolerance in a contaminated river. *Water Research* 44, 1941-1949.
- Pester, M., Knorr, K.H., Friedrich, M.W., Wagner, M., Loy, A., 2012. Sulfate-reducing microorganisms in wetlands - fameless actors in carbon cycling and climate change. *Frontiers in Microbiology* 3, 72.
- Petrovic, M., Farre, M., de Alda, M.L., Perez, S., Postigo, C., Kock, M., Radjenovic, J., Gros, M., Barcelo, D., 2010. Recent trends in the liquid chromatography-mass spectrometry analysis of organic contaminants in environmental samples. *Journal of Chromatography A* 1217, 4004-4017.
- Postigo, C., Barcelo, D., 2014. Synthetic organic compounds and their transformation products in groundwater: Occurrence, fate and mitigation. *Science of the Total Environment*.
- Qin, K., Struckhoff, G.C., Agrawal, A., Shelley, M.L., Dong, H., 2015. Natural attenuation potential of trichloroethene in wetland plant roots: Role of native ammonium-oxidizing microorganisms. *Chemosphere* 119, 971-977.
- Qiu, S., Gozdereliler, E., Weyrauch, P., Lopez, E.C., Kohler, H.P., Sorensen, S.R., Meckenstock, R.U., Elsner, M., 2014. Small (13)C/(12)C fractionation contrasts with large enantiomer fractionation in aerobic biodegradation of phenoxy acids. *Environmental Science & Technology* 48, 5501-5511.
- Ramette, A., 2007. Multivariate analyses in microbial ecology. *FEMS Microbiology Ecology* 62, 142-160.
- Ranjard, L., Poly, F., Nazaret, S., 2000. Monitoring complex bacterial communities using culture-independent molecular techniques: application to soil environment. *Research in Microbiology* 151, 167-177.
- Rebich, R.A., Coupe, R.H., Thurman, E.M., 2004. Herbicide concentrations in the Mississippi River Basin-the importance of chloroacetanilide herbicide degradates. *Science of the Total Environment* 321, 189-199.
- Reemtsma, T., Alder, L., Banasiak, U., 2013. A multimethod for the determination of 150 pesticide metabolites in surface water and groundwater using direct injection liquid chromatography-mass spectrometry. *Journal of Chromatography A* 1271, 95-104.
- Reid, B.J., Jones, K.C., Semple, K.T., 2000. Bioavailability of persistent organic pollutants in soils and sediments-a perspective on mechanisms, consequences and assessment. *Environmental Pollution* 108, 103-112.
- Reinicke, S., Simonsen, A., Sørensen, S.R., Aamand, J., Elsner, M., 2012. C and N isotope fractionation during biodegradation of the pesticide metabolite 2,6- dichlorobenzamide (BAM): Potential for environmental assessments. *Environmental Science & Technology* 46, 1447-1454.
- Rice, P.J., Arthur, E.L., Barefoot, A.C., 2007. Advances in pesticide environmental fate and exposure assessments. *Journal of Agriculture and Food Chemistry* 55, 5367-5376.
- Richardson, J.R., Roy, A., Shalat, S.L., von Stein, R.T., Hossain, M.M., Buckley, B., Gearing, M., Levey, A.I., German, D.C., 2014. Elevated serum pesticide levels and risk for Alzheimer disease. *JAMA Neurology* 71, 284-290.
- Richnow, H.H., Annweiler, E., Michaelis, W., Meckenstock, R.U., 2003. Microbial *in situ* degradation of aromatic hydrocarbons in a contaminated aquifer monitored by carbon isotope fractionation. *Journal of Contaminant Hydrology* 65, 101-120.

- Rooney, R.C., Bayley, S.E., 2012. Community congruence of plants, invertebrates and birds in natural and constructed shallow open-water wetlands: Do we need to monitor multiple assemblages? *Ecological Indicators* 20, 42-50.
- Rosell, M., Gonzalez-Olmos, R., Rohwerder, T., Rusevova, K., Georgi, A., Kopinke, F.D., Richnow, H.H., 2012. Critical evaluation of the 2D-CSIA scheme for distinguishing fuel oxygenate degradation reaction mechanisms. *Environmental Science & Technology* 46, 4757-4766.
- Runes, H.B., Jenkins, J.J., Bottomley, P.J., 2001. Atrazine degradation by bioaugmented sediment from constructed wetlands. *Applied Microbiology and Biotechnology* 57, 427-432.
- Saha, S., Dutta, D., Karmakar, R., Ray, D.P., 2012. Structure-toxicity relationship of chloroacetanilide herbicides: relative impact on soil microorganisms. *Environmental Toxicology and Pharmacology* 34, 307-314.
- San Miguel, A., Roy, J., Gury, J., Monier, A., Coissac, E., Ravanel, P., Geremia, R.A., Raveton, M., 2014. Effects of organochlorines on microbial diversity and community structure in *Phragmites australis* rhizosphere. *Applied Microbiology and Biotechnology* 98, 4257-4266.
- Sanyal, D., Kulshrestha, G., 2002. Metabolism of metolachlor by fungal cultures. *Journal of Agriculture & Food Chemistry* 50, 499-505.
- Schafer, R.B., Bundschuh, M., Rouch, D.A., Szocs, E., von der Ohe, P.C., Pettigrove, V., Schulz, R., Nuggeoda, D., Kefford, B.J., 2012. Effects of pesticide toxicity, salinity and other environmental variables on selected ecosystem functions in streams and the relevance for ecosystem services. *Science of the Total Environment* 415, 69-78.
- Schenker, U., Scheringer, M., Hungerbühler, K., 2007. Including degradation products of persistent organic pollutants in a global multi-media box model. *Environmental Science and Pollution Research* 14, 145-152.
- Scheublin, T.R., Deusch, S., Moreno-Forero, S.K., Muller, J.A., van der Meer, J.R., Leveau, J.H., 2014. Transcriptional profiling of Gram-positive *Arthrobacter* in the phyllosphere: induction of pollutant degradation genes by natural plant phenolic compounds. *Environmental Microbiology* 16, 2212-2225.
- Schmidt, T.C., Jochmann, M.A., 2012. Origin and fate of organic compounds in water: characterization by compound-specific stable isotope analysis. *Annual Review of Analytical Chemistry* 5, 133-155.
- Schneider, M., Endo, S., Goss, K.-U., 2013. Volatilization of pesticides from the bare soil surface: Evaluation of the humidity effect. *Journal of Environmental Quality*, 844-851.
- Schulz, R., 2004. Field studies on exposure, effects, and risk mitigation of aquatic nonpoint-source insecticide pollution: a review. *Journal of Environmental Quality* 33, 419-448.
- Schurig, C., Melo, V.A., Miltner, A., Kaestner, M., 2014. Characterisation of microbial activity in the framework of natural attenuation without groundwater monitoring wells?: a new Direct-Push probe. *Environmental Science and Pollution Research* 21, 9002-9015.
- Schütte, U.M., Abdo, Z., Bent, S.J., Shyu, C., Williams, C.J., Pierson, J.D., Forney, L.J., 2008. Advances in the use of terminal restriction fragment length polymorphism (T-RFLP) analysis of 16S rRNA genes to characterize microbial communities. *Applied microbiology and biotechnology* 80, 365-380.
- Seghers, D., Bulcke, R., Reheul, D., Siciliano, S.D., Top, E.M., Verstraete, W., 2003a. Pollution induced community tolerance (PICT) and analysis of 16S rRNA genes to evaluate the long-term effects of herbicides on methanotrophic communities in soil. *European Journal of Soil Science* 54, 679-684.

- Seghers, D., Verthé, K., Reheul, D., Bulcke, R., Siciliano, S.D., Verstraete, W., Top, E.M., 2003b. Effect of long-term herbicide applications on the bacterial community structure and function in an agricultural soil. *FEMS Microbiology Ecology* 46, 139-146.
- Serkebaeva, Y.M., Kim, Y., Liesack, W., Dedysh, S.N., 2013. Pyrosequencing-based assessment of the bacteria diversity in surface and subsurface peat layers of a northern wetland, with focus on poorly studied phyla and candidate divisions. *PLoS One* 8, e63994.
- Sette, L.D., de Oliveira, V.M., Manfio, G.P., 2005a. Isolation and characterization of alachlor-degrading actinomycetes from soil. *Antonie Van Leeuwenhoek* 87, 81-89.
- Sette, L.D., de Oliveira, V.M., Manfio, G.P., 2005b. Isolation and characterization of alachlor-degrading actinomycetes from soil. *Antonie Van Leeuwenhoek* 87, 81-89.
- Sette, L.D., Mendonca Alves Da Costa, L.A., Marsaioli, A.J., Manfio, G.P., 2004. Biodegradation of alachlor by soil streptomycetes. *Applied Microbiology and Biotechnology* 64, 712-717.
- Seybold, C.A., Mersie, W., McNamee, C., 2001. Anaerobic degradation of atrazine and metolachlor and metabolite formation in wetland soil and water microcosms. *Journal of Environmental Quality* 30, 1271-1277.
- Sharma, C.M., Vogel, J., 2014. Differential RNA-seq: the approach behind and the biological insight gained. *Current Opinion Microbiology* 19, 97-105.
- Si, Y., Takagi, K., Iwasaki, A., Zhou, D., 2009. Adsorption, desorption and dissipation of metolachlor in surface and subsurface soils. *Pest management science* 65, 956-962.
- Sierka, R.A., 2013. Activated carbon adsorption and chemical regeneration in the food industry. in: Coca-Prados, J., Gutiérrez-Cervelló, G. (Eds.). *Economic sustainability and environmental protection in mediterranean countries through clean manufacturing methods*. Springer Netherlands, pp. 93-105.
- Sims, A., Horton, J., Gajaraj, S., McIntosh, S., Miles, R.J., Mueller, R., Reed, R., Hu, Z., 2012. Temporal and spatial distributions of ammonia-oxidizing archaea and bacteria and their ratio as an indicator of oligotrophic conditions in natural wetlands. *Water Research* 46, 4121-4129.
- Sims, A., Zhang, Y., Gajaraj, S., Brown, P.B., Hu, Z., 2013. Toward the development of microbial indicators for wetland assessment. *Water Research* 47, 1711-1725.
- Singh, N., Megharaj, M., Kookana, R.S., Naidu, R., Sethunathan, N., 2004. Atrazine and simazine degradation in *Pennisetum* rhizosphere. *Chemosphere* 56, 257-263.
- Skarpeli-Liati, M., Pati, S.G., Bolotin, J., Eustis, S.N., Hofstetter, T.B., 2012. Carbon, hydrogen, and nitrogen isotope fractionation associated with oxidative transformation of substituted aromatic N-alkyl amines. *Environmental Science & Technology* 46, 7189-7198.
- Smit, E., Leeftang, P., Gommans, S., van den Broek, J., van Mil, S., Wernars, K., 2001. Diversity and seasonal fluctuations of the dominant members of the bacterial soil community in a wheat field as determined by cultivation and molecular methods. *Applied and Environmental Microbiology* 67, 2284-2291.
- Smith, C.J., Danilowicz, B.S., Clear, A.K., Costello, F.J., Wilson, B., Meijer, W., 2005. T-Align, a web-based tool for comparison of multiple terminal restriction fragment length polymorphism profiles. *FEMS Microbiology Ecology* 54, 375-380.

- Spahr, S., Huntscha, S., Bolotin, J., Maier, M.P., Elsner, M., Hollender, J., Hofstetter, T.B., 2013. Compound-specific isotope analysis of benzotriazole and its derivatives. *Analytical and Bioanalytical Chemistry* 405, 2843-2856.
- Springael, D., Top, E.M., 2004. Horizontal gene transfer and microbial adaptation to xenobiotics: new types of mobile genetic elements and lessons from ecological studies. *Trends in Microbiology* 12, 53-58.
- Stamper, D.M., Tuovinen, O.H., 1998. Biodegradation of the acetanilide herbicides alachlor, metolachlor, and propachlor. *Critical Reviews in Microbiology* 24, 1-22.
- Steele, G.V., Johnson, H.M., Sandstrom, M.W., Capel, P.D., Barbash, J.E., 2008. Occurrence and fate of pesticides in four contrasting agricultural settings in the United States. *Journal of Environmental Quality* 37, 1116-1132.
- Stehle, S., Elsaesser, D., Gregoire, C., Imfeld, G., Niehaus, E., Passeport, E., Payraudeau, S., Schäfer, R.B., Tournebize, J., Schulz, R., 2011. Pesticide risk mitigation by vegetated treatment systems: a meta-analysis. *Journal of Environmental Quality* 40, 1068–1080.
- Stelzer, N., Imfeld, G., Thullner, M., Lehmann, J., Poser, A., Richnow, H.H., Nijenhuis, I., 2009. Integrative approach to delineate natural attenuation of chlorinated benzenes in anoxic aquifers. *Environmental Pollution* 157, 1800-1806.
- Thullner, M., Centler, F., Richnow, H.H., Fischer, A., 2012. Quantification of organic pollutant degradation in contaminated aquifers using compound specific stable isotope analysis – Review of recent developments. *Organic Geochemistry* 42, 1440–1460.
- Tobler, N.B., Hofstetter, T.B., Schwarzenbach, R.P., 2008. Carbon and hydrogen isotope fractionation during anaerobic toluene oxidation by *Geobacter metallireducens* with different Fe(III) phases as terminal electron acceptors. *Environmental Science & Technology* 42, 7786-7792.
- Tournebize, J., Passeport, E., Chaumont, C., Fesneau, C., Guenne, A., Vincent, B., 2013. Pesticide decontamination of surface waters as a wetland ecosystem service in agricultural landscapes. *Ecological Engineering* 56, 51-59.
- Truu, M., Juhanson, J., Truu, J., 2009. Microbial biomass, activity and community composition in constructed wetlands. *Science of the Total Environment* 407, 3958–3971.
- Uhlik, O., Leewis, M.C., Strejcek, M., Musilova, L., Mackova, M., Leigh, M.B., Macek, T., 2013. Stable isotope probing in the metagenomics era: a bridge towards improved bioremediation. *Biotechnology Advances* 31, 154-165.
- Uhlik, O., Strejcek, M., Vondracek, J., Musilova, L., Ridl, J., Lovecka, P., Macek, T., 2014. Bacterial acquisition of hexachlorobenzene-derived carbon in contaminated soil. *Chemosphere* 113, 141-145.
- Valentin-Vargas, A., Toro-Labrador, G., Massol-Deya, A.A., 2012. Bacterial community dynamics in full-scale activated sludge bioreactors: operational and ecological factors driving community assembly and performance. *PLoS One* 7, e42524.
- Vega, F.A., Covelo, E.F., Andrade, M.L., 2007. Accidental organochlorine pesticide contamination of soil in Porrino, Spain. *Journal of Environmental Quality* 36, 272-279.
- Vila-Costa, M., Rinta-Kanto, J.M., Sun, S., Sharma, S., Poretsky, R., Moran, M.A., 2010. Transcriptomic analysis of a marine bacterial community enriched with dimethylsulfoniopropionate. *The ISME journal* 4, 1410-1420.



- Vilchez-Vargas, R., Junca, H., Pieper, D.H., 2010. Metabolic networks, microbial ecology and 'omics' technologies: towards understanding in situ biodegradation processes. *Environmental Microbiology* 12, 3089-3104.
- Villeneuve, A., Larroudé, S., Humbert, J.F., 2011. Herbicide contamination of freshwater ecosystems: Impact on microbial communities. in: Stoytcheva, M. (Ed.). *Pesticides - Formulations, Effects, Fate*. InTech.
- Vogt, C., Cyrus, E., Herklotz, I., Schlosser, D., Bahr, A., Herrmann, S., Richnow, H.H., Fischer, A., 2008. Evaluation of toluene degradation pathways by two-dimensional stable isotope fractionation. *Environ. Sci. Technol.* 42, 7793-7800.
- Vryzas, Z., Papadakis, E.N., Oriakli, K., Theodoros, P.M., Papadopoulou-Mourkidou, E., 2012. Biotransformation of atrazine and metolachlor within soil profile and changes in microbial communities. *Chemosphere* 89, 1330–1338.
- Vuilleumier, S., Pagni, M., 2002. The elusive roles of bacterial glutathione S-transferases: new lessons from genomes. *Applied Microbiology and Biotechnology* 58, 138-146.
- Vymazal, J., 2011a. Constructed wetlands for wastewater treatment: five decades of experience. *Environmental Science & Technology* 45, 61-69.
- Vymazal, J., 2011b. Plants used in constructed wetlands with horizontal subsurface flow: a review. *Hydrobiologia* 674, 133-156.
- Wang, H., Yang, Z., Liu, R., Fu, Q., Zhang, S., Cai, Z., Li, J., Zhao, X., Ye, Q., Wang, W., Li, Z., 2013a. Stereoselective uptake and distribution of the chiral neonicotinoid insecticide, Paichongding, in Chinese pak choi (*Brassica campestris* ssp. *chinensis*). *Journal of Hazardous Materials* 262, 862-869.
- Wang, S., He, J., 2013. Phylogenetically distinct bacteria involve extensive dechlorination of aroclor 1260 in sediment-free cultures. *PLoS One* 8, e59178.
- Wang, Y.S., Liu, J.C., Chen, W.C., Yen, J.H., 2008. Characterization of acetanilide herbicides degrading bacteria isolated from tea garden soil. *Microbial Ecology* 55, 435-443.
- Wang, Z., Deng, H., Chen, L., Xiao, Y., Zhao, F., 2013b. *In situ* measurements of dissolved oxygen, pH and redox potential of biocathode microenvironments using microelectrodes. *Bioresource Technology* 132, 387-390.
- Weber, K.P., Mitzel, M.R., Slawson, R.M., Legge, R.L., 2011. Effect of ciprofloxacin on microbiological development in wetland mesocosms. *Water Research* 45, 3185-3196.
- Werner, J.J., Zhou, D., Caporaso, J.G., Knight, R., Angenent, L.T., 2012. Comparison of Illumina paired-end and single-direction sequencing for microbial 16S rRNA gene amplicon surveys. *The ISME journal* 6, 1273-1276.
- Wessén, E., Hallin, S., 2011. Abundance of archaeal and bacterial ammonia oxidizers – Possible bioindicator for soil monitoring. *Ecological Indicators* 11, 1696-1698.
- White, J.C., Mattina, M.I., Eitzer, B.D., Lannucci-Berger, W., 2002. Tracking chlordane compositional and chiral profiles in soil and vegetation. *Chemosphere* 47, 639-646.
- Whitehorn, P.R., O'Connor, S., Wackers, F.L., Goulson, D., 2012. Neonicotinoid pesticide reduces bumble bee colony growth and queen production. *Science* 336, 351-352.

- Widenfalk, A., Bertilsson, S., Sundh, I., Goedkoop, W., 2008. Effects of pesticides on community composition and activity of sediment microbes--responses at various levels of microbial community organization. *Environmental Pollution* 152, 576-584.
- Wiegert, C., Aeppli, C., Knowles, T., Holmstrand, H., Evershed, R., Pancost, R.D., Machackova, J., Gustafsson, O., 2012. Dual carbon-chlorine stable isotope investigation of sources and fate of chlorinated ethenes in contaminated groundwater. *Environmental Science & Technology* 46, 10918-10925.
- Winderl, C., Anneser, B., Griebler, C., Meckenstock, R.U., Lueders, T., 2008. Depth-resolved quantification of anaerobic toluene degraders and aquifer microbial community patterns in distinct redox zones of a tar oil contaminant plume. *Applied and Environmental Microbiology* 74, 792-801.
- Winderl, C., Penning, H., Netzer, F., Meckenstock, R., Lueders, T., 2010. DNA-SIP identifies sulfate-reducing *Clostridia* as important toluene degraders in tar-oil-contaminated aquifer sediment. *The ISME Journal* 4, 1314-1325.
- Winsley, T., van Dorst, J.M., Brown, M.V., Ferrari, B.C., 2012. Capturing greater 16S rRNA gene sequence diversity within the domain Bacteria. *Applied and Environmental Microbiology* 78, 5938-5941.
- Wong, C.S., Hoekstra, P.F., Karlsson, H., Backus, S.M., Mabury, S.A., Muir, D.C., 2002. Enantiomer fractions of chiral organochlorine pesticides and polychlorinated biphenyls in standard and certified reference materials. *Chemosphere* 49, 1339-1347.
- Wu, L., Yao, J., Trebse, P., Zhang, N., Richnow, H.H., 2014. Compound specific isotope analysis of organophosphorus pesticides. *Chemosphere* 111, 458-463.
- Xu, D., Wen, Y., Wang, K., 2010. Effect of chiral differences of metolachlor and its (*S*)-isomer on their toxicity to earthworms. *Ecotoxicology and Environmental Safety* 73, 1925-1931.
- Xu, J., Qiu, X., Dai, J., Cao, H., Yang, M., Zhang, J., Xu, M., 2006. Isolation and characterization of a *Pseudomonas oleovorans* degrading the chloroacetamide herbicide acetochlor. *Biodegradation* 17, 219-225.
- Xue, B., Tang, Q.Z., Jin, M.Q., Zhou, S.S., Zhang, H.S., 2014. Residues and enantiomeric profiling of organochlorine pesticides in sediments from Xinghua Bay, southern East China Sea. *Journal of Environmental Science and Health Part B* 49, 116-123.
- Ye, J., Wang, L., Zhang, Z., Liu, W., 2013. Enantioselective physiological effects of the herbicide diclofop on cyanobacterium *Microcystis aeruginosa*. *Environmental Science & Technology* 47, 3893-3901.
- Ye, J., Zhao, M., Liu, J., Liu, W., 2010. Enantioselectivity in environmental risk assessment of modern chiral pesticides. *Environmental Pollution* 158, 2371-2383.
- Yergeau, E., Lawrence, J.R., Sanschagrin, S., Waiser, M.J., Korber, D.R., Greer, C.W., 2012. Next-generation sequencing of microbial communities in the Athabasca River and its tributaries in relation to oil sands mining activities. *Applied and Environmental Microbiology* 78, 7626-7637.
- Yu, Y.L., Chen, Y.X., Luo, Y.M., Pan, X.D., He, Y.F., Wong, M.H., 2003. Rapid degradation of butachlor in wheat rhizosphere soil. *Chemosphere* 50, 771-774.
- Yu, Y.L., Wu, X.M., Li, S.N., Fang, H., Zhan, H.Y., Yu, J.Q., 2006. An exploration of the relationship between adsorption and bioavailability of pesticides in soil to earthworm. *Environmental Pollution* 141, 428-433.

- Zeng, T., Arnold, W.A., 2013. Pesticide photolysis in prairie potholes: probing photosensitized processes. *Environmental Science & Technology* 47, 6735-6745.
- Zeng, T., Ziegelgruber, K.L., Chin, Y.P., Arnold, W.A., 2011. Pesticide processing potential in prairie pothole porewaters. *Environmental Science & Technology* 45, 6814–6822.
- Zhang, C., Bennett, G.N., 2005. Biodegradation of xenobiotics by anaerobic bacteria. *Applied Microbiology and Biotechnology* 67, 600-618.
- Zhang, D.Q., Gersberg, R.M., Zhu, J., Hua, T., Jinadasa, K.B.S.N., Tan, S.K., 2012. Batch versus continuous feeding strategies for pharmaceutical removal by subsurface flow constructed wetland. *Environmental Pollution* 167, 124–131.
- Zhang, J., Fu, Q., Wang, H., Li, J., Wang, W., Yang, Z., Zhang, S., Ye, Q., Li, C., Li, Z., 2013a. Enantioselective uptake and translocation of a novel chiral neonicotinoid insecticide cycloxaprid in Youdonger (*Brassica campestris* subsp. *Chinensis*). *Chirality* 25, 686-691.
- Zhang, J., Zheng, J., Liang, B., Wang, C., Cai, S., Ni, Y., He, J., Li, S., 2011a. Biodegradation of chloroacetamide herbicides by *Paracoccus* sp. FLY-8 in vitro. *Journal of Agricultural and Food Chemistry* 59, 4614–4621.
- Zhang, N., Bashir, S., Qin, J., Schindelka, J., Fischer, A., Nijenhuis, I., Herrmann, H., Wick, L.Y., Richnow, H.H., 2014. Compound specific stable isotope analysis (CSIA) to characterize transformation mechanisms of  $\alpha$ -hexachlorocyclohexane. *Journal of Hazardous Materials* 280, 750-757
- Zhang, P., Sun, H., Yu, L., Sun, T., 2013b. Adsorption and catalytic hydrolysis of carbaryl and atrazine on pig manure-derived biochars: impact of structural properties of biochars. *Journal of Hazardous Materials* 15, 244-245:217-224.
- Zhong, F., Wu, J., Dai, Y., Yang, L., Zhang, Z., Cheng, S., Zhang, Q., 2014. Bacterial community analysis by PCR-DGGE and 454-pyrosequencing of horizontal subsurface flow constructed wetlands with front aeration. *Applied Microbiology and Biotechnology*. doi:10.1007/s00253-014-6063-2
- Zhou, W., Wan, M., He, P., Li, S., Lin, B., 2002. Oxidation of elemental sulfur in paddy soils as influenced by flooded condition and plant growth in pot experiment. *Biology and Fertility of Soils* 36, 384-389.

## Omnia ELSAYED

### Biodegradation of chloroacetanilide herbicides in wetlands

#### Résumé

Les chloroacétanilides sont une famille d'herbicides largement utilisée en agriculture, et contribuent de ce fait à la pollution environnementale. Leur devenir, y compris dans les écosystèmes rédox-dynamiques récepteurs comme les zones humides, est encore mal compris. Dans ce travail, la dégradation microbienne de chloroacétanilides (métolachlore, acétochlore et l'alachlore) a été étudiée par des approches innovantes de chimie analytique et de biologie moléculaire, à l'échelle du laboratoire en utilisant des microcosmes en colonnes, et *in situ* dans des zones humides construites à ciel ouvert et conçues pour traiter les intrants chimiques issus de l'agriculture.

Une nouvelle méthode d'analyse isotopique composés-spécifiques a été développée. Les résultats indiquent la biodégradation des chloroacétanilides dans les zones humides, également suggérée par la détection des produits de dégradation correspondants (acides éthane sulfonique et oxanilique). Dans les expériences en microcosme de laboratoire, les chloroacétanilides ont principalement été dégradés dans les zones anoxiques de la rhizosphère, suggérant un rôle prépondérant des processus anaérobies. L'analyse par chromatographie chirale du métolachlore a en outre révélé la dégradation préférentielle de l'énantiomère *S* du métolachlore, confirmant l'importance des processus biologiques dans la dissipation des chloroacétanilides. Les corrélations qui ont pu être observées entre les changements de variables hydrochimiques et de conditions hydrauliques et des différences de composition bactérienne détectées par génotypage par polymorphisme de longueur des fragments de restriction (T-RFLP) et par pyroséquençage du gène ARNr 16S confirme le potentiel de bio-indicateurs basés sur l'ADN pour suivre le fonctionnement des écosystèmes.

Sur la base de ce travail, la détection et l'identification des micro-organismes et des voies biochimiques responsables de la dégradation de chloroacétanilides dans les zones humides, ainsi que l'élaboration d'indicateurs génétiques bactériens pour le suivi de la dégradation de chloroacétanilides en zones humides, émergent comme autant d'objectifs de recherche à court-terme.

**Mots-clés:** chloroacétanilides, biodégradation de pesticides, biogéochimie des zones humides, CSIA, T-RFLP, pyroséquençage, bioindication basée sur l'ADN

#### Summary

Chloroacetanilide herbicides are widely used in agriculture, and thereby contribute to environmental pollution. Their fate, including in redox-dynamic receptor ecosystems such as wetlands, remains poorly understood. In this work, microbial degradation of chloroacetanilides (metolachlor, acetochlor and alachlor) was investigated by emerging chemical and molecular biological approaches, at the lab-scale using microcosm columns, and *in situ*, in outdoor constructed wetlands designed for the treatment of chemical pollutants originating from agriculture.

A novel compound-specific isotope analysis (CSIA) method was developed, and the results indicated biodegradation of chloroacetanilides in wetlands, which was also suggested by detection of ethane sulfonic acid and oxanilic acid degradation products. In lab-scale wetland microcosms, chloroacetanilides were mainly degraded in anoxic rhizosphere zones, suggesting a predominant role of anaerobic processes. Chiral chromatographic analysis of metolachlor revealed preferential degradation of the (*S*) enantiomer of metolachlor, and further confirmed the role of biological processes in chloroacetanilide dissipation. Changes in hydrochemical variables and hydraulic conditions correlated with differences in wetland bacterial composition detected by terminal restriction fragment length polymorphism (T-RFLP) and pyrosequencing analyses of the bacterial 16S rRNA gene, confirming the potential of DNA-based bioindicators for follow-up of ecosystem functioning.

On the basis of this work, detecting and identifying the microorganisms and biochemical pathways responsible for chloroacetanilide degradation in wetlands, as well as developing bacterial gene-based indicators of wetland functioning, emerge as research objectives for the near future.

**Keywords:** chloroacetanilides, pesticide biodegradation, wetland biogeochemistry, CSIA, T-RFLP, pyrosequencing, DNA-based bioindication